Perfluorosulfonic acid (PFSA)/nanoclay composite membranes as low relative humidity and intermediate temperature electrolytes for proton exchange membrane fuel cell (PEMFC)

Sahng Hyuck Woo

PSL UNIVERSITÉ PARIS

THÈSE DE DOCTORAT
DE L'UNIVERSITÉ PSL

Préparée à MINES ParisTech

Perfluorosulfonic acid (PFSA)/nanoclay composite membranes as low relative humidity and intermediate temperature electrolytes for proton exchange membrane fuel cell (PEMFC)

Membranes composites acide perfluorosulfonique (PFSA)/argile pour un fonctionnement à faible humidité relative et haute température des piles à combustible à membrane échangeuse de protons (PEMFC)

Soutenue par
Sahng Hyuck Woo
Le 21 juin 2019

Ecole doctorale n° 621
ISMME – Ingénierie des Systèmes, Matériaux, Mécanique, Énergétique

Spécialité
Énergétique et Génie des Procédés

Composition du jury :

Mourad Benabdesselam Professeur, University of Nice, France	*Président*
Sara Cavaliere Maître de conférence, ICGM, University of Montpellier, France	*Rapporteur*
Claire Longuet Ingénieur de recherche, IMT Mines Alès, France	*Rapporteur*
Patrick Achard Directeur de recherche, PSL-MINES ParisTech, France	*Examinateur*
Jochen Kerres Dr. rer. nat., University of Stuttgart, Germany	*Invité*
Christian Beauger Maitre de recherche, PSL-MINES ParisTech, France	*Directeur de thèse*
Arnaud Rigacci Professeur, PSL-MINES ParisTech, France	*Co-directeur*

MINES ParisTech | PSL

For those I love,

Acknowledgements

As a Ph.D. student, I started studying in France in 2016. Until I finished this Ph.D. thesis, many people have worked together for electrolyte membrane and fuel cell studies, and helped me. I would like to express my gratitude to Prof. Christian Beauger and Prof. Arnaud Rigacci who gave a lot of cooperation and teaching in the study of electrolyte membranes and proton exchange membrane fuel cells (PEMFCs). I would also like to thank the professors and research engineers who gave me various advices through Ph.D. seminars. In particular, Prof. Patrick Achard gave me a lot of help with useful comments. I was nervous during the evaluation each year, but now I think it was a great teaching. Thanks also to my partners Prof. Aurélie Taguet and Prof. Belkacem Otazaghine for their help with mechanical strength test and nanoclay functionalization. I would like to thank Aurélie and Belkacem for helping me make the experiment when I visited Alès. Especially, Belkacem has also helped to analyze the funtionalized nanoclays using ATR-FTIR, TGA and Py-GC/MS for the study.

I am also greatful to Prof. Byoung Ryul Min, Prof. Joo-Sik Kim and Prof. Jinhee Choi for giving me various advices for Ph.D.

I want to thank Pierre Ilbizian (PERSEE center), Patrick Leroux (PERSEE center), Cedric Sernissi (PERSEE center), Suzanne Jacomet (CEMEF center), Gabriel Monge (CEMEF center), Loïc Dumazert (C2MA center) and Benjamin Gallard (C2MA center) for technical support until this thesis has been successfully completed.

I wish to thank Prof. Sara Cavaliere, Dr. Claire Longuet, Prof. Jochen Kerres, Prof. Mourad Benabdesselam, Prof. Arnaud Rigacci, Prof. Christian Beauger and Prof. Patrick Achard for their efforts on reviewing Ph.D. thesis and participating in Ph.D. defense.

I am going to miss lots of other professors, research engineers and Ph.D. students studying hard and having a good time together at the PERSEE center, as well as CEMEF, CMA, CRC and OIE centers: Lluis Sola-Hernandez, Dr. Alexi Gerossier, Dr. Youling Wang, Antoine Rogeau, Giovanni Muratore, Dr. Raounak Loudad, Dr. Guillaume Ozouf, Fian Assemien, Dr. Yossef Abdo, Di Li, Dr. Qiang Chen, Shaojie Zhang, Dr. Carlos Adrian Correa Florez, Dr. Aravind Ramaswamy, Dr. Lucia Ianniciello, Dr. Fabien Labbe, Dr. Gislan Agoua, Dr. Etta Grover-Silva, Julien Fausty, Rag Ghandour, Feng Gao, Valentin Mahler, Dr. Kevin Nocentini, Kevin Bellinguer, Simon Camal, Thomas Carriere, Charlotte Gervillie, Dr. Pedro Affonso Nobrega, Dr. Maxime Gautier, Dr. Papa Gueye, Dr. Thibaut Barbier, Dr. Aumaury Bazalgette, Dr. Gediminas Markevicious, Shitij Arora, Dr. Lucile Druel, Dr. Sophie Groult, Pacco Bailly, Sylvain Fenot, Juhi Sharma, Dr. Alexander V Surov, Prashanth Thirunavukkarasu, Dr. Andrea Michiorri, Diego Alejandro Uribe Suárez, Corentin Perderiset, Dr. Romain Dupin, Diana Paola Moreno Alarcon, Dr. Fabian Claudel, Romane Quéré, Dr. Sabri Takali, Dr. Elena Magliaro, Mathieu Gaulène, Chahrazade Bahbah, Dr. Ghalia Guiza, Wafa Daldoul, Dr. Robin Girard, Dr. Pierrick Rambaud, Dr. Quentin Schmid, Dr. Yuki Kobayashi, Fanny Romeo, Dr. Zhang Yancheng and Dr. Welington De Oliveira. Everything seems just like yesterday and time really flies.

I thank also to Lyliane Louault, Christine Gschwind, Brigitte Leprat, Marie-Jean Condo, Laurent Schiatti de Monza and Sophie Pierini for the help regarding the administration.

I would like to thank the PERSEE center that provided funding for the use of chemical reagents, experimental machines and laboratory equipments for Ph.D. I am also grateful to the ARMINES that provided me with salary, Allianz health insurance and other benefits until I finished studying and developing the fuel cell, especially, new

electrolyte composite membranes and membrane electrode assemblies (MEAs). This study was supported by funding under the COMEHTE project (contract number ANR-15-CE05-0025-01) granted from French National Research Agency (ANR).

I would also like to thank the neighborhoods who helped me during staying in France. They were so friendly and kind. In particular, Claudia and Danielle, who lived downstairs, were almost my family while staying in France.

Through the ASCoF (Association des Scientifiques Coréens en France) and the South Korean communities, I have experienced a lot and enjoyed having the parties and meetings together. They were the only good opportunity to speak Korean in foreign land, and it was so good to feel Korean culture again. I would also like to thank Korean friends who contacted me on mobile phone during studying in France.

My lovely family, I especially appreciate my parents who helped me in various ways in South Korea. They were with my mind at any time. I am also grateful to my wife, my mother-in-law and my father-in-law who are raising my son, Joonhee. Many thanks to my maternal grandfather who always supported me during Ph.D.

Once again, thank you all.

Sahng Hyuck Woo
PERSEE
Ecole des mines de Paris (MINES ParisTech)
Paris Sciences et Lettres - PSL University
Paris
24th June 2019

Contents

Abbreviation

[BVBI][Cl], 1-butyl-3-(4-vinylbenzyl)imidazolium chloride;

[HMIM][Cl], 1-hexyl-3-methylimidazolium chloride;

[TMG][BF4], 1,1,3,3-tetramethylguanidine tetrafluoroborate;

1,3-PS, 1,3 propane sultone

1,4-BS, 1,4 butane sultone

3-MPTMS, 3-(mercaptopropyl)trimethoxysilane;

AAc, acrylic acid;

ABPBI, poly(2,5-benzimidazole);

ACA, 6-aminocaproic acid; BHB, behenyl betaine;

AFC, alkaline fuel cell;

AIBN, 2,2′-azobisisobutyronitrile;

AMPS, 2-acrylamido-2-methyl-1-propanesulfonic acid;

AP, anionic polymerization;

ATRP, atom transfer radical polymerization;

BCPS, bis-(4-chlorophenylsulfone);

BMC, bulk molding compound;

CS, chitosan;

CTAB, cetyltrimethylammonium bromide;

CTAC, hexadecyltrimethylammonium chloride;

DABA, 3,4-diaminobenzoic acid;

DCDPS, 4,4'-dichlorodiphenyl sulfone;

DFB, 4,4'-diflluorobenzophenone;

DMA, dynamic mechanical analysis;

DMAc, dimethylacetamide;

DMDOC, dimethyl dioctadecylammonium chloride;

DMF, N,N-dimethylformamide;

DMOSPA, dimethyloctadecyl(3-sulfopropyl) ammonium hydroxide;

DMSO, dimethyl sulfoxide;

DOA, dodecylamine;

EDS, energy-dispersive X-ray spectroscopy;

EHTES, 2(3, 4 epoxy cyclo hexyl)ethyltriethoxy silane;

FE-SEM, field emission scanning electron microscopy

FMES, 1,2,2-tri-fluoro-hydroxy-l-trifluomethylethane sulfonic acid sultone

GA, glutaraldehyde;

GPTMS, 3-glicidoxy propyltrimethoxysilane;

HDDA, hexanediol diacrylate;

HDTMA, hexadecyltrimethylammonium;

HEMA, 2-hydroxyethyl methacrylate;

HNT, halloysite nanotube;

IEC, ion exchange capacity;

IPA, isopropyl alcohol;

MCFC, molten carbonate fuel cell;

MEA, membrane electrode assembly;

MMT, montmorillonite;

MPS, propyltrimethoxysilan;

MWNT, multi-walled carbon nanotube;

NaSS, sodiumstyrene sulfonate;

NMP, 1-methyl-2-pyrrolidinone;

PAFC, phosphoric acid fuel cell;

PBI, polybenzimidazole;

PBP, 4,40-(1,4-phenylene diisopropylidene)bisphenol;

PEG, polyethylene glycol;

PEM, proton exchange membrane;

PEMFC, proton exchange membrane fuel cell;

PEO, poly(ethylene oxide);

PES, poly(ether sulfones);

PFPE-NR3, quaternized ammonium perfluoropolyether;

PFSA, perfluorosulfonic acid;

PFSI, perfluorosulfonate ionomer;

pHNT, pretreated halloysite nanotube;

pHNT-F, pretreated and fluorinated halloysite nanotube;

pHNT-FQ, pretreated and fluorinated-quercetin-grafted halloysite nanotube;

pHNT-NQ, pretreated and aminized-quercetin-grafted halloysite nanotube;

pHNT-S, pretreated and sulfonated halloysite nanotube;

pHNT-SF, pretreated and perfluorosulfonated halloysite nanotube;

pHNT-Q, pretreated and quercetin-grafted halloysite nanotube;

POPD, poly(oxyproplene)-backboned diamine cation;

PPA, polyphosphoric acid;

PPA, polyphosphoric acid;

PPO, poly(p-phenylene oxide);

PSA, phenylsulfonic acid;

pSEP, pretreated sepiolite;

pSEP-F, pretreated and fluorinated sepiolite;

PSSA, poly(styrene sulfonic acid);

PSU, polysulfone;

PTFE, polytetrafluoroethylene;

PVOH, poly(vinyl alcohol);

PWA, Phosphotungstic acid;

RH, relative humidity;

RIP, radiation-induced polymerization;

ROP, ring opening polymerization;

RP, radical polymerization;

SEP, sepiolite nanofiber;

SFRP, stable free radical polymerization;

SOFC, solid oxide fuel cell;

SPAES, sulfonated poly(arylene ether sulfonate);

SPAS, sulfonated poly(arylene sulfone);

SPEEK, sulfonated poly(ether ether ketone);

SPEK, poly(ether ketone);

SPPESK, sulfonated poly(phthalazinone ether sulfone ketone);

SPSEBS, sulfonated polystyrene block-poly(ethylene-ran-butylene)-block-polystyrene;

SPSU, sulfonated polysulfone;

SPSU-BP, sulfonated poly (biphenyl ether sulfone);

SSEBS, (Sulfonated poly(styrene-b-ethylene/butylene-b-styrene);

St, styrene;

STA, silicotungstic acid;

TAP, 2,4,6-triaminopyrimidine;

TGA, thermal gravimetric analysis;

TMSCS, trimethyl silyl chlorosulfonate.

List of figures

List of tables

General introduction

1. Background

The increasing amount of greenhouse gas, e.g., carbon dioxide (CO_2), released in the atmosphere due to the consumption of fossil fuels is causing climate change. Hence, Earth has been suffering from climate change during 20^{th} century because CO_2 gas resulted in global warming impacting Earth's surface and the lower atmosphere. Greenhouse effect has a negative influence and change of sea level, precipitation pattern, glacier retreat, and agricultural yields. Accordingly, an attempt to reduce CO_2 gas emissions is necessary for humankind and all living creatures [1, 2].

One eco-friendly alternative to energy conversion from fossil fuels is the fuel cell. The fuel cell is a useful electrochemical device which converts chemical energy from various fuels to electrical energy and heat. This is an environmental-friendly solution in lieu of alleviating carbon dioxide emission from combustion and it will have a positive impact on the climate change. In general, fuel cells include proton exchange membrane fuel cell (PEMFC), solid oxide fuel cell (SOFC), phosphoric acid fuel cell (PAFC), alkaline fuel cell (AFC) and molten carbonate fuel cell (MCFC). Depictions of the various fuel cells were described in the literatures [3, 4]. In particular, PEMFC is attractive in the field of automobile application due to low operating temperature, high efficiency, portable power generation, high power density, and innocuous electrolyte, which is a hydrated proton conducting polymer [5, 6].

The evolution of PEMFC has mainly be accompanied by spaceflight and automobile development. In the early 1960s, the first PEMFC was used as power source for Gemini space flights under NASA's space program, which is started in late 1950s. In late 1960s, PEMFC was displaced by AFC for NASA's Apollo and Space Shuttle flights. However, since the late 1980s, interest in the introduction of PEMFC technology has been on the rise in NASA's space station and Mars program due to the major strides in PEMFC performance [5]. Application of PEMFC as power sources for electric vehicles first developed by General Electric (GE) in 1958 but it also took until 1993 for the vehicle demonstrations. In mid-to-late 1990s, many major automakers developed the fuel cell vehicles using PEM. Recently, automakers in France, Germany, Japan, South Korea, USA and other countries are spurring the development of PEMFC used for hydrogen fuel cell vehicle (HFCV) in line with the Paris climate change conference, which came into force in 2016, and the HFCV market is currently increasing in the fields of car, truck, boat, train, air plane and heavy equipment.

Power generated by PEMFC systems is based on electrochemical reactions involving hydrogen and oxygen gases as shown in Fig. 1. Hydrogen reacts with Pt catalyst to form protons and release electrons from the anode (i.e., oxidation reaction). The protons form water in the cathode by combining with O_2 and electrons (i.e., reduction reaction). The role of the proton exchange membrane (PEM) used as an electrolyte in PEMFC is to conduct protons from the anode towards the cathode [7]. The chemical reactions occurring in PEMFC could be elucidated as follows:

Anode: $2H_2 \rightarrow 4H^+ + 4e^-$

Cathode: $O_2 + 4e^- + 4H^+ \rightarrow 2H_2O$

Cell reaction: $2H_2 + O_2 \rightarrow 2H_2O$

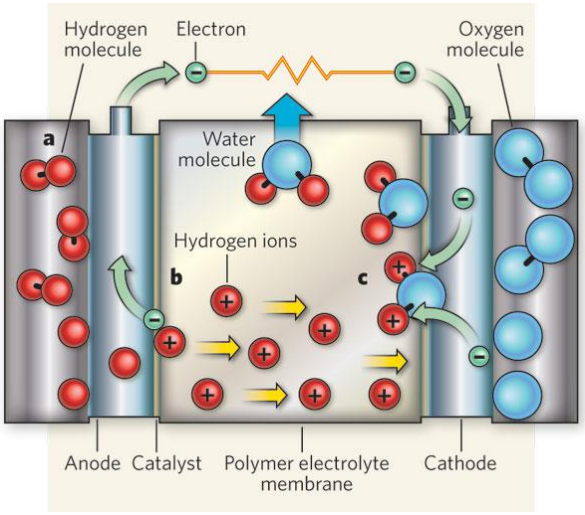

Fig. 1. Electrochemical conversion of hydrogen in a fuel cell: (a) H_2 molecules split into hydrogen atoms at anode. (b) A catalyst allows the hydrogen atoms to split into hydrogen ions (H^+) and electrons. (c) At cathode, oxygen reacts with hydrogen ions (H^+) and electrons to form pure water molecules [7]. Copyright 2009, Reproduced with permission from Macmillan Publishers.

Among the broad range of polymers used as proton exchange membranes (PEMs), Nafion, one of PFSA materials, has been widely adopted as a standard because of its rather good thermal and chemical stability, mechanical strength, hydrophilicity and MEA (membrane electrode assembly) performance at low temperature, resulting from both its chemical composition and chain organization: PTFE-like backbones and polyethers having side chains terminated with sulfonic acid groups ($-SO_3H$) [8, 9]. However, physicochemical characteristics of pristine Nafion membrane are limiting the PEMFC operation range. The proton conductivity of the electrolyte membrane declines due to dehydration as PEMFCs are operated at intermediate temperature, which is above 100℃.

Clean water is produced from the cathode through oxygen reduction and is removed by reactant gas flow during PEMFC operation. PFSA electrolyte membranes-contained hydrogen fuel cells have a significant influence on performance and durability depending on the relative humidity as hydrogen protons moves through water molecules inside the electrolytes. More specifically, dried membranes lacking moisture can affect performance degradation caused by increased resistance [10], as well as form pinholes to generate hydrogen crossover [11]. On the other hand, excessive water content at the cathode and the anode decreases the performance by blocking the pores of the catalyst or gas diffusion layers, and eventually limiting the reactant mass transport [12]. Therefore, sufficient water content is required to improve the operational efficiency of the electrolyte membranes and accordingly it affects an electrochemical reaction for fuel cells.

Various inorganic fillers have been used as additives to develop electrolyte membranes suitable for use at low relative humidity. The incorporation of such fillers results in improved water uptake and sometimes proton conductivity and mechanical resistance. Inorganic fillers added in composite membranes include inorganic oxides, e.g., TiO_2, SiO_2, ZrO_2, and ZrO_2/SO_4^{2-}[13-23]; and zeolites, e.g., NaA zeolite, ETS-10 (engelhard corporation titanosilicate), umbite, mordenite, analcime, faujasite, b-zeolite, ZrP-modified zeolite, and H-type of b-zeolite [13, 24-28], and nanoclays, e.g., montmorillonite, laponite, sepiolite or halloysite [13, 24, 29-36].

Incorporation of nanoclays into a polymer matrix helps to overcome some of the limitations regarding thermo-

mechanical resistance and sensitivity to relative humidity at intermediate temperature. Blending of nanoclays particularly prevents dehydration due to their hygroscopic property. Composite membranes can be in turn operated at low relative humidity [33, 37-41]. Mechanical property may also be improved through fillers homogeneous dispersion, functionalization for better compatibility with the polymer selected for the composite membrane or exfoliation in case of some nanoclays [39, 41-44]. The presence of fillers can, moreover, decrease the hydrogen crossover. Also, according to literature published by Peighambardoust, S. Jamai et al, nanoclay-based membranes are cost competitive compared with inorganic oxide materials and zeolites-based composite membrane [13, 45]. In particular, sepiolite (SEP), a natural nanoclay, has a fibrous morphology (so called needle-like structure) and consists of parallel tunnels formed by blocks. Hence, it is able to improve the tensile strength of the membrane by effect of chain packing [38, 39, 42, 46, 47]. Previous works achieved in the group already demonstrated that the incorporation of sepiolite can lead to improved properties of Nafion composite membranes [38, 39]. Halloysite nanotube (HNT), a natural nanoclay, is composed of cylinder form wrapping by the nanoclay layer. Accordingly, the tensile strength of the composite membrane can be enhanced by the influence of reinforcement [42, 48].

However, aggregated nanoclays inside polymer matrix can interfere with performance within the polymer matrix and hinder the expected benefit. Hence, controlling the dispersion state has been considered as a crucial challenge in order to enhance the performance and numerous researchers have tried various methods to improve the dispersion state [63]. To this end, surface modification has been achieved, namely sulfonation [32, 39, 49] or perfluorosulfonation [38].

Afore-mentioned background and state-of-the-art review are presented in more detail in Chapter 2.

2. Challenge

Briefly, as above-mentioned, numerous researchers reported the work principle of PEMFC and why PEMFC should be operated at low relative humidity and high temperatures, and the advantages and disadvantages of polymers and inorganic additives used in electrolyte membranes. Particularly, the problems of Nafion, a PFSA which has been widely used so far, were discussed. In addition, it was explained why nanoclays should be used among various inorganic fillers. A detailed description of the various functionalization methods and modified nanoclays will be also presented in chapter 2.

To date, however, the physicochemical properties of electrolyte membranes composed of short-side-chain PFSA (i.e., Aquivion) and nanoclays have not yet been fully studied. More specifically, sepiolite with nanofiber morphology and halloysite with nanotube shape have not been incorporated to the Aquivion matrix as fillers. In addition, although iron in sepiolites and halloysites may cause oxidation, the studies have not been fully conducted to verify it using anti-oxidant material such as quercetin. Furthermore, composite membranes prepared in this manner have not been applied to fuel cells. If these studies are confirmed to improve performance, the approach will be of significant benefit for PEMFC to operate over a broad range of conditions.

3. Objective

The objective of the Ph.D. thesis focused on novel nanoclay-based Aquivion electrolyte membranes that can be operated at low relative humidity. The thesis takes benefit from hygroscopicity and fiber morphology of sepiolite and halloysite. The effect of halloysite and sepiolite on PFSA composite membranes were questioned as follow:

- What effect does the blend time of halloysite or sepiolite have on Nafion matrix of composite membranes?
- Does the performance of the composite membrane improve? What about composite homogeneity?
- What is the performance of functionalized nanoclay-incorporated membranes compared with that of pristine nanoclay-blended membranes?
- Does the antioxidative activity of quercetin improve the composite membrane chemical stability once grafted on halloysite?
- What are the influence of pretreated nanoclays and their various contents on Aquivion composite membranes?

In the study, impact of sepiolite or halloysite on PFSA composite membranes was demonstrated through various analyses. Water uptake, swelling ratio, IEC, mechanical strength and proton conductivity were conducted to characterize. Furthermore, nanoclay sulfonation, fluorination and perfluoro-sulfonation to enhance the proton conductivity and the dispersion state and compatibility with PFSA polymer were realized. Afterwards, improvement of the durability through pretreatment (to remove iron from the nanoclays) and addition of antioxidant (i.e., quercetin) were verified. Last, it was demonstrated that modifying nanoclays (functionalization and pretreatment) improved the physicochemical properties of composite membrane electrolytes compared with those of pristine Aquivion or commercially available Nafion HP and Gore Select M820. MEA test was also performed through several selected membranes.

Chapter 1

State-of-the-art review

Summary

Proton exchange membrane (PEM) is pivotal among various components used in proton exchange membrane fuel cell (PEMFC). In a wide range of PEMs, perfluorosulfonic acid (PFSA) and non-fluorinated membranes are used for operation in PEMFC, but it has a limitation of reduced performance above 90℃ and at low relative humidity. Hence, a study to incorporate nanoclay, one of inorganic fillers, into polymer matrix has been attempted in order to improve performance of PEM. Nanoclays, e.g., montmorillonite (MMT) and Laponite as layered silicate morphology; and sepiolite nanofiber (SEP) and halloysite nanotube (HNT) as fiber morphology, are attractive for composite membrane as these allow composite membrane to have influence on improved hydrophilicity, hygroscopicity and thermal stability at high temperature and low relative humidity. Mechanical property also exhibits positive deviation by introduction of nanoclay, as well polymer/nanoclay composite membrane is cost competitive compared with composite membranes containing inorganic oxides and zeolites. This review highlights the 1) preparation of composite membranes containing sulfonic, perfluorosulfonic and amine groups, and other types of functionalized nanoclays, as well as 2) characterization of composite membranes composed of polymer and functionalized nanoclay.

Résumé

La membrane échangeuse de protons (PEM) joue un rôle central parmi les divers composants utilisés dans la pile à combustible à membrane échangeuse de protons (PEMFC). Les membranes perfluorosulfoniques acides (PFSA) et les membranes non fluorées sont utilisés dans une large gamme de PEM, mais leur performance est réduite au-dessus de 90℃ et à faible humidité relative. Par conséquent, des études visant à incorporer des nanoargiles, une charge inorganique, dans la matrice polymère ont été tentées afin d'améliorer les performances de ces membranes. Les nanoargiles, par exemple la montmorillonite (MMT) et la Laponite, argiles lamellaires, la sépiolite (SEP) et l'halloysite (HNT), argiles fibreuses sont d'intérêt pour les membranes composites car elles permettent d'agir sur l'amélioration de l'hydrophilie, de l'hygroscopicité et de la stabilité thermique à haute tempéraure et basse humidité relative. Les propriétés mécaniques présentent également une déviation positive par introduction de nanoargile. Les membranes composites polymère/nanoargile sont par ailleurs compétitives par rapport aux membranes composites contenant des oxydes inorganiques et des zéolithes. Cette revue résume 1) la préparation de membranes composites contenant des groupes sulfoniques, perfluorosulfoniques et amines, ainsi que d'autres types de nanoargiles fonctionnalisées, ainsi que 2) la caractérisation de membranes composites composées de polymère et de nanoargile fonctionnalisée.

Numerous research groups have studied perfluorosulfonic acid and non-fluorinated hydrocarbon composite membranes containing functionalized nanoclay as electrolyte used in PEMFC, in order to improve performance. This literature review aims to highlight 1) preparation of electrolyte membranes composed of polymer and functionalized nanoclays, and 2) properties i.e., water uptake, thermal stability (chemical degradation), mechanical resistance (including compatibility), and proton conductivity, on PEMs incorporated with functionalized MMT, Laponite, HNT, or SEP.

1. Basic polymer matrix and nanoclay additive

1.1. Fluorinated and non-fluorinated polymers used as electrolyte membrane in PEMFC

Materials used for polymer based membrane fall into two different categories: 1) perfluorosulfonic acid ionomer, 2) non-fluorinated polymer (i.e., hydrocarbon), and 3) partially fluorinated polymers.

Among a broad range of polymers, Nafion has for long been selected as a standard material to prepare PFSA membrane. Physicochemical properties of Nafion include relatively high thermal and chemical stability and MEA (membrane electrode assembly) performance. This is caused by tetrafluoroethylene (i.e., PTFE-like backbone) and polyether side chain ending with sulfonic group ($-SO_3H$). Nafion also allows membranes to have good mechanical stability and hydrophilicity [8, 9].

Aquivion-based membrane displays similar or better properties compared with Nafion electrolyte membrane. Aquivion has been selected for its enhanced proton conductivity and thermal stability compared with those of Nafion due to short-side-chain, larger crystallinity and higher glass transition temperature (T_g) [50-52]. It is noteworthy that T_g of Nafion, 3M and Aquivion respectively show 100, 125 and 140℃, which means augmentation in operating temperature of Aquivion membrane. In the same equivalent weight (EW), the crystallinity is smaller with long side chain ionomers than with short side chain to such an extend that the membranes with short side chain ionomers display crystallinity in EW that long side chain ionomers are amorphous [53]. Aquivion membranes are also chemically stable and can operate at temperatures higher than Nafion membrane. According to result of Aricò's group, Nafion membrane has a maximum operating temperature of 95℃, while Aquivion membrane can be operated up to 110℃, under 500 h of operation [54]. Higher PEMFC operating temperature can lead to carbon monoxide (CO) tolerance, easier heat and water management and better reaction kinetics during operation [55, 56]. For membrane durability, Aquivion is considerably less sensitive to radical attack compared to Nafion based on Fenton's test, due to absence of the $-O-CF_2-CF(CF_3)-$ segment in Aquivion, thereby improved side chain stability [53].

Other PFSA ionomers manufactured by 3M, Dow and Solvay Solexis have not been used as nanoclay-incorporated electrolyte membranes so far.

Pristine PFSA membrane has a limitation of physicochemical characteristics during PEMFC performance. Ionic conductivity of electrolyte membranes suffer from high temperature, i.e., above 100℃ because of dehydration. Degradation of PFSA membrane is also caused by hydrogen peroxide (H_2O_2) and free radical species such as $HO\cdot$ and $HO_2\cdot$ formed in the presence of metal cation, e.g., Fe^{2+}. With strong oxidative property, the formed radical chemically attacks C-F bonds [57]. Formation of H_2O_2 and decomposition intermediate products, i.e., free radicals, is generated by two different pathways at cathode and anode in MEA. More specifically, two-electron

reduction of oxygen and chemical combination of hydrogen and oxygen can form H_2O_2, thereby H_2O_2 reacts with metal ions in membrane to form free radical species, i.e., $HO\cdot$ and $HO_2\cdot$, at cathode. The occurrence at cathode is as following reaction [58, 59]:

1) $O_2 + 2H^+ + 2e^- \rightarrow H_2O_2$

2) $H_2O_2 + M^{2+} \rightarrow M^{3+} + HO\cdot + HO^-$

3) $HO\cdot + H_2O_2 \rightarrow H_2O + HO_2\cdot$ (hydrogen peroxide radical chemically attacks C-F bonds of PEM)

In addition to this, chemical combination of hydrogen and oxygen at the anode also can occur on Pt catalyst, resulting in generation of $HO_2\cdot$ radical and H_2O_2 as below [59-61]:

1) $H_2 + O_2 \rightarrow [O] + H$ (on Pt surface)

2) $H_2 \rightarrow 2H\cdot$ (by Pt catalyst)

3) $H\cdot + O_2$ (diffused through PEM to anode) $\rightarrow HO_2\cdot$

4) $HO_2\cdot + H\cdot \rightarrow H_2O_2$ (diffused into PEM)

Mechanical degradation of electrolyte membrane is also important. PFSA membranes usually indicate that higher relative humidity and temperature lead to lower Young's modulus. The intermolecular forces are reduced by the interference between water and chain-to-chain secondary bonding in the presence of water, thereby the chains with greater mobility and increased free volume reduce glass transition temperature and mechanical strength of membranes [62]. Also, the higher the operating temperature, the lower the amorphous domain, leading to lower Young's modulus [63]. As a solution to this problem, one approach is to transform into ionomer with multi-acid side chain. Another strategy is to crosslink the polymer to improve mechanical property through sulfonamide functionalization [64] and crosslinkable side chains [65]. Other effect method is to use the partially fluorinated bi-functional monomeric units containing sulfonyl group [66].

Nafion HP and Gore Select M820 (EW = 820) used as reference in Chapters 4, 5 and 6 are needed to compare membrane properties.

Fuel cell Store company provides the physicochemical properties of Nafion HP. However, for Gore Select (EW = 820), it was difficult to find bibliographies published in journals or described in manufacturer's website. For this reason, two Gore Selects (with EW = 900 and 1100) analyzed by W. L. Gore & Associates, Inc. were introduced in this section [67]. Three kinds of commercially available membranes are listed in Table 1.1.

Water uptake and tensile strength of Nafion HP are higher compared to that of Gore Selects, whereas proton conductivity has improved values for Gore Selects. The lower the equivalent weight (EW) of Gore Select, the higher the proton conductivity.

Table 1.1. Properties of Nafion HP, Gore Select EW1100 and Gore Select EW900.

Membranes	Nafion HP [1) Feul Cell Store]	Gore Select EW1100 [67]	Gore Select EW900 [67]
Equivalent weight (EW)	Unkown	1100	900
Thickness (μm)	20	20	12
Water uptake (%)	50 ± 5 (100℃)	32	43
Tensile strength (MPa)	38 - 41 (23℃, 50%RH)	Transverse direction: 17.7 (wet) Machine direction: 32.5 (wet)	-
Proton conductivity (through-Plane) (mS/cm)	50.5 (23℃, 100%RH)	52 – 53 (Gore Select immersed in DI water was measured)	96 (Gore Select immersed in DI water was measured)

Numerous research groups have reported alternative membranes made of non-fluorinated hydrocarbons used as alternative materials, such as PEEK (polyetheretherketone), PVOH (polyvinyl alcohol), PBI (polybenzimidazole), PPO (polyphenylene oxide), PSU (polysulfone), and other polymers in recent years. Hydrocarbon-type membranes have benefit of low cost and good durability at high temperature.

Among alternative materials, PEEK, aromatic structure (i.e., $C_{21}H_{18}O_3$), is popular as polymer for fuel cell membrane. Beside low preparation cost, PEEK includes high chemical stability, mechanical characteristics, and thermal stability [34]. Table 1.1 provides the information on thermal and mechanical properties of polymer used for membrane fabrication. Moreover, proton conductivity can be obtained through sulfonation of PEEK (SPEEK). It depends on the degree of sulfonation, which is improved according to sulfonation conditions (e.g., concentration, temperature and reaction time of sulfuric acid) [68-70]. SPEEK membranes generally were made of commercial PEEK, which was manufactured by Victrex and Poly Science Inc.

PVOH [$(C_2H_4O)_n$] is also a good candidate as an alternative polymer in lieu of Nafion. PVOH membrane has higher hydrophilicity, but low thermal stability at high temperature. For this reason, even though cross-linked PVOH membrane is used for hydrogen fuel cell, it displays low proton conductivity because it doesn't contain proton conductive sulfonic acid ($-SO_3H$) or carboxylic (-COOH) group. In order to enhance the proton conductivity of membrane, PVOH is blended or grafted with negative charged ions [71-74]. PVOH was sulfonated by addition of sulfosuccinic acid in PVOH solution according to publication [75]. Major suppliers of PVOH are Sigma-Aldrich and Fluka Inc. for fabrication of nanoclay-based PVOH composite membrane.

PBI [$(C_{20}H_{12}N_4)_n$] is also one of a promising nonfluorinated-hydrocarbon ionomer as membrane material for fuel cell operating at temperature higher than 100 ℃ because its characteristics include high thermal and mechanical stability (see Table 1.1). However, it is difficult for PBI to dissolve in common organic solvents

because of its very tight molecular structure, and hence incorporating nanoclay into PBI is hard. To solve this problem, fluorine-containing PBI has been introduced [76]. PBI is sulfonated to have stable proton conductivity of the membrane above 100℃ prior to preparation of PBI membrane [77]. There are other attempts to make H_3PO_4-PBI by doping PBI with phosphoric acid, and it has influence on high chemical and thermal stability of membrane [78, 79]. However, PBI membrane series operated above 160℃ show creep, and reduce proton conductivity below 100℃ due to certain amount of dehydration [77, 80].

In addition, PPO [$(C_6H_2(CH_3)_2O)_n$] has been introduced as another alternative membrane material instead of Nafion owing to high chemical and thermal stability, as well as good mechanical characteristic (see Table 1). However, PPO membrane had to be sulfonated in order to generate ionic conductivity of membrane [81].
PSU [$C_{27}H_{24}Cl_2O_4S$] is also used for non-fluorinated polymer for membrane preparation because of high thermal and chemical stability of PSU membrane in fuel cell application (see Table 1.2) [82, 83]. Blending PSU with Aquivion displays improved mechanical properties of composite membranes, as compared to pristine Aquivion membrane [52].

Various other polymers used for membrane preparation were reported in the literatures in recent years [30, 46, 84-95]. However, attempts to grow proton conductivity of non-fluorinated polymer–based membrane by phosphonation or sulfonation, in turn, can cause excessive swelling of the membrane operated at high temperature between 60 and 80℃, resulting in reduced performance. This is because high molar concentration usually can lead to decreased mechanical property of the membrane as large sulfonation makes the polymer soluble in water [80, 87].

Table 1.2. Thermal and mechanical stability of various polymers used as fuel cell membrane.

Polymer properties	Nafion	Aquivion	PEEK	PVOH	PBI	PPO	PSU
Thermal stability							
Melting point (℃)	200 [96]	240 [96]	340-343	230	760	268	180-190
Glass transition temperature (℃)	67 [97]	127 [97]	140-143	75-85	410	211	170-185
Thermal expansion coefficient (10^{-6}/℃)	-	-	55-140	70-100	23-33	40	19-57
Mechanical stability							
Tensile modulus (Gpa)	-	-	4-24	3.9	5.9	2.4	2.5-8.7
Tensile strength (Mpa)	-	-	97-200	78	160	63-140	70-140
Elongation at break (%)	-	-	1.6-43	9.90	3	3.5-28	2-59

1.2. Nanoclays used in electrolyte membrane in PEMFC

Numerous attempts have been made to incorporate various inorganic fillers into polymer membrane as the selected polymers cannot be adapted to operating temperature above 90℃. The proton conductivity of the PFSA membrane declines during operation at 90℃ or higher because of dehydration of the membrane. However, membranes operating at intermediate temperature (120 - 150℃) can provide advantages related to better reaction kinetics, carbon oxide (CO) tolerance (i.e., lower sensitivity of platinum to pollution), easier heat and water management for PEMFC application [55, 56]. Hence, membranes which can be operated at high temperature are necessary, but they have limitations in thermo-mechanical resistance and sensitivity to relative humidity resulting

from high temperature. Therefore, we are faced with the need to develop membranes that can be applied at low relative humidity and relatively high temperature.

Inorganic fillers can provide better gains at high proton conductivity, water uptake and mechanical resistance to composite membranes. In general, major inorganic fillers used for polymer/inorganic composite membranes include inorganic oxides, e.g., TiO_2, SiO_2, ZrO_2, and ZrO_2/SO_4^{-2} [14-16, 18-23, 59, 98]; and zeolites, e.g., NaA zeolite, ETS-10, umbite, mordenite, analcime, faujasite, b-zeolite, ZrP-modified zeolite, and H-type of b-zeolite [24-28, 59]; and nanoclays, e.g., MMT, Laponite, HNT, and SEP [24, 29-36, 59].

Among these inorganic materials, addition of nanoclay inside polymer matrix can overcome the limitations regarding sensitivity to relative humidity and thermo-mechanical resistance at high temperature. Nanoclay with hygroscopic characteristics incorporated in polymeric phase can prevent dehydration allowing composite membrane to conduct protons at low relative humidity [33, 37-41]. Too much humidification can cause flooding of membranes, thereby increase in diffusion over-potential due to insufficient oxygen and hydrogen supply [35]. Mechanical property also exhibits positive deviation by introduction of nanoclay, which is due to homogeneous dispersion, exfoliation of nanoclay, or good interfacial compatibility between the polymer and nanoclay inside the composite membrane [39, 41-44]. In particular, fibrous shaped sepiolite (SEP) and halloysite (HNT) can provide additional increase in tensile strength of the membrane, resulting from chain packing [38, 39, 42, 46, 47]. Addition of nanoclay also can improve mechanical stability, resulting in reduced occurrence of hydrogen (H_2) crossover at high temperature [99]. That is, cracks and pinholes are likely to occur in membranes comprising low mechanical strength. Accordingly, reactant crossover decreases the performance, the efficiency as well as the durability of PEMFC. Peighambardoust, S. Jamai et al, moreover, reported that polymer/nanoclay composite membrane is cost competitive compared to polymer composite membranes containing zeolite and inorganic oxide materials [45, 59].

Since 2003, nanoclays added in polymer membranes have been studied and first appeared in international journals. In the early days, Montmorillonite (MMT), a natural layered magnesium and aluminum silicate, was introduced by GKSS research center [100]. Research on MMT has been the oldest and most studied. Since then, Laponite, a synthetic layered clay, was used as an additive first by O-Ok Park's research group [34]. Sepiolite (SEP), a microfibrous natural magnesium silicate, has been reported since 2007 by Compan's group [49]. Even more recently, halloysite nanotubes (HNT), a natural tubular aluminum silicate, has been studied since 2013 by Cavallaro's group [30]. Currently, research on SEP and HNT as a filler is increasing as much as Laponite. When we calculate the proportion of research papers according to nanoclay type, HNT and SEP accounts for 8% and 9% of the total, respectively, while Laponite and MMT represent 10% and 72%, respectively, between 2003 and 2018.

Silicate nanoclays can be classified into fibrous shape (so called needle-like) or layered shape depending on the morphology. Detailed information regarding different kinds of nanoclays is described in section 1.2.1 and 1.2.2.

1.2.1. Layered silicate-shaped nanoclay

Two types of layered nanoclays, i.e., Montmorillonite (MMT) and Laponite, have been used as fillers in polymer for PEMFC application.

MMT, multi-layered alumino-magnesio-silicate, is substantially incorporated into composite membrane as nanoclay filler. This belongs to smectite group of 2:1 layered silicate family, and it consists of negatively charged

silica sheets. MMT has 2D plate-like layers, which are coupled with weak interatomic forces. This generally has chemical formula given by $(Al_{2-y}Mg_y)(Si_{4-x}Al_x)O_{10}(OH)_2,M_y^+$, as shown in Fig. 1.1. Where, M_y^+ and y represents the exchangeable interlayer cations (e.g., Na^+, K^+, Mg^{2+}, Ca^{2+}) and the substitution degree, respectively. Aforementioned cations balance the negative charge originated from the isomorphous substitution of Fe^{2+} and Mg^{2+} for Al^{3+} in the octahedral sheet, and Al^{3+} for Si^{4+} in the tetrahedral sheet. In addition to this, the cations help to absorb water molecules in interlayer [95, 101]. Moreover, MMT has been added into various polymer dispersions in order to improve performance of the composite membrane [102]. Strength of interfacial interactions between polymer and layered nanoclay (e.g., Laponite, MMT) can lead to three kinds of different polymer-layered nanoclay composites. That is, the dispersion state of polymer/multi-layered nanoclay could be typically classified as follows [41, 44]:

- No chain penetration (microcomposite): polymers don't penetrate the silicate layers, and hence formation of conventional phase separated composite as shown in Fig. 1.2a.
- Chain intercalation: polymer chains are intercalated into silicate layers as can be seen in Fig. 1.2b. Layered stacking leads to well-ordered multilayers with alternating polymer/silicate layers.
- Nanoclay exfoliation (nanocomposite): individual layers of nanoclay lose the layered stacking, thereby the silicate layers are exfoliated and homogeneously distributed with polymer chains as shown in Fig. 1.2c.

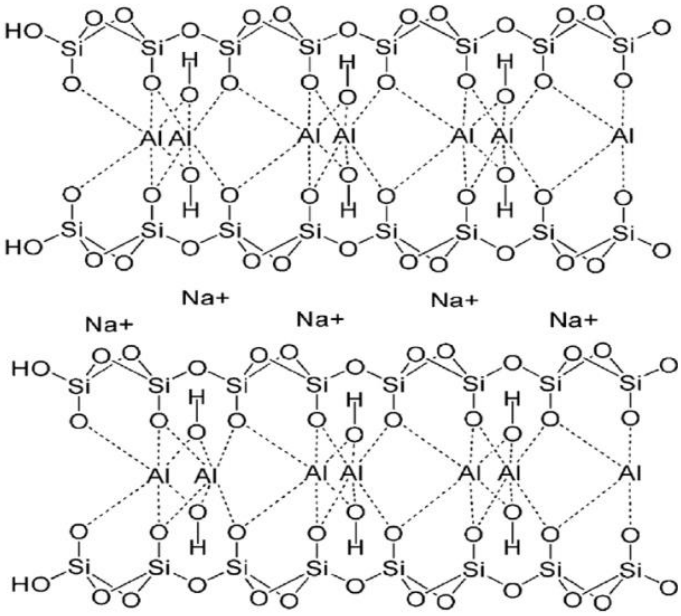

Fig. 1.1. Structure of unmodified montmorillonite nanoclay (trade name: Cloisite Na^+) [86]. Copyright 2015, Reproduced with permission from Elsevier Ltd.

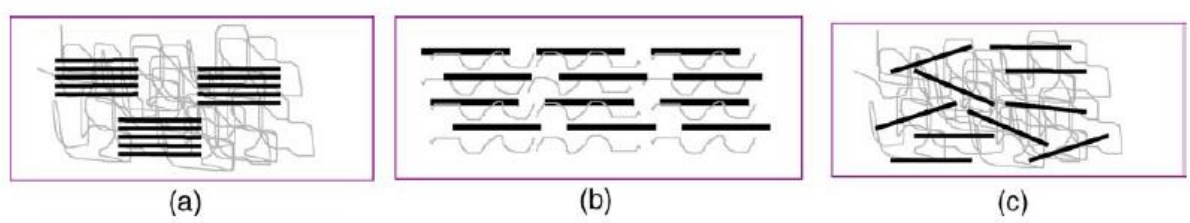

Fig. 1.2. Typical dispersion state of polymer/layered nanoclay composites: (a) no chain penetration (i.e., microcomposite), (b) chain intercalation, and (c) nanoclay exfoliation (i.e., nanocomposite) [44]. Copyright 2006, Reproduced with permission from Elsevier Ltd.

Laponite is the layered silicate often used for nanoclay-based polymer composite membrane in PEMFC application. In terms of structure and composition, this resembles hectorite clay with chemical formula of $Na_{0.3}(Mg,Li)_3Si_4O_{10}(OH)_2$. More specifically, Laponite is a type of commercially synthesized hectorite and it has chemical composition of $Na_{0.7}^{+}[(Si_8Mg_{5.5}Li_{0.3})O_{20}(OH)_4]^{-0.7}$ as shown in Fig. 1.3. Laponite is relatively small in particle size which has thickness of about 1 nm and diameter of 25-30 nm. The basic unit consists of layered hydrous magnesium silicate platelets. The unit cell is composed of six octahedral sheets coordinated with Mg^{2+} ions, which are sandwiched between two layers made of four tetrahedral sheets coordinated with Si^{4+} ions. Twenty oxide ions and four hydroxyl groups (-OH) forms positive charge, and anions are formed by isomorphic substitution of Mg^{2+} and Li^{+} ions on the layers. Laponite has the delaminated structure and sodium hydrate is exchangeable in the platelets to balance the surface with negative charge. Incorporation of Laponite in composite membrane helps to augment in mechanical characteristic, as well have hygroscopic charges at high temperature and low relative humidity conditions during performance [33, 37, 103]. Based on strength of interfacial interaction, Laponite also shows three types of dispersion state between polymer matrix and layered nanoclay composites as aforementioned [44].

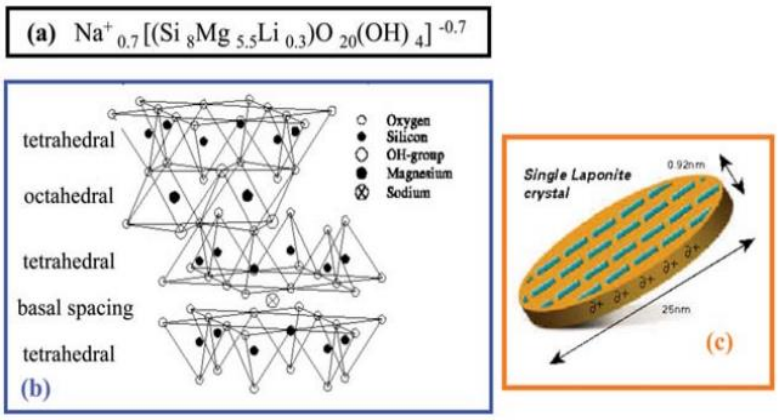

Fig. 1.3. Images on (a) Laponite chemical formula, (b) Laponite structure, and (c) single Laponite crystal [104]. Copyright 2011, Reproduced with permission from Royal Society of Chemistry.

1.2.2. Fibrous shaped nanoclay

SEP has fibrous shapes, and shows a tunnel formed by various blocks, thereby these fibers are parallel to each other. This has porous structure similar to palygorskite and the hydrated magnesium silicate is based on SiO_4 tetrahedra layers with half-unit cell formula of $Mg_8Si_{12}O_{30}(OH)_4 \cdot 12H_2O$ as shown in Fig. 1.4. These layers are interconnected with the MgO_6 octahedron, which constitutes a nano-channels with a cross-sectional area of 3.5 × 10.6 $Å^2$ [39, 105, 106]. SEP, used as the filler in PEM, has been selected to enhance the performance of PFSA. This is because high hygroscopic property of SEP helps composite membrane to have improved mechanical strength and proton conduction. On the other hand, if sepiolite is not blended with ionomer, dehydration of the membrane becomes easier., which lowers mechanical strength, which tends to cause cracking of the membranes. [38, 39]. In addition to this, fibrous shaped SEP can be dispersed easy due to lower specific surface area compared with layered nanoclay such as MMT, and hence relatively small contact surface and reduced aggregation results in mechanical reinforcement of composite membrane [107]. Recently, SEP-based polymer composite membrane has been prepared, and characterized using MEA under condition of high temperature and low relative humidity [31, 32, 49, 108].

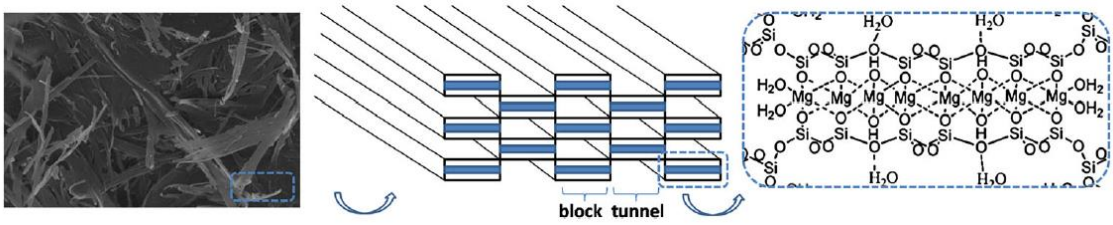

Fig. 1.4. Schematic diagram concerning structure of sepiolite nanofiber [106]. Copyright 2015, Reproduced with permission from Wiley.

HNT has also fibrous shape (so called nanotube shape), and this is a clay mineral of two-layered aluminosilicate type which is composed of unitary cell with $Al_2Si_2O_5(OH)_4 \cdot 2H_2O$ molecular formula as can be seen in Fig. 1.5. HNT is tubular with a meso/macroscopic superstructure, which is formed by wrapping of the clay layer under favorable geological conditions. This lapping process is caused by mismatch in the periodicity between the oxygen-shared tetrahedral SiO_4 sheets and the adjacent octahedral AlO_6 sheet (1:1 layer). The external and inner diameters of HNT are 30 to 50 nm and 1 to 30 nm, respectively. The external surface consists of siloxane groups (Si-O-Si), but the inner surface is composed of gibbsite-like array of aluminol groups (Al-OH). HNT with sufficient Si-OH and Al-OH groups has hydrophilicity and facile functionalization/modification ability, specifically inside and outside of cylindrical surface. Also, weak van der Waals attraction between HNTs makes the dispersion in polymeric phase easy. Well-dispersed HNT within composite membrane determines thermal stability and mechanical property because effect of nanotube shape on chain packing increases the mechanical resistance [30, 40, 42, 47, 109, 110].

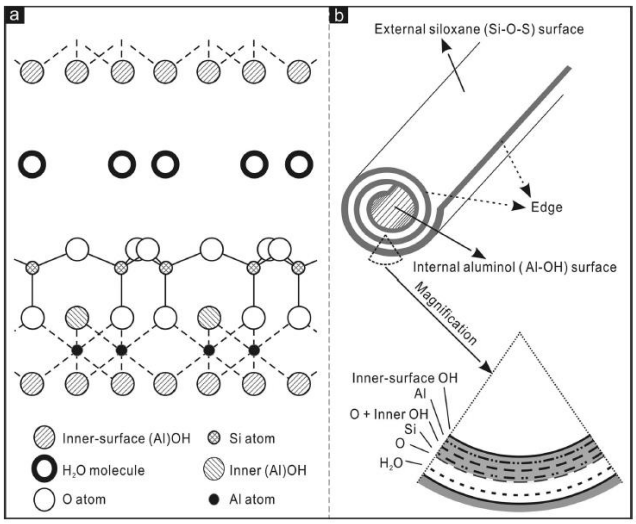

Fig. 1.5. Schematic representation regarding (a) crystalline structure and (b) structure of halloysite nanotube [109]. Copyright 2008, Reproduced with permission from American Chemical Society.

1.2.3. Functionalized nanoclay

As above-mentioned, pristine nanoclays can be incorporated inside polymeric phase in order to improve characteristics of proton exchange membranes. Nevertheless, this method still has limitations regarding the restricted temperature and sensitive relative humidity resulting in reduced proton conductivity during operation. This result is due to aggregated nanoclay inside polymer matrix, and hence dispersion of nanoclay is an important aspect for formation of homogeneous membranes. Controlling dispersion state of nanoclay within polymeric phase has been a key issue for numerous researchers, but the achievement is difficult as relationship between polymer and inorganic filler shows limited compatibility caused by poor affinity [111, 112]. PFSA materials have hydrophobicity and hydrophilicity respectively originated from PTFE-backbone and acid side chains. This is influencing the specific organization of the ionomer as well as the dispersion state of nanoclays during membrane formation, depending on the hydrophilic - hydrophobic balance. However, if fibrous and layered nanoclays can be functionalized, the modified nanoclays ultimately can help composite membranes to have improved homogeneous characteristic. For example, fluorinated nanoclays improve the compatibility by controlling hydrophilic – hydrophobic balance between polymer and nanoclay, thereby the resulting composite membrane has improved hydrophilic/hygroscopic, and mechanical characteristics. Accordingly, an attempt to incorporate the modified nanoclays into membranes ultimately achieved the enhancement of proton conductivity. Various nanoclays have been functionalized by introduction of monomers upon the surface. Usually, physical adsorption and grafting methods were used to modify the nanoclay surface [113-116]. MMT, Laponite, HNT, and SEP have been functionalized into sulfonated, perfluorosulfonated, fluorinated or amininated nanoclays. In particular, MMT modified with quaternary ammonium salt, named Cloisite, were developed as commercially available nanoclay. For example, there are Cloisite 10A, Cloisite 15A, Cloisite 20A, Cloisite 30B and Cloisite 93A manufactured by Southern Clay Products Inc. Since 2005, Cloisite series have been added into the polymer membrane as modified MMT. The modification not only has improved the characteristics of MMT as described in Table 1.3, but also increased hydrophobic surface and interaction with polymer [117].

Table 1.3. Properties of Cloisite Na^+, Cloisite 10A, Cloisite 15A, Cloisite 20A, Cloisite 30B, Cloisite 93A manufactured by Southern Clay Products Inc.

Trade name	Cloisite Na^+	Cloisite 10A	Cloisite 15A	Cloisite 20A	Cloisite 30B	Cloisite 93A
Organic modifier (chemical structure of surfactant)	None	Dimethyl, benzyl, hydrogenated tallow, quaternary ammonium	Dimethyl, dihydrogenatedtallow, quaternary ammonium	Dimethyl, dihydrogenatedtallow, quaternary ammonium	Methyl, tallow, bis-2-hydroxyethyl, quaternary ammonium	Methyl, dihydrogenated tallow ammonium
Modifier concentration (meq/100 g·clay)	None	125	125	95	90	95
Cation exchange capacity (meq/g)	0.926	-	1.25	0.95	0.90	-
Moisture (%)	< 2	< 2	< 2	< 2	< 2	≤ 2
Weight loss on ignition (%)	7	39	43	38	30	40
Specific gravity (g/cc)	2.86	1.90	1.66	1.77	1.98	1.88
d_{001} (Å)	11.7	19.2	31.5	24.2	18.5	23.6
References	[118, 119]	[118, 119]	[118, 119]	[118, 119]	[118, 119]	[119]

2. Preparation of composite membrane based on polymer and nanoclay

Homogeneous dispersion of nanoclay inside polymer phase is a key issue for good performance. Hence, numerous research engineers have functionalized nanoclay at first, and then added it into polymer dispersion before composite membranes are prepared using various methods. This section summarizes preparation and modification of composite membranes. Tables A1 and 1.3-1.5 provide the chemical composition of the polymer, nanoclay, and solvent/non-solvent for the casting dispersion made to prepare the fuel cell membranes. The latest published works was introduced in order, but they are organized according to the type of nanoclays. HNT modification as filler was most recently published since 2013, followed by SEP functionalization in 2007. Among the additives, MMT and Laponite are the longest studied materials ever published since 2003.

(a) Membrane preparation: Composite membranes containing various nanoclays are prepared following different basic processes: casting – evaporation, electric field process [100], dual electrospinning [31], IR ramp [91], doctor blade method [120-122], bulk molding compound (BMC) process [94] and hot pressing process [123]. Most of casting dispersions are prepared using casting-evaporation process. Polymer was dissolved in the casting dispersion containing solvent and nonsolvent. Nanoclay of casting dispersion was usually distributed using ultrasound, after which composite membranes are cast and evaporated at high temperature. In another method, specialized experimental device was used for membrane preparation under electric field to heat the mold [100]. For dual electrospinning, an electrical charge is used to draw the submicro fibers. Submicro fibers are drawn from

a polymer solution made to the appropriate concentration. In the dual electrospinning process, two polymer solutions are simultaneously electrospun. The membrane made in this way has a porous structure [31]. IR ramp is used to evaporate solvent or nonsolvent blended in the casting dispersion [91]. For doctor blade, the thickness of electrolyte membranes can be manually adjusted using this process. Therefore, the desired thickness can be obtained more easily than casting – evaporation. Bulk molding compound (BMC) is a process to blend a thermoset plastic resins. Various materials (e.g., polymers, thickening agents and inorganic fillers) are used for injection molding compound. BMC makes the end-use application with good mechanical and thermal properties, and low shrink. The characteristics of the electrolyte membrane produced using the BMC process depend on the process time and temperature [94]. Hot pressing is used to make the electrolyte membrane as well as the anode and cathode as shown in Fig. 1.6. Hot pressing is used for membrane preparation, but mainly for the preparation of MEAs. This process can improve performance of the fuel cell by leading to good interface between the electrodes and the electrolyte membrane. The physicochemical properties of membranes prepared via hot pressing process are affected by various parameters, e.g., temperature, pressure, time, and casting solution loading. In particular, there is a benefit of reducing ohmic resistance to gas diffusion electrodes (GDE) [124-126]

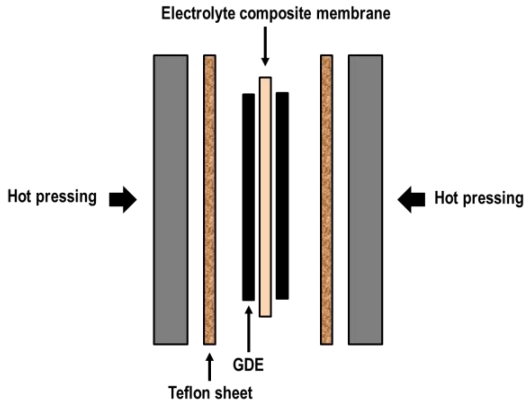

Fig. 1.6. Appearance example of membrane electrode assembly (MEA) prepared using hot pressing process.

(b) Nanoclay modification: The main approaches to modify nanoclay are physical adsorption and chemical grafting of functionalized polymer to nanoclay surface. More specifically, physical adsorptionis controlled by thermodynamic criteria. This modification improves physicochemical characteristics of surface, whereas this can have weak force between adsorbed molecules and nanoclay. In terms of chemical grafting, they are one-step grafting and two-step grafting of functional polymer group. One-step grafting method is to condense the functional polymer with reactive group of a solid substrate as shown in Fig. 1.7a. This method does not provide high density of polymer brushes on nanoclay surface. This is because diffusion of the following chains to the surface for further attachments is hindered by chemisorption of the first fraction of chains. However, two-step grafting was considered to give higher density compared with one-step grafting. Monolayer of polymerizable molecule (macromonomer) or initiator (macroinitiator) is covalently bound to nanoclay (see Fig. 1.7b). After activation the chains grow from the interface then the only limit to propagation is the diffusion of monomers to the active species. The macromonomers used for nanoclay modification contain carbon-carbon double bond and reactive groups, e.g., silane compounds. Macroinitiators are the other class of reactive groups which initiate further chain polymerizations such as RP, AP, ROP, SFRP and ATRP [42, 127, 128]. Between 2003 and 2018, Laponite has not

only been sulfonated, but also MMT has been usually modified by synthetic process such as sulfonation, sulfofluorination and aminization. HNT and SEP used for membrane additive have been sulfonated, fluorinated and perfluorosulfonated.

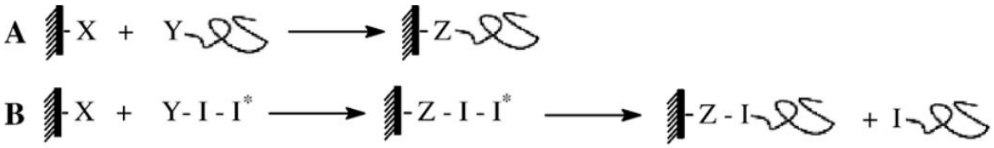

Fig. 1.7. Grafting reaction of (a) one-step and (b) two-step methods [42]. Copyright 2007, Reproduced with permission from Elsevier Ltd.

(c) Polymer modification: In order to obtain proton conductive polymer used for nanoclay-incorporated composite membranes, the polymers were functionalized with sulfonic acid and perfluorosulfonic acid groups. Among various ionomers, Nafion and SPEEK were mainly used for preparation of composite membranes and account for approximately 42.1% and 15.0%, respectively (see Tables A1, 1.3, 1.4 and1.5). In general, SPEEK was obtained by sulfonation. More specifically, PEEK was dissolved in highly concentrated sulfonic acid solution, and then SPEEK precipitated by stirring was washed with DI water until about pH 7. Following this, SPEEK was dehydrated under vacuum [34, 47, 68]. Nafion, perfluorosulfonate ionomer, was manufactured DuPont and Ion Power Inc. and most of them were used for membrane preparation without modification [39, 129]. Until now, however, 3M^{TM}, Hyflon®, Flemion®, Aciplex®, and Fumion® have not been used as ionomers for nanoclay-based composite membranes.

3. Effect of nanoclay additives on composite membrane

In section 1.1, the properties of pristine polymer membrane (no additives) were already introduced. Briefly, pure polymer membranes used as a reference classify into PFSA membrane and hydrocarbon membrane. Nafion, PFSA ionomer, allows membranes to have good mechanical stability and hydrophilicity [8, 9]. However, pristine PFSA membrane has a limitation of proton conductivity above 90℃. In terms of hydrocarbon-based pristine membranes, PEEK and PPO membranes are characterized by good mechanical strength and thermal stability, but exhibit low proton conductivity [34, 81]. PEEK membranes are sulfonated to enhance proton conductivity [68, 69]. PVOH membranes have the disadvantage of low thermal property and poor proton conductivity [71-74]. The PBI membrane has good mechanical property and thermal stability, but it has low proton conductivity below 100℃ and therefore requires high operating temperature of above 160℃ [76-79].

This section summarizes the effects of MMT, Laponite, SEP and HNT additives to improve water uptake, thermal stability (chemical degradation), mechanical resistance (including dispersion state of additives), and proton conductivity. These can be a parameter to understand performance of polymer/nanoclay composite membrane. Typical characterization methods are introduced in section 3.1, and physicochemical properties of the unmodified nanoclays- and modified nanoclays-blended composite membranes are described from section 3.2 to 3.5.

3.1. Analysis method of electrolyte membrane used for PEMFC

(a) Water uptake: Water uptake value of membrane is important because the amount of water absorbed on the membrane affects the microstructure (i.e., clusters and channel size) and is ultimately related to proton conductivity [130]. Incorporation of nanoclay to composite membrane delays dehydration with hygroscopic property, and accordingly composite membrane can perform under condition of low relative humidity [37, 38]. Occasionally, water storage capacity and ion channels are reduced, resulting in decreased water uptake of the composite membrane. The water uptake is measured by weight difference of wet and dried membranes. Water uptake of the prepared membranes is calculated by the following equation:

$$W_{ut}\ (\%) = \frac{W_w - W_d}{W_d} \times 100 \qquad (1)$$

Where W_w and W_d are weight of the wet and dried membranes, respectively.

(b) Mechanical stability: Mechanical resistance of electrolyte membrane is also necessary for high durability. High mechanical property requires 1) complete dispersion of nanoclay, 2) nanoclay exfoliation (for MMT and Laponite®) or 3) good interfacial compatibility between polymer and functionalized nanoclay within composite membrane [39, 41, 42, 44, 131]. Mechanical stability is generally evaluated with tensile strength, Young's modulus and elongation measured at room temperature and 50% RH. Tensile strength is the maximum load that a material can withstand when pulled to cut, divided by the cross-sectional area of the material, and the result is expressed in megapascals (MPa). Elongation is percentage value (%) obtained by dividing the elongated length at the moment of rupture by the initial length of the membrane. Young's modulus, known as elastic modulus, is the degree to which the membrane stretches and deforms when the membrane is stretched from both sides, and the result is expressed in gigapascals (GPa).

Also, membrane tends to swell, leading to mechanical constraints in the MEA stack in the presence of hot water [39], and hence swelling ratio of membrane samples is measured as the percentage of thickness and area difference and then is calculated based on the following equation [38, 40]:

$$S_{th}(\%) = \frac{Th_{\mathrm{rt}} - Th_{\mathrm{bt}}}{Th_{bt}} \times 100 \qquad (2)$$

Where Th_{rt} and Th_{bt} are thickness of the membranes at room and boiling temperatures, respectively.

$$\mathrm{S}_a(\%) = \frac{A_{wet} - A_{dry}}{A_{dry}} \times 100 \qquad (3)$$

Where A_{wet} and A_{dry} represent area of dried and hydrated membranes, respectively.

PEM exhibits fast proton transport under condition of high temperature thereby better performance, and hence thermal stability of membrane is necessary during fuel cell performance [42]. High thermal stability of the membrane is obtained from 1) homogenous distribution of nanoclay without aggregations and voids, 2) exfoliated nanoclay or 3) fluorinated nanoclay inside composite membrane [38, 39, 49, 93, 129].

(c) Thermal property: In general, thermal property of the membrane is characterized using TGA between 25 and 800℃. Polymer/nanoclay composite reveals three stage weight losses: 1) evaporation of water molecules adsorbed in membrane, 2) pyrolysis of polymer side-chain, and 3) chemical decomposition of polymer backbone

[46]. Electrolyte composite membrane shows the improved thermal stability due to interaction between polymer and additive. Moreover, too much high temperature leads to chemical decomposition of polymeric side-chain (220 – 330℃) and backbone (480 – 800℃) upon the surface of functionalized nanoclay [46, 49, 132].

(d) Proton conductivity: The membrane requires good proton conductivity originated from high mobility of ion carrier. Proton transfer phenomena in ionomeric polymer matrix could be classified into 1) hopping mechanism, i.e., Grotthouss mechanism, and 2) vehicular mechanism as shown in Fig. 1.8a. Hopping mechanism means that protons randomly jump between neighboring protonic species (e.g., H^+, H_3O^+ and NH_4^+) through the H-bond network inside ionomer matrix. Protons are quickly distributed by rotation of the side chains with sulfonate functional groups (see Fig. 1.8a). Secondly, vehicular mechanism represents that carrier ions are diffused through aqueous medium caused by electrochemical difference as shown in Fig. 1.8b. The rate of proton conductivity is based on vehicular diffusion rate and free volume within polymer matrix, and hence nanocomposite membrane composed of polymer and the modified nanoclay can show better performance at high temperature and low relative humidity, compared with the unmodified membrane [133-136]. Moreover, radical attack can lead to increased chemical degradation of membranes through Fenton reaction caused by the oxidation of organic substrates by divalent iron and hydrogen peroxide, and accordingly decomposed membranes "may" display relatively declined proton conductivity, compared with that of pristine membranes. This is because the membrane are too brittle and crumble during analysis [121]. In terms of real Fenton test procedure, divalent iron (Fe^{2+}) is oxidized to trivalent iron (Fe^{3+}) by hydrogen peroxide to form hydroxyl radicals and hydroxide ions in the process. Trivalent iron is reduced to divalent iron by other hydrogen peroxide molecules to form hydroperoxyl radicals and protons. The final effect is the disproportionation of hydrogen peroxide to create two different oxygen-radical species with water ($H^+ + OH^-$) as a by-product. The process of free radical generation in real Fenton test is as follow:

$$Fe^{2+} + H_2O_2 \rightarrow Fe^{3+} + HO\cdot + OH^-$$

$$Fe^{3+} + H_2O_2 \rightarrow Fe^{2+} + HOO\cdot + H^+$$

$$2H_2O_2 \rightarrow HO\cdot + HOO\cdot + H_2O$$

Proton conductivity is calculated with membrane resistance obtained using impedance spectroscopy under condition of various temperature and relative humidity according to the following equation:

$$\sigma = \frac{L}{RA} \qquad (4)$$

Where *L* and *R* represent membrane thickness and membrane resistance, respectively. *A* is surface area of the membrane.

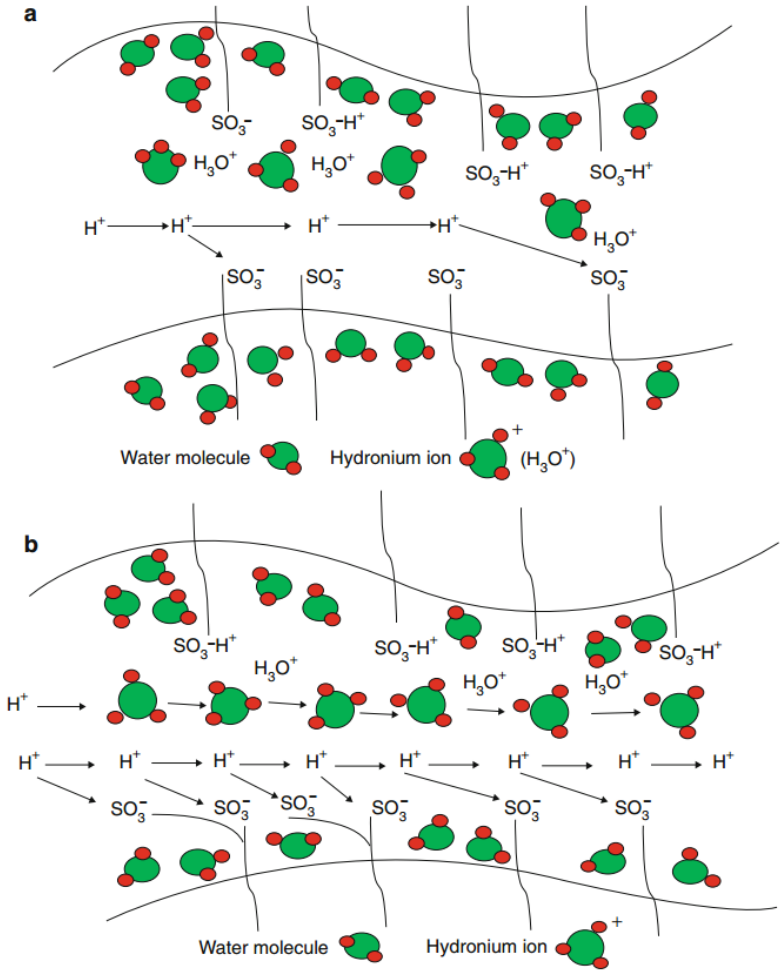

Fig. 1.8. Schematic diagram of a) hopping (i.e., Grotthus) and b) vehicular mechanisms in polymer ionomer matrix of proton exchange membrane [133]. Copyright 2015, Reproduced with permission from Springer.

3.2. Effect of montmorillonite type additive

MMT was used as a filler in two types of polymer matrices: PFSA (e.g., Nafion®) and hydrocarbons (e.g., PVOH, PVOH/PSSA, ABPBI, SPEEK, Cross-linked SPEEK, SPPESK, PBI, PBI/PPA, H_3PO_4-doped PBI, PSU, SPSU, styrene, HEMA, Acrylic acid, CS, CS/PWA, Poly(St-co-NaSS), Poly(HEMA-co-NaSS), Poly(AAc-co-NaSS), PEO, SPAES, SSEBS, SPES, SPPO, GPTMS/EHTES, 6F-PEAA and Vinyl ester). Among the wide range of polymers, MMT series are generally mixed with Nafion or SPEEK to prepare casting dispersion.

Modification of MMTs includes hydroxylation, sulfonation, perfluorosulfonation, aminization and bio-functionalization. M^{x+}-MMT or Cloisite® was also added to prepare casting dispersion of composite membranes. M^{x+} represents Ca^{2+}, K^+, Mg^{2+}, Na^+ and H^+. The above-mentioned modified MMTs were introduced to improve electrolyte membrane properties. Table A1 provides summary data concerning the casting dispersion and proton conductivity of electrolyte composite membranes.

References for above-mentioned polymer materials used to prepare each composite membrane are listed in Table A1 (annex).

3.2.1. M^{x+}-MMT additive

3.2.1.1. Nafion matrix

Nanocomposite membrane composed of Nafion/Ca^{2+}-MMT, Nafion/K^{+}-MMT, Nafion/Mg^{2+}-MMT, Nafion/Na^{+}-MMT, and Nafion/H^{+}-MMT was prepared by casting method, according to paper published by Wu, Xiu-Wen, et al [129]. Karthikeyan, C. S., et al. introduced Nafion-based unmodified MMT composite membrane prepared using the specialized experimental device under electric field to heat the plate for casting temperature control, as shown in Fig. 1.9. 5 - 6 kV of voltage was applied with the simultaneous evaporation of dispersion [100]. Nicotera, et al prepared composite membrane as following order: 1) all solvents, i.e., water and isopropanol, in Nafion dispersion were removed by heating; 2) Nafion was dissolved in DMF or IPA; 3) M^{x+}-MMT was dispersed in Nafion/DMF or Nafion/IPA mixture prior to casting. Here M^{x+} represents Na^{+}, H^{+}, K+, Ca^{2+}, and Mg^{2+}. Afterwards, prepared membranes were treated by HNO_3, H_2O_2, H_2SO_4 and DI water [35]. The proton conductivity of composite membranes is from 0.0360 to 0.0385 S cm^{-1} in the order of Na^{+}-MMT > H^{+}-MMT > K^{+}-MMT > Mg^{2+}-MMT > Ca^{2+}-MMT > Mg^{2+}MMT. The membrane samples were fully hydrated in DI water at 293 K prior to analysis. These results may be because proton transfer channels of composite membranes are partly blocked by the larger groups [129].

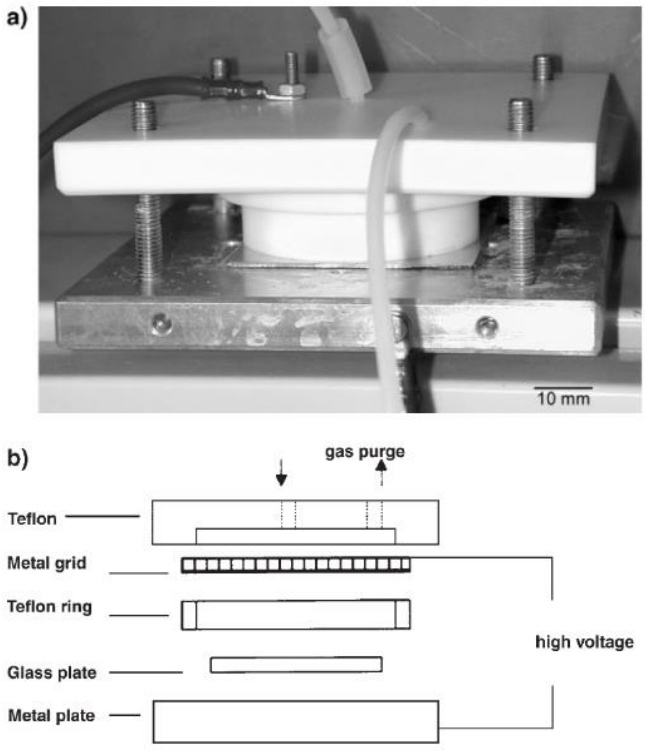

Fig. 1.9. (a) Photo image and (b) scheme of the experimental device for membrane prepared under electric field [100]. Copyright 2003, Reproduced with permission from Wiley.

3.2.1.2. PVOH and sulfonated PVOH matrices

(a) Membrane preparation: Palani, P. Bahavan, et al prepared composite membrane consisting of PVOH and H^+-MMT [137]. Yang, Chun-Chen, and Ying-Jeng Lee reported composite membrane based on PVOH/MMT prepared by casting method. Na^+-MMT was converted into H^+-MMT by treatment using H_2SO_4 [73, 138]. Biopolymer-based nanocomposite membrane containing CS and GPTMS-modified MMT was prepared by Purwanto, Mochammad, et al. In the study, MMT was added into toluene with GPTMS at 110℃ [85].

Sulfonated PVOH/Cloisite Na^+ composite membranes were prepared by Duangkaew, P., and J. Wootthikanokkhan. Sulfonated PVOH was acheived by addition of sulfosuccinic acid in PVOH solution [75].

(b) Thermal property: Yang, Chun-Chen, and Ying-Jeng Lee measured TGA of PVOH/H^+-MMT composite membrane. TGA curve of composite membrane displayed three weight loss regions. More specifically, water within composite membrane was evaporated between 60 and 200℃, and then degradation of side chain of composite membrane was revealed from 350 to 390℃. Afterwards, C-C backbone of composite membrane had cleavage at approximately 435℃ [73, 138]. Pristine Laponite showed decomposition at around 300℃, whereas PWA did not degrade until 900℃. Also, blending of Cloisite Na^+ and PWA into PVOH matrix improved thermal resistance of composite membrane [44].

(c) Mechanical stability: Thomassin, et al confirmed that blending PWA with PVOH has no influence on mechanical strength [44]. Addition of Cloisite Na^+ led to 9 times increased elongation of composite membranes compared with that of sulfonated PVOH membrane due to the reduced crystallinity of the polymer with silicate [75].

(d) proton conductivity: Proton conductivity of PVOH/H^+-MMT composite membrane showed the highest values when 10% of H^+ MMT loading content was blended in PVOH solution, but no additive led to about 0.004 S cm^{-1} higher than addition of 20% H^+ MMT in PVOH matrix [73, 138]. Moreover, incorporation of Cloisite Na^+ and PWA into PVOH matrix decreased proton conductivity with reduced water uptake as shown in Fig. 1.10 [44].

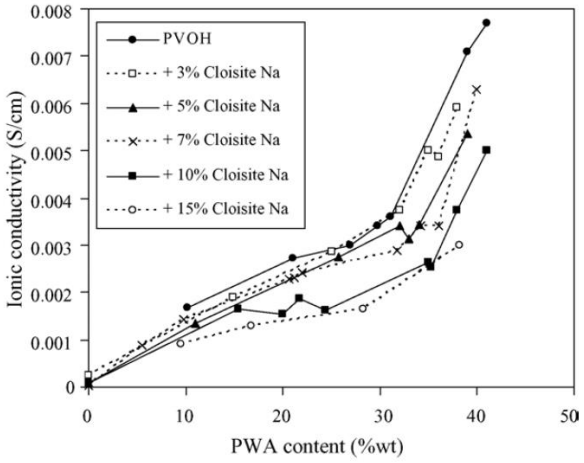

Fig. 1.10. Proton conductivity of pristine PVOH, PVOH/Cloisite Na^+ and PVOH/Cloisite Na^+/phosphotungstic acid membranes [44]. Copyright 2006, Reproduced with permission from Elsevier Ltd.

3.2.1.3. PBI and ABPBI matrix

(a) Membrane preparation: Ublekov et al reported PBI/PA membrane blended with H^+-MMT, which made from Cloisite Na^+ with HCl [80]. ABPBI/Cloisite Na^+/ionic liquid dispersions were used to prepare composite membranes according to literature published by Bao, Xujin, Fan Zhang, and Qingting Liu. ABPBI, PBI family, has high thermal and mechanical stability. In the study, ionic liquids composed of liquid state salts include [HMIM][Cl] and [TMG][BF_4] which were synthesized as can be seen in Fig. 1.11. More specifically, [HMIM][Cl] was modified by mixing 1-Methylimidazole and 1-chlorohexane; and [TMG][BF_4] was synthesized with 1,1,3,3-Tetramethylguanidine and fluoroboric acid [139]. In the study, ABPBI was obtained from mixture containing P_2O_5 and methanesulfonic acid by polymerization at 150℃ as shown in Fig. 1.12 [140].

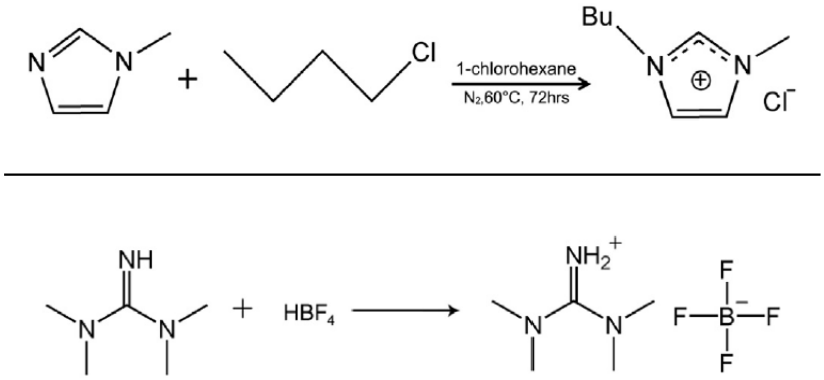

Fig. 1.11. Synthetic illustration of (up) [HMIM][Cl] and (down) [TMG][BF_4] ionic liquids [139]. Copyright 2015, Reproduced with permission from Elsevier Ltd.

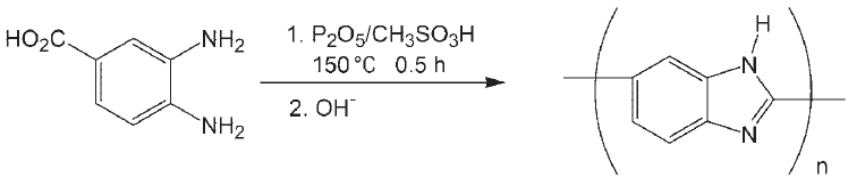

Fig. 1.12. Polymerization process of ABPBI in mixture containing P_2O_5 and methanesulfonic acid [140]. Copyright 2004, Reproduced with permission from Wiley.

(b) Mechanical stability: The ultimate tensile strength of pristine ABPBI membrane showed 46.4 ± 16.4 MPa, whereas composite membranes displayed improved value with increasing the nanoclay content, and finally reached to maximum 88.8 ± 25.3 MPa at 3 wt% loading [139].

(c) Proton conductivity: The doping level of the ionic liquid, caused by the good dispersion of the nanoclay, was grown, leading to an increased proton conductivity of the composite membranes. More specifically, 3 wt% ABPBI/Cloisite Na^+ composite membrane with 1.32 [HMIM][Cl] doping level displayed 4.0×10^{-2} S/cm of proton conductivity at 220°C. 3 wt% ABPBI/Cloisite Na^+ composite membrane with 1.37 [TMG][BF_4] doping level led to the highest proton conductivity, which is 9.6×10^{-3} S/cm at 220°C [139].

3.2.1.4. SEBS and sulfonated SEBS matrixes

(a) Membrane preparation: Ganguly, Anirban, and Anil K. Bhowmick. synthesized SEBS with acetyl sulfate to form SSEBS as shown in Fig. 1.13, and then prepared SSESB/Na^+-MMT nanocomposite membrane [93].

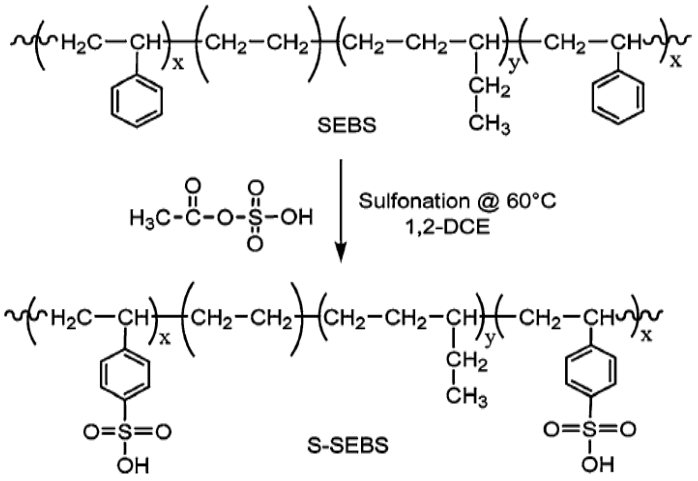

Fig. 1.13. Sulfonation process of SSEBS, which was reacted with acetyl sulfate and SEBS [93] . Copyright 2008, Reproduced with permission from Springer.

(b) Mecanical property: As shown in Fig. 1.14, blending of MMT in pure SEBS solution formed composite membrane with thick stack, whereas incorporating MMT into sulfonated SEBS matrix allowed composite membrane to form intercalation and exfoliation. Exfoliation of sulfonated SEBS/MMT composite membrane in turn led to enhancement of tensile strength (41%) compared with pure SEBS/MMT composite membrane which shows distorted morphology [93].

(c) Proton conductivity: H^+ ions hopped inside SSEBS matrix due to H-bonded network between protonated water molecules, and blending of MMT with SSEBS allowed H^+ ion interaction with the acid group and hydrocyl group of nanoclay, thereby controlling the proton transfer [93].

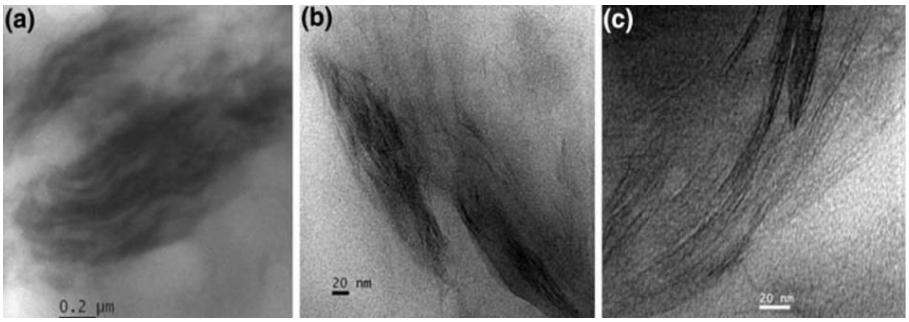

Fig. 1.14. TEM morphology of (a) thick stacks of pure SEBS/MMT (4 wt%) composite membrane, (b) intercalated-exfoliated membrane composed of sulfonated SEBS (3 wt%)/MMT (4 wt%) and (c) exfoliated membrane composed of sulfonated SEBS (6 wt%)/MMT (4 wt%) membranes [93]. Copyright 2007, Reproduced with permission from Springer.

3.2.1.5. Other types of matrix (Styrene, HEMA, Acrylic acid, SPEK, PAA and vinyl)

Kim, Young-Seok et al prepared composite membrane via radiation-induced polymerization (RIP) as shown in Fig. 1.15. To begin with, Na^+-MMT/[BVBI][Cl] was synthesized with [BVBI][Cl] and Na^+-MMT by cation-exchange method, after which NaSS was added into St/Na^+-MMT/[BVBI][Cl], AAc/Na^+-MMT/[BVBI][Cl] and HEMA/Na^+-MMT/[BVBI][Cl] dispersions to obtain sulfonate group (–SO_3Na). Following this, the nanocomposite membranes were prepared by casting method after RIP, which is polymerization reaction that occurs by irradiating the ionized radiation onto the unit. RIP has benefit to prepare composite membrane composed of vinyl-based polymer and nanoclay because radical-initiator is unnecessary.

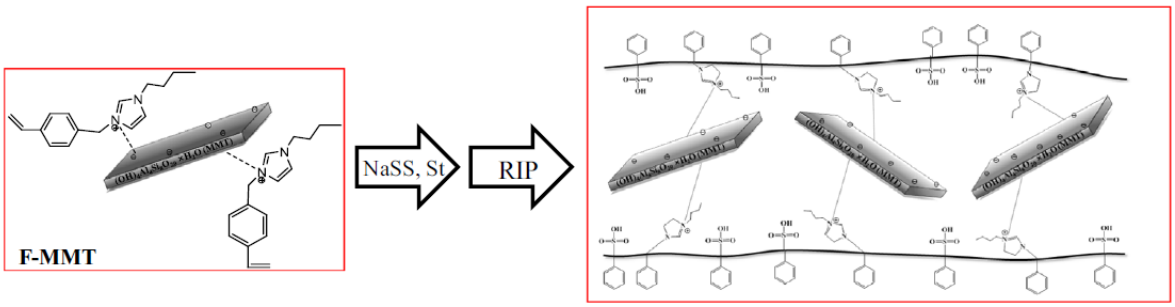

Fig. 1.15. Schematic illustration of vinyl group functionalized polymer/Na^+-MMT/[BVBI][Cl] composite membranes prepared by RIP [84]. Copyright 2016, Reproduced with permission from Elsevier Ltd.

Karthikeyan, C. S. and co-workers also prepared SPEK membranes with 10 and 20 wt% pristine MMT [141]. Prasad, M., Smita Mohanty, and Sanjay K. Nayak prepared PEO/Cloisite Na^+/PAA hybrid membrane. PEO/Cloisite Na^+ dispersion was added to PAA aqueous solution to make casting dispersion [89]. Kim, Yoon-Seob, Yun Ok Kang, and Seong-Ho Choi reported a preparation method of three different kinds of vinyl/Cloisite Na^+ composite membrane by casting, as can be seen in Fig. 1.16. St, HEMA, Nass, and AAc were used as polymers for membrane fabrication [142]. Properties of above-mentioned membranes are gathered in the literatures [84, 89, 141, 142].

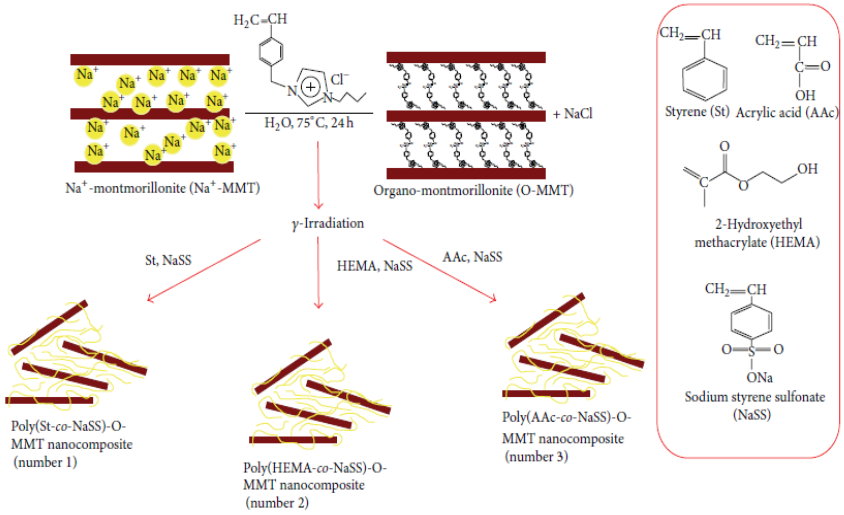

Fig. 1.16. Schematic diagram of three kinds of vinyl polymer/Cloisite Na^+ nanocomposite prepared by radiation-induced polymerization [142]. Copyright 2014, Reproduced with permission from Hindawi.

3.2.2. Sulfonated MMT additive

3.2.2.1. Nafion matrix

(a) Membrane preparation: Lee, Jang-Woo, Yoo, Young-Tai, and Lee, Jae Yeol made Nafion/HSO_3-functionalized MMT composite membranes. Na^+-MMT was converted into MMT sulfonated with H_2SO_4 [143]. Zhang, Limin, et al. reported that Na^+-MMT was converted into H^+-MMT by 1 M H_2SO_4. Following this, MMT was synthesized with dodecylamine via conventional sol-gel intercalation, and accordingly dodecylamin modified MMT was obtained [144]. For Nafion composite membrane preparation, Kim, Youngkwon, et al. functionalized MMT with organic sulfonic acid such as HSO_3-R-modified MMT and HSO_3-RSR-modified MMT as can be seen in Fig. 1.17. To begin with, Na^+-MMT was converted into H^+-MMT. Concerning modification of HSO_3-R-modified MMT, HS-MMT was made by 3-MPTMS, subsequently HSO_3-R-modified MMT was obtained by oxidation of H_2O_2. In addition to this, 3-MPTMS condensed hydroxyl group of H^+-MMT surface, and then the grafted thiol group was reacted with 1,3-PS so as to render HSO_3-RSR-modified MMT with long chain length [145].

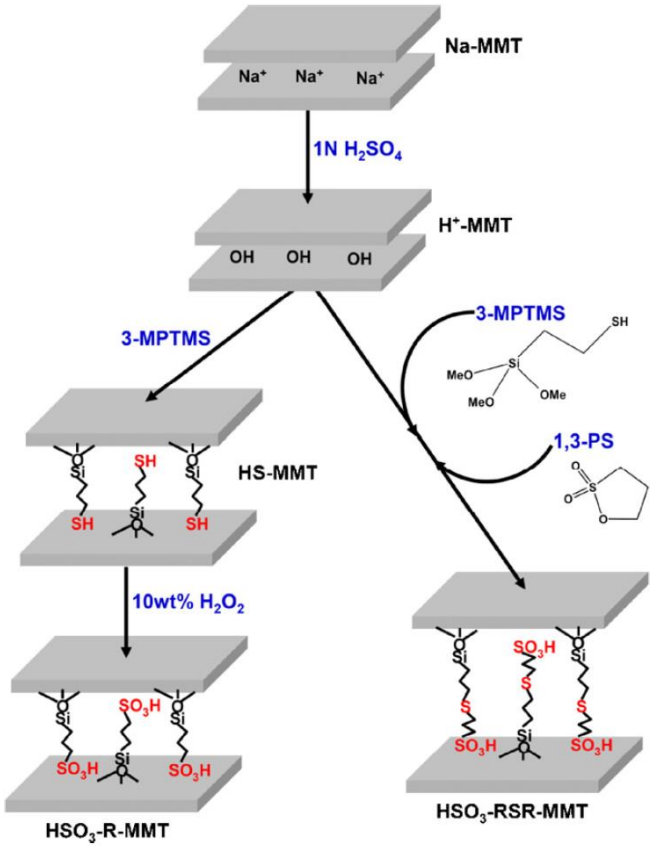

Fig. 1.17. Synthesis process of HSO_3-R-MMT and HSO_3-RSR-MMT [145]. Copyright 2010, Reproduced with permission from Elsevier Ltd.

Thomassin, Jean-Michel, et al. reported three types of different MMTs synthesized with DMOSPA, ACA and BHB as shown in Fig. 1.18. That is, Na^+-MMT and H^+-MMT were modified with ammonium cations, which contain carboxylic acid and sulfonic groups, respectively [102].

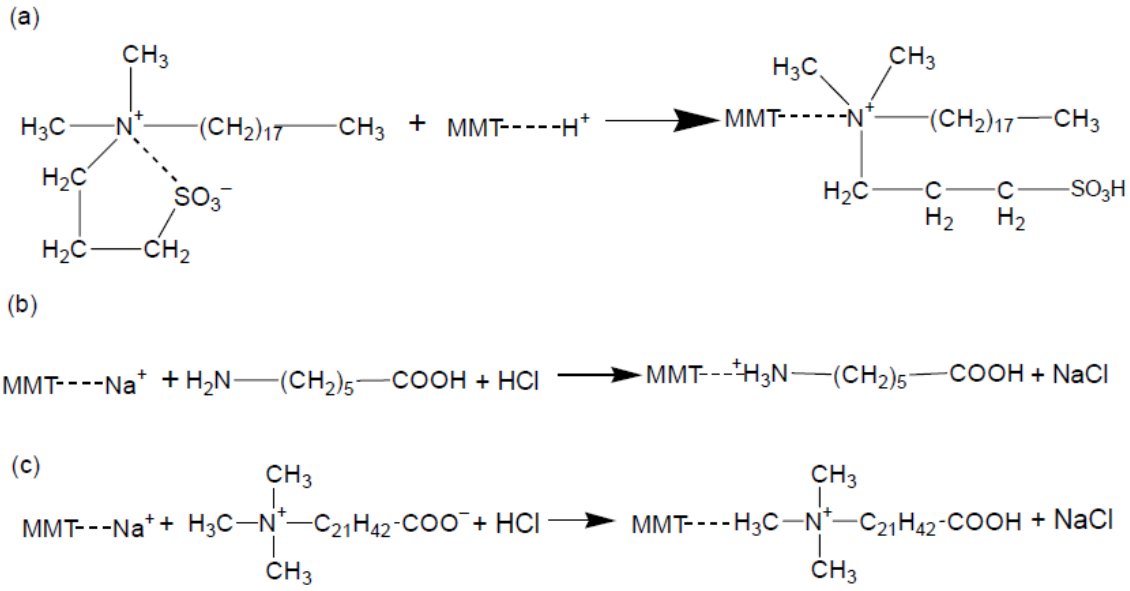

Fig. 1.18. Schematic representation of the ammonium cations synthesized with the cation exchange with MMT: (a) dimethyloctadecyl(3-sulfopropyl) ammonium (hydroxide) (DMOSPA), (b) 6-aminocaproic acid (ACA), and (c) behenyl betaine (BHB) [102]. Copyright 2005, Reproduced with permission from Elsevier Ltd.

Kim, Youngkwon, et al. synthesized different kind of HSO_3-modified MMTs prior to preparation of Nafion/sulfonated MMT composite membranes. To begin with, it was converted Na^+-MMT into H^+-MMT by 1M H_2SO_4 treatment, accordingly sulfonated MMT (i.e., HSO_3-modified MMT) was obtained as shown in Fig. 1.19. That is, different types of sulfonated MMT were prepared by dehydration with 1,4-BS, 1,3-PS and FMES as sulfonic acid precursors [146].

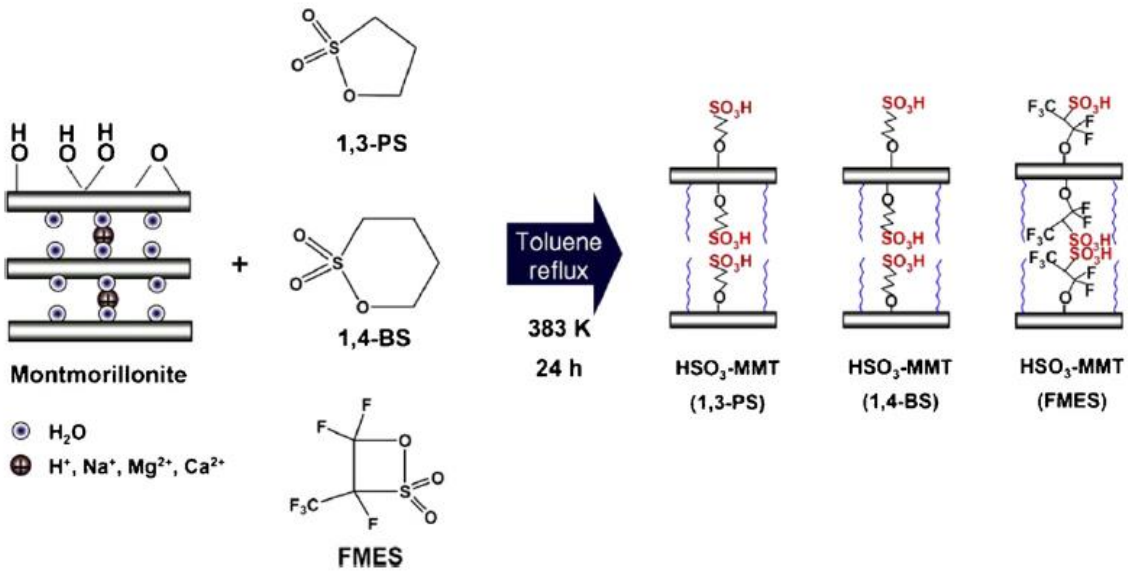

Fig. 1.19. Schematic structure of functionalization procedure for 1,4-BS-modified MMT, 1,3-PS-modified MMT and FMES-modified MMT [146]. Copyright 2006, Reproduced with permission from Elsevier Ltd.

Kim, Tae Kyoung, et al. prepared sulfonated MMT-based Nafion membrane by film coating process using a pilot coating machine, i.e., Inokin 2 roll reverse die coater. In the study, sulfonated MMT was modified from Na^+-MMT via cation exchange with sulfonic acid. DMAc/NMP solution led to dense membrane due to azeotropic vaporization, and also it made reorganization of the sulfonic acids to form ion clusters [147]. Moreover, prior to preparation of Nafion/POPD400-modified MMT composite membranes, POPD400-modified MMT was synthesized with amines, 1,3-propane sultone, and poly(propylene oxide)-backboned diamines as shown in Fig. 1.20 [148].

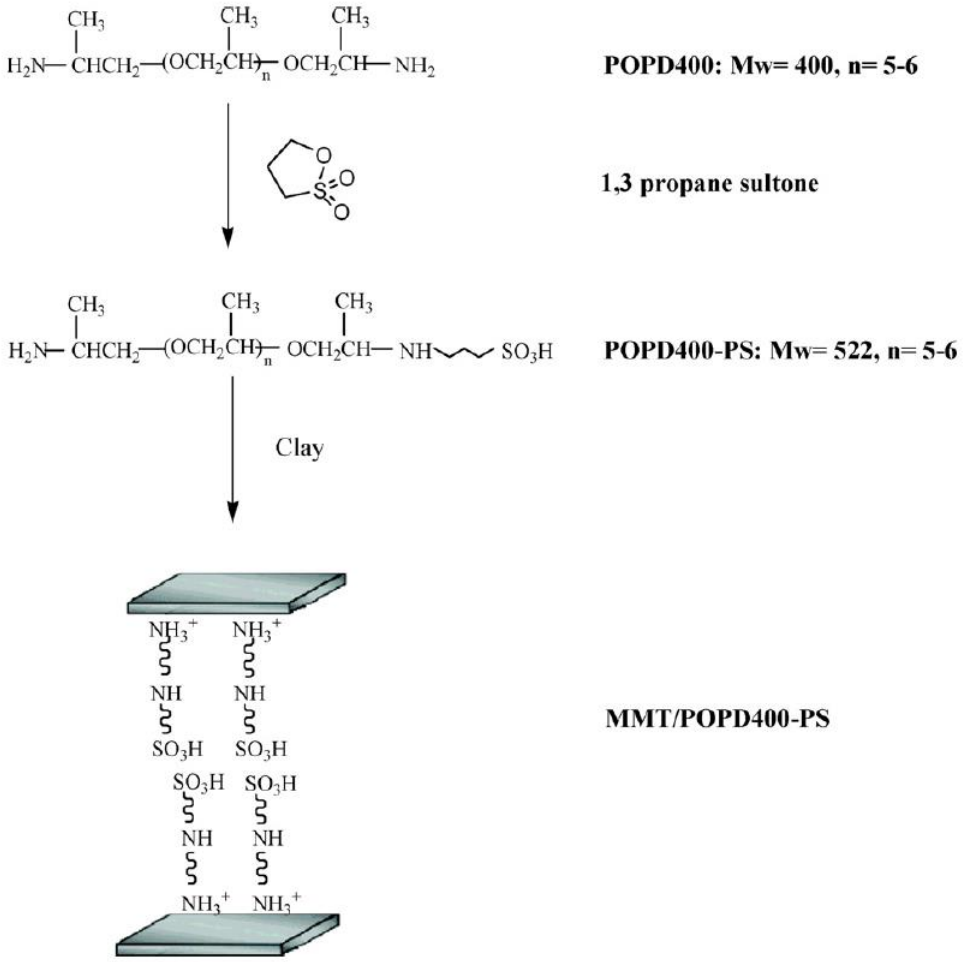

Fig. 1.20. Synthesis process of POPD400 and POPD400-PS [148]. Copyright 2007, Reproduced with permission from Elsevier Ltd.

Xiuchong, He, and his co-workers modified MMT with dodecylamine, which was changed to H^+ form by addition of H_2SO_4, subsequently they introduced perfluorosulfonylfluroride into the interlayer of modified MMT at high pressure and temperature so as to obtain Nafion/dodecylamine-modified MMT composite membrane as shown in Fig. 1.21 [149]. Hasani-Sadrabadi, Mohammad Mahdi, et al. reported that MMT was distributed in water and then it was mixed with AMPS prior to preparation of Nafion composite membrane [150].

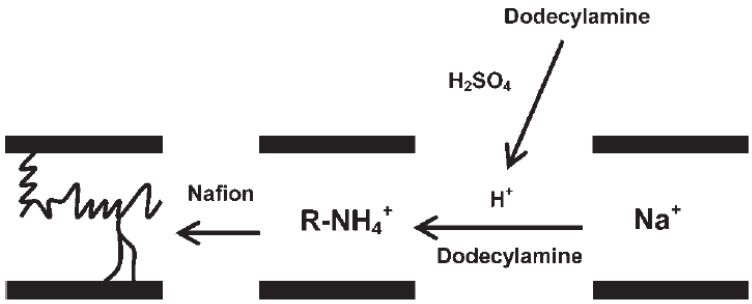

Fig. 1.21. Preparation process of Nafion/dodecylamine-exchanged MMT composite membranes [149]. Copyright 2008, Reproduced with permission from Wiley.

(b) Water uptake, thermal property and mechanical stability: Water uptake values of Nafion/HSO_3-R-modified MMT and Nafion/HSO_3-RSR-modified MMT composite membranes were 17% and 20.1%, respectively. Incorporating HSO_3-RSR-modified MMT, which is large interlayer distance caused by long chain sulfonic acid group, led to the slightly higher water content and better thermal stability (between 420- 550K) compared to pristine Nafion membrane and composite membrane containing HSO_3-R-MMT with shorter chain length [145] . Xiuchong's group reported that the mechanical strength of dodecylamine-exchanged MMT-incorporated Nafion membrane augmented with increasing content and was suitable for operation in fuel cell [149].

(c) Proton conductivity: Blending of 5wt% HSO_3-RSR-modified MMT in Nafion dispersion formed composite membrane with improved proton conductivity ($\leq$ 0.16 S/cm) compared with composite membranes containing HSO_3-R-modified MMT, and Nafion/HSO_3-R-modified MMT composite membrane showed maximum 0.09 S cm^{-1} of proton conductivity value [145]. Also, Nafion/POPD400-PS-modified MMT (6 wt%) composite membrane displayed about 0.115 S cm^{-1} of proton conductivity, which is the improved value compared with Nafion membrane at room temperature [148]. Blending 1 wt% pure Cloisite B30 slightly reduced to 0.090 S/cm in proton conductivity. Incorporating with BHB-modified Cloisite B30 into Nafion phase showed improvement by 0.005 S/cm, but addition of ACA-modified reached to similar proton conductivity (0.098 S/cm) compared to that of pure MMT under 100% relative humidity condition [102]. Blending with 1,4-BS-modified MMT, 1,3-PS-modified MMT or FMES-modified MMT with Nafion showed negative effect on proton conductivity [146]. Xiuchong's group compared the proton conductivity of composite membranes with that of commercially available Nafion 211 while changing the content of dodecylamine-exchanged MMTs (1, 3, 5, 8 or 10 wt%). Filling 5 wt% additive into Nafion matrix showed higher values (0.7 S/cm without external humidification at 80℃) than the other contents, which is even better than Nafion 211 [149].

3.2.2.2. SPEEK matrix

(a) Membrane preparation: Gosalawit, Rapee, et al. prepared sulfonated MMT/4-sulfophthalic acid-modified MMT composite membrane. MMT with silane coupling agent was modified with 4-sulfophthalic acid, in order to obtain sulfonated MMT as shown in Fig. 1.22 [151]. Mohtar, S. S., Ahmad Fauzi Ismail, and T. Matsuura impregnated STA onto pristine MMT prior to preparation of SPEEK/STA-modified MMT composite membrane [152]. Doğan, Hacer, et al modified MMT with DMDOC, sulfanilic acid, and AMPS before preparation of SPEEK

composite membrane [153]. Samberan, Mehrab Fallahi, et al prepared nanocomposite membrane based on SPEEK/MMT modified with AMPS. Na^+-MMT was dispersed with AMPS in DI water for AMPS functionalized MMT [154].

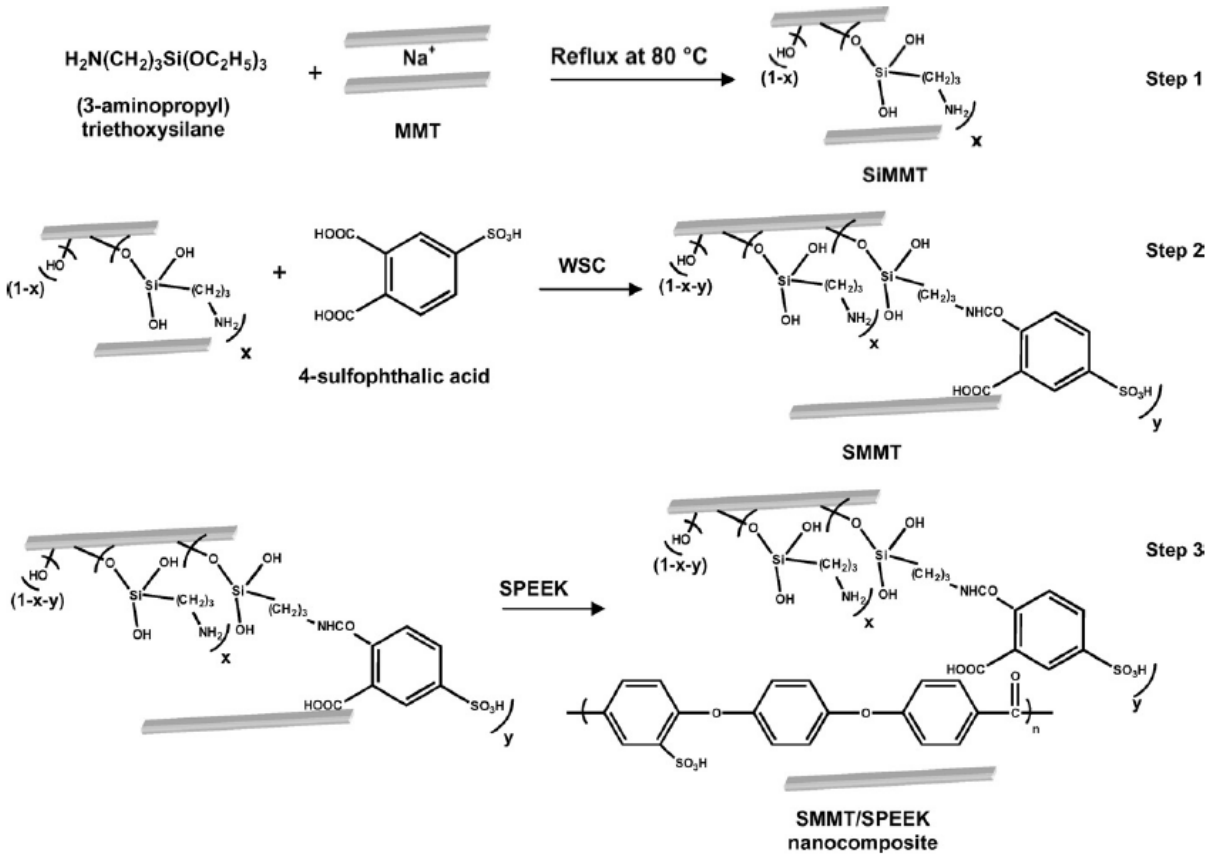

Fig. 1.22. Synthetic process of sulfonated MMT [151]. Copyright 2008, Reproduced with permission from Elsevier Ltd.

(b) Water uptake and mechanical stability: Silicate-layered aggregation, resulted from sulfonated MMT/4-sulfophthalic acid-modified MMT addition, allowed composite membrane to reduce water uptake from 28% to 10%. Composite membrane also had the enhanced strength at break from 38.6 to 51.2 MPa with the increased loading contents of sulfophthalic acid-modified MMT (i.e., 0 - 3 wt%) [151].

(c) Proton conductivity: According to literature reported by Gosalawit, Rapee, et al, functionalization of 4-sulfophthalic acid with MMT led to enhanced proton conductivity of SPEEK composite membrane with 3% loading content as shown in Fig. 1.23, compared with that of pristine SPEEK membrane, even though the aggregation of 4-sulfophthalic acid-modified MMT blocked the proton transferring within composite membrane [151].

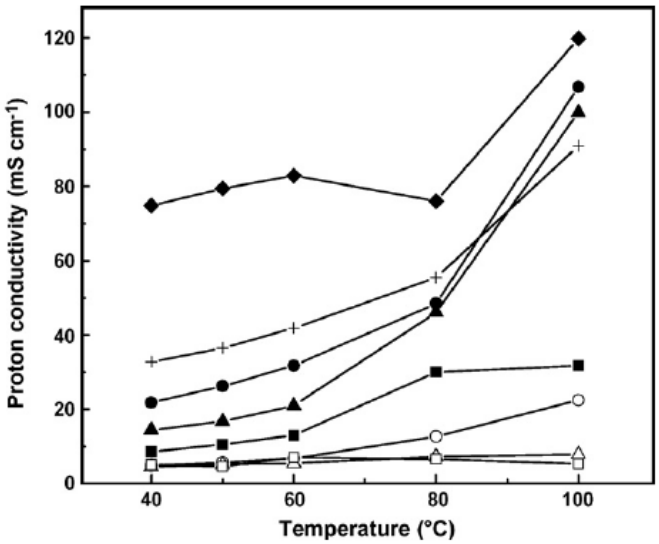

Fig. 1.23. Proton conductivity of Nafion117 (◆) and pristine SPEEK (+) membranes. Proton conductivity of SPEEK composite membrane containing 1wt% (○), 3wt% (△) and 5wt% (□) of unmodified MMT; and containing 1wt% (●), 3wt% (▲) and 5wt% (■) of sulfophthalic acid-modified MMT [151]. Copyright 2008, Reproduced with permission from Elsevier Ltd.

3.2.2.3. PVOH matrix

(a) Membrane preparation: Yang's group made PVOH/sulfonated MMT/PSSA/GA composite membranes via casting procedure. MMT was blended with PSSA polymer solution at room temperature with a weight ratio of 1:1, thereby MMT was impregnated with SO_3H groups prior to membrane preparation [71, 155].

(b) Thermal property: Chemical degradation analyzed using TGA of cross-linked PVA/MMT/PSSA/glutaraldehyde composite membrane was delayed and the peak was shifted to higher temperature, which means thermal property showed stable, caused by MMT and cross-linking effect between PVOH and glutaraldehyde [155].

(c) Mechanical stability and proton conductivity: Mechanical stability of cross-linked PVA/MMT/PSSA/glutaraldehyde composite membrane showed improved value at 120°C. This is due to the annealing effect on cross-linking between the PVOH (-OH group) and glutaraldehyde (-CHO group). PVA/20 wt%MMT/10wt% PSSA composite membrane displayed 12×10^{-3} S/cm of proton condutvity at 70℃ [155].

3.2.2.4. Sulfonated PSU/PTFE matrix

(a) Membrane preparation: Xing, Danmin, et al. prepared STA-modified MMT/SPSU-BP and sulfonated MMT/SPSU-BP/PTFE composite membranes. As shown in Fig. 1.24, H^+-MMT was refluxed with 1,3-propane sultone in toluene to synthesize STA-modified MMT, as well SPSU-BP was copolymerized using 4,40-biphenol, 4,40-difluorodiphenylsulfone, and 3,3-disulfonate-4,40-difluorodiphenylsulfone [156].

(b) Water uptake: The water uptake of STA-modified MMT/SPSU-BP/PTFE composite membrane was lower

than that of sulfonated MMT/SPSU-BP membrane due to hydrophobicity of PTFE. STA-modified MMT/SPSU-BP and STA-modified MMT/SPSU-BP/PTFE composite membranes respectively showed 160 wt% and about 100 wt% at 90℃ [156].

(c) Mechanial strength: The reinforcing effect of the PTFE addition led to improved tensile strength of STA-modified MMT/SPSU-BP/PTFE composite membrane, thereby the higher value compared to sulfonated MMT/SPSU-BP composite membrane [156].

(d) Proton conductivity: The through-plane conductivities/the in-plane conductivities of STA-modified MMT/SPSU-BP and STA-modified MMT/SPSU-BP/PTFE composite membranes respectively exhibited 0.028/0.073 S/cm and 0.032/0.088 S/cm. The in-plane conductivities of the two membranes are higher than the through-plane conductivities of the two membranes because the parallel distribution of sulfonated MMT causes the proton conduction channel to twist further in the plane direction [156].

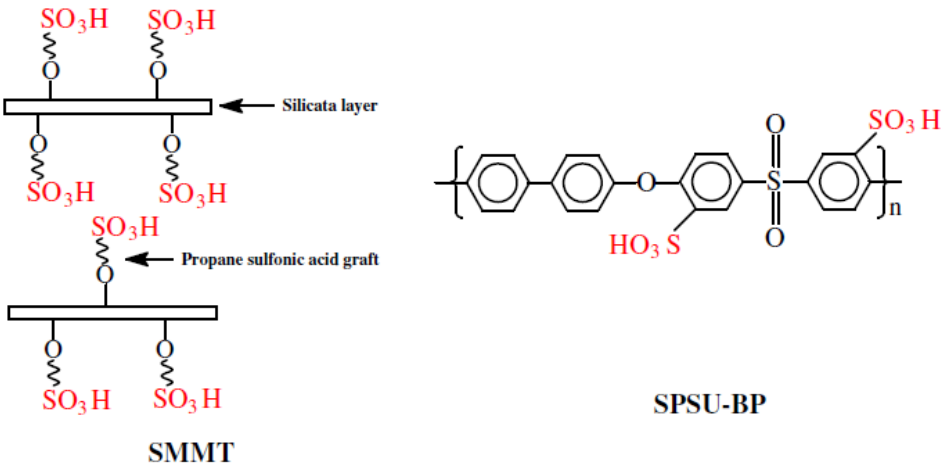

Fig. 1.24. Synthetic process of STA-modified MMT (left) and SPSU-BP (right) [156]. Copyright 2011, Reproduced with permission from Elsevier Ltd.

3.2.2.5. SPAES matrix

(a) Membrane preparation: Kim, Deuk Ju, et al fabricated SPAES/sulfonated MMT blended membrane. Na^+-MMT was added to a sulfuric acid solution and then 3-MPTMS/MMT/toluene was blended with the MMT dispersion for preparation of sulfonated MMT as shown in Fig. 1.25. Following this, SPAES solution was mixed with 3-MPTMS-modified MMT dispersion, after which composite membrane was fabricated by casting and evaporation process [91].

(b) Water uptake: The water uptake analyzed at 80 celcius degree of composite membrane was lower than the SPAES pure membranes. The water uptake of the SPASE/sulfonated MMT membrane was lower than the SPAES/Na^+-MMT membrane because the inorganic aggregation made the hydrogen bond between water and hydrophilic groups on sulfonated MMT layer weakened. As the sulfonated MMT content increased, the water uptake improved [91].

(c) Mechanical stability: SPAES/0.5 wt% Na^+-MMT and SPAES/0.5 wt% sulfonated MMT composite membranes respectively displayed approximately 48 MPa and 27 MPa, which are lower than pristine SPAES. In addition, as the content of sulfonated MMT grew, the hydrophilic property increased leading to mechanical

stability decreased. This is because hydrophilic groups (-SO_3H and -OH) created void spaces, and limited stress transfer of sulfonated MMT nanoparticles inside polymer matrix [91].

(d) Proton conductivity: SPAES composite membranes containing same sulfonated MMT content with higher sulfonation degree showed higher proton conductivity under 100%RH and 80℃ due to the augmented proton donators and carriers (sulfonation group). However, SPAES/0.5 wt% sulfonated MMT composite membrane exhibited reduced value (0.5 S/cm at 100%RH and 80℃) compared to pristine SPAES membrane (0.7 S/cm) because of the low density of ion clusters [91].

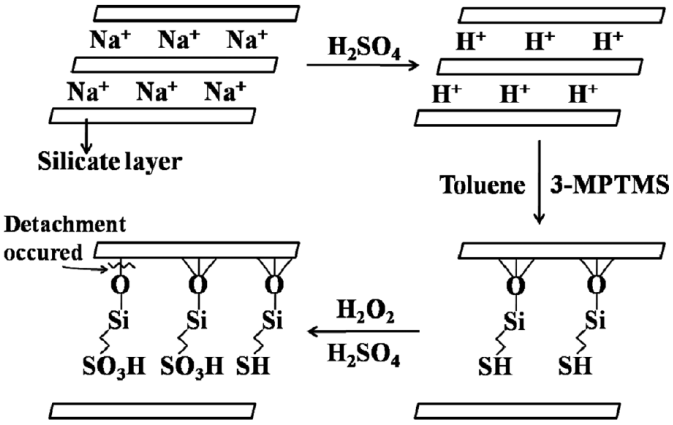

Fig. 1.25. Schematic diagram of sulfonated MMT synthesized with 3-MPTMS and toluene [91]. Copyright 2012, Reproduced with permission from Springer.

3.2.3. Perfluorosulfonated MMT additive

(a) Membrane preparation: MMTs with perfluorosulfonation groups were incorporated into the Nafion phase. Thomassin, Jean-Michel, et al. synthesized MMT with cationic fluorosurfactants. PFPE-NR_3 and Zonyl were used as fluorinated ammonium cations as shown in Fig. 1.26. The sulfonylfluoride groups were hydrolyzed in KOH/water/dimethylsulfoxide solution before Nafion composite membranes [8].

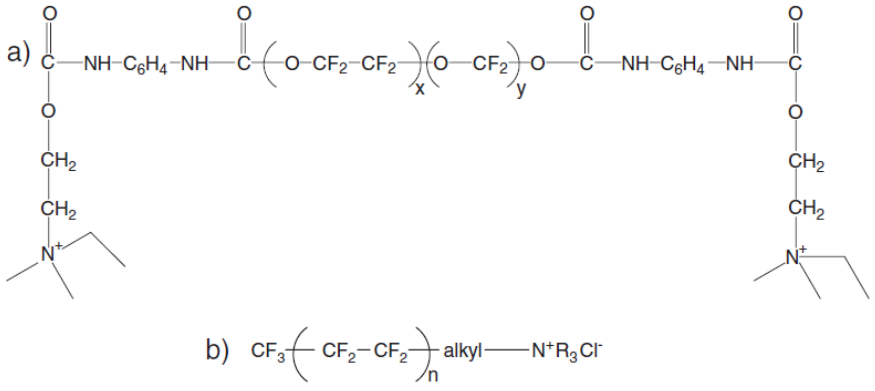

Fig. 1.26. Chemical structure of (a) PFPE-NR_3 (x = y = 14) and (b) Zonyl (n = ±5) [8]. Copyright 2006, Reproduced with permission from Elsevier Ltd.

Lee, Wonmok, et al. synthesized H^+-MMT with 1,3-PS, 1,4-BS, FMES. Afterwards, MMTs with perfluorinated sulfonic acid group were blended in Nafion dispersion for membrane preparation [157]. The same process was introduced by Y.K. Kim and co-workers [158]. Gosalawit, Rapee, et al. reported the preparation method of the membrane containing MMT synthesized with Krytox and Nafion according to Fig. 1.27. Synthesis process was achieved as follows [130]:

1) The hydrolyzed (3-aminopropyl)triethoxysilane was mixed with MMT in ethanol.

2) Aminosilane-functionalized MMT was filtrated and washed with water.

3) Krytox was blended with aminosilane and WSC, and then the mixture was added into Nafion/DMAc dispersion to obtain homogeneous casting dispersion.

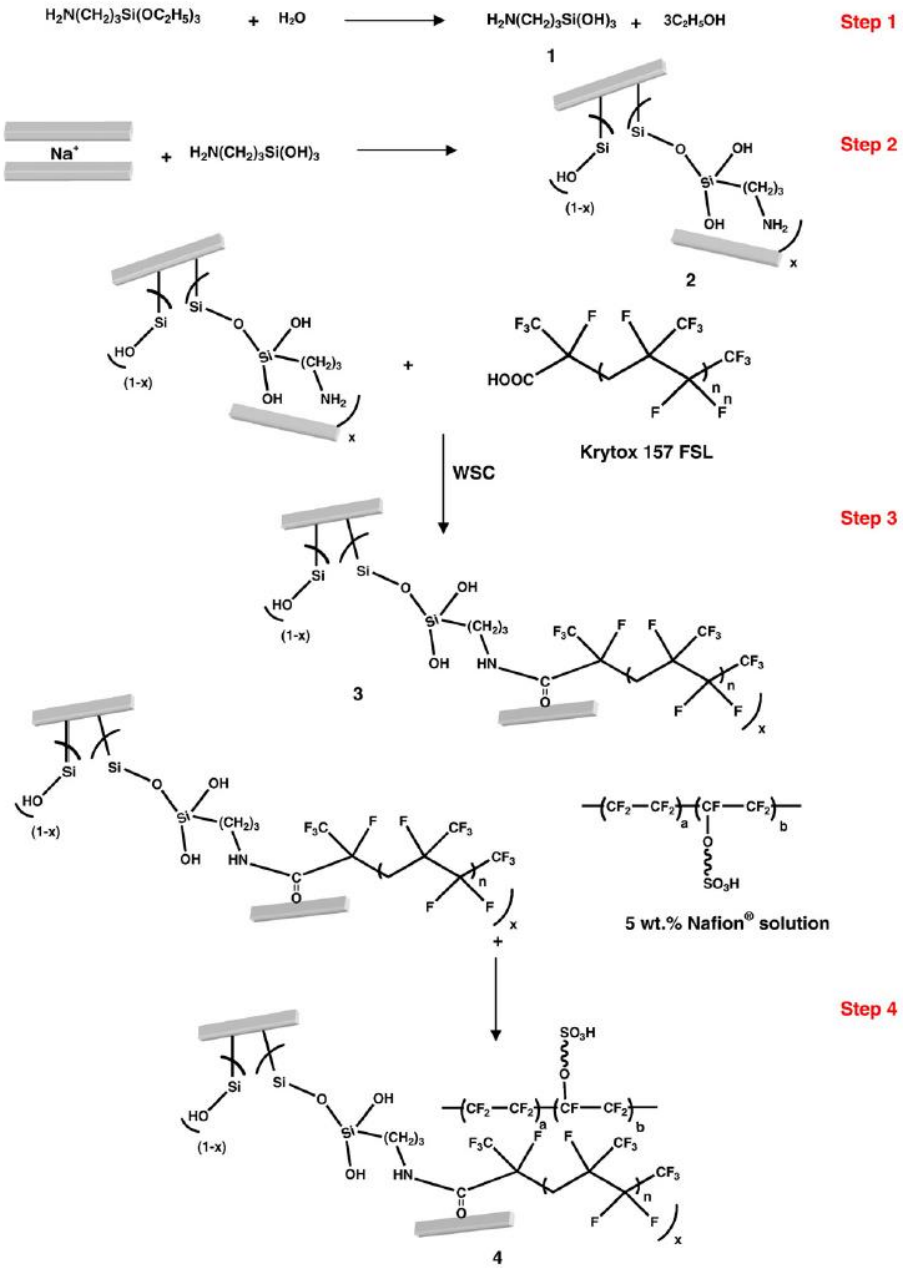

Fig. 1.27. Modification process of MMT synthesized with Krytox and Nafion [130]. Copyright 2007, Reproduced with permission from Elsevier Ltd.

(b) Water uptake: Water uptake of composite membrane blended with Nafion/Krytox-modified MMT improved by about 10% due to its hydrophilic property, compared with that of the recast Nafion membrane [130].

(c) Thermal property: Sulfonic acid of perfluorosulfonic group (i.e., $-OCF_2CF_2SO_3H$) and PTFE-like backbone (i.e., $-CF_2-CF_2-$) of recast Nafion membrane respectively showed degradation at 296 and 402°C, whereas composite membrane based on Nafion and Krytox-modified MMT had degradation at higher temperature (i.e., 309.8 and 417.6℃) due to interaction between PTFE-like backbones of Nafion and multilayered silicates of organophilic nanoclay [130]. Moreover, at around 150 - 300℃, functionalized MMT showed weight loss which is in the order of H^+ MMT < 1,4-BS-modified MMT < 1,3-PS-modified MMT < FMES-modified MMT because $-SO_3H$ groups were thermally cracked [146, 157].

(d) Proton conductivity: FMES-modified MMT-based Nafion composite membrane, respectively, allowed about 0.01 and 0.015 S cm^{-1} higher proton conductivity, compared with 1,4-BS-modified MMT- and 1,3-PS-modified MMT-based composite membranes. On the other hand, pristine Nafion membrane showed the highest proton conductivity among all membranes tested[146, 157]. In addition, the proton conductivity measured using AC impedance spectroscopy of composite membrane containing perfluorosulfonic group (i.e., $-OCF_2CF_2SO_3H$) was reduced with increased loading of Krytox-modified MMT [130].

3.2.4. Aminized MMT additive

3.2.4.1. Nafion matrix

(a) Membrane preparation: Nafion-based membranes were blended with Cloisite 10A [43] or POPD-modified MMT [94]. MMT was modified via cation exchange between Na^+ in MMT and poly(oxypropylene) (POP)-backboned diamines cations in aqueous solution [94]. Jung's group reported a method to recast Nafion membrane containing dodecylamine-modified MMT via hot pressing [123, 159].

(b) Thermal property: Thermal decomposition behavior of Nafion/Cloisite 10A membrane was verified at 300 - 370℃. Interaction between hydrophobic backbones (i.e., PTFE-like structure) of Nafion and Cloisite 10A led to lower thermal decomposition of the composite membrane than that of pristine Nafion membrane [43]. The coefficient of thermal expansion (CTE) of POPD-modified MMT/Nafion composite membrane showed an improved value in comparison to that of unmodified membrane due to decreased composite porosity caused by addition of clays [94]. Blending 3, 5, 7wt% dodecylamine-modified MMT with Nafion resulted in improved thermal stability (at 400℃), compared to pristine Nafion [123, 159].

(c) Mechanical stability: Blending of POPD-modified MMT in Nafion dispersion led to flexural and impact strength in the order of POPD2000-modified MMT > POPD400-modified MMT > POPD230-modified MMT > pristine MMT. The reinforcing effect of organo-nanoclays is increasing with the increase of modified MMT basal spacing. Blending of POPD2000-modified MMT in Nafion dispersion formed composite membrane with increased about 15 MPa for flexural strength compared with pristine MMT-based Nafion composite membrane as shown in Fig. 1.28 [94]. Addition of Cloisite 10A resulted in remarkably improved mechanical resistance compared with pristine Nafion membrane. The highest strength and elongation at break of pristine Nafion membrane were about 30 MPa and 200%, respectively. However, the maximum strength of Nafion/Cloisite 10A composite membrane showed approximately 45 MPa at a loading of 3wt% nanoclay, and also the elongation at break of the

composite membrane was about 500%, which is almost doubled compared with that of pristine Nafion membrane. The results are due to homogeneous dispersion or exfoliation of Cloisite 10A nanolayer [43].

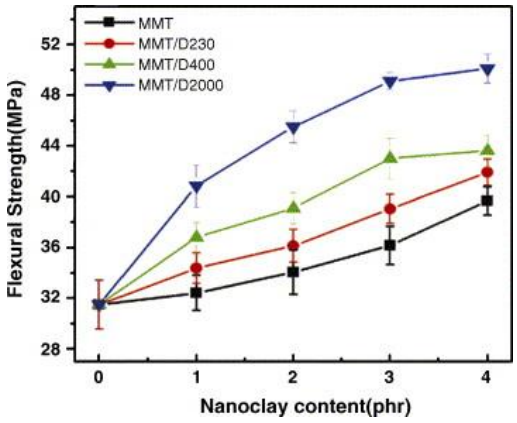

Fig. 1.28. Flexural strength (MPa) of vinyl ester composite membranes containing pristine MMT; and POPD230-, POPD400- and POPD2000-modified MMT [94]. Copyright 2006, Reproduced with permission from Elsevier Ltd.

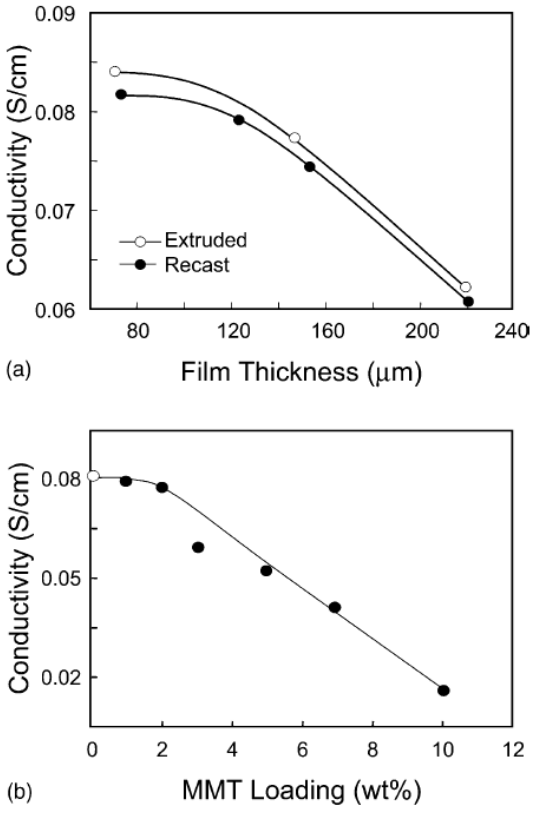

Fig. 1.29. Data on (a) proton conductivity (under ambient temperature) of pristine Nafion membrane made by extruding and recasting, and (b) proton conductivity (under room temperature and dry state) of Nafion/Cloisite 15A composite membrane according to filler loading [43]. Copyright 2004, Reproduced with permission from Elsevier Ltd.

(c) Proton conductivity: Proton conductivity of pristine Nafion membranes prepared by extruding as well as recasting was in inverse proportion to the membrane thickness as can be seen in Fig. 1.29a. The highest conductivity of Nafion/Cloisite A10 composite membrane was displayed at 1 wt% loading as shown in Fig. 1.29b, but the grown amount of 2 – 10 wt% Cloisite 15A within Nafion membrane resulted in gradually decreased conductivity up to 0.01 S cm^{-1} owing to the hydrophobicity of Cloisite 15A [43]. In addition, based on Bragg's law, Xiuchong, He, et al. confirmed that Nafion matrix was intercalated into interlayer of dodecylamine-modified MMT. The interlayer distance (d001) of modified MMT (15.9518 nm) was larger than that of MMT/Nafion composites (about 32-36 nm), accordingly water uptake, mechanical strength and even proton conductivity of composite membranes were superior to that of Nafion 211 membrane [149]. Incorporating 3 wt% dodecylamine-modified MMT with Nafion (0.0772 S/cm) led to lower proton conductivity compared to pristine Nafion (0.089 S/cm) at 110℃ [123, 159].

3.2.4.2. PBI and ABPBI matrices

(a) Membrane preparation: According to literature of Chuang et al, MMT was modified by cation exchange method, with ammonium salt of DOA. PBI/DOA-modified MMT composite membranes were prepared and then the membranes were doped by immersion in 11 M aqueous phosphoric acid. PBI was synthesized with 3,3-diaminobenzidine and 2,2-bis(4-carboxyphenyl)hexafluoropropane in PPA by means of condensation polymerization [76]. Eren, Bilge, Reyhan Aydin, and Erdal Eren fabricated ABPBI/HDTMA-modified MMT composite membrane. ABPBI was made via condensing DABA with PPA, and MMT was modified with HDTMA solution at 80℃ [88]. Also, H_3PO_4-doped PBI/Cloisite 15A membranes were prepared by Hasani-Sadrabadi, Mohammad Mahdi, et al [78].

(b) Thermal propert and mechanical stability: For thermal property analyzed using DTG, the temperature at maxiumum decomposition rate of ABPBI/15 wt% HDTMA-modified MMT composite membranes was 603°C [88]. Exfoliated dispersion of DOA-modified MMT inside PBI matrix showed improved mechanical characteristics. To be specific, PBI/5wt% DOA-modified MMT composite membrane, respectively, led to the enhanced tensile modulus and stress by about 0.7 Gpa and 20 Mpa, compared with phosphoric acid-doped PBI/5wt% DOA-modified MMT membrane due to the plasticizing effect of phosphoric acid [76].

(c) Proton conductivity: Blending of PBI and DOA-modified MMT together with PBI resulted in the decreased values by 21 - 27% compared with blending of PBI alone as dispersed DOA-modified MMT in polymer matrix retarded the mobility of proton within membrane [76]. Blending 3 wt% Cloisite 15A with H_3PO_4-doped PBI showed 0.0173 S/cm for proton conductivity [78].

3.2.4.3. SPEEK matrix

(a) Membrane preparation: Gaowen, Zhang and co-worker reported organic modification of Na^+-MMT. Na^+ ions of Na^+-MMT was exchanged with hexadecyltrimethylammonium ions. SPEEK was blended with CTAC-modified MMT in DMAc, and then the dispersion was cast on glass plate [160]. Hasani-Sadrabadi, Mohammad Mahdi, et al. sulfonated PEEK, and then it was blended with Cloisite 15A to prepare composite membrane

composed of SPEEK and Cloisite 15A [161]. Jaafar, Jafariah and co-workers used PEEK and sulfuric acid for obtaining sulfonated PEEK. Afterwards, SPEEK, Cloisite 15A and TAP were blended in DMSO solution for preparation of composite membranes. Addition of TAP improved the compatibility between SPEEK and Cloisite 15A. In general, low molecular weight material is selected as a compatibilizer due to simultaneous interaction with polymer and nanoclay. The compatibilizer should be soluble in the solvent and form strong bonding (i.e., hydrogen bonding) with polymer and nanoclay. It also should keep solid state at room temperature in order to prevent evaporation of the compatibilizer [162]. Hasani-Sadrabadi, Mohammad M., et al. sulfonated PEEK as various degree. Specifically, SPEEK was precipitated, filtrated, washed and dried, after which SPEEK, Cloisite 15A and DMAc were blended prior to membrane preparation [70]. In addition to this, Jaafar, Juhana, Ahmad Fauzi Ismail, and T. Matsuura also used TAP as compatibilizer in order to make SPEEK/Cloisite 15A/TAP composite membrane [68]. Hasani-Sadrabadi, Mohammad Mahdi, et al. prepared SPEEK/SPPO/Cloisite 15A. SPPEK and SPPO sulfonated using sulforic acid and chlorosulfonic acid, respectively [163]. Hande, Varsha R., et al. prepared composite membrane containing BHMB cross-linked SPEEK with Cloisite 30B order to increase thermal and mechanical stability. Fig. 1.30 displays schematri procedure, which is hydroxyl groups of Cloisite 30B with sulfonic acid group regarding BHMB cross-linked SPEEK [164].

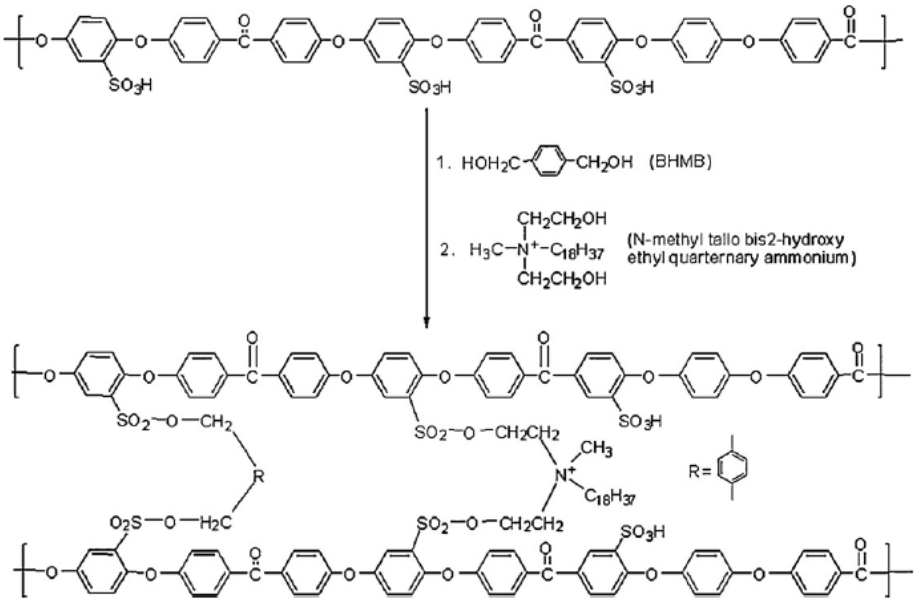

Fig. 1.30. Cross-linking process of 1,4-bis (hydroxymethyl) benzene (BHMB) cross-linked SPEEK [164]. Copyright 2011, Reproduced with permission from Elsevier Ltd.

(b) Water uptake and mechanical stability: Cloisite 15A/TAP/SPEEK membrane showed low water uptake values compared with Nafion membrane because blending of Cloisite 15A with TAP formed narrow and branched water channel inside SPEEK membrane. In particular, presence of TAP improved compatibility, caused by uniform dispersion state of additive and compactness, and hence mechanical strength of Cloisite 15A/TAP/SPEEK membrane in turn raised (51 Mpa) compared with SPEEK membrane [121]. Blending Cloisite B30 with cross-linked SPEEK exibited approximately 40% improvement in tensile strength compared to pristine SPEEK. However, as the addition amount of Cloisite 30B augmented, the composite homogeneity decreased, leading to

the tensile strength of the composite membrane being reduced [164]. The higher the degree of sulfonation of SPEEK (up to 75%) and SPPO (up to 21.9%), the better the water uptake of pristine membranes. For water uptake analysis, SPEEK/SPPO ratio was 75:25, which was up to 121.5% at 70℃ [163].

(c) Thermal property: Jaafar, Jafariah et al observed that incorporation of Cloisite 15A into SPEEK with TAP helped to decrease the thermal degradation of SPEEK due to increased crystallinity and steric hindrance of the methyl groups which lead to reduction of molecular mobility [162]. Decomposition temperature verified using TGA delayed and slightly reduced at 250℃, leading to improved themal stability of cross-linked SPEEK/Cloisite 30B composite membranes compared with pristine SPEEK membrane. Additionally, glass transition temperature (T_g) of composite membranes shifted to higher values compared to pristine SPEEK accoridng to DSC analysis. This is due to immobilization of the polymeric chains, caused by the covalent bonding of the sulfonyl groups of SPEEK phase with the reactive Cloisite 30B [164].

(d) Proton conductivity: For proton conductivity in the Fenton reagent test, Cloisite 15A/TAP/SPEEK and Nafion 117 membranes displayed 1.75×10^{-2} S/cm and 1.87×10^{-2} S/cm, respectively. Nafion membrane with wider water channels compared to composite membrane made better proton movement [121]. Incorporating Closite B30 with cross-linked SPEEK displayed 11.8 mS/cm (at 80℃) of proton conductivity, whereas pristine SPEEK showed 65 mS/cm, which is higher values thant composite membrane [164]. With respect to the proton conductivity of SPEEK/SPPO composite membrane, 50:50 of SPEEK/SPPO ratio showed 0.0455 S/cm under 70℃ and hydration conditions [163].

3.2.4.4. PSU and SPSU matrixes

(a) Membrane preparation: Unnikrishnan, Lakshmi, et al prepared nanocomposite membranes composed of PSU/Cloisite 93A and PSU/Cloisite 30B [82]. Unnikrishnan, Lakshmi, et al and sulfonated PSU by using chlorosulfonic acid and trimethyl silyl chlorosulfonate (TMSCS), and then SPSU/Cloisite 30B dispersion was cast on glass plate via casting - evaporation [165]. Shami, Zahed, et al also sulfonated PSU using trimethyl silyl chlorosulfonate before SPSU/Cloisite 30B blended membrane is prepared [166].

(a) Water uptake: PSU/Cloisite 30B and PSU/Cloisite 93A nanocomposite membranes decreased in water uptake compared to pristine PSU owing to reduced free volume and swelling ability caused by blending of nanoclays. As the sulfonation degree was raised, the water uptake of SPSU membrane was improved (up to 32.2% at 60℃), but the addition of Cloistie 30B didn't help to multiply the water uptake [165].

(b) Mechanical stability: Tensile modulus of pristine PSU, PSU/1 wt%Cloisite 30B and PSU/1wt% Cloisite 93A membranes displayed 1142.56 ± 36.87 MPa, 2899.73 ± 42.23 Mpa and 2179.13 ± 59.40 Mpa, respectively. However, when the content of additives was augmented to 2 wt%, the mechanical stability was deteriorated compared to 1 wt% content due to agglomeration of silicate layers inside PSU matrix.

(c) Thermal property: Better interaction between PSU matrix/Cloisite 93A or PSU matrix/Cloisite 30B led to delayed thermal decomposition of composite membranes compared to pristine PSU at approximately 200℃. The glass transition temperature (T_g) of pristine PSU displayed 185℃, whereas that of SPSU/1 wt% Cloisite 30B composite membranes showed improved values by around 20℃ [165].

(d) Proton conductivity: No exciting results can be found for proton conductivity of pristine PSU, PSU matrix/Cloisite 93A and PSU matrix/Cloisite 30B membranes and their values are similar to each other between 3.31×10^{-7} and 3.51×10^{-7} S/cm [82]. SPSU modified with sulfonic acid group showed better proton conductivity of the membrane than pristine PSU , and the addition of 1 wt% Cloisite 30B inside SPSU matrix sulfonated with TMSCS improved it to 2.126×10^{-3} S/cm at 25℃. On the other hand, incorporating 1 wt% Cloisite 30B into SPSU sulfonated with chlorosulfonic acid showed a reduced value, which is 5.581×10^{-4} S/cm at the same temperature [165].

3.2.4.5. PVOH matrix

Thomassin, Jean-Michel, et al. reported phosphotungstic acid (PWA)-modified PVOH/Na^+-MMT composite membranes [44]. Pristine PVOH membrane has a strong hydrophilicity, resulting in 128% of water uptake. Incorporating 3 wt% Cloisite Na^+ into PVOH phase reduced to 110% in water uptake. Blending 10 wt% PWA/3 wt% Cloisite Na+ led to reduced water uptake (100%) of PVOH composite membrane. The inorganic acid improves proton movement of PVOH membrane. Doping by 40 wt% content of phosphotungstic acid showed 0.008 S/cm in proton conductivity (see Fig. 1.31). Filling 7% Cloisite Na^+ into PVOH matrix led to the highest proton conductivity among the composite membranes containing 3, 5, 7, 10 or 15% Cloisite Na^+, but this still displayed lower conductivity than the pristine PVOH.

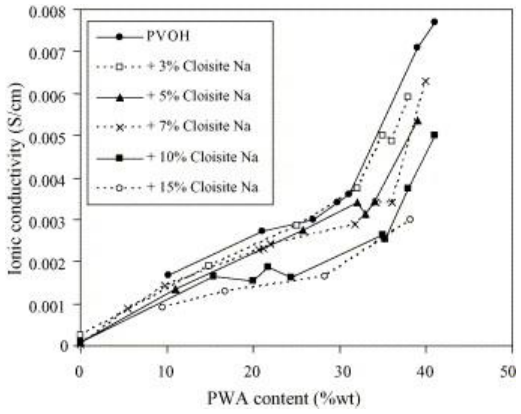

Fig 1.31. Proton Conductivity of PVOH composite membranes according to the content of phosphotungstic acid and Cloisite Na^+. Copyright 2005, Reproduced with permission from Elsevier Ltd [44] .

3.2.4.6. GPTMS/H_3PO_4 and SPPO matrices

(a) Membrane preparation: PPO was sulfonated with chlorosulfonic acid and then sulfonated PPO/Cloisite 15A composite membrane was prepared by Hasani-Sadrabadi et al [81]. Jana, R. N., and H. Bhunia prepared silane-based composite membranes containing GPTMS, EHTES, H_3PO_4 and Cloisite 30B via sol-gel method, as shown in Fig. 1.32 [132].

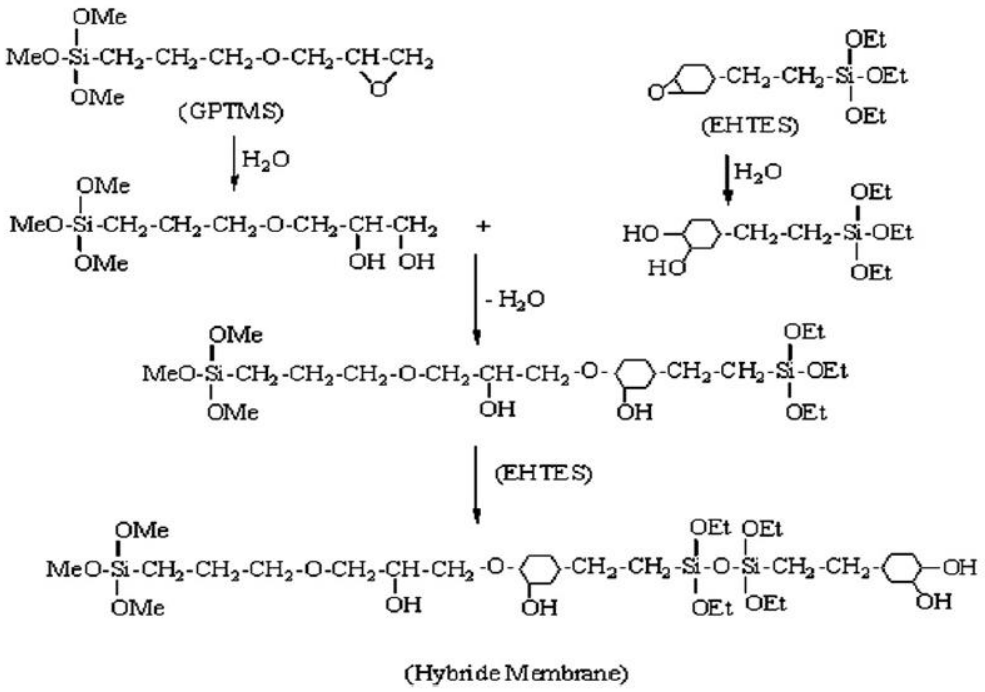

Fig. 1.32. Synthetic procedure of silane-based composite membranes by sol-gel method [132]. Copyright 2008, Reproduced with permission from Elsevier Ltd.

(b) Thermal property: GPTMS/EHTES/H_3PO_4/Cloisite 30B membrane prepared by sol-gel method has thermal stable characteristic because of C–O–C bonds and Si–O–Si bonds between two silane groups of EHTES. Thermal stability reduced with increased contents of GPTMS and H_3PO_4 used for polymer. Also, interaction between Cloisite 30B and polymer matrix forms ether linkage from the condensation –OH groups, thereby delayed chemical decomposition of composite membrane [132].

(c) Water uptake and proton conductivity: SPPO/Closite 15A composite membrane showed proton conductivity (up to 1.08×10^{-2} S cm^{-1}) with decreased loading content of Cloisite 15A due to relatively hydrophobicity [81]. Incorporating Closite 30B and MWNTs helped GPTMS/EHTES composite membranes to display augmented proton conductivity with improved chemisorbed water by capillary action [132].

2.1.4.7. Other types of polymer matrixes (SPES, Vinyl ester, CS, SSEBS and SPPESK)

Hasani-Sadrabadi, Mohammad Mahdi, et al. prepared SPES/Cloisite 15A composite membranes. In the study, PES was dissolved in chloroform and then mixed with chlorosulfonic acid in order to obtain SPES as shown in Fig. 1.33 [167]. Yen, Chuan-Yu, et al prepared Vinyl ester membranes with MMT/POPD organoclay (MW = 230, 400 and 2000 g/mol) by BMC process [94]. Tohidian, Mahdi, et al reported preparation method of CS/PWA/Cloisite Na, CS/PWA/Cloisite 15A and CS/PWA/Cloisite 30B composite membrane [168]. Hwang, Hae Young, et al. prepared SSEBS copolymer membrane containing Cloisite 15A, Cloisite 20A and Cloisite 30B. SSEBS copolymer was sulfonated with SEBS which consists of glassy polystyrene and rubbery ethylene butylene blocks. The glassy polystyrene parts provide sulfonation-possible regions that can be modified to polymer with hydrophilicity. Besides, the rubbery ethylene-butylene blocks offer improvement of mechanical strength caused

by elasticity [118]. Hu, Zhengwen, et al synthesized SPPESK with PPESK by using sulfuric acid and fuming sulfuric acid solution (4.6 : 5.4 as a volume ratio), and then prepared SPPESK composite membrane containing CTAB-modified MMT made by mixing Na^+-MMT with CTAB solution [169]. Pphysicochemical properties of composite membranes are described in the literacutres [167], [94], [168], [118] and [169].

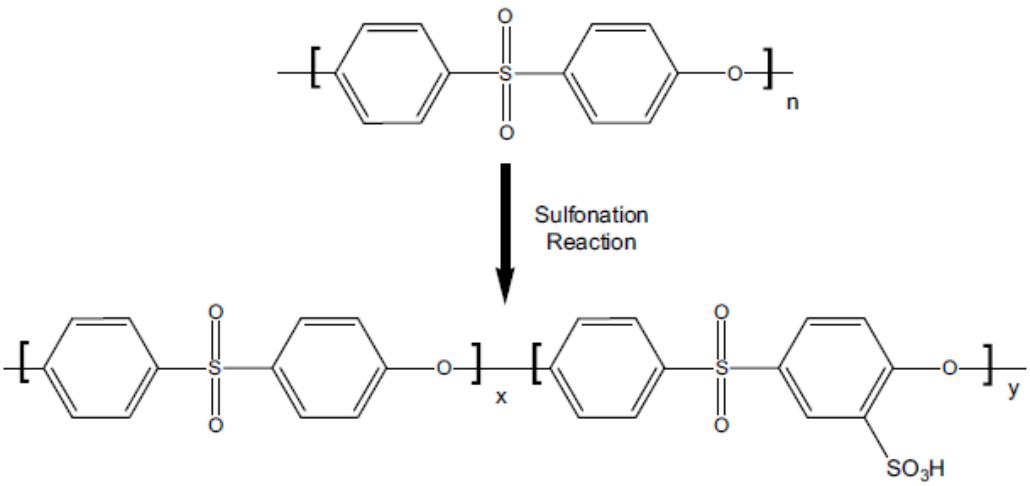

Fig. 1.33. Structure of PES and S-PES [167]. Copyright 2010, Reproduced with permission from Elsevier Ltd.

3.2.5. Bio-functionalized MMT additive

(a) Membrane preparation: Hasani-Sadrabadi, Mohammad Mahdi, et al. reported MMT bio-functionalized with CS as additive within Nafion composite membrane because macromolecular polycationic intercalating agent provides improvement of transport characteristic. In the synthetic process, unmodified MMT was dispersed in DI water and CS in acetic acid aqueous solution prior to drying. Afterwards, casting dispersion containing Nafion and CS-modified MMT was used for membrane preparation [170, 171].

(b) Thermal property: CS, biopolymer, appears the promising candidate for intercalation in unmodified Na^+-MMT by cationic exchange processes due to cationic state of CS in acidic media. Hasani-Sadrabadi, Mohammad Mahdi, et al. reported that exfoliation of MMT improved thermal stability, and TGA thermogram displayed three-step degradation pattern: CS degradation at 220℃, decomposition of sulfonic side-chains of Nafion at about 300℃, and degradation of PTFE backbone of Nafion ionomer after 360℃ [171].

(c) Proton conductivity: Addition of 10wt% CS-functionalized MMT into Nafion matrix improved proton conductivity compared with the membranes containing unmodified MMT and Cloisite 15A as shown in Fig. 1.34. This is due to ionic interaction between amino group of CS polycation and negatively charged Nafion ionomer [171].

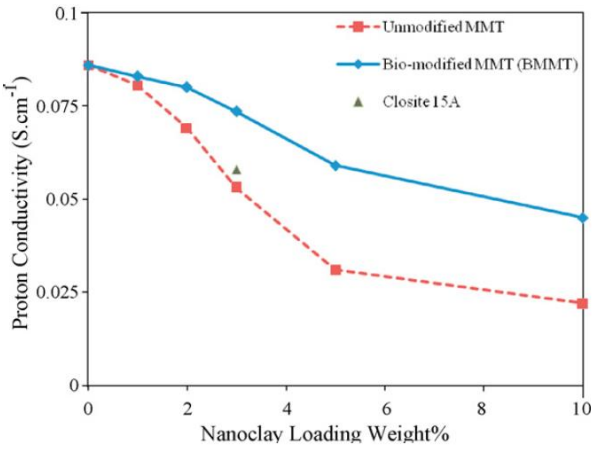

Fig. 1.34. Proton conductivity of Nafion/unmodified MMT, Nafion/Cloisite 15A and Nafion/CS-modified MMT composite membranes [171]. Copyright 2009, Reproduced with permission from Elsevier Ltd.

3.3. Effect of Laponite® (synthetic Hectorite) type additive

Laponite was added into Nafion, SPAS, SPAES, PBI or SPEEK. Laponites are usually incorporated into Nafion or SPEEK to prepared casting dispersion. Functionalized Laponites can be classified in sulfonation and other type. Table 1.4 summarizes the chemical composition of membrane casting dispersion, proton conductivity and reference.

Table 1.4. Summary data on membrane casting dispersions composed of Laponite and ionomer, and proton conductivity of prepared membranes.

Filler type	Additives	Polymer powder/ polymer dispersion	Solvent/ non-solvent	Preparation method of composite membrane	Additive content over the casting dispersion (wt%)	Operating temp. (℃)	RH (%)	Proton conductivity of modified membrane (S cm^{-1})	Year of publication	Ref.
Laponite	Laponite®	Crosslinked SPAS	NMP	Doctor blade method	10	-	-	0.035	2017	[122]
Laponite	Laponite®	Nafion	DMF; IPA	Casting-evaporation process	-	-	-	-	2015	[103]
Laponite	3-MPTMS-modified laponite	SPAES	NMP	Casting-evaporation process	2	60	100	0.11	2012	[90]
Laponite	Laponite® Laporte	Nafion	DMF; IPA	Casting-evaporation process	-	-	-	-	2012	[35]
Laponite	$Na_4P_2O_7$-modified Laponite	Nafion	Ethanol/ water	Casting-evaporation process	3	110	100	0.2702	2012	[41]

Filler type	Additives	Polymer powder/ polymer dispersion	Solvent/ non-solvent	Preparation method of composite membrane	Additive content over the casting dispersion (wt%)	Operating temp. (℃)	RH (%)	Proton conductivity of modified membrane (S cm^{-1})	Year of publication	Ref.
Laponite	*p*-styrene sulfonate-grafted Laponite	Nafion	DMF	Casting-evaporation process	3	90	-	0.011	2011	[37]
Laponite	1,3-propane sultone-grafted Laponite®	Nafion	DMF	Casting-evaporation process	3	90	-	0.0105	2011	[37]
Laponite	Imidazole salt-modified Laponite® RD	PBI	NMP	Casting-evaporation process	-	-	-	-	2011	[172]
Laponite	Dequaliniu m chloride salt-modified Laponite® RD	PBI	NMP	Casting-evaporation process	15	150	12	0.12	2011	[172]
Laponite	p-styrene sulfonate-grafted Laponite®	Nafion	DMF	Casting-evaporation process	1.2	85	-	0.05	2011	[173]
Laponite	Laponite® grafted with SO_2 gas by plasma treatment	Nafion	DMF	Casting-evaporation process	1.2	85	-	0.011	2011	[173]
Laponite	Styrene sulfonic-grafted Laponite®	Nafion	DMF	Casting-evaporation process	10	95	98	0.08	2006	[33]
Laponite	Laponite® Solvay	SPEEK	DMF; NMP	Casting-evaporation process	10	-	-	0.111	2005	[141]
Laponite	Laponite® Southern Clay treated with 1 M H_2SO_4	SPEEK	DMAc	Casting-evaporation process	10	60	-	0.003	2003	[34]

3.3.1. Pristine Laponite additive

3.3.1.1. Nafion and SPAS matrices

(a) Membrane preparation: Nicotera, Isabella, et al. introduced that Nafion chain was incorporated into layered Laponite by solution intercalation method [35]. Lee, Sun Hwa, et al prepared UV-cross-linked SPAS/Laponite composite membranes. DCDPS, Na-sDCDPS, BPA and DABPA were blended with K_2CO_3 in NMP,

and then the mixture was heated for condense polymerization at 180℃. Following this, Laponite dispersed in NMP was transferred into with SPAS sample to prepare UV-crosslined SPAS-Laponite nanocomposite. HDDA and benzophenone (as photoinitiator) were added to UV-crosslined SPAS/Laponite dispersion. Composite membranes were prepared via Doctor blade method [122].

(b) Composite homogeneity: Nicotera, Isabella, et al. studied the self-diffusion coefficients of composite membrane, which was prepared using Nafion/Laponite dispersion containing DMF and IPA solvents. Nafion and Laponite exhibited higher dispersing effects when blended into DMF instead of IPA. Also, the composite membranes prepared using DMF were observed according to different Laponite loadings under various temperature (i.e., from 20℃ to 140℃), as shown in Fig. 1.35 [35]. Blending of Laponite with SPAS showed good compatibility because UV-crosslinked SPAS has polarity property, thereby augmented concentration of sulfonic acid [122].

(c) Thermal property, mechanical stability and proton conductivity: It was confirmed that 3 - 6 wt% of Laponite loading led to improved mechanical stability and homogeneous distribution in Nafion matrix compared with 1 wt% of Laponite loadings above 80℃ as lower loading (1 wt%) of Laponite has a discrete effect within composite membrane. Accordingly, strong interaction between polymer main chains and Laponite allowed composite membrane to have thermal resistance [35]. Laponite-based membrane containing SPAS crosslinked by UV enhanced elastic modulus and hardness by 15% (7.1 Mpa) and 5% (31.5 MPa), compared with UV-crosslinked SPAS membrane. However, incorporation of Laponite inside UV-crosslinked SPAS phase did not affect proton conductivity (i.e., 0.038 - 0.035 S cm^{-1}) [122].

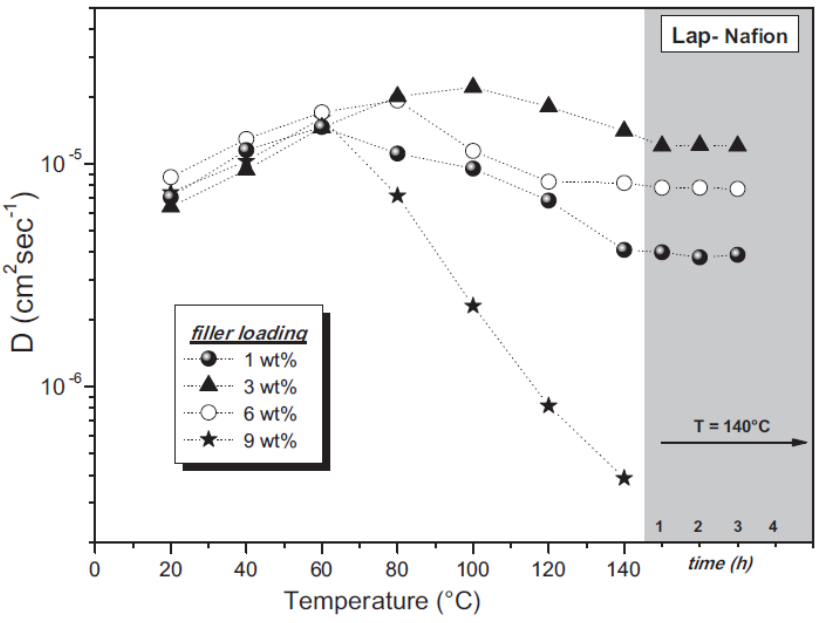

Fig. 1.35. Self-diffusion coefficients based on different temperature and laponite loadings within composite membrane prepared using DMF [35]. Copyright 2012, Reproduced with permission from Elsevier Ltd.

3.3.1.2. SPEEK matrix

Chang, Jae-Hyuk, et al. dissolved PEEK in 95% sulfonic acid so as to obtain SPEEK, after which Laponite was incorporated into SPEEK phase of composite membrane [34].

Volume fraction of laponite flakes has an influence on uniformity of distribution throughout SPEEK composite membrane. This is because flakes are present at the bottom of membrane resulted from flake settling. For this reason, higher amount (20 wt%) of Laponite in SPEEK composite membrane reduced proton conductivity compared with SPEEK composite membrane containing lower amount (10 wt%) of Laponite [141].

3.3.2. Sulfonated Laponite additive

3.3.2.1. Nafion matrix

(a) Membrane preparation: Fatyeyeva, Kateryna, et al. synthesized sulfonated Laponite by using coupled Radio Frequency (RF) plasma reactor. Laponite was grafted with sodium salt of p-styrene sulfonic acid or 1,3-propane sultone by plasma treatment as shown in Fig. 1.36. Afterward, Nafion dispersion containing grafted Laponite was blended with PEG 1500 prior to membrane casting [37]. Bébin, Philippe and co-workers synthesized Laponite with p-styrene sulfonate in DMF. Sulfonated Laponite was grafted using helium plasma. Laponite particles modified in this manner were blended in Nafion dispersion [33].

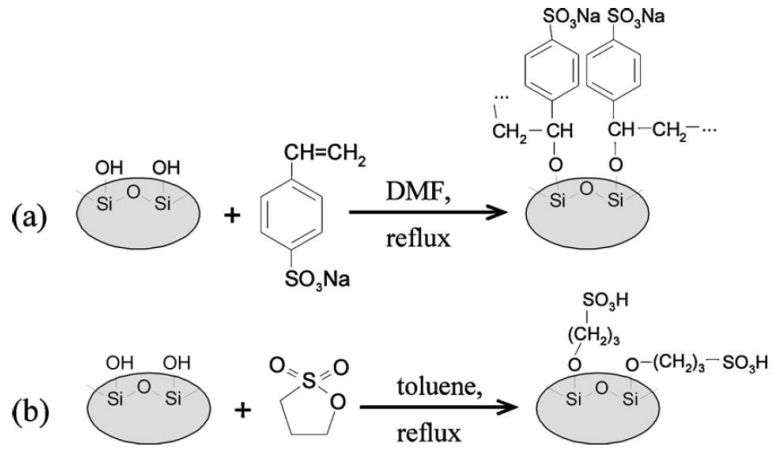

Fig. 1.36. Modification process of sulfonated Laponite synthesized with (a) p-styrene sulfonic acid sodium salt and (b) 1,3-propane sultone sodium salt [37]. Copyright 2011, Reproduced with permission from Elsevier Ltd.

(b) Water uptake and swelling: Water uptake measured at 85℃ of pristine Nafion membrane reduced with increased time, whereas Nafion/p-styrene sulfonate-grafted Laponite and Nafion/1,3-propane sultone-grafted Laponite composite membranes resulted in the raised water uptake. The reason for the improved value is that introduction of modified Laponite delayed dehydration of the composite membrane. [37]. Water loss of pristine Nafion and Nafion/styrene sulfonic-grafted Laponite membranes was analyzed by Bébin, Philippe and co-workers. Pristine Nafion membrane showed 4% higher water loss than the composite membrane, and this result is due to the high water uptake and the slow dehydration kinetics of the composite membrane. Also, water adsorption ratio was proportional to thickness swelling [33].

(c) Proton conductivity: Nafion/p-styrene sulfonate-grafted Laponite and Nafion/1,3-propane sultone-grafted Laponite composite membranes showed reduced proton conductivity despite good water uptake compared with commercial Nafion membrane as shown in Fig. 1.37. This is due to different distribution of ion-conducting domains for membrane [37]. Operating under high relative humidity improved the proton conductivity of Nafion/styrene sulfonic-grafted Laponite membranes as shown in Fig. 1.38. Also, proton conductivity of composite membrane tested at 98%RH and 25℃ led to better performance (i.e., about 0.03 S cm^{-1}) compared with that of commercially available Nafion 115 membrane (see Fig. 1.38) [33].

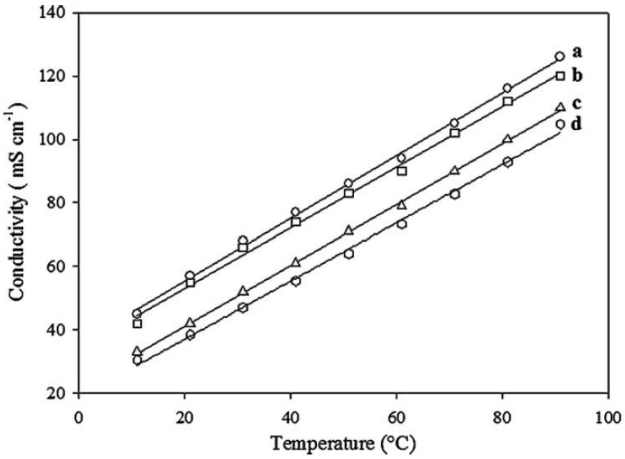

Fig. 1.37. Proton conductivity of (a) commercial Nafion – NRE212, (b) commercial Nafion – NRE211, (c) Nafion/p-styrene sulfonate-grafted Laponite and (d) Nafion/1,3-propane sultone-grafted Laponite composite membranes [37]. Copyright 2011, Reproduced with permission from Elsevier Ltd.

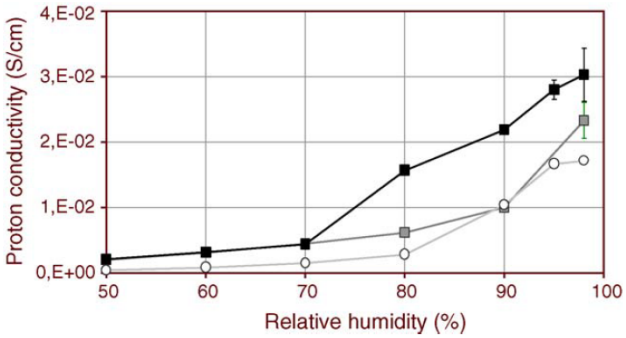

Fig. 1.38. Proton conductivity of the membranes measured under condition of 25℃ and various relative humidity: (○) Nafion 115, (■) Nafion/unmodified Laponite and (■) Nafion/styrene sulfonic-grafted Laponite membranes [33]. Copyright 2006, Reproduced with permission from Elsevier Ltd.

3.3.2.2. SPAES matrix

(a) Membrane preparation: Kim, Deuk-Ju, et al. reported synthesis of sulfonated Laponite with 3-MPTMS via cation exchange method as can be seen in Fig. 1.39 [90]. To begin with, 3-MPTMS was dropped into Laponite suspension and then it was oxidized prior to obtaining sulfonated Laponite. SPAES and sulfonated Laponite were blended with NMP solution in order to obtain SPAES/sulfonated Laponite dispersion [90]. UV-crosslinkable SPAS was functionalized with Laponite

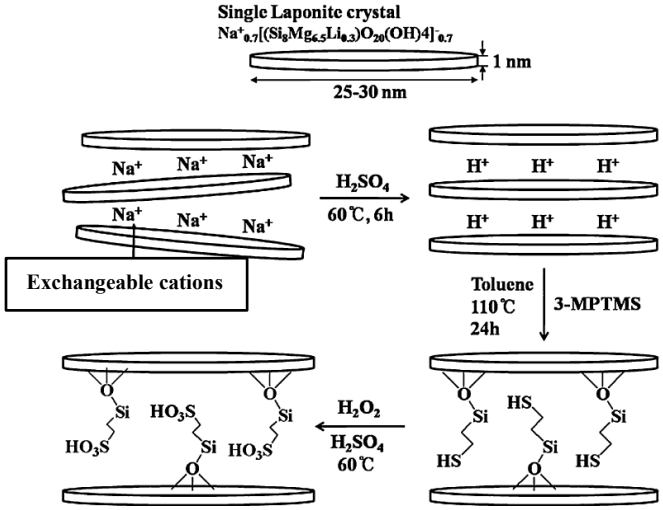

Fig. 1.39. Laponite sulfonated using H_2SO_4 and H_2O_2 through exchangeable cations [90]. Copyright 2012, Reproduced with permission from Elsevier Ltd.

(b) Water uptake: Kim, Deuk-Ju, et al. compared water uptake of pristine SPAES and SPAES/3-MPTMS-modified Laponite (i.e., SPAES SLa20 series) membranes under various temperatures. Water uptake of all membranes improved with increasing temperature because higher temperature results in augmented polymer chain mobility and free volume for water absorption as shown in Fig. 1.40. Addition of 3-MPTMS-modified Laponite showed higher water uptake than SPAES/pristine Laponite membrane due to the increased hydrophilic property caused by the sulfonated Laponite [90].

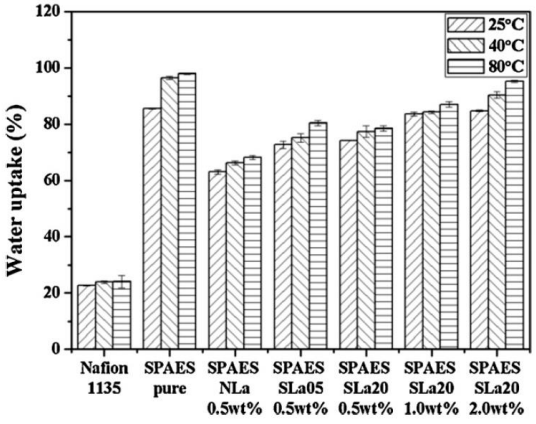

Fig. 1.40. Water uptake of pristine Nafion, pristine SPAES, SPAES/Laponite and SPAES/3-MPTMS-modified laponite membranes [90]. Copyright 2012, Reproduced with permission from Elsevier Ltd.

(c) Thermal property, mechanical stability and proton conductivity: Incorporation of 3-MPTMS-modified Laponite within SPAES membrane led to about 2 times higher tensile strength than pure SPAES membrane, but slightly grew proton conductivity. In addition, blending of Laponite augmented thermal resistance, whereas sulfonic acid group of 3-MPTMS-modified Laponite thermally cracked between 200 and 500℃ [90].

3.3.3. Other type of Laponite addtivie

3.3.3.1. Nafion matrix

(a) Membrane preparation: Mishra, Ananta Kumar, et al. replaced Na^+ ion to H^+ for Laponite by acid activation peptizer ($Na_4P_2O_7$) before membrane formation. Acid activation led to hydrogen bonding between *in-situ* generated phosphoric acid and Nafion due to hydrolysis on nanoclay [41].

(b) Water uptake: Addition of Laponite activated by peptizer ($Na_4P_2O_7$) into Nafion ionomer led to a raised water uptake compared to pristine Nafion membrane due to the hydrophilicity. However, strong hydrogen bonding between H_3PO_4 and H_2O molecule (i.e., *in-situ* generated phosphoric aicd and Nafion) allowed Nafion/H_3PO_4-activated Laponite composite membrane to have superior water uptake compared with that of Nafion/$Na_4P_2O_7$-activated Laponite composite membrane [41].

(c) Mechanical and thermal properties: Mishra, Ananta Kumar, et al. also conducted dynamic mechanical analysis of Nafion membrane containing Laponite activated by peptizer ($Na_4P_2O_7$). More specifically, pristine Nafion membrane showed 39.2 - 721 MPa of storage modulus at between -30 and 100℃, whereas incorporation of 3 wt% $Na_4P_2O_7$-activated Laponite into Nafion matrix reduced the storage modulus due to augmented incompatibility between Nafion and phosphoric acid-activated Laponite. However, addition of H_3PO_4-activated Laponite (3 wt%) resulted in maximum value (100 - 1600 Mpa). Moreover, The composite membrane had increased thermal stability compared with pristine Nafion membrane [41].

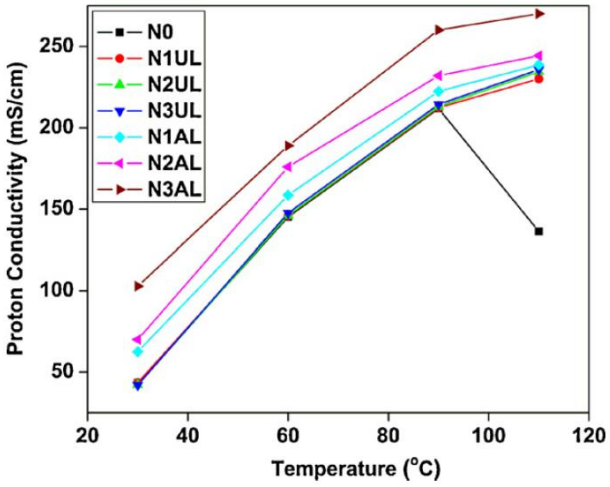

Fig. 1.41. Proton conductivity of (a) pristine Nafion (i.e., N0), (b) Nafion/$Na_4P_2O_7$-activated Laponite (i.e., N*x*UL series) and (c) H_3PO_4-activated Laponite (i.e., N*x*AL series) membranes [41]. Copyright 2012, Reproduced with permission from Elsevier Ltd.

(d) Proton conductivity: Nafion/3 wt% H_3PO_4-activated Laponite composite membrane exhibited higher proton conductivity than pristine Nafion and Nafion/3 wt% $Na_4P_2O_7$-activated Laponite composite membranes, as can be seen in Fig. 1.41. This result is due to highly conductive H_3PO_4 modified on Laponite surface. Pristine Nafion membrane showed the outstanding decrease as the membrane was dehydrated above 90℃, thereby blocking the ion pathway within Nafion [41].

3.3.3.2. PBI matrix

(a) Membrane preparation: Plackett, David, et al prepared PBI/modified Laponite composite membranes. In the study, imidazole salt-modified and dequalinium chloride salt-modified Laponites were used for preparation of composite membranes. PBI was modified from isophthalic acid and 3,3'-diaminobenzidine tetrahy-drochloride and in PPA via polycondensation [172].

(b) Water uptake and Swelling: Plackett, David, et al. studied acid doping test in order to understand volume swelling of pristine PBI, PBI/imidazole salt-modified Laponite, and PBI/dequalinium chloride salt-modified Laponite composite membranes. The swelling of composite membranes immersed in 65 - 75 wt% H_3PO_4 at room temperature reduced to approximately 12%. This swelling ratio decreased with decreasing water uptake. [172].

(c) Mechanical stability and proton conductivity: The composite membranes exhibited a stable mechanical strength due to much less swelling, and thus this property improved the proton conductivity to 0.12 S/cm at 150℃ and 12%RH.

3.4. Effect of halloysite type additive

HNT was incorporated into Nafion, SPEEK or PEG phase of electrolyte membranes. HNTs were functionalized with sulfonic, amino or other type group. Table 1.5 summarizes the data on chemical composition and proton conductivity of composite membranes containing modified HNT.

Table 1.5. Summary data on membrane casting dispersions composed of halloysite and ionomer, and proton conductivity of prepared membranes.

Filler type	Additives	Polymer powder/ polymer dispersion	Solvent/ non-solvent	Preparation method of composite membrane	Additive content over the casting dispersion (wt%)	Operating temp. (℃)	RH (%)	Proton conductivity of modified membrane (S cm^{-1})	Year of publication	Ref.
HNT	Pristine HNT	Nafion	DMF	Casting-evaporation process	-	-	-	-	2015	[29]
HNT	HNT/PWA	SPEEK	DMAc	Doctor blade method	30	Room	-	0.02037	2018	[120]
HNT	Pt-modified HNT	Nafion	DMF	Casting-evaporation process	-	-	-	-	2016	[174]

Filler type	Additives	Polymer powder/ polymer dispersion	Solvent/ non-solvent	Preparation method of composite membrane	Additive content over the casting dispersion (wt%)	Operating temp. (℃)	RH (%)	Proton conductivity of modified membrane (S cm^{-1})	Year of publication	Ref.
HNT	MPS-modified HNT	SPEEK	DMF	Casting-evaporation process	10	80	100	0.0521	2014	[47]
HNT	Dopamine-modified HNT	SPEEK	DMF	Casting-evaporation process	30	25	100	0.018	2013	[40]
HNT	SSA-modified HNT	SPEEK	DMAc	Casting-evaporation process	15	25	-	0.043	2016	[42]
HNT	MPS-modified HNT/CS/SPNF	SPEEK	Acetic acid/water	Casting-evaporation process	5	90	100	0.12	2016	[46]
HNT	Pristine HNT	PEG	Water	Casting-evaporation process	-	-	-	-	2013	[30]

3.4.1. Pristine HNT additive

3.4.1.1. Nafion matrix

Filippov, Anatoly, et al. fabricated Nafion membrane blended with pristine HNT, and analyzed the diffusion permeability for Nafion/HNT composite membrane according to Nernst-Planck approach. In the study, it was demonstrated that blending of 5 wt% HNT in Nafion dispersion showed improved ion exchange capacity compared to blending of 8 wt% HNT due to effective averaged mobility. This implies that control of HNT amount can be important factor to improve proton conductivity of electrolyte composite membrane [29].

3.4.1.2. PEG matrix

Cavallaro, G., et al. prepared PEG/HNT membrane by blending of HNT in PEG 20000 solution [30]. Addition of 10 wt% HNT in PEG 20000 resulted in compact nanomaterial, whereas blending of 50 wt% HNT led to sponge-like structure of the membrane. More specifically, incorporation of 10 wt% HNT displayed membrane structure with compact nanocomposite, accordingly it showed higher thermal stability compared with membrane containing 50 wt% HNT, due to craters and voids. Activation energy for PEG crystallization decreased with increasing concentration of HNT. This implies that PEG crystallization is more diffused by blending of HNT compared with blending of no additive [30].

3.4.2. Sulfonated HNT additive

3.4.2.1. SPEEK matrix

(a) Membrane preparation: Zhang, Haoqin, et al. prepared SPEEK/sulfonated HNT membrane by casting. Sulfonated HNT was blended in SPEEK and chitosan solutions for preparation of sulfonated HNT-based membranes. In order to enhance proton conductivity, HNT was sulfonated with sulfuric acid by distillation-precipitation polymerization. Also, PEEK pellets were dispersed in sulfuric acid solution in order to obtain SPEEK [47]. Zhang, Haoqin, et al, moreover, prepared CS membranes with dual-interfacial proton-conducting pathways. The dual interfaces form two pathways for efficient proton transfer inside membrane. The membrane with interfacial regions was prepared by blending of MPS-modified HNT in SPEEK/CS solutions. MPS was dispersed in mixture of styrene, sodium-p-styrenesulfonate and AIBN in order to synthesize sulfonated HNT [46].

(b) Water uptake and swelling ratio: Addition of MPS-modified HNT in SPEEK allowed membrane to reduce water uptake because the decreased ionic channel size led to small water storage space in cross section. Incorporation of SSA-modified HNT allowed SPEEK membrane to form the uniform morphology with voids, accordingly it improved hydrophilicity. More specifically, SPEEK membrane blended with SSA-modified HNT displayed approximately 10% higher water uptake than SPEEK membrane containing HNT and dopamine-modified HNT. Swelling ratio grew with improved water uptake, caused by water adsorption of membrane [42].

(c) Thermal and mechanical properties: Incorporation of MPS-modified HNT in SPEEK phase exhibited improved thermal and mechanical properties for composite membranes due to interfering with SPEEK chain motion and packing, compared with SPEEK membrane [46, 47]. In addition, SPEEK/SSA-modified HNT (15 wt%) showed the highest mechanical properties for elastic modulus (i.e., 1393 MPa) and tensile strength (i.e., 84 MPa) [42]

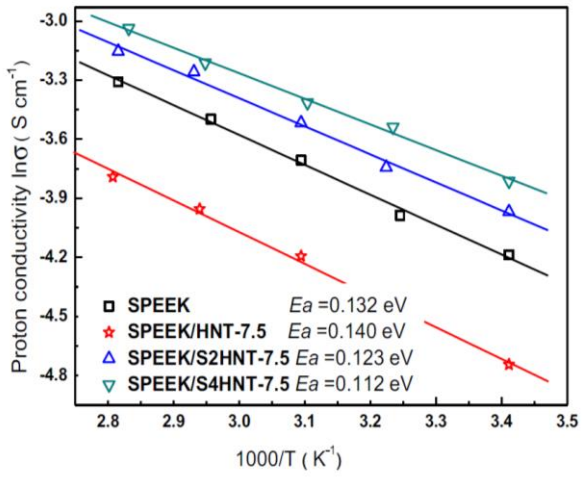

Fig. 1.42. Data on proton conductivity of SPEEK/sulfonated HNT composite membrane measured at 100% RH [47]. Copyright 2014, Reproduced with permission from Elsevier Ltd.

(d) Proton conductivity: As shown in Fig. 1.42, proton conductivity of SPEEK/HNT sulfonated with MPS displayed increased value due to the presence of sulfonic (i.e., $–SO_3H$) group on HNT surface [46, 47]. Reduced activation energy was achieved for promoted proton transport of composite membrane containing SSA-modified HNT. SPEEK/SSA-modified HNT composite membrane improved proton conductivity due to long shaped-

nanotube and well-organized matrix. However, high concentration (i.e., ≥15 wt%) of pure HNT, dopamine-modified HNT and SSA-modified HNT blocked membrane pathway for proton transport, resulting in reduced proton conductivity as shown in Fig. 1.43 [42].

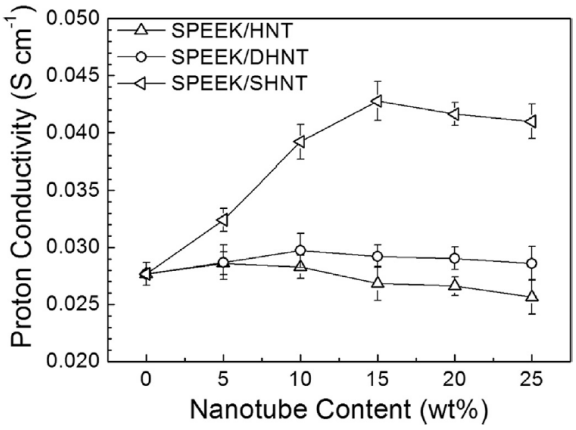

Fig. 1.43. Proton conductivity of SPEEK/HNT, SPEEK/dopamine-modified HNT and SPEEK/SSA-modified HNT membranes [42]. Copyright 2016, Reproduced with permission from Elsevier Ltd.

3.4.2.2. CS/SPNF matrix

Addition of MPS-modified HNT into CS/SPNF polymer showed lower water uptake value compared with that of pristine CS and CS/SPNF membranes. Mechanical strain stress and swelling ratio of membranes reduced in the order of pristine CS > CS/SPNF > CS/SPNF/sulfonated HNT. Also, hydrated (100% RH) and anhydrous (under 0% RH) proton conductivity of CS/SPNF/sulfonated HNT membrane displayed higher values compared with those of CS and CS/SPNF membranes at 25 – 90 ℃ due to the dual-interfacial proton-conducting pathways (see Fig. 1.44) [46].

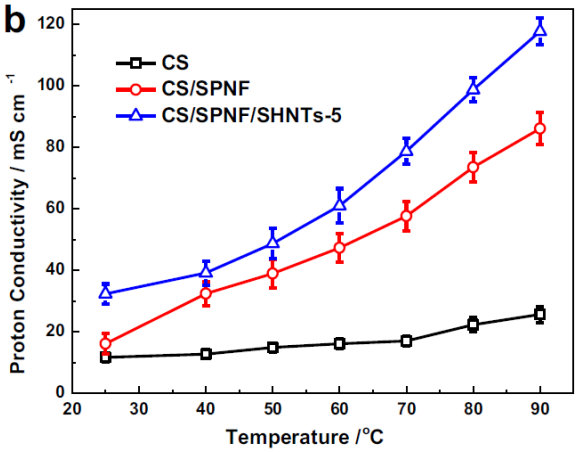

Fig. 1.44. Temperature-dependent conductivity of CS, CS/SPNF and CS/SPNF/MPS-modified HNT composite membrane measured at 100% RH [46]. Copyright 2016, Reproduced with permission from Elsevier Ltd.

3.4.3. Aminized HNT additive

(a) Membrane preparation: Zhang, H., et al. prepared SPEEK composite membrane containing dopamine-modified HNT with –NH and $–NH_2$ groups. Dopamine-modified HNT was synthesized by the bioadhesion principle. Aqueous dopamine solution was dissolved in Tris solution, and then mixture was immersed with HNT [40]. X. Liu et al. prepared pristine SPEEK, SPEEK/HNT, SPEEK/DHNT and SPEEK/DHNT-SSA membranes. HNT was sulfonated with grafting PSSA (polystyrene sulfonic acid) by ATRP process, on dopamine-modified HNT [42].

(b) Water uptake, thermal stability and proton conductivity: Addition of dopamine-modified HNT into SPEEK phase of composite membrane led to improved water uptake and proton conductivity as can be seen in Fig. 1.47 due to effective electrostatic interaction and acid-base paired structure resulted from dopamine-modified HNT and SPEEK interface, but area swelling was augmented. Also, thermal decomposition of composite membrane was not altered by blending with aminized HNT. However, blending of pristine HNT decreased water uptake of SPEEK/ HNT composite membrane due to reduced size of ion channels and water storage capacity, thereby reduction of proton conductivity (see Fig. 1.45) [40].

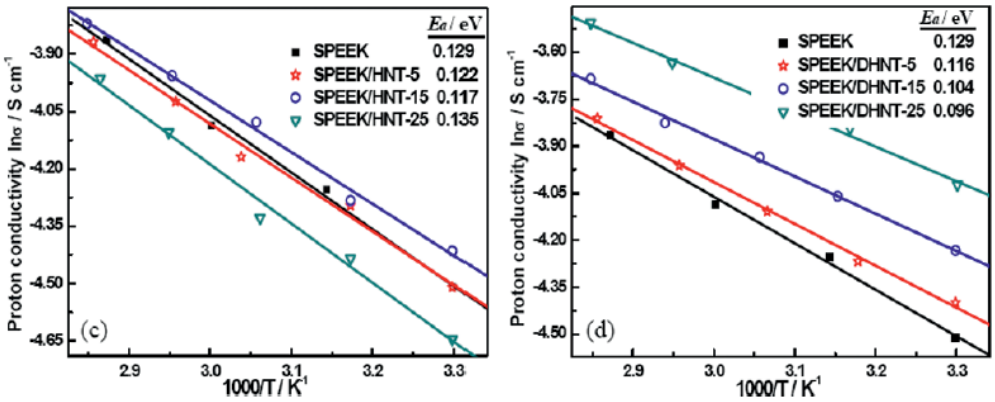

Fig. 1.45. Temperature-dependent conductivity of SPEEK, SPEEK/unmodified HNT and SPEEK/dopamine-modified membranes [40]. Copyright 2016, Reproduced with permission from Wiley.

3.4.4. Other type of HNT additive

3.4.4.1. Nafion matrix

Filippov, Anatoly, et al. developed a new model by using Nafion/platinum-modified HNT and Nafion/iron nanoparticle-modified HNT hybrid membranes. The model was made based on fine porous membrane in order to calculate the physic-chemical parameters such as ambipolar diffusion and equilibrium distribution coefficients of the electrolyte within the membrane. Based on new method, it was demonstrated that Nafion membrane containing HNT encapsulated by platinum is desirable for the use in fuel cells while exhibiting high proton conductivity compared to pristine Nafion and Nafion/iron nanoparticle-modified HNT membranes [174].

3.4.4.2. SPEEK matrix

In order to obtain HNT impregnated with PWA, HNT was dried and then dispersed in water/PWA solution. HNT/PWA-blended SPEEK composite membranes were prepared via Doctor blade method [120]. The composite membranes showed improved mechanical resistance, low crossover and proton conductivity (88%), but decreased water uptake compared with pristine SPEEK membrane. According to analysis evaluated by hydrogen pumping system, 15% of HNT/PWA led to low energy consumption for proton transport from anode to cathode at 0.4 A cm^{-2} due to improved proton conductivity provided by the phosphotungstic acid, as well as delayed dehydration caused by HNT [120].

3.5. Effect of sepiolite type additive

Sepiolite series were incorporated into Nafion, PES, SPEK and SPSEBS matrices. Sepiolites were functionalized with sulfonic or perfluorosulfonic group. Table 1.6 summarizes the data regarding chemical composition and proton conductivity of composite membranes blended with modified sepiolite.

Table 1.6. Summary data on membrane casting dispersions composed of sepiolite and ionomer, and proton conductivity of prepared membranes.

Filler type	Additives	Polymer powder/ polymer dispersion	Solvent/ non-solvent	Preparation method of composite membrane	Additive content over the casting dispersion (wt%)	Operating temp. (°C)	RH (%)	Proton conductivity of modified membrane (S cm^{-1})	Year of Publi-cation	Ref.
SEP	Pristine SEP	PES (55 wt%)	DMF/ THF	Dual electrospinning process	4	80	-	0.28	2015	[31]
SEP	Pristine SEP	SPEK (35 wt%)	DMF/ THF	Dual electrospinning process	8	80	-	0.133	2015	[31]
SEP	Pristine SEP	Nafion	ethanol/ water	Casting-evaporation process	10	80	-	0.0624	2010	[175]
SEP	SSA-modified SEP	Nafion	1-propa-nol	Casting-evaporation process	10 (corresponding to Nafion amount)	-	-	-	2013	[39]
SEP	PSA-modified SEP	SPSEBS	THF	Casting-evaporation process	10	100	< 100	0.013	2010	[32]
SEP	PSA-modified SEP	Nafion	THF	Casting-evaporation process	10	80	< 100	0.024	2010	[32]
SEP	PSA-modified SEP	SPSEBS	Chlorof orm/ ethanol	Casting-evaporation process	10	80	100	0.0354	2007	[49]
SEP	PSA-modified SEP	Nafion	Chlorof orm/ ethanol	Casting-evaporation process	10	80	100	0.031	2007	[49]
SEP	SEP modified with SSA and perfluoroocta noic acid	Nafion	1-propa-nol	Casting-evaporation process	10 (corresponding to Nafion amount)	25	100	0.021	2015	[38]

3.5.1. Pristine SEP additive

Oroujzadeh, Maryam et al reported non-sulfonated PES/raw SEP and SPEK/raw SEP composite membranes prepared by dual electrospinning process as shown in Fig. 30a-c. Initially, electrospun mats were prepared and then the blended composite mats were pressed. Afterwards, hot-pressing was conducted at hot temperature of 220℃ (see Fig. 1.46bc). For polymer modification, non-sulfonated PES was prepared by addition of BCPS, PBP and DMAc in three necked flask, as well SPEK was synthesized with PBP and SDFB which was sulfonated with sulfuric acid and DFB as can be seen in Figs. 46de [31, 176].

Introduction of SEP into Nafion matrix presents good interaction, thereby enhanced glass transition temperature and mechanical property of composite membrane. Also, addition of SEP did not block the pathway of proton movement within membrane [32]. According to literature [39], it was demonstrated that the composite membrane based on Nafion and unmodified SEP showed improvement of water uptake and mechanical characteristic, but reduced proton conductivity [39].

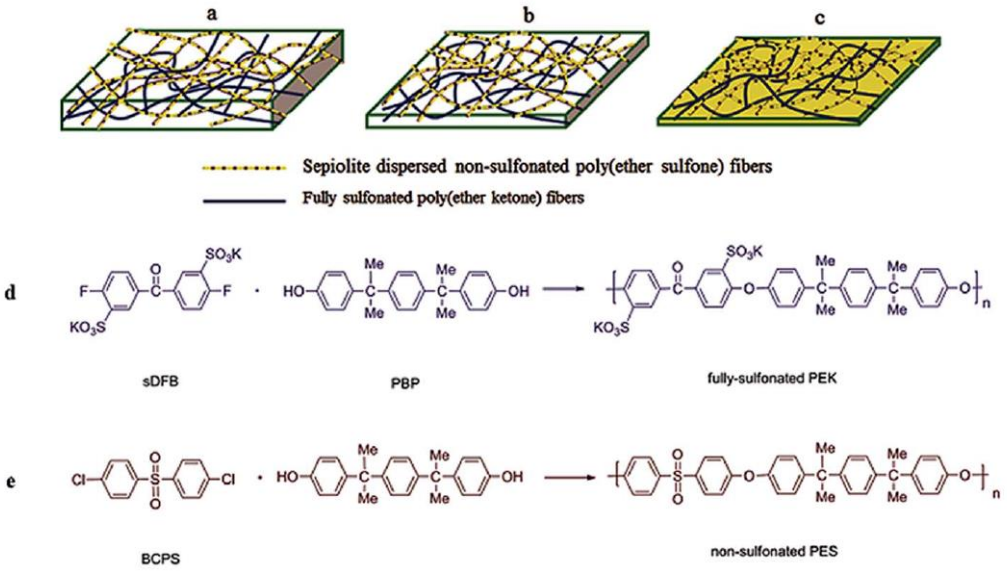

Fig. 1.46. Schematic illustration of (a) the prepared electrospun mat, (b) the compressed membrane, and (c) the hot-pressed membrane. Synthesis process of (d) SPEK and (e) non-sulfonated PES [31]. Copyright 2015, Reproduced with permission from Royal Society of Chemistry.

3.5.2. Sulfonated SEP additive

3.5.2.1. Nafion matrix

(a) Membrane preparation: Fernandez-Carretero's group prepared Nafion/PSA-modified SEP. For sulfonated nanoclay, SEP was synthesized by addition of phenyl-tri-ethoxy-silane, HCl and isopropanol under stirring [32, 49, 175]. Beauger's research group synthesized epoxy functionalized SEP with sulfonic acid group (i.e., $-SO_3H$) as shown in Fig. 1.47. Afterward, Nafion membranes incorporated with SSA-modified SEP were prepared in order to compare Nafion/SEP membrane with Nafion/sulfonated SEP membranes [39].

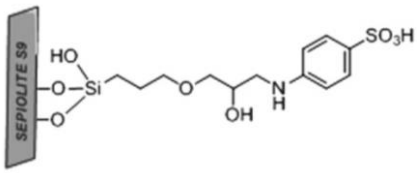

Fig. 1.47. Structure of SEP functionalized with sulfonic acid [39]. Copyright 2013, Reproduced with permission from Elsevier Ltd.

(b) Water uptake, swelling and mechanical strength: Blending of PSA-modified SEP with Nafion decreased water uptake and enhanced mechanical characteristics compared to pristine Nafion. The reason why introduction of PSA-modified SEP led to reduced water uptake is low sulfonation index. Incorporation of SSA-modified SEP into Nafion matrix (i.e., M112S10SH series) led to raised hygroscopic property as SEP was synthesized with SSA containing sulfonic group. Swelling ratio was grew according to high SEP contents and sulfonation, caused by better water adsorption, and improved homogeneity of composite membrane had influence on the mechanical strength [39]

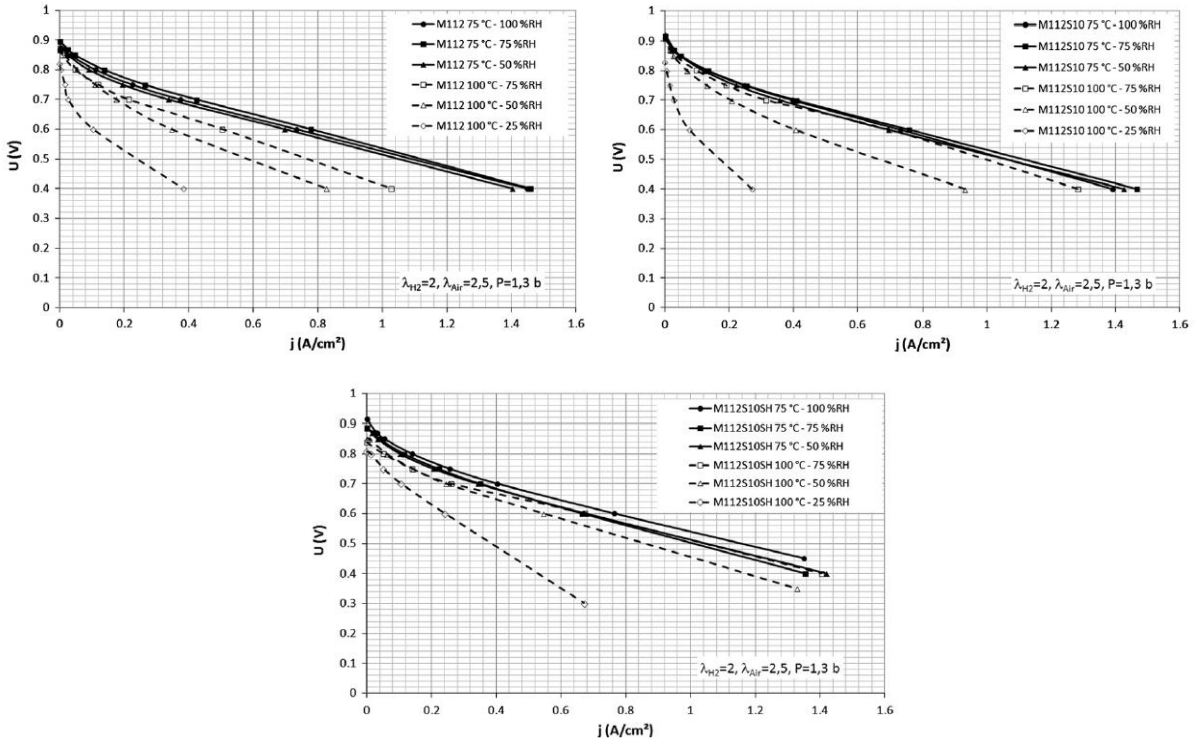

Fig. 1.48. Polarization curves obtained during MEA test of (top left) pristine Nafion (i.e., M112), (top right) Nafion/SEP (i.e., M112S10), and (bottom) Nafion/SSA-modified SEP (i.e., M112S10SH) membranes measured at 75℃ (solid lines) and 100℃ (dashed lines), between 25 and 100% RH [39]. Copyright 2013, Reproduced with permission from Elsevier Ltd.

(c) Proton conductivity: Nafion/SSA-modified SEP composite membrane improved performance for fuel cell application compared with pristine Nafion (i.e., M112 series) and Nafion/pure SEP membranes (i.e., M112S10 series). That is, as shown in Figs. 1.48a-c, composite membrane composed of Nafion and SSA-modified SEP resulted in improved performance under condition of high temperature and low relative humidity, based on polarization curve obtained by MEA test [39].

3.5.2.2. SPSEBS matrix

Fernandez-Carretero's group prepared made SPSEBS/PSA-modified SEP membranes. In the study, SPSEBS was sulfonated *in situ* by reaction of acetyl sulfonate, acetic anhydride, sulfuric acid, and dichloro ethane solution. PSA-modified SEP was sulfonated by phenyl-tri-ethoxy-silane, HCl and isopropanol [32, 49, 175].

SPSEBS composite membrane containing PSA-modified SEP was characterized for water uptake, conductivity and mechanical properties. SPSEBS/PSA-modified SEP composite membranes displayed decreased water uptake compared with pristine SPSEBS membranes. Proton conductivity measured at 80℃ showed 1.6 and 2.4 S/cm for Nafion/PSA-modified SEP and SPSEBS/PSA-modified SEP composite membranes, respectively. However, pristine Nafion membrane showed 2.3 S/m for proton conductivity at same condition. Mechanical stress of membrane composed of Nafion and PSA-modified SEP displayed the highest value among all the membranes tested at the breaking point [32, 49].

3.5.3. Perfluorosulfonated SEP additive

(a) Membrane preparation: Beauger, Christian, et al. synthesized double functionalized SEP, i.e., SEP perfluorosulfonated using SSA and $-C_7F_{15}$ group, as shown in Fig. 1.49 prior to Nafion composite membrane blended with the modified SEP was prepared via casting and evaporation [38].

(b) Mechanical stability: Introduction of perfluorosulfonated SEP (synthesized with SSA and $-C_7F_{15}$ group) within Nafion membrane has good mechanical resistance with decreased swelling ratio. More specifically, the elastic modulus of Nafion/sulfo-fluorinated SEP hybrid membrane was 200 - 250 Mpa superior to that of Nafion/SSA-modified SEP (i.e., sulfonated SEP) hybrid membrane. This is because the fluorination ($-C_7F_{15}$ group) of SEP improved the mechanical property caused by affinity with Nafion matrix [38].

(c) Water uptake and proton conductivity: In terms of hydrophilicity of composite membrane, incoporation of sulfo-fluorinated SEP (10 wt%) into Nafion matrix showed similar water uptake to Nafion membrane containing SSA-modified SEP, but the increased amount (20 wt%) of sulfo-fluorinated SEP resulted in the improved value by about 4 wt%. Nafion/sulfo-fluorinated SEP also displayed approximately 50% improved output power at 100 ℃ and 50% RH compared with pristine Nafion membrane as shown in Fig. 1.50 [38].

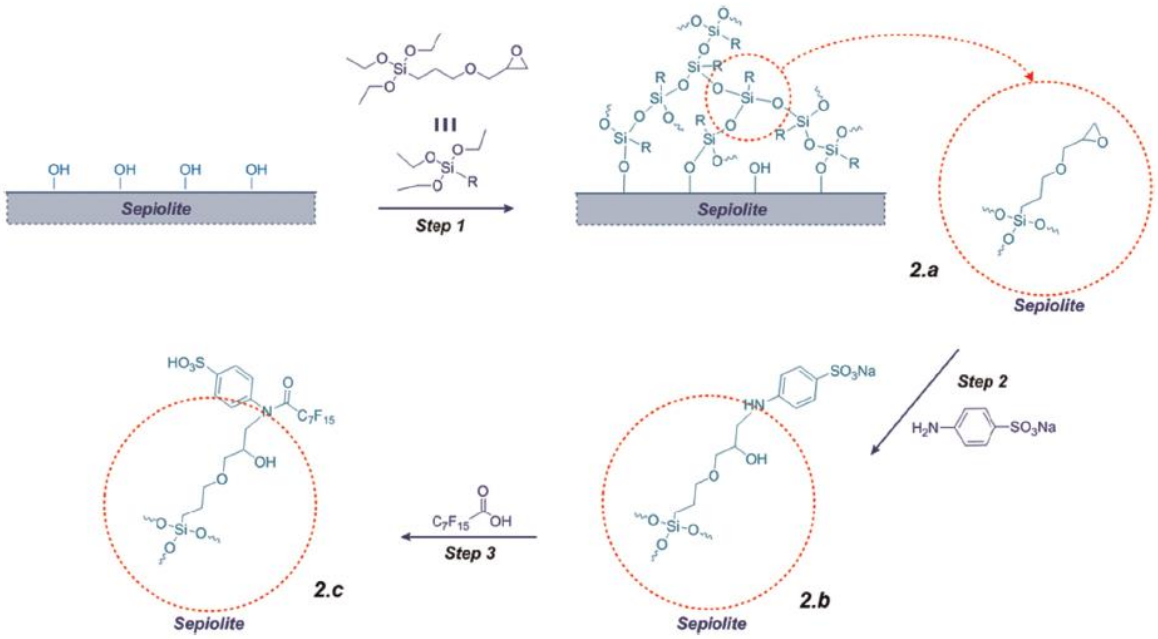

Fig. 1.49. Perfluorosulfonated SEP, which introduces $–SO_3H$ and $–C_7F_{15}$ groups [38]. Copyright 2015, Reproduced with permission from Elsevier Ltd.

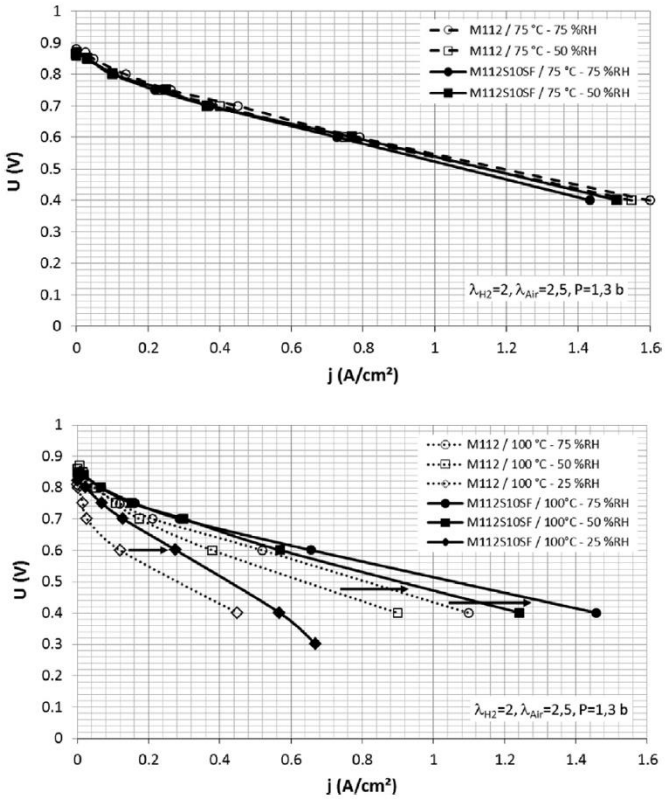

Fig. 1.50. Polarization curves of pristine Nafion (dotted lines) and Nafion/sulfo-fluorinated SEP membranes (solid lines) measured at 75 °C and 100 °C between 25% RH and 75% RH [38]. Copyright 2015, Reproduced with permission from Elsevier Ltd.

Conclusion

Perfluorosulfonic acid (i.e., PFSA) and non-fluorinated hydrocarbon membranes as electrolyte are used in PEMFC. Nanoclay-based PFSA composite membranes are typically made of Nafion. The polymer matrix of the hydrocarbon electrolyte membranes consists of polyetheretherketone (PEEK), polyvinyl alcohol (PVOH), polybenzimidazole (PBI), polyphenylene oxide (PPO) or polysulfone (PSU). However, Nafion, PEEK, PVOH, PPO and PSU membranes have the limitation of the reduced performance caused by the decreased proton conductivity under condition of low relative humidity and high temperature above 90℃. PBI membrane shows low proton conductivity below 100℃, and hence requires high temperature of above 160℃ during fuel cell operation. Hence, numerous research engineers have attempted to overcome the limitation by development of various composite membranes. Improved physicochemical properties of electrolyte membranes can be obtained by incorporating different kinds of inorganic additives into polymer matrix. Generally, inorganic fillers include inorganic oxides, zeolites and nanoclays. Nanoclays have been used for a long time as montmorillonite (MMT) and Laponite as additives for composite membranes, and recently halloysite (HNT) or sepiolite (SEP) has also been used. Hydroscopicity of clay nanoparticles can prevent dehydration so that the composite membrane conducts at low relative humidity. Also, incorporating the nanoclays functionalized with fluorination, sulfonation, perfluorosulfonation or amino group into polymer phase can offer a promising strategy on improved properties, e.g., water management, mechanical resistance (including compatibility), chemical degradation, and proton conductivity, of composite membranes. The results of membrane characteristics can be summarized as follows.

Composite membrane could have delayed dehydration with hygroscopic property, thereby good performance of composite membrane at low relative humidity. Sulfonated, perfluorosulfonated, aminized and phosphated nanoclays lead to increased hydrophilicity and hygroscopicity of PFSA and non-fluorinated hydrocarbon composite membranes. To be specific, composite dispersions blended with sulfonated and perfluorosulfonated nanoclays form composite membranes which have hydrophilic sulfonic acid groups, hydrophobic fluorinated groups, and uniform morphology with voids. Sulfonated polymers lead to augmented water uptake with functionalized nanoclays, e.g., aminized HNT which forms acid-base paired structure. Presence of –OH and $–NH_2$ groups of aminized MMT, moreover, allows to grow in hydrophilicity of composite membrane, but incorporation of Cloisite 15A and TAP inside SPEEK formed composite membrane with narrow and branched water channel. Phosphated laponite also improves water uptake owing to strong hydrogen bonding between phosphate group and water molecules. However, decreased ionic channel size caused by MPS-modified HNT, one of sulfonated HNT, incorporated in SPEEK matrix in turn results in small water storage space, which is the structure that is not easy to absorb the water molecules, thereby reducing water uptake.

High durability and mechanical resistance of composite membrane could require complete dispersion or exfolication of nanoclay, thereby good interfacial compatibility between polymer and nanoclay. In general, functionalized nanoclay generally augments mechanical resistance but decrease swelling ratio of composite membranes. This is due to decreased crystallinity of polymer with layered silicate nanoclays such as MMT and Laponite. Effect of nanotube shape of HNT on chain packing as well as good hygroscopicity of SEP also causes improved mechanical property and reduced swelling of membranes. In particular, presence of fluorinated groups synthesized on nanoclay surface helps composite membrane to grow mechanical resistance. However, plasticizing effect of phosphoric acid within aminized MMT-based composite membrane reduces mechanical resistance, and

also phosphated laponite decreases mechanical stability due to incompatibility between polymer and phosphoric acid group, whereas TAP is used as compatibilizer for SPEEK/Cloisite 15A/TAP composite membrane, thereby improved homogeneity and mechanical property.

Functionalized nanoclay-incorporated membranes generally show increased thermal stability compared with pristine membranes due to interaction between the nanoclays and polymer matrix. Accordingly, incorporating nanoclays delay the chemical degradation of composite membranes. For example, interaction between Cloisite 30B and polymer matrix forms ether linkage from the condensation of -OH groups, and hence blending of nanoclay delays the chemical decomposition of composite membrane. Composite membrane based on Nafion and Krytox-modified MMT is also good example of degradation at high temperature (i.e., 309.8 - 417.6℃) due to the interaction between the PTFE-like backbone of Nafion and the multilayer silicate of lipophilic nanoclays. In addition, the homogeneous distribution of nanoclay without aggregations and voids is also good factor to improve thermal stability of composite membranes, especially incorporation of HSO_3-RSR-modified MMTs, which are large interlayer distance caused by long chain sulfonic acid groups, lead to stable thermal property. Moreover, exfoliation of layered-silicate-shaped MMT, caused by e.g., chitosan functionalization, inside polymer phase also contributes to improved thermal property. Interaction of cross-linked polymers, without the help of nanoclay effect, could also cause the thermal properties of the membrane to stabilize.

Good proton conductivity can result from high mobility of ion carrier. The rate of proton conductivity is based on diffusion rate and free volume of ion channels within composite membrane. Proton conductivity of electrolyte membranes can be enhanced through introducing functionalized nanoclay, acid-base paired structure, dual interfacial proton-conducting pathways, hydrophilic-hydrophobic balance of sulfonated polymer/Cloisite series, or/and polymers synthesized with sulfonic acid group. However, high loading contents of functionalized nanoclay within PFSA and non-fluorinated membranes can lead to aggregation, resulting in low proton conductivity as nanoclay causes the blocking of ion pathway, and exfoliation. In addition to this, different distribution of ion-conducting domains leads to decreased proton conductivity of Nafion/p-styrene sulfonate-grafted laponite and Nafion/1,3-propane sultone-grafted laponite composite membranes despite having high water uptake. Weak interaction between inter-chains and basal spacing of vinyl ester and POPD-modified MMT, one of amizied MMT, also leads to composite membrane with reduced proton conductivity. Proton conductivity performed on the composite membranes was summarized as listed in Tables A1 and 1.3-1.5.

Based on this review, it can be summarized that water uptake, mechanical resistance, thermal stability, and proton conductivity of PEMs are likely to be enhanced by homogeneous dispersion, long chain functional group and loading content control of nanoclay, and introduction of compatibilizer, thereby improvement in PEMFC performance at high temperature and low relative humidity. Hence, aforementioned properties ultimately can allow polymer/nanoclay composite membranes to be suitable for use in PEMFC.

Further attempt to introduce perfluorosulfonated HNT and aminized SEP may be needed in order to analyze performance in PEMFC. Moreover, chemical stability regarding radical attack of composite membranes needs to be studied for future work.

Chapter 2

Experimental and characterization method

Summary

This chapter introduces experimental and analytical methods. Sepiolite or halloysite is functionalized with sulfonated and/or fluorinated groups. In the case of halloysite, quercetin was also grafted as an antioxidant group. The pure nanoclay and modified nanoclay were filtered to obtain uniform particles, and another was additionally pretreated using acidic solutions to remove iron inside sepiolites and halloysites. Modified nanoclays were characterized using ATR-FTIR (attenuated total reflection-fourier-transform infrared spectroscopy), TGA (thermal gravimetric analysis) and Py-GC/MS (pyrolysis-gas chromatography mass spectrometry). Detailed analysis results are described in chapters 4 - 6.

The sepiolites and halloysites, modified or not, were incorporated into Nafion or Aquivion matrix to prepare composite membranes. The electrolyte membranes were prepared via casting – evaporation method. How physicochemical properties of prepared membranes are analyzed through various analytical instruments is introduced. Cross section of prepared membranes was examined using FE-SEM to observe composite homogeneity. The chemical degradation of the membrane caused by C-F bond attack of radicals was verified using fluoride concentration. Mechanical strength of the membranes was measured at various temperatures. EIS (electrochemical impedance spectroscopy) was used to analyze the proton conductivity of electrolyte membranes. Preparation and test protocols of MEA (Membrane electrode assembly) were conducted under various conditions. In addition, analytical method on membrane thickness, water uptake, IEC (ion exchange capacity) and swelling ratio is introduced.

Résumé

Ce chapitre présente les méthodes expérimentales et analytiques. La Sepiolite ou l'halloysite est fonctionnalisée avec des groupes sulfonés et / ou fluorés. Dans le cas de l'halloysite une fonction antioxydante de type quercétine a été greffée. Les argiles pures et modifiées ont été filtrées pour obtenir des particules uniformes. Elles ont également été prétraitées à l'aide de solutions acides pour éliminer le fer pouvant être présent à l'intérieur des sépiolites et des halloysites. Les argiles ont été caractérisées par ATR-FTIR (spectroscopie infrarouge à transformée de Fourier, réflection totale atténuée), ATG (analyse thermique gravimétrique) et Py-CPG/SM (spectrométrie de masse à pyrolyse en phase gazeuse). Les résultats de l'analyse détaillée sont décrits aux chapitres 4 à 6.

Les sépiolites et halloysites, modifiées ou non, ont été incorporées à la matrice Nafion ou Aquivion pour préparer des membranes composites. Les membranes électrolytiques ont été préparées par coulée - évaporation. Les divers instruments utilisés pour caractériser les propriétés physicochimiques des membranes préparées sont présentées. La section transversale des membranes préparées a été examinée par microscopie électronique à balayage (MEB) pour observer l'homogénéité des composites. La dégradation chimique de la membrane provoquée par l'attaque des liaisons C-F par les radicaux a été vérifiée à l'aide d'une mesure de concentration en fluorure. La résistance mécanique des membranes a été mesurée à différentes températures. La spectroscopie d'impédance électrochimique (SIE) a été utilisée pour calculer la conductivité protonique des membranes électrolytiques. Les protocoles de préparation des assemblages membrane-électrodes (AME) et les conditions dans lesquelles les essais ont été réalisés sont présentés. De plus, les méthodes de mesure de l'épaisseur des membranes, de l'absorption d'eau, de la capacité d'échange ionique (CEI) et du taux de gonflement sont introduites.

1. Materials

Sepiolite was provided by Tolsa. N-(3-triethoxysilylpropyl)perfluorooctanoamide (SPFOA) was purchased from ABCR. Ethanol, acetone and tetrahydrofuran (THF) were purchased from Fisher Chemical. All these products were used for functionalization without further purification.

Halloysite was provided by Sigma Aldrich. Sodium 2,3-dihydroxynaphthalene-6-sulfonate and N-(3-triethoxysilylpropyl)perfluorooctanoamide were purchased from ABCR. Ethanol, acetone and tetrahydrofuran (THF) were purchased from Fisher Chemical. All these products were used for functionalization without further purification. Quercetin hydrate, N-(3-triethoxysilylpropyl)perfluorooctanoamide and (3-aminopropyl)triethoxysilane (APTES) were purchased from ABCR. Ethanol, acetone and tetrahydrofuran (THF) were purchased from Fisher Chemical. All these products were used for functionalization without further purification.

Nafion (15wt%, 1000 EW) was purchased by LQ1015, Ion Power, USA. Aquivion (24t%, D83-24B) was purchased by Solvay. Sulfuric acid (H_2SO_4, 5N), sodium hydroxide (NaOH, 98%) and hydrogen chloride (HCl, 0.1N) were purchased from Alfa Aesar, Germany. Hydrogen peroxide (H_2O_2, 6%) and oxalic acid (0.45M) were purchased from Fisher Scientific, UK. Sodium chloride (NaCl, 99.5%) and isopropanol (99.5%) were purchased from Acros Organics. Deionized (DI) water (18.2 MΩ·cm) was supplied from ultrapure water plants (Smart2Pure, Thermo Scientific).

Sepiolite or halloysite was functionalized with sulfonated and/or fluorinated groups; or grafted with quercetin with fluorinated or aminized group. A specific nomenclature was chosen to name samples:

- SEP and SEP-F represent pristine sepiolite and fluorinated sepiolite, respectively.
- HNT represents pristine halloysite. HNT-S, HNT-F and HNT-SF represent sulfonated halloysite, fluorinated halloysite, and sulfofluorinated halloysite, respectively.
- HNT-Q, HNT-FQ and HNT-NQ represent respectively pristine, fluorinated and aminized halloysite modified with quercetin.
- Prefix p represent pretreatment process using acidic solutions (see sections 2.2.4. and 2.2.5).

2. Experimental methods

2.1. Sepiolite modification

Sepiolite was functionalized with fluorine group. Functionalizations will be introduced in detail in the nanoclay functionalization section of each chapter.

2.2. Halloysite modification

Halloysite was functionalized by fluorination, sulfonation, or perfluorosulfonation. In addition, halloysite was grafted into pure quercetin, quercetin/fluorine group, or quercetin/amino group. Detailed explanation will be introduced in the nanoclay functionalization section of each chapter.

2.3. Filtration and acidic pretreatment of nanoclays

2.3.1. Filtration

Every nanoclay, modified or not, pretreated or not, were purified by filtration to remove bigger alien particles.

Filtration process was conducted in order to obtain uniform sized-nanoclays. 1 g of nanoclay was stirred in 100 ml DI-water for 4 h and then precipitated for 1 day before supernatant was removed. Aforementioned process was repeated 3 times under identical condition. Afterwards, remaining clay was distributed using ultrasound (HD 2070, Bandelin, Germany) for 2 min at 60 W power and 20% pulsation level. Filtration was performed by membrane filters with 45 μm and 25 μm pore size, after which filtrated nanoclay was dehydrated in oven at 80 ℃ for 16 h.

2.3.2. Pretreatment

Pretreatment was conducted in order to leach cations, especially iron ions, out from nanoclays to limit any further membrane chemical degradation. 1 g of nanoclay was pretreated by stirring in 100 cm^2 of 0.5 M oxalic acid solution at 80℃ for 2.5 h, and then it was filtrated using membrane filter (0.4 μm of pore size, Merck Millipore). Following this, nanoclay was washed using DI-water, after which nanoclay dispersion in DI-water was distributed using ultrasound (HD 2070, Bandelin, Germany) for 2 min at 60 W power and 20% pulsation level. Afterward, nanoclay was added into 0.001 M HCl solution (i.e., 1 g/100 cm^2) before it was stirred at 80 ℃ for 2.5 h for treatment. Filtration and ultrasound were repeated under identical condition. After that, pretreated nanoclay was precipitated in water and supernatant was removed. Last, filtration was conducted according to filtration protocol presented in section 2.3.

Prefix p represents pretreated nanoclay (e.g., pSEP-F, pretreated fluorinated sepiolite; pHNT-Q, pretreated halloysite modified with quercitine); no prefix means non-pretreated nanoclay (e.g., SEP, non-pretreated sepiolite; HNT, non-pretreated halloysite).

2.4. Membrane preparation

All membranes were prepared via a casting-evaporation process.

Dispersions were poured in a mold and heated in an oven in two steps, for “solvent” evaporation and membrane annealing.

The dispersions were actually poured on a cleaned glass plate which cannot be seen on Fig. 2.1.b. The size of the membrane is determined by that of the Teflon frame (white part on Fig. 2.1.b). After annealing, the membrane was recovered by dipping the glass plate in deionized (DI) water.

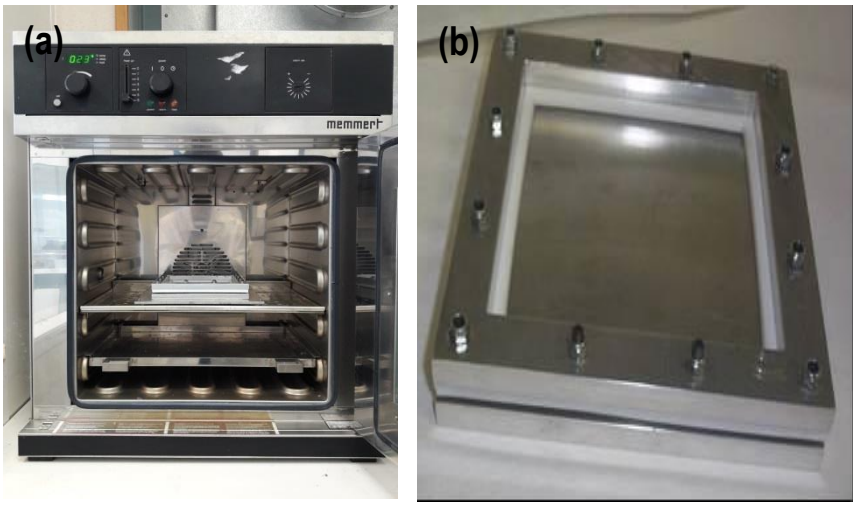

Fig. 2.1. Photo of (a) oven and (b) mold used for casting the membrane.

2.4.1. Nafion-based composite membranes

Nine different kinds of membranes (5 × 5 cm^2), as listed in Table 2.1, were prepared via casting-evaporation process with identical 10 wt% content of SEP and HNT. Each of the nanoclay dispersions was blended for 24 h, 5 h and 1 h. Following this, nanoclay dispersions were mixed with Nafion 1000 dispersion for 1 h. Stirring rate was set at 80 rpm. Afterward, Nafion/nanoclay dispersions were dispersed using ultrasound (HD 2200, Bandelin, Germany) titanium alloyed microtip (MS73-529, Sonopuls, Bandelin) for 2 min at 60 W power and 20% pulsation level. 2.5 g of the resultant dispersions were poured in a 5x5cm^2 mold and heated at 80 °C for 2 h and 120 °C for 1 h. The obtained membranes were treated for each 1 h in boiling 1) 0.5 M HNO_3, 2) 6% H_2O_2 and 3) 0.5 M H_2SO_4. Between each step, the membranes were washed in boiling (DI) water for 1 h.

Table 2.1. Chemical compositions of Nafion casting dispersions with sepiolite or halloysite.

Membranes	Nafion dispersion (g)	Sepiolite (g)	Halloysite (g)	Isopropanol (g)	Blending time of nanoclay dispersion(h)	Blending time of casting dispersion (h)
Nafion 1000-24h	2	0	0	4	-	24
Nafion 1000-5h	2	0	0	4	-	5
Nafion 1000-1h	2	0	0	4	-	1
Nafion/SEP-24h	2	0.03	0	4	24	1
Nafion/SEP-5h	2	0.03	0	4	5	1
Nafion/SEP-1h	2	0.03	0	4	1	1
Nafion/HNT-24h	2	0	0.03	4	24	1
Nafion/HNT -5h	2	0	0.03	4	5	1
Nafion/HNT -1h	2	0	0.03	4	1	1

Fig. 2.2. Photo of the ultrasound equipment (HD 2070, Bandelin, Germany)used to disperse nanoclay in the casting dispersion.

2.4.2. Aquivion-based composite membranes

All membrane samples with a size of 13 × 13 cm^2 were prepared via casting and evaporation. Aquivion and nanoclay were blended within casting dispersion in vials.

To begin with, 3.23 g of Aquivion dispersion (24 wt%, D83-24B), 0.078 g of nanoclay and 12.27 g of isopropanol were blended so as to obtain a 5 wt% Aquivion casting dispersion resulting in a 10 wt% clay loaded composite membrane.

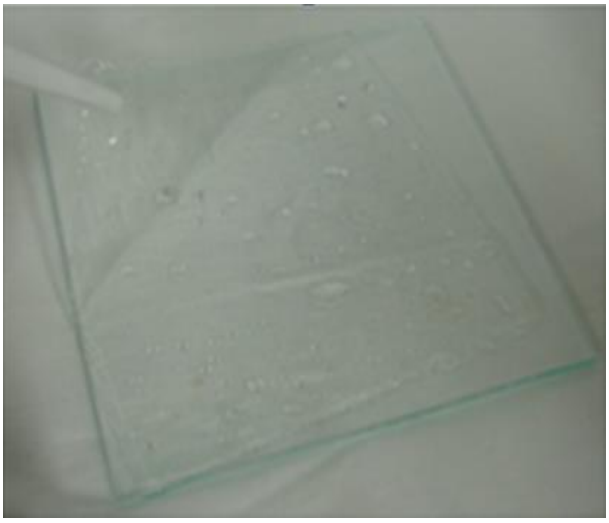

Fig. 2.3. Photo of wet membrane detached from glass plate.

Different kinds of casting dispersions, obtained with different clays, were stirred for 15 mins by stirrer at 80 rpm. Afterward, nanoclay dispersions in vials were dispersed using ultrasound (HD 2070, Bandelin, Germany) for

2 min at 60 W power and 20% pulsation level (see Fig. 2.2). The resultant dispersions were poured on a 13x13cm² mold at 15.578 g, after which it was heated at 80℃ for 18 h and then at 170℃ for 2 h. Prepared membranes were treated using 0.5M H_2SO_4 for 1 h and rinsed with DI-water for 1 h, at 100℃.

All the membranes were prepared using mold to have thickness of around 20 μm, in order to follow commercial trends and reduce resistance. Various membranes were prepared by addition of nine available nanoclays and they were labeled as listed in table 2.2.

Table 2.2. Information on nineteen different kinds of membranes prepared based on the available nanoclays.

Membrane reference	PFSA ionomer	Nanoclay reference/content (wt%)	Type of nanoclay	Modification of nanoclay	Pretreatment of nanoclay
Aquivion		-	-	-	
Aq/SEP		SEP10	Sepiolite	Pristine	
Aq/SEP-F		SEP-F10		Fluorination	
Aq/pSEP		pSEP2/5/10	Sepiolite	Pristine	○
Aq/pSEP-F		pSEP-F2/5/10		Fluorination	○
Aq/HNT		HNT10	Halloysite	Pristine	
Aq/HNT-F		HNT-F10		Fluorination	
Aq/HNT-S		HNT-S10		Sulfonation	
Aq/HNT-SF	Aquivion	HNT-SF10		Sulfo + Fluo	
Aq/pHNT		pHNT2/5/10	Halloysite	Pristine	○
Aqn/pHNT-F		pHNT-F2/5/10		Fluorination	○
Aq/pHNT-S		pHNT-S2/5/10		Sulfonation	○
Aq/pHNT-SF		pHNT-SF2/5/10		Sulfo + Fluo	○
Aq/HNT-Q		HNT-Q10	Halloysite	Quercetine	
Aq/HNT-FQ		HNT-FQ10		Fluo + Quer	
Aq/HNT-NQ		HNT-NQ10		Amino + Quer	
Aq/pHNT-Q		pHNT-Q2/5/10	Halloysite	Quercetine	○
Aqn/pHNT-FQ		pHNT-FQ2/5/10		Fluo + Quer	○
Aq/pHNT-NQ		pHNT-NQ2/5/10		Amino + Quer	○

3. Analytical methods

3.1. ATR-FTIR

The surface modification of sepiolite was investigated at IMT Mines-Alès by Fourier transform infrared (FTIR) spectroscopy. FTIR was performed on a spectrometer IFS 66 (Bruker) in ATR mode. Spectra were obtained by collecting 32 scans between 400 and 4000 cm^{-1} with a resolution of 4 cm^{-1}.

3.2. TGA

The thermal stability of the sepiolite samples was studied at IMT Mines-Alès by thermal gravimetric analysis (TGA). The analyses were performed by a thermogravimetric analyzer (Perkin Elmer Pyris-1 instrument). In order to remove all the physisorbed water, an isothermal step (10 min, 110 °C) was performed before starting the analysis and then the samples were heated to 900 °C at a heating rate of 10 °C/min. Measurements were carried out under nitrogen atmosphere with a flow rate of 20 ml/min on samples of approximately 10 mg.

3.3. Py-GC/MS

Pyroprobe 5000 pyrolyzer (CDS analytical) was used at IMT Mines-Alès to flash pyrolyze the samples in a helium environment. This pyrolyzer is equipped with an electrically heated platinum filament. One coil probe enables the pyrolysis of samples (< 1 mg) placed in a quartz tube between two pieces of rockwool. The sample was heated at 900°C. The temperature was held for 15 s, and then the gases were drawn to the gas chromatograph for 5 min. The pyroprobe 5000 is interfaced to a 450-GC chromatograph (Varian) by means of a chamber heated at 270 °C. In the oven, the initial temperature of 70 °C was raised to 310 °C at 10 °C/min. The column is a Varian Vf-5 ms capillary column (30 m × 0.25 mm; thickness = 0.25 µm) and helium (1 *l*/min) was used as the carrier gas, a split ratio was set to 1:50. The gases were introduced from the GC transfer line to the ion trap analyzer of the 240-MS mass spectrometer (Varian) through the direct-coupled capillary column.

3.4. FE-SEM and EDS

The cross section of prepared membranes was examined on cryofractures using FE-SEM (Field emission scanning electron microscopy, FEI XL30, Philips) at 2000× magnification. Si/F atomic ratio (%) across the membrane was calculated using EDS (Energy dispersive X-ray spectroscopy), in order to analyze the clay distribution inside the polymer matrix.

3.5. Membrane thickness

Wet membranes were cut into seven pieces and the thickness of three pieces selected diagonaly was measured on three different locations using a micrometer (Mitutoyo 293-344, Japan). The average thickness of each membrane could then be calculated based on nine measurement data.

3.6. Water uptake

The water uptake was measured by weight difference between wet and dried membranes. The membranes were first immersed in DI water at room temperature and their weight measured after wiping the excess of water (W_w). The weight of dried membranes (W_d) was then measured after drying in an oven at 80℃ for 18 hr. The water uptake was finally calculated according to the following equation:

$$W_{ut}\ (\%) = \frac{W_w - W_d}{W_d} \times 100 \qquad (1)$$

Where W_w and W_d are the weight of the wet and dried membranes, respectively.

3.7. Swelling ratio

The swelling was calculated as the percentage of thickness difference between membranes immersed 2 h in water at room and boiling temperature. The thickness was averaged at three points for all membranes, and the swelling was calculated based on the following equation:

$$S_{th}(\%) = \frac{th_{bt} - th_{rt}}{th_{rt}} \times 100 \qquad (3)$$

Where th_{rt} and th_{bt} are the thickness of the membranes at room temperature and 100℃, respectively.

3.8. IEC (Ion exchange capacity)

IEC was measured by titration. The membranes were fully immersed for 24 h in 40 ml of 2 M NaCl solution for Na^+ ions to replace H^+ ones in the membrane. H^+ ions were then titrated with 0.005 M NaOH solution. IEC was calculated according to the following equation:

$$IEC\ (meq/g) = \frac{V_{NaOH} \times C_{NaOH}}{W_d} \qquad (4)$$

Where V_{NaOH} and C_{NaOH} are the volume and the concentration of NaOH, respectively. W_d is the weight of dried membranes.

3.9. Chemical stability

The chemical degradation of the membrane due to the presence of iron occurs through C-F bond attack during fuel cell operation. Such a process results in an increase of the fluorine concentration in the water produced by the fuel cell. The chemical stability can thus be assessed through the analysis of the fluorine concentration.

4.4 M H_2O_2/1.25 mM H_2SO_4 solution was prepared for verifying the chemical stability of the prepared membranes, assuming that iron may come from the nanoclay. One piece of wet membrane was immersed in the afore-mentioned solution using brown glass bottle in order to reach 0.16 wt%. The solution temperature and stirrer speed were set at 70℃ and 100 rpm, respectively. The membrane was dipped into the solution for 4 h, 17 h, 48 h, 72 h and 96 h after which fluoride concentration in the solution was analyzed using an ion meter and a specific electrode (781 pH/Ion meter, Metrohm AG, Swizerland). TISAB IV was blended with the above-mentioned solution before 0.001 N NaF solution was added as a standard during analysis. A blank test of the solution was conducted prior to any analysis.

3.10. EIS (Electrochemical impedance spectroscopy)

The resistance of membranes was accurately conducted with electrochemical impedance spectroscopy (EIS) equipment (Bio-Logic Scientific Instruments, France). The equipment was connected to a proprietary cell made in hydrogen lab of PERSEE center as shown in Fig. 2.4. Experiments were conducted to study the effect of temperature and relative humidity on membrane resistance with this equipment. Membrane sample cut into 0.5 × 0.5 cm^2 was put into the cell and it was subsequently evaluated 50 times under condition of 50℃, 70℃ and 90℃ of temperature, and 25%, 50%, 75% and 90% of relative humidity. The operating temperature and relative humidity were controlled using self-made software on computer. EIS equipment was operated under frequency range between 1 mHz and 1 kHz with an amplitude of ± 20 mV. All resistance values (Ohm) of membranes were automatically calculated by EC-Lab® software and homemade program.

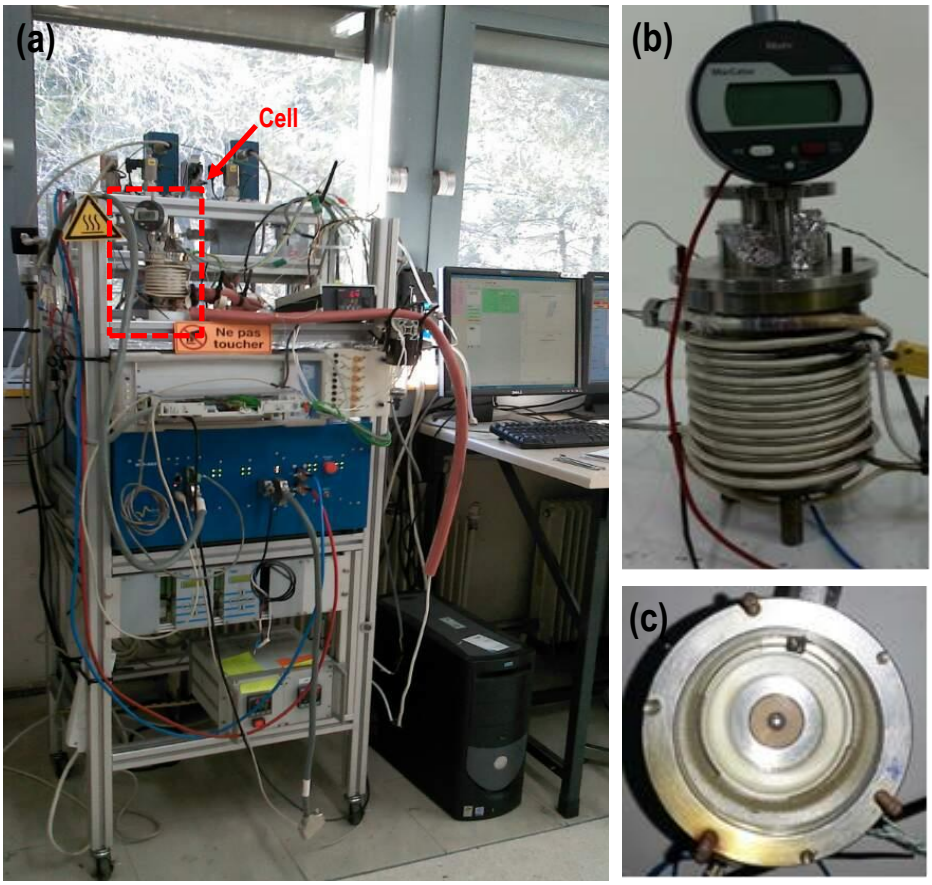

Fig. 2.4. Photo images on (a) electrochemical impedance spectroscopy (EIS) equipment, (b) appearance of proprietary cell, and (c) inner part of proprietary cell.

The proton conductivity (S cm^{-1}) of membranes was calculated using the following equation:

$$\sigma = \left(\frac{1}{R}\right)\left(\frac{l}{S}\right) \qquad (5)$$

Where σ represents the proton conductivity (S cm^{-1}). R and l are the resistance (ohm) and the thickness (cm) of the membrane, respectively. S represents the contract surface with platinum electrodes (0.0346 cm^2).

It was not possible to measure the thickness during the resistance measurement. Since the membrane was hydrated in the measurement cell we chose to consider the thickness measured in wet conditions to calculate the

proton conductivities. The real conductivities may vary from the calculated ones. Nevertheless, it is noteworthy that the conductivities calculated for Aquivion at 90°C and 25 %RH or 90 %RH are close to values reported in literature (cf. Fig. 5.13).

3.11. DMA (Dynamic mechanical analysis)

The viscoelastic behavior of the membranes was determined using dynamic mechanical analysis (DMA50 from Metravib, Acoem) under shear jaws for film test configuration (characterizations were performed at IMT Mines-Alès). The samples dimension was 30 mm length, 10 mm height and the thickness of the membrane (between 30 and 50 µm). The results were analyzed with DYNATEST software. A temperature scanning was performed on membranes from 50 to 200°C at a heating rate of 1°C/min. It was verified previously that the deformation (3 µm) was in the linear domain. The frequency was 1Hz. Since membranes are very thin (around 40 µm) the reproducibility is not high but still some trends can be observed.

3.12. MEA preparation

Catalyst Coated Membranes were made at Symbio with a SonoTek ExactaCoat ultrasonic spray-coating machine. The ExactaCoat coating machine is a programmable 3-axis robot with an integrated Accumist ultrasonic atomizing nozzle. The system is easily configured to customize spray patterns and to deposit precise amounts of ink. A syringe pump was used to supply the catalyst ink to the ultrasonic atomizing nozzle. The flow rate of the catalyst ink delivery is controlled by the program software. The amount of ink deposited on the membrane, and hence the Pt loading of the CCM, is controlled by the ink flow rate and the x-y speed of the nozzle. The membranes were held down on a vacuum plate heated to 80°C.

The catalyst used to prepare the ink for both the anode and cathode sides of the CCMs was Tanaka TEC10E40E. The anode and cathode catalyst loadings were programmed for 0.3 and 0.5 mg Pt/cm² respectively. Mass measurements made before and after coating confirmed the Pt loadings to be 0.26 $\pm$ 0.08 mg Pt/cm² for the anode and 0.50 $\pm$ 0.06 mg Pt/cm² for the cathode. 5L+SG MEAs (5-layer MEA + subgasket) were prepared by hot-pressing the gas diffusion layers (Freudenberg H23C6) and the PET subgaskets onto both sides of the CCMs at 170°C and 50 kg/cm² for the Aquivion based membranes and 140°C and 50 kg/cm² for the Nafion HP membrane. The anode and cathode GDLs were the same. Hot-pressing was carried out using a Carver 30-12H Press.

3.13. Single cell set-up and test protocols

The 5L+SG MEAs were set up in a 25 cm² single cell with graphite monopolar plates with a single channel flow field and with an integrated O-ring gasket. The cell was tightened with 8 nuts and bolts with a dynamometric wrench set at 6 Nm.

Fuel cell electrochemical tests were carried out at Symbio with a BioLogic FCT-150S fuel cell test station. H_2 crossover tests were carried out with a BioLogic VSP potentiostat and a BioLogic VMP3 Booster.

Each MEA was activated at 0.6 V for 2-3 h until stabilization of the current.

Polarization curves (IV) were conducted at 80°C in the co-flow configuration using pure hydrogen on the anode (stoichiometry = 1.5, outlet pressure = 2.5 bara, relative humidity = 30%) and air on the cathode

(stoichiometry = 2.0, outlet pressure = 2.5 bara, relative humidity = 100% in wet mode and 30 % in dry condition). A more severe condition was also applied: low pressure = dry conditions + outlet pressure = 1.5 bara on both sides.

For resistance measurements, impedance spectroscopy (EIS) was carried out in the galvanostatic mode. An AC sinus signal (10% I amplitude) was applied around a fixed current I of 1.25 A, 20 A and 30 A (frequency range = [10 kHz – 10 Hz]).

The hydrogen crossover was calculated after linear sweep voltammetry results obtained under H_2/N_2 at 3/3 bara. The voltage was scanned from 0.05 V to 0.55 V at 5 mV/sec. The extrapolation of the straight linear portion between 0.4 and 0.5 V vs. RHE of the anodic current to zero cell voltage corresponds to the addition of the charging current and the current due to the oxidation of hydrogen crossed over from anode to cathode. The shorting resistance is the calculation of the ratio (slope) ($\Delta v/\Delta I$, [$\Omega.cm^2$]) between 0,4 V and 0,5 V vs. RHE.

To assess the durability of the membranes a highly accelerated stress test (HAST) from General Motor protocol was also conducted (dry conditions + cell temperature = 90°C and outlet pressure = 3 bara): 1) Current Scan from 1.25 A to 20 A in 10 s (1875 mA/s), 2) Current Scan from 20 A to 30 A in 60 s (167 mA/s), 3) 30 A for 35 s and 4) Current Pulse at 1.25 A for 160 s. The durability test is comprised of blocks of 48 h of HAST cycles (265 s) followed by shorting/crossover measurements, chronoamperometry, GEIS and IV tests. The AST test is stopped when the voltage reaches a value of 0.7 V at 0.05 A/cm² (or at OCV).

Chapter 3

Effect of blending time on composite homogeneity

Summary

This chapter introduces the relationship between physicochemical properties and blending time for two different nanoclays, sepiolite nanofibers (SEP) and halloysite nanotubes (HNT) inside Nafion matrix of electrolyte membrane used in proton exchange membrane fuel cell (PEMFC). In the study, based on the blending time (24, 5 and 1 h), composite homogeneity, thickness, water uptake, swelling ratio and IEC of Nafion composite membranes were investigated. Short blending time (1 h) resulted in better homogeneity of Nafion/SEP and Nafion/HNT composite membranes which moreover displayed improved physicochemical properties compared with those of pristine Nafion membrane.

Résumé

Ce chapitre présente la relation entre les propriétés physicochimiques et le temps de mélange de deux nanoargiles différentes, les nanofibres de sépiolite (SEP) et les nanotubes d'halloysite (HNT) à l'intérieur d'une matrice Nafion utilisée comme membrane électrolytique pour pile à combustible à membrane échangeuse de protons (PEMFC). Dans l'étude, l'homogénéité des composites, l'épaisseur, l'absorption d'eau, le taux de gonflement et la capacité d'échange ionique des membranes composites ont été étudiés en fonction du temps de mélangeage (24, 5 et 1 h). Un temps de mélangeage court (1 h) a permis d'obtenir une meilleure homogénéité des membranes composites Nafion/SEP et Nafion/HNT, qui présentent en outre des propriétés physicochimiques améliorées par rapport à celles de la membrane Nafion seule.

1. Introduction

Among a broad range of polymers used for PEM, Nafion is selected as a standard material to prepare perfluorosulfonic acid (PFSA) membranes, due to its physicochemical properties such as chemical stability, good mechanical stability, and proton conductivity at intermediate temperature [177]. However, Nafion membrane has limitations of reduced thermal stability and proton conductivity above 90℃. Hence different additives were used to improve its performance, among which different types of clay. Sepiolite nanofibers (SEP) and halloysite nanotubes (HNT) are two interesting examples. Addition of such nanoclays into a Nafion matrix can overcome the limitations of performance at high temperature, due to their properties. Also, improving the dispersion state of SEP and HNT has been considered by research engineers in order to enhance the characteristics of composite electrolyte membranes [39, 47].

So far, the correlation between physicochemical properties and blending time inside Nafion matrix of composite membrane has not yet been studied. That is, most researchers have not realized and mentioned that the increased blending time affects the nanoclay aggregation within composite membranes even though such phenomenon in turn leads to raised swelling and decreased homogeneity of the membrane. Obtaining information on the clay dispersion through the membrane according to blending time will be useful for preparation of homogeneous Nafion composite membranes incorporated with nanoclays.

This chapter focuses on relationship between physicochemical properties and blending time within polymer matrix of Nafion/SEP and Nafion/HNT composite membrane used as PEMFC. In the study nanoclay dispersions in isopropanol were blended under magnetic stirring for 24 h, 5 h and 1 h, after which Nafion dispersion was added and composite membranes were prepared via casting-evaporation process. Following this, the homogeneity of the composite was analyzed through observation of the cross section and analysis of the Si/F atomic ratio using FE-SEM/EDS (Field emission scanning electron microscopy/Energy-dispersive X-ray spectroscopy). Moreover, water uptake, swelling and ion exchange capacity (IEC) values of composite membranes were analyzed with respect of clay incorporation and blending time.

2. Preparation of Nafion-based composite membranes

Nine different kinds of membranes (5 × 5 cm^2), as listed in Table 3.1, were prepared via casting-evaporation process with identical 10 wt% content of SEP and HNT. Each of the nanoclay dispersions containing isopropanol was blended for 24 h, 5 h and 1 h. Following this, nanoclay dispersions were mixed with Nafion LQ1015 dispersion for 1 h. Stirring rate was set at 80 rpm. Afterward, Nafion/nanolay dispersions were dispersed using ultrasound (HD 2200, Bandelin, Germany) for 2 min at 60 W power and 20% pulsation level (see Fig. 3.1). 2.5 g of the resultant dispersions were poured in a 5 x 5cm^2 mold and heated at 80 °C for 2 h and 120 °C for 1 h. The obtained membranes were treated for each 1 h in boiling 1) 0.5 M HNO_3, 2) 6% H_2O_2 and 3) 0.5 M H_2SO_4. Between each step, the membranes were washed in boiling (DI) water for 1 h.

Table 3.1. Chemical compositions of Nafion casting dispersions with sepiolite or halloysite (reproduced from chapter 2).

Membranes	Nafion dispersion (g)	Sepiolite (g)	Halloysite (g)	Isopropanol (g)	Blending time of nanoclay dispersion(h)	Blending time of casting dispersion (h)
Nafion LQ1015-24h	2	0	0	4	-	24
Nafion LQ1015-5h	2	0	0	4	-	5
Nafion LQ1015-1h	2	0	0	4	-	1
Nafion/SEP-24h	2	0.03	0	4	24	1
Nafion/SEP-5h	2	0.03	0	4	5	1
Nafion/SEP-1h	2	0.03	0	4	1	1
Nafion/HNT-24h	2	0	0.03	4	24	1
Nafion/HNT -5h	2	0	0.03	4	5	1
Nafion/HNT -1h	2	0	0.03	4	1	1

Fig. 3.1. Photo images of the ultrasound equipment used to disperse nanoclay in the casting dispersion (reproduced from chapter 2).

3. Composite homogeneity of Nafion electrolyte membranes

Membrane surfaces were first observed in order to study the appearance of prepared composites as shown in Fig. 3.2. Sepiolite and halloysite based membranes behave quite differently. The dispersion of halloysite seems to be much more difficult, resulting in larger and numerous white dots than sepiolite. In both cases the shorter the blending time the nicer the membrane. That is, 1 h blending time resulted in the preparation of homogeneous Nafion/HNT-1h and Nafion/SEP-1h compared with Nafion/SEP and Nafion/HNT membranes blended for 5 h or 24 h.

In addition, the thickness of membranes was measured on 5 different locations to calculate an average value (see Fig. 3.3). 24 h blending time resulted in 20 μm thicker composite membranes than shorter blending time. This may be attributed to nanoclay aggregation and sponge-like structure with voids, caused by incomplete dispersions,

as observed on composites cross section (see Fig. 3.4a-d) [42, 178]. 1h and 5h blending time resulted in thickness similar to that of the pristine Nafion membrane.

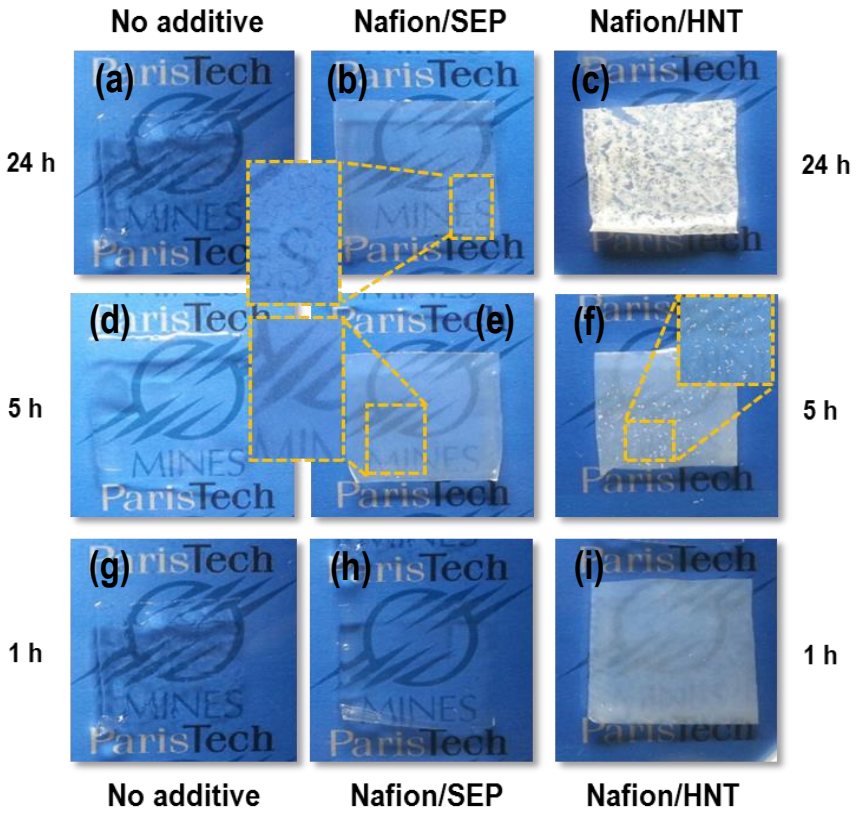

Fig. 3.2. Photo images of pristine Nafion blended for (a) 24h, (d) 5h, (g) 1h, Nafion/SEP blended for (b) 24h, (e) 5h, (h) 1h, and Nafion/HNT blended for (c) 24h, (f) 5h, (i) 1h.

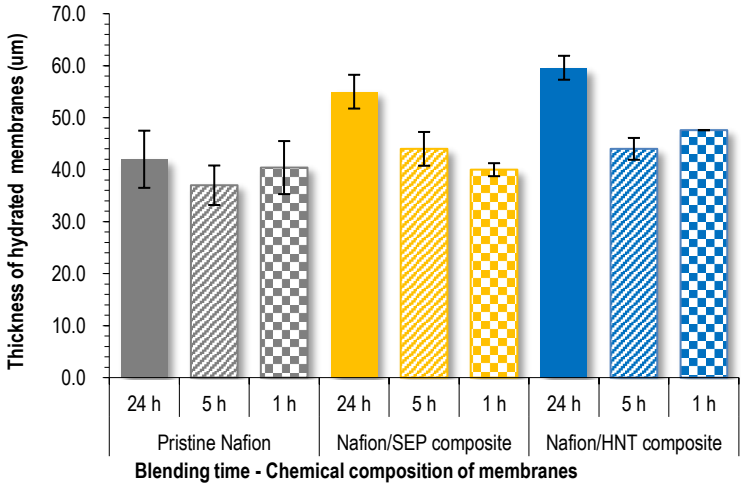

Fig. 3.3. Thickness of membranes with respect of blending time, measured under wet condition: pristine Nafion, and SEP- or HNT-based composite membranes.

Figs. 3.4a-h show cross sectional micrographs of composite membranes, across which Si/F atomic ratio (%) was calculated (see Fig. 3.5). Considering that Si and F originated from nanoclays and Nafion, respectively, uniform Si/F atomic ratio across the membrane is representative of a good homogeneity (Si traces the amount of nanoclay inside the polymer phase). Looking at Fig. 3.4, sepiolite based membranes look much more homogeneous than halloysite based ones, in good agreement with previous observations. This is confirmed with the EDS results: the longer the blending time, the larger the difference between Si/F ratios across the membrane and thus the less homogeneous the composite membrane. Data collected here show again that sepiolite more easily mixes with Nafion than halloysite. Long blending time probably led to aggregated nanoclay, from 5 h in the case of halloysite and only 24 h for sepiolite. The large difference of Si/F values implies the presence of large agglomerates. In addition, particles were discovered in Nafion/SEP-24h as shown in Fig 3.4c. According to EDS, Fig 3.5, the main atom of these particles was silicon originated from Si-OH bonds (silanol group) of SEP aggregation. However, 1 h and 5 h of blending time allowed membranes to have relatively homogeneous SEP distribution.

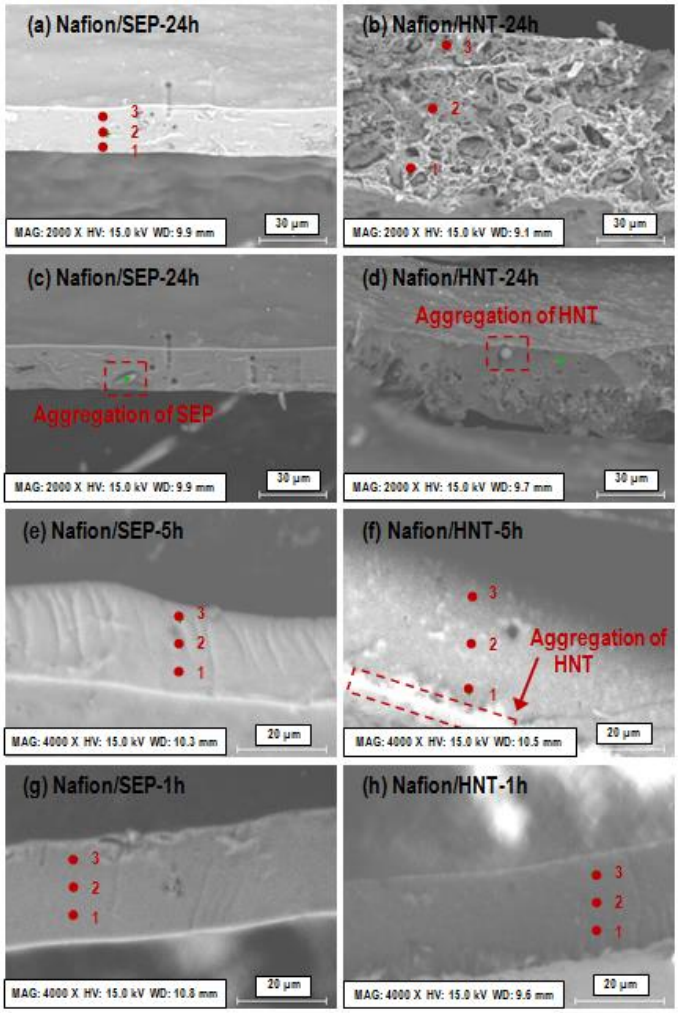

Fig. 3.4. Cross sectional images of (a, c) Nafion/SEP-24h, (b, d) Nafion/HNT-24h, (e) Nafion/SEP-5h, (f) Nafion/HNT-5h, (g) Nafion/SEP-1h and (h) Nafion/HNT-1h membranes observed using FE-SEM. Reprinted with permission from CSJ journal [179].

Nafion/HNT-24 h formed large or partial sponge-like structure with voids as shown in Figs. 3.4b and 3.4d. Fig. 3.4d also exhibited silicon particles resulted from HNT aggregation within dotted red box. A similar aggregation was observed with Nafion/HNT-5 h as can be seen in dotted red box of Fig 3.4f. On the other hand, aggregated HNT was not discovered in the membrane blended for 1 h, and accordingly its EDS data showed relatively uniform Si/F atomic ratio (%) compared with Nafion/HNT membranes stirred for 24 h and 5 h. Based on characterizations in composite homogeneity, it was demonstrated that relationship between Si/F atomic ratio and surface appearance of membranes is consistent. It could be attributed that the long blending time between Nafion dispersion and nanoclays leads to sedimentation by making the aggregated nanoclays, which may eventually interfere with the dispersion inside the polymer matrix. More research is needed to reveal the exact mechanism.

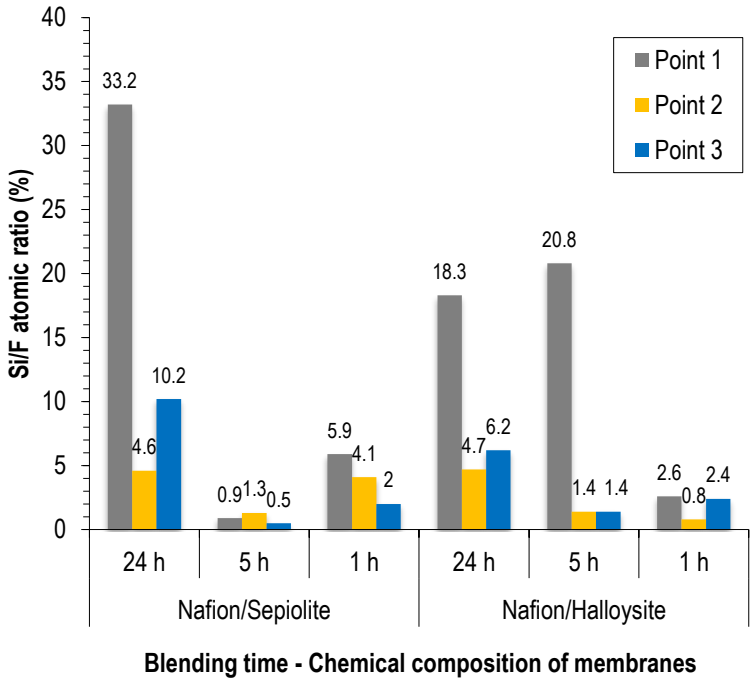

Fig. 3.5. Si/F atomic ratio (%) of pristine Nafion, Nafion/SEP and Nafion/HNT composite membranes analyzed using EDS.

4. Water uptake

Water uptake is an important parameter in judging membrane performance since it partially governs the proton conductivity. As shown in Fig. 3.6a, the incorporation of nanoclay, sepiolite or halloysite, in Nafion dispersion generally led to improved water uptake due to their hygroscopic feature, resulting from surface hydroxyl groups. That is, blending of SEP improved water uptake by about 20% - 30% compared with no addition. The blending time has little effect on sepiolite based membranes. On the contrary, it impacts significantly the water uptake of halloysite based composites. If a similar value was obtained for 1h blending the water uptake is much larger for 24h.This result may be due to the sponge-like structure as can be seen in Fig. 3.4b [6].

5. Swelling ratio and ion exchange capacity

Membrane swelling has to be reduced at maximum because it leads to constraints in MEA (membrane electrode assembly) and stack during operation. In order to analyze their thickness swelling ratio, membranes were boiled in water. As can be seen in Fig. 3.6b. in general, the introduction of nanoclays in Nafion results in limited thickness swelling compared to that of pristine Nafion membranes. If the blending time has no effect on the thickness swelling of pristine Nafion membranes (12.4 - 14.4 %) it impacts that of composites, similarly for sepiolite and halloysite, the shorter the blending time the lower the swelling. The limited effect observed after long blending may be related to the inhomogeneity of composite membranes showing weaker cohesion between the polymer phase and the additives.

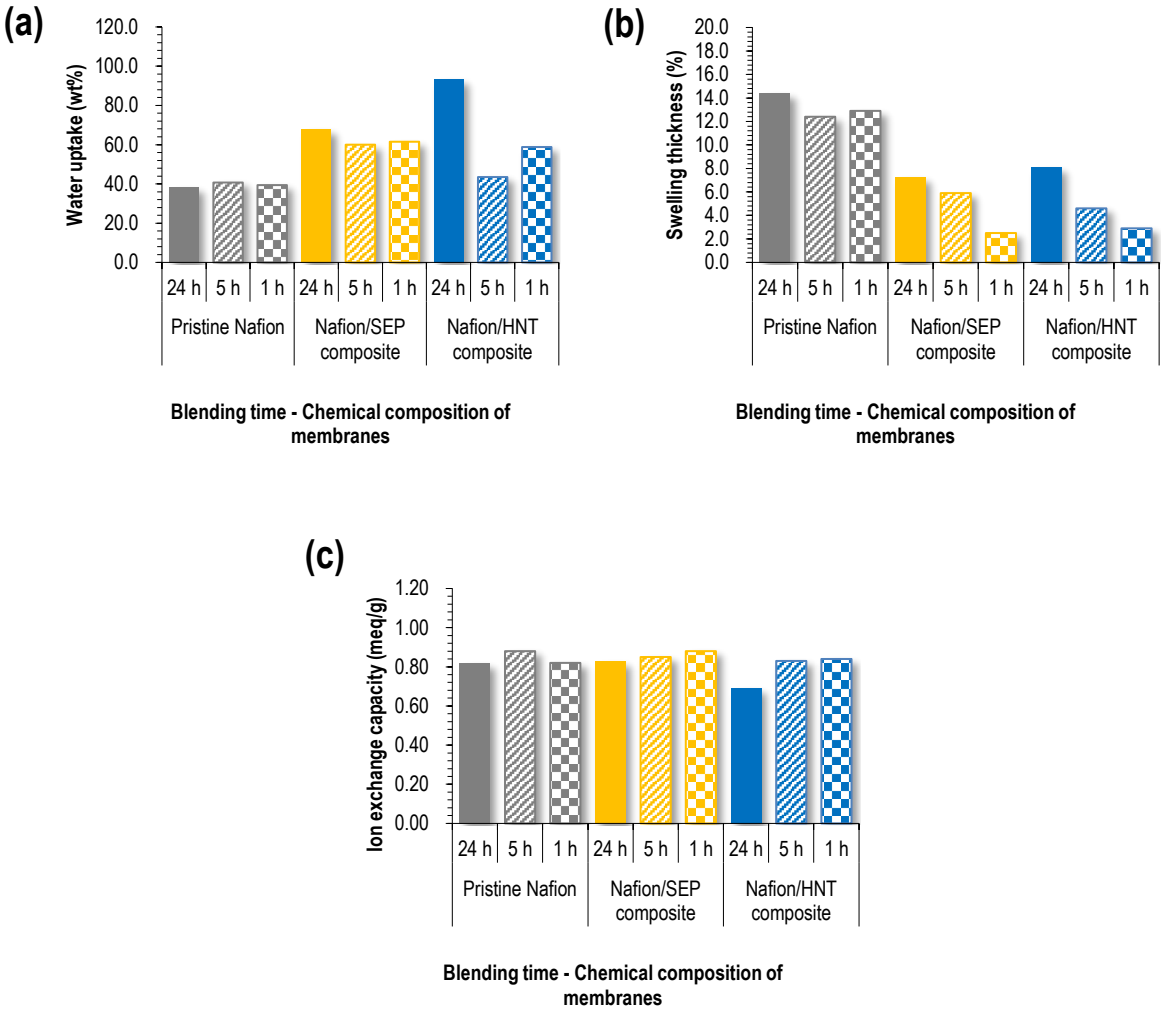

Fig. 3.6. Data on (a) water uptake, (b) swelling ratio and (c) IEC regarding pristine Nafion and composite membranes incorporated with SEP and HNT.

Ion exchange capacity (IEC) data of membranes was obtained via titration method. They showed similar values between approximately 0.7 and 0.8 meq/g, regardless of blending time. All data on IEC values was gathered in Fig. 3.6c. These are slightly lower than the IEC value measured in other labs. The deviation of the measured values is due to the limitations of the calculation and weighing procedures to determine the amount of polymer

added into the casting dispersion. It is notable that IEC of pristine casting membranes composed of Nafion EW1000 show 0.91 – 1.0 meq/g according to literature [180, 181]. In addition, Walsh's group reported that IEC of commercially available Nafion N112 (EW1026), N1135 (EW1021), N115 (EW1012), and N117 (EW1071) showed 0.98, 0.98, 0.99 and 0.93 meq/g, respectively.

Conclusions

In conclusion, SEP and HNT nanoclays were incorporated in Nafion dispersions and PEMs were prepared via casting-evaporation process.

In general, the addition of these nanoclays resulted in improved membrane properties: larger water uptake and reduced swelling compared with pristine Nafion membranes, without any impact on the IEC. It is noteworthy that the introduction of sepiolite and halloysite resulted in similar improved performance: 60% water uptake and 2 - 3% swelling ratio for 1 h blending, versus 40% and 14% respectively for the Nafion membrane prepared in the same conditions.

Moreover, it is clear from our results that the shorter the blending the better the homogeneity and as a consequence the performance, especially the water uptake. The impact seems to be more pronounced for halloysite than for sepiolite. In the first case macroscopic inhomogeneity appeared from 5 h blending, 24 h in the second case.

Additionally, it can be concluded that sepiolite is much easier to disperse than halloysite inside Nafion matrix.

As a consequence, in the rest of study the membranes will be prepared with a short blending time in order to favor a good distribution of the clay inside the composite membrane.

Chapter 4

Influence of fluorinated, sulfonated and perfluorosulfonated - pretreated halloysites on electrolyte membranes

Summary

Different composite membranes have been prepared mixing Aquivion and halloysite.

Halloysite nanotubes were grafted with the fluorine group, sulfonated group, or perfluoro-sulfonated group prior to removing divalent iron inside nanoclays through pretreatment with oxalic acid and hydrogen chloride. Pristine halloysite or modified halloysite was incorporated into Aquivion phase of composite membranes to improve physicochemical properties. Electrolyte membranes tested in this chapter were prepared by casting and evaporation. As reference sample, Nafion HP and Gore Select M820 were used to compare the membrane characteristics.Different kinds of functionalized halloysites were analyzed using ATR-FTIR (attenuated total reflection-fourier-transform infrared spectroscopy), TGA (thermal gravimetric analysis) and Py-GC/MS (pyrolysis-gas chromatography mass spectrometry).

According to FTIR analysis, HNT-F and HNT-SF spectra exhibited the presence of two peaks at 1535 and 1250 cm^{-1} attributed respectively to the N-H (bending) of the amide function and C-F bonds of the perfluorinated fragment.

In terms of TGA data, HNT-F and HNT-S display weight losses of approximately 1.2 and 0.4 wt%, respectively. The second step of functionalization to obtain HNT-SF from HNT-S was also analyzed with an increase of the weight loss of around 1.2 wt% attributed to the fluorinated grafting agent.

Concerning Py-GC/MS result, Presence of fluorinated molecules is observed for HNT-F and HNT-SF due to the release of fluorinated molecules by decomposition of the fluorinated grafting agent. Different aromatic molecules are observed for HNT-S due to the thermal decomposition of the naphthalene part of the grafting agent. The above mentioned analysis means that halloysites were successfully grafted with fluorination, sulfonation or perfluoronation group.

Blending with halloysite with Aquivion dispersion led to augmented water uptake, reduced swelling ratio and improved mechanical strength. Compared with commercially available membranes, composite membranes exhibited similar IEC, but reduced proton conductivities. In addition, they showed a thicker thickness compared to commercial membranes and pristine Aquivion.

With respect to functionalization, functionalized nanoclay-incoporated membranes showed thinner thickness and improved mechanical strength compared to pristine halloysite-blended membrane. On the other hand, similar composite homogeneity, swelling, antioxidant activity, hydrophilicity, and IEC values were verified, regardless of functionalization type.

Functionalized and pretreatment halloysites contribute to improve composite homogeneity and proton conductivity. In particular, pretreated and perfluoro-sulfonated halloysite helped to provide the highest proton conductivity of composite membrane among the membranes tested. Furthermore, it has a benefit to enhanced mechanical strength with better stiffness. On the other hand, it had no effect on the antioxidant function.

Reduced addition of clay nanotubes affected membrane properties. For example, blending 5 wt% of pretreated and perfluoro-sulfonated halloysite resulted in the highest IEC, water uptake, and proton conductivity of electrolyte membrane among the membrane tested. However, the smaller the addition amount, the better homogeneity was observed in the membrane cross section.

Résumé

Différentes membranes composites ont été préparées en mélangeant Aquivion et halloysite.

L'halloysite a été modifiée par fluoration, sulfonation ou fluoro-sulfonation avant d'éliminer le fer divalent dans les nanoargiles par prétraitement avec de l'acide oxalique et de l'acide chlorhydrique. De l'halloysite vierge ou de l'halloysite modifiée a été incorporée à la phase Aquivion de membranes composites afin d'améliorer les propriétés physicochimiques. Les membranes électrolytiques testées dans ce chapitre ont été préparées par coulée et évaporation. À titre de référence, Nafion HP et Gore Select M820 ont été utilisés pour comparer les caractéristiques des membranes.

Les différents halloysites fonctionnalisées ont été analysés par ATR-IRTF (spectroscopie infrarouge à transformée de Fourier-à réflexion totale atténuée), ATG (analyse thermogravimétrique) et Py-GC/MS (spectrométrie de masse par pyrolyse en phase gazeuse).

Selon l'analyse IRTF, les spectres HNT-F et HNT-SF ont montré la présence de deux pics à 1535 et 1250 cm^{-1} attribués respectivement à la liaison N-H (flexion) de la fonction amide et aux liaisons C-F du fragment perfluoré. En termes de données ATG, HNT-F et HNT-S affichent des pertes de poids d'environ 1,2 et 0,4% en masse, respectivement. La deuxième étape de la fonctionnalisation pour obtenir HNT-SF à partir de HNT-S a également été analysée avec une augmentation de la perte de poids d'environ 1,2% en masse attribuée à l'agent de greffage fluoré.

En ce qui concerne le résultat Py-GC/MS, la présence de molécules fluorées est observée pour HNT-F et HNT-SF en raison de la libération de molécules fluorées par décomposition de l'agent de greffage fluoré. Différentes molécules aromatiques sont observées pour HNT-S en raison de la décomposition thermique de la partie naphtalène de l'agent de greffage. L'analyse mentionnée ci-dessus signifie que les halloysites ont été greffés avec succès avec un groupe de fluoration, sulfonation ou perfluoronation.

Le mélange avec l'halloysite et la dispersion d'Aquivion a entraîné une augmentation de l'absorption d'eau, du gonflement ainsi que de la résistance mécanique. Comparées aux membranes disponibles dans le commerce, les membranes composites présentaient une capacité d'échange ionique similaire, mais une conductivité protonique réduite. En outre, elles ont montré une épaisseur plus épaisse par rapport aux membranes commerciales et à la membrane Aquivion non chargée.

L'utilisation d'halloysites fonctionnalisées a produit des membranes plus fines et plus résistantes mécaniquement par rapport à la membrane mélangée à de l'halloysite non modifiée. Elles présentent par ailleurs une homogénéité, ungonflement, une activité antioxydante, une hydrophilie et des capacités déchanges ioniques similaires, quel que soit le type de fonctionnalisation.

Les halloysites fonctionnalisés prétraitées contribuent à améliorer l'homogénéité des composites et la conductivité protonique. En particulier, l'halloysite prétraitée et perfluorosulfonée a permis d'obtenir la conductivité protonique la plus élevée de toutes les membranes testées. En outre, elle présente l'avantage d'améliorer la résistance mécanique avec une meilleure rigidité. Par contre, cela n'a aucun effet sur la fonction antioxydante.

La diminution de la quantité d'argile a affecté les propriétés de la membrane. Par exemple, le mélange de 5% en masse d'halloysite prétraitée et perfluoro-sulfoné a permis d'obtenir la plus haute capacité déchange ionique, l'absorption d'eau et la conductivité protonique les plus élevées parmi les membranes testées. Plus la quantité ajoutée était faible, meilleure était l'homogénéité de la membrane.

1. Introduction

The addition of nanoclay into the polymer matrix can overcome the limitations associated with thermomechanical resistance and sensitivity to relative humidity, even when operated at high temperatures. Mixing the nanoclay prevents dehydration, especially by improving hygroscopicity, and hence composite membranes can be operated at low relative humidity [38, 39]. Mechanical properties can be enhanced by homogenous dispersion of the filler, affinity improvement with the polymer used in the composite membrane, or exfoliation in some nanoclays [86]. Moreover, the addition of filler can reduce the occurrence of hydrogen crossover during operation [38]. Also, Peighambardoust, S. Jamai et al reported that Nanoclay as a membrane additive is more cost competitive compared with inorganic oxide or zeolite as afore-mentioned in literature review [16, 59]. In particular, halloysite nanotube (HNT), natural nanoclay, is composed of cylinders formed by silica and alumina layers. Accordingly, the tensile strength of the composite membrane can be enhanced by the influence of reinforcement [42, 48]. In some cases, however, aggregated nanoclays can interfere with performance within the polymer matrix. Hence, numerous research engineers have tried various methods to improve fuel cell performance by controlling the dispersion state of halloysites. For this purpose, halloysite surface has been modified using, namely sulfonation [42, 46, 47], aminization [40, 42], or other type of functionalization (i.e., HNT impregnated with phosphotungstic acid, PWA) [120]. Changing the blending time for the casting dispersion is another good method [179].

To date, an influence of halloysite nanotube inside Aquivion membrane electrolytes has not been fully investigated for PEMFC applications, even if Aquivion is considered as a prominent candidate among various PFSA ionomers. Moreover, it has not been fully evidenced that the perfluoro-sulfonation of halloysite can improve certain properties regarding Aquivion composite membranes. If improved performance is confirmed through halloysite modification and pretreatment, this approach will be of significant benefit for the PEMFC to operate over a wide range of conditions.

This chapter focused on novel halloysite nanotube-based Aquivion membranes that can be operated at low relative humidity.

2. Membrane preparation

All membrane samples with a size of 13 × 13 cm^2 were prepared via casting and evaporation. Aquivion and nanoclay were blended within casting dispersion in vials.

To begin with, 3.23 g of Aquivion dispersion (24 wt%, D83-24B), 0.078 g of nanoclay and 12.27 g of isopropanol were blended so as to obtain a 5 wt% Aquivion casting dispersion resulting in a 10 wt% clay loaded composite membrane.

Different kinds of casting dispersions, obtained with different clays, were stirred for 15 mins by stirrer at 80 rpm. Afterward, nanoclay dispersions in vials were dispersed using ultrasound (HD 2070, Bandelin, Germany) and titanium alloyed microtip (MS73-529, Sonopuls, Bandelin) for 2 min at 60 W power and 20% pulsation level. The resultant dispersions were poured on a 13x13cm^2 mold at 15.578 g, after which it was heated at 80℃ for 18 h and then at 170℃ for 2 h. Prepared membranes were treated using 0.5M H_2SO_4 for 1 h and rinsed with DI-water for 1 h, at 100℃.

All the membranes were prepared using mold to have a dry thickness of around 20 μm, in order to follow

development trends and reduce resistance.

Various membranes were prepared by addition of four available nanoclays: pristine halloysite (HNT), sulfonated halloysite (HNT-S), fluorinated halloysite (HNT-F) and sulfo-fluorinated halloysite (HNT-SF). The modification of halloysite is briefly presented in chapter 2. The obtained membanes were labeled as listed in table 2.2.

Table 2.2. Information on nine different kinds of membranes prepared based on the available nanoclays (reproduced from chapter 2).

Membrane reference	PFSA ionomer	Nanoclay reference/content (wt%)	Type of nanoclay	Modification of nanoclay	Pretreatment of nanoclay
Aquivion		-	-	-	
Aq/HNT	Aquivion	HNT10	Halloysite	pristine	
Aq/HNT-F		HNT-F10		fluorination	
Aq/HNT-S		HNT-S10		sulfonation	
Aq/HNT-SF		HNT-SF10		Sulfo + fluo	
Aq/pHNT		pHNT2/5/10		pristine	○
Aqn/pHNT-F		pHNT-F2/5/10		fluorination	○
Aq/pHNT-S		pHNT-S2/5/10		sulfonation	○
Aq/pHNT-SF		pHNT-SF2/5/10		Sulfo + fluo	○

3. Nanoclay functionalization and characterization

3.1. Functionalization of halloysites

3.1.1. Fluorinated halloysite (HNT-F)

Into a 250 ml flask fitted with a condenser were introduced 10 g of halloysite, 1 g (1.6×10^{-3} mol) of N-(3-triethoxysilylpropyl)perfluorooctanoamide and 100 ml of an ethanol/water (90/10 wt%) solution. The mixture was then stirred and heated at solvent reflux for 15 h. The mixture was next centrifuged (5000 rpm) to eliminate the liquid phase and washed twice with acetone and THF. Finally, the modified filler was dried under vacuum before characterization.

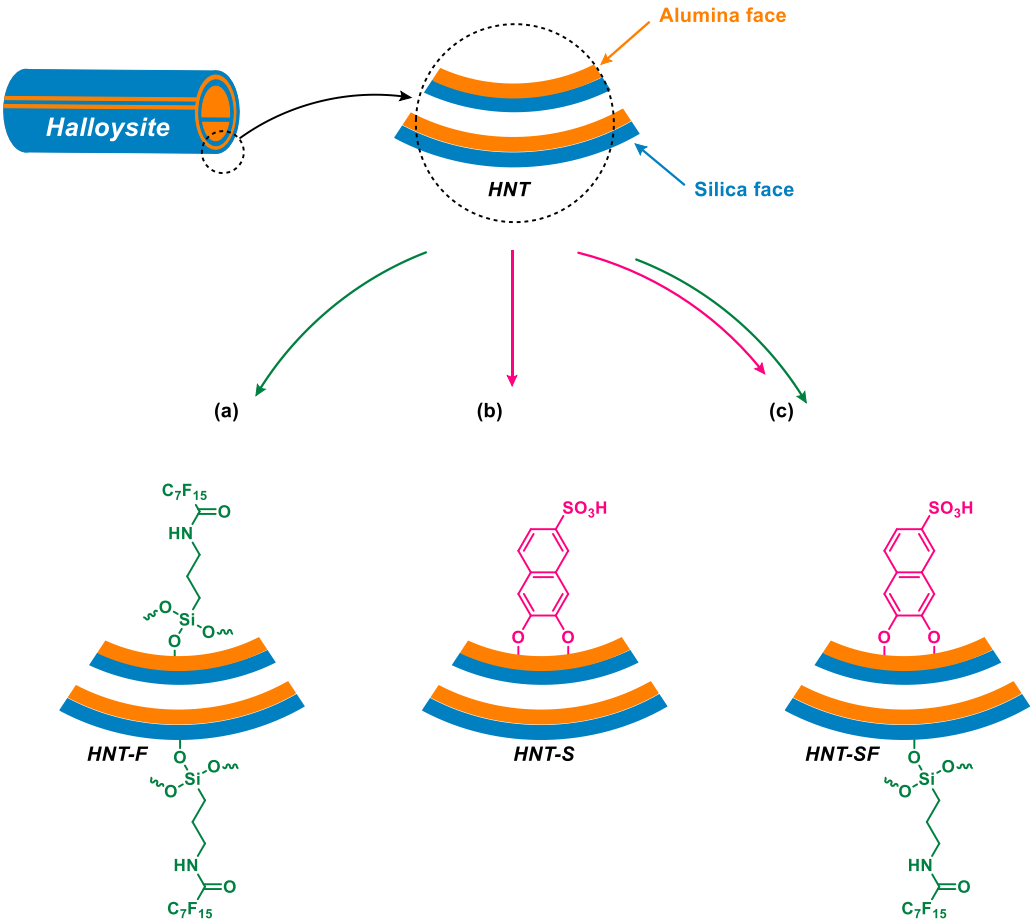

Scheme 4.1. Schematic representation of halloysite nanotubes (a) fluorinated, (b) sulfonated, and (c) perfluorosulfonated.

3.1.2. Sulfonated halloysite (HNT-S)

Into a 250 ml flask fitted with a condenser were introduced 10 g of halloysite, 1 g (3.8×10^{-3} mol) of sodium 2,3-dihydroxynaphthalene-6-sulfonate and 100 ml of deionized water. The mixture was then stirred and heated at solvent reflux for 15 h. The mixture was next centrifuged (5000 rpm) to eliminate the liquid phase and washed twice with water and acetone. Finally, the modified filler was dried under vacuum before characterization.

3.1.3. Perfluoro-sulfonated halloysite (HNT-SF)

Into a 250 ml flask fitted with a condenser were introduced 10 g of sulfonated halloysite previously obtained, 1 g (1.6×10^{-3} mol) of N-(3-triethoxysilylpropyl)perfluorooctanoamide and 100 ml of an ethanol/water (90/10 wt%) solution. The mixture was then stirred and heated at solvent reflux for 15 h. The mixture was next centrifuged (5000 rpm) to eliminate the liquid phase and washed twice with acetone and THF. Finally, the modified filler was dried under vacuum before characterization.

3.2. Characterization of halloysites (ATR-FTIR, TGA, Py-GC/MS)

All characterizations were performed at IMT MINES Alès.

FTIR was used to investigate the pristine and modified HNTs. As shown in Fig. 4.1, the different HNT samples show almost similar spectra. Characteristic peaks are observed at 3693 and 3628 cm^{-1}, assigned to the O–H stretching vibrations of inner-surface Al–OH and inner Al–OH, respectively [109]. The band for O–H deformation of inner Al–OH can also be observed at 908 cm^{-1}. The band at 1647 cm^{-1} corresponds to strongly bending vibrations of the adsorbed water. The band at 1124 cm^{-1} is ascribed to the perpendicular Si–O stretching vibration, and the band at 1020 cm^{-1} can be assigned to in-plane Si–O stretching vibrations. The bands for deformations of Al-O-Si and Si-O-Si can also be observed at 530 and 465 cm^{-1} respectively. Compared to the unmodified halloysite, the introduction of the fluorinated grafting agent onto halloysite surface exhibits some new peaks between 1200 and 1800 cm^{-1}. Indeed HNT-F and HNT-SF spectra show the presence of two peaks at 1535 and 1250 cm^{-1} attributed respectively to the N-H (bending) of the amide function and C-F bonds of the perfluorinated fragment. Moreover, the modification of the shape of the band centered at 1647 cm^{-1} (with an enlargement of the peak for the highest wavenumbers) was attributed to the C=O stretching vibration of the amide function. Finally, the HNT-S spectrum does not show significant differences with that of HNT.

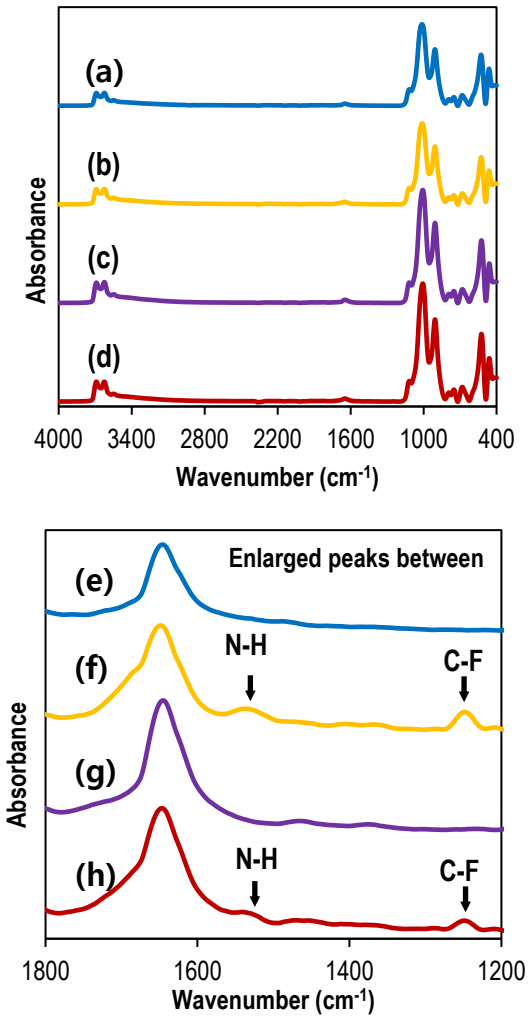

Fig. 4.1. ATR-FTIR spectra of (a, e) pristine halloysite, (b, f) HNT-F, (c, g) HNT-S and (d) (h) HNT-SF.

Thermogravimetric analyses were also used to characterize the different functionalizations of the halloysite as shown in Fig. 4.2. For all modifications an augmentation of the weight loss after grafting was observed. These weight losses were attributed to the decomposition of the grafted organic parts which tends to prove, along with FTIR results, the efficiency of the functionalization procedures used. HNT-F and HNT-S show weight losses of about 1.2 and 0.4 wt% respectively. Moreover, the second step of functionalization to obtain HNT-SF from HNT-S was also verified with an increase of the weight loss of about 1.2 wt% attributed to the fluorinated grafting agent.

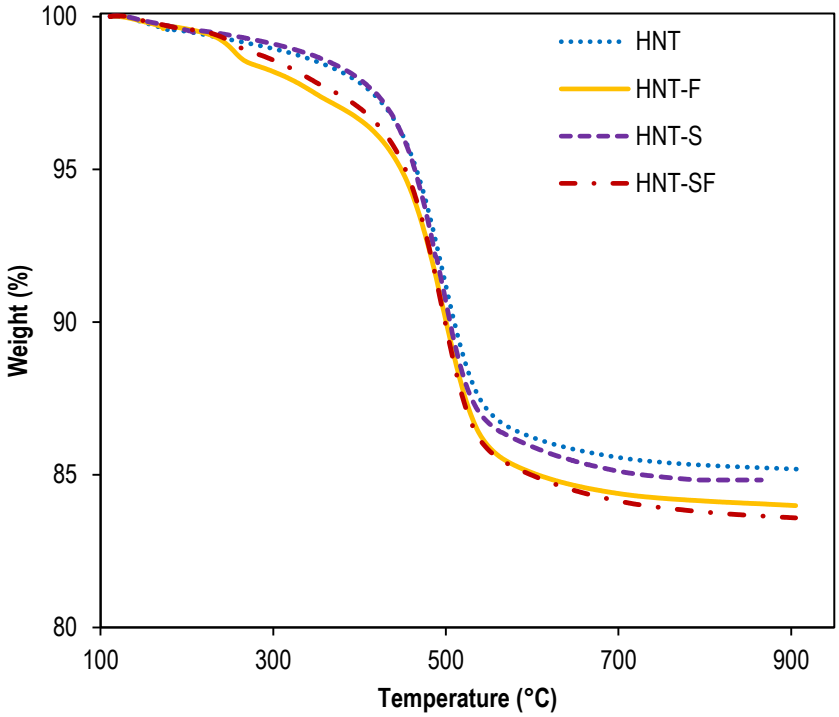

Fig. 4.2. TGA under nitrogen of pristine halloysite, HNT-F, HNT-S and HNT-SF samples from 110 °C to 900 °C after an isotherm at 110 °C for 10 min.

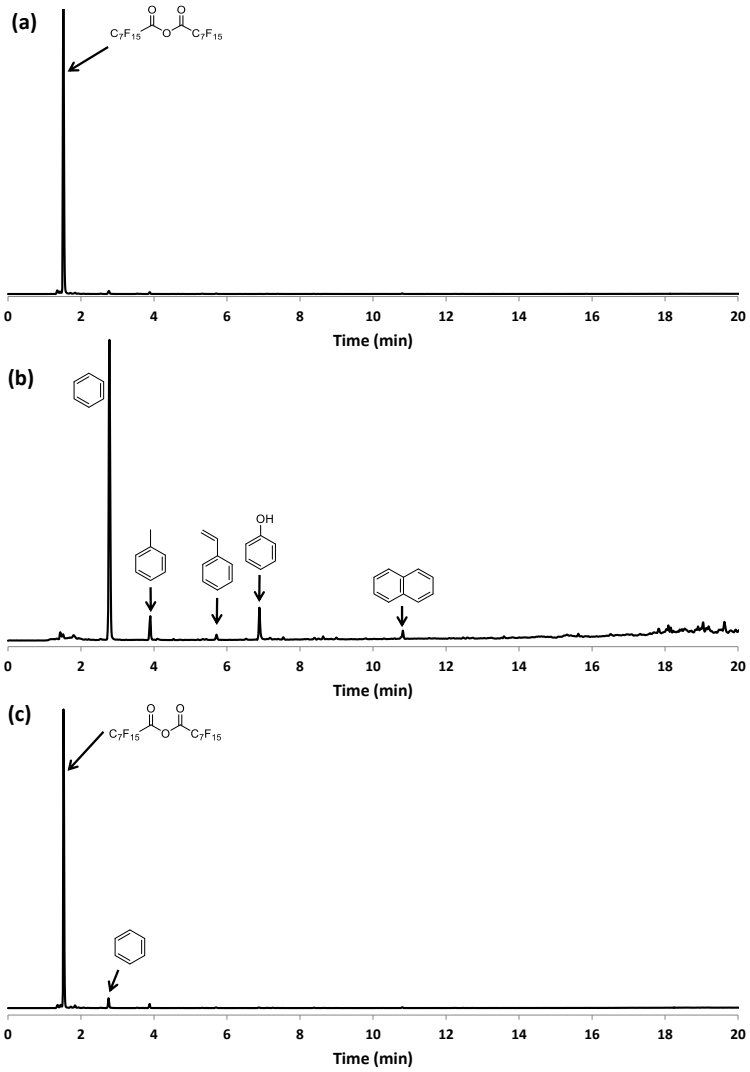

Fig. 4.3. Py–GC/MS chromatograms obtained for (a) HNT-F, (b) HNT-S and (c) HNT-SF samples pyrolyzed at 900°C.

Finally, Py–GC/MS was used to verify the different functionalization of halloysite. The analyses used a pyrolysis step at 900 °C to evaluate the presence and the nature of the organic molecules on the fillers surface after the grafting procedures. The results obtained for HNT-F, HNT-S and HNT-SF (see Fig. 4.3) confirmed the presence of the grafting agents after the halloysite functionalization. Whereas no peak was observed for pristine halloysite, chromatograms of functionalized clays show peaks corresponding to organic molecules obtained by thermal degradation of the grafted parts. Presence of fluorinated molecules is observed for HNT-F and HNT-SF due to the release of fluorinated molecules by decomposition of the fluorinated grafting agent. Different aromatic molecules are observed for HNT-S due to the thermal decomposition of the naphthalene part of the grafting agent. We have to note that for HNT-SF when a multi-grafting procedure was used, the obtained chromatogram shows essentially a peak due to the fluorinated part. This can be due to a fewer grafting rate obtained with the sulfonic grafting agent as observed from TGA results.

Based on the above description, Py-GC/MS analysis confirmed the presence of the grafting agents on the modified halloysite nanotubes after the grafting procedures.

4. Membrane characterization

4.1. Thickness of hydrated membranes (micrometer)

The membrane thickness is considered as crucial characteristic to reduce the ohmic losses during PEMFC operation [182], often at the expense of a higher hydrogen crossover. To achieve the benefits, the membrane thickness was targeted to 20 µm at room temperature and dry condition. State-of-the-art membranes such as Nafion HP and Gore Select M820 are approximately 23 – 27 µm thick, in wet condition, a value close to that measured for our pristine Aquivion membrane. It is noted that the manufacturers have made Nafion HP and Gore Select 20 µm thick in factories. All data is displayed in Fig. 4.4.

Pristine Aquivion membrane was slightly thicker (32 µm) compared with commercially available membranes. Adding 10 wt% of halloysite, pristine or modified, resulted in even thicker membranes (32-54 µm). It is common for the membrane thickness to increase as additives are added. The thickest membrane (54 µm) was obtained with 10 wt% pristine halloysite (Aq/HNT10).

The incorporation of modified halloysite (after fluorination, sulfonation, or perfluoro-sulfonation) resulted in intermediate thickness of composite membranes, between 40 and 45 µm. The thickness of membranes with functionalized halloysite was less than that of membrane to which pristine halloysite was added. Such thickness is probably due to density changes caused by functionalized halloysites inside membranes. That is, functionalized nanoclays can lead to thinner membranes due to better dispersing effect than the relatively more agglomerated pristine halloysite.

The pretreatment of halloysites in oxalic acid and hydrogen chloride, has a very limited impact on the thickness, regardless of functionalization type and nanoclay content (2 wt%, 5wt%, and 10 wt%). The only exception is Aq/pHNT10 (10 wt% of pre-treated halloysite) whose thickness is equal to that of our pristine Aquivion membrane. This means that introduction of pretreated pure halloysite induced the membrane to have a high density.

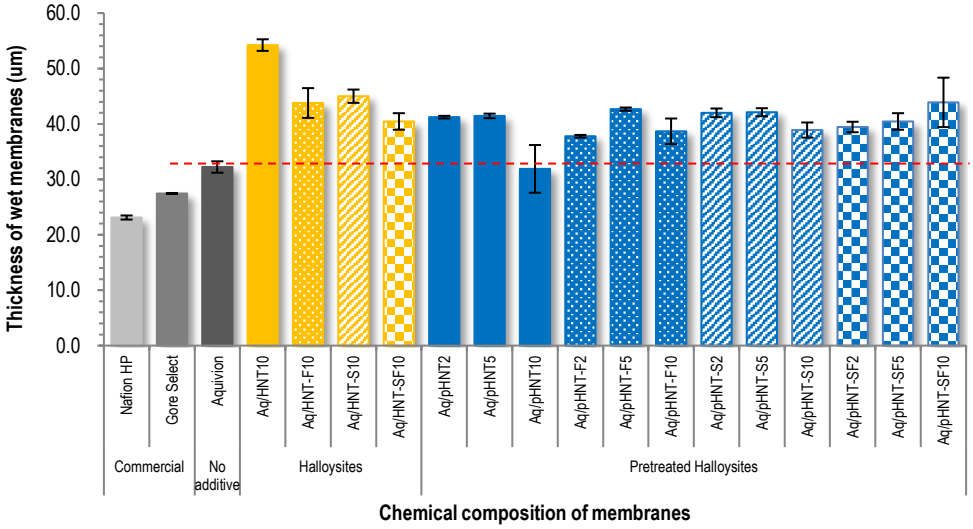

Fig. 4.4. Data on thickness: commercially available Nafion HP and Gore Select M820, and pristine Aquivion and Aquivion composite membranes containing various halloysites, HNT, HNT-F, HNT-S and HNT-SF. Yellow and blue bars represent non-pretreated and pretreated nanoclays, respectively.

Generally, the difference in the thicknesses of the membranes depending on the clay content, functionalization and pretreatment process is not large. However, another reason for the finely different thicknesses of the membranes (e.g., Aq/pHNT10) is that the moisture evaporates over a long time when the thickness is measured, and accordingly the membrane shrinks. The strategy to overcome these subtle differences is further work to be considered.

4.2. Ion exchange capacity

IEC is a crucial factor to verify the available number of ion exchange groups. It affects the proton conductivity of PEMs according to Grotthuss type theory [183]. Since the IEC value is inversely proportional to the equivalent weight of the ionomer, IEC grows as the equivalent weight decreases. The IEC of commercially available, pristine and composite membranes displayed values between 0.94 and 1.20 meq/g, as shown in Fig. 4.5.

Except for perfluoro-sulfonated halloysite, the addition of halloysite (pristine, fluorinated, or sulfonated) resulted in slightly higher IEC: 1.2 meq/g versus 1 for pristine Aquivion and Aq/HNT-SF10.

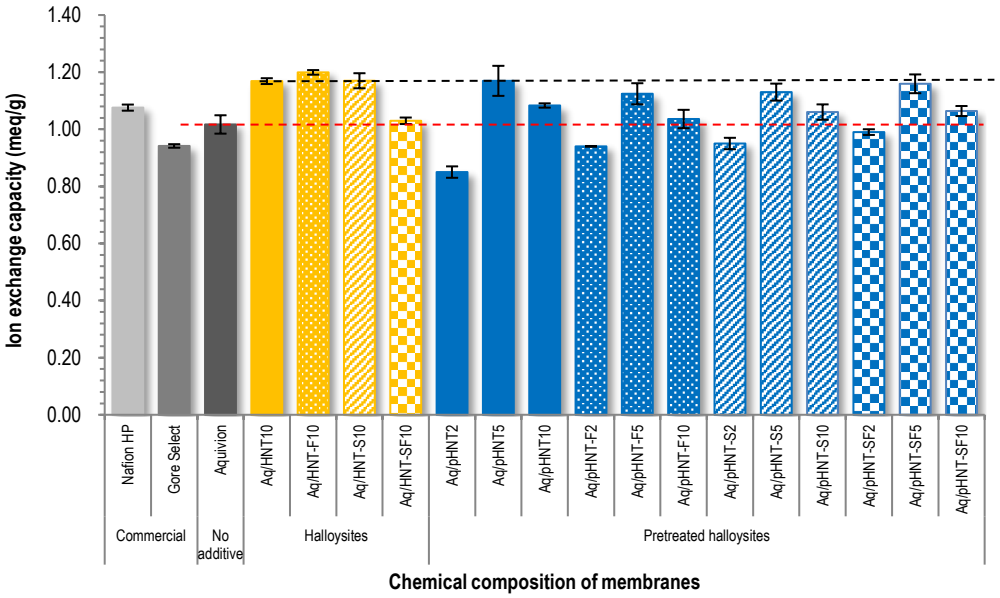

Fig. 4.5. Data on ion exchange capacity: commercially available Nafion HP and Gore Select M820, and pristine Aquivion and Aquivion composite membranes containing various halloysites, HNT, HNT-F, HNT-S and HNT-SF. Yellow and blue bars represent non-pretreated and pretreated nanoclays, respectively.

The pretreatment has no impact on the IEC which is for 10 wt% added halloysite (modified or not) at maximum 0.05 meq/g higher than for pristine Aquivion, i.e. within the margin error. For pretreated clay nanotubes, the amount of fillers seems to impact the IEC. For every pretreated HNT, the higher IEC is obtained for 5 wt% (around 1.15 meq/g). It is significantly lower for 2 wt% at least for pretreated pure hallosysite (0.85 meq/g for Aq/pHNT2). 10 wt% halloysite addition showed lower IEC of composite membranes rather than 5 wt%.. This may be because the clay nanotubes are blocking the side chain of the Aquivion, that is, the sulfonic group due to too

much added amount. Blocked sulfonic groups eventually interfere with ion movement. It is interesting to note that the evolution of the IEC is following that of the water uptake (Fig. 4.6). It is well known by many research engineers that the relationship between water uptake and IEC is closely related.

4.3. Water uptake

Proton transfer is affected by water molecules inside the ionomeric polymer matrix according to Grotthuss and vehicle mechanisms [182, 184]. Water uptake (%) is an essential parameter to evaluate the proton transfer in PEMFC application.

As shown in Fig. 4.6, the water uptake of the Aquivion membrane (38%) stands in between that of the Nafion HP (30 %) and that of the Gore Select (45%).

Due to their hygroscopicity, the addition of halloysite in Aquivion clearly resulted in an augmentation of water uptake, reaching similar values to Gore Select M820, with a maximum for the sulfonated halloysite (54%).

Comparing 10 wt% loaded composites prepared with the same type of halloysite, it is clear from Fig.4.6 that the pretreatment has a limited impact on the water uptake. As for IEC, the amount of fillers seems to impact the water uptake of pretreated halloysites which shows a maximum for 5 wt% loading, whatever the type of functionalization, reaching values between 65 % and 75%. Surprising data was obtained. Actually, a continuous increase of water uptake with the increasing amount of clay has been expected.

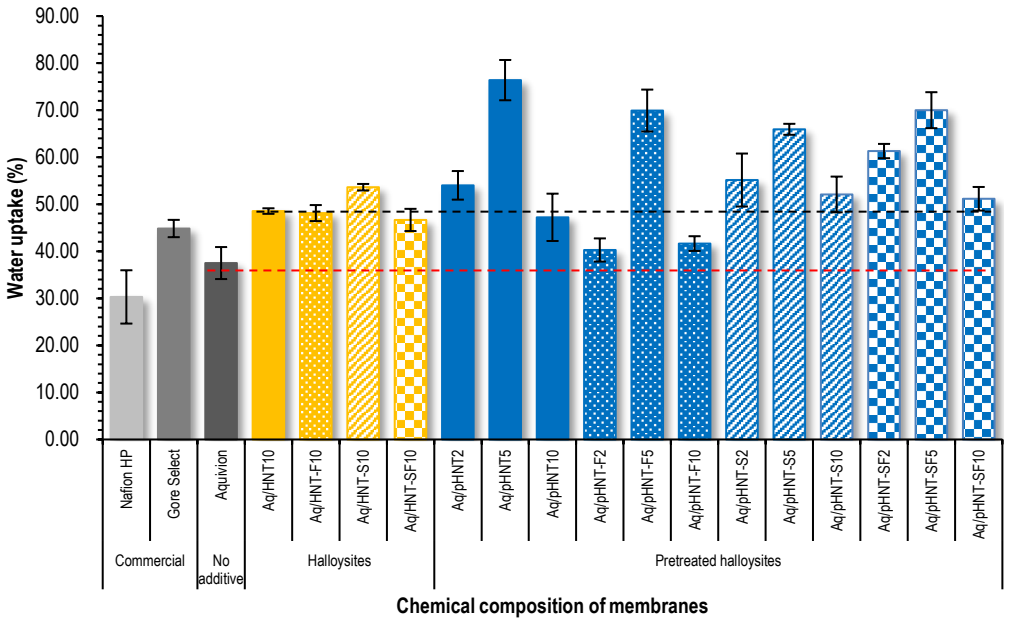

Fig. 4.6. Data on water uptake: commercially available Nafion HP and Gore Select M820, and pristine Aquivion and Aquivion composite membranes containing various halloysites, HNT, HNT-F, HNT-S and HNT-SF. Yellow and blue bars represent non-pretreated and pretreated nanoclays, respectively.

4.4. Swelling ratio

Fig. 4.7 displays the swelling ratio of different kinds of membranes, which is another crucial factor for fuel cell performance.

Commercially available membranes, Nafion HP and Gore Select, were analyzed as reference and they showed relatively lower swelling ratio compared with pristine Aquivion.

The addition of 10 wt% halloysites tremendously reduced the thickness swelling of all composite membranes, from 15% for Aquivion to about 4% for composites regardless of functionalization. This is attributed to improved reinforcement caused by the cylinder morphology of HNT nanotubes as discussed in former publications [30, 40, 42]. The fluorination may have a positive effect since Aq/HNT-F10 and Aq/HNT-SF10 membranes showed lower swelling.

The pretreatment had no significant impact. After pretreatment of the various halloysites,the composite membranes still showed rather limited swelling values, between 1.1% - 5.8%.

No real trend could be drawn either concerning the amount of pretreated clay. A decrease from 10 wt% to 5 wt% entailed a swelling increase after pretreatment for unmodified and fluorinated halloysites, whereas it raised for sulfonated and perfluorosulfonated ones.

Hence, the evolutions observed cannot be considered as representative. So, it is probably the impact of fluorination discussed above.

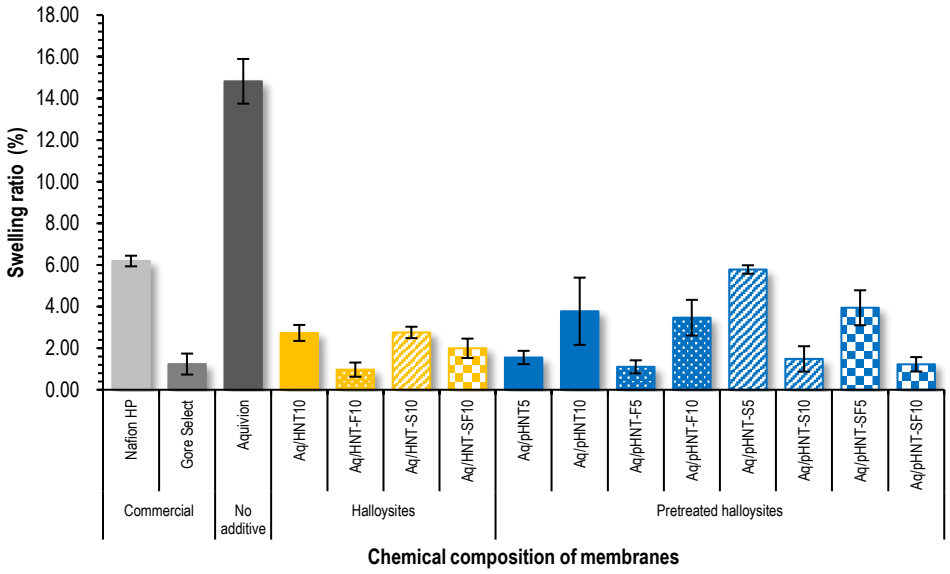

Fig. 4.7. Data on swelling ratio: commercially available Nafion HP and Gore Select M820, and pristine Aquivion and Aquivion composite membranes containing various halloysites, HNT, HNT-F, HNT-S and HNT-SF. Yellow and blue bars represent non-pretreated and pretreated nanoclays, respectively.

4.5. Homogeneity of composite membranes (FE-SEM and EDS)

Fig. 4.8 shows FE-SEM cross-section of the different kinds of membranes studied here, the commercally available ones and those prepared according to section 2. Both edge of membranes as well as the center of the cross section were chemically analyzed in order to get insights on the nanoclay repartition across the membrane thickness. Silicon and fluorine originating from halloysite and Aquivion respectively, were considered as markers to discuss about the distribution of nanoclays inside the polymer phase.

Blending of pristine halloysite with Aquivion displays large aggregates-loaded cross section, compared with that of functionalized halloysites as shown in Figs. 4.8d, h, l, and p. If the functionalization of halloysite allowed to largely avoid the formation of agglomerates, it hardly impacted the fine repartition of the clay within the polymer matrix. Indeed, the Si/F atomic ratio calculated from EDS results of all the composite membranes differs from one side to the other of the membranes. Concerning 10 wt% loaded composites, similar values have been morevover obtained (between 15 – 18 at the edges of cross section), regardless of functionalization as shown in yellow bars of Fig. 4.9.

Generally speaking, the pretreatement of halloysite resulted in a significative improvement of the clay repartition within the membrane. The difference of Si/F between both sides is divided by a factor two. The effect is more pronounced with sulfonated and fluorosulfonated halloysites, the latter resulting even in quite homogenous composites.

The amount of added clay nanotubes does not seem to impact the homogeneity of the composite whatever the type of nanoclay.

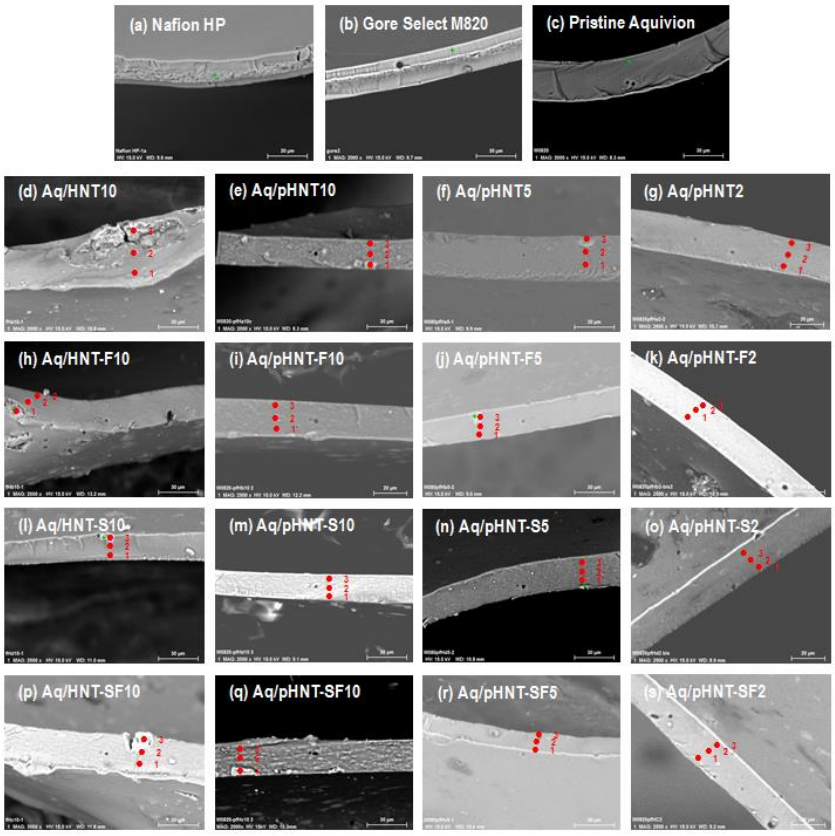

Fig 4.8. FE-SEM images regarding (a) commercially available Nafion HP, (b) Gore Select M820, (c) pristine Aquivion, and (d - s) Aquivion composite membranes blended with HNT, HNT-F, HNT-S and HNT-SF.

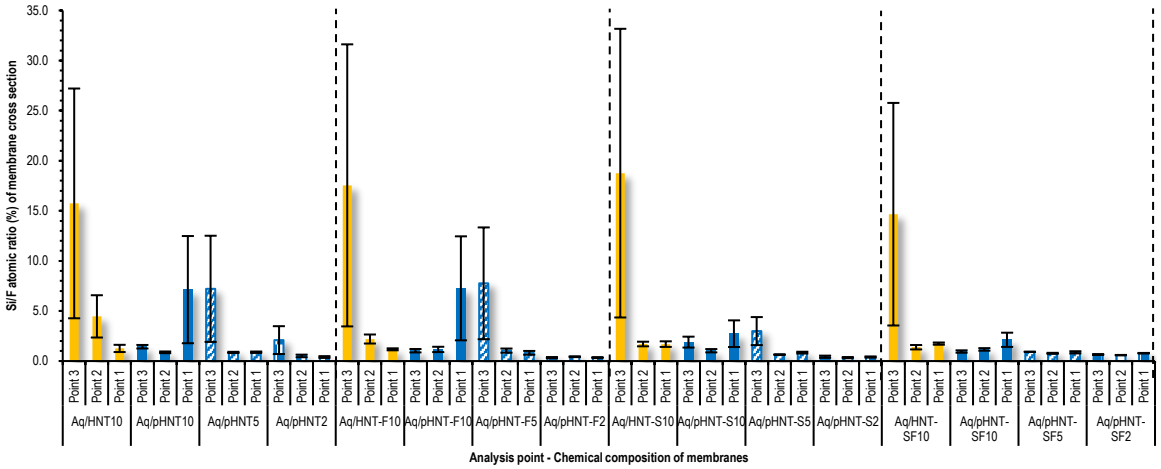

Fig. 4.9. Si/F atomic ratio calculated from EDS measurements, regarding commercially available Nafion HP, Gore Select, pristine Aquivion, and Aquivion composite membranes incorporated with HNT, HNT-F, HNT-S and HNT-SF. Yellow and blue bars represent non-pretreated and pretreated nanoclays, respectively.

4.6. *Dynamic mechanical analysis (DMA)*

DMA tests were performed in order to evaluate the influence of the different functionalizations on the storage and loss modulus. In the first test, in which temperature was varied, membranes containing 10wt% of non-pretreated or pretreated unmodified and modified HNT were tested (Figs. 4.10a-d).

It is shown that, up to 120°C, hybrid membranes containing non-pretreated and functionalized HNT have a lower storage modulus than the unmodified HNT one (Fig. 4.10a). Those non-pretreated HNT membranes are interesting because they maintain their stiffness (especially Aq/HNT-SF10) to very high temperatures. The results are totally different for hybrid membranes containing pretreated HNT. Indeed, Aq/pHNT-F10, Aq/pHNT-S10 and Aq/pHNT-SF10 membranes are all more rigid than Aq/pHNT10. Aq/pHNT-SF10 is particularly interesting at low T as it exhibits the highest stiffness. According to Fig. 4.10cd, the glass transition temperatures (peak of tan delta) are almost all the same between 80 and 90°C, whatever the membrane (except for Aq/HNT-SF10).

In the second test performed at low temperature (50°C), the relative humidity was varied for a long period of time. Only non-pretreated HNT bearing hybrid membranes were tested. As seen in Fig. 4.11, for all the membranes, an increase in RH induces a decrease in storage modulus G' as water plasticizes the membrane. For all the membranes, the response to a change in relative humidity is instantaneous and G' is always higher than G'' all along the test. These results are in good agreement with Fig. 4.10 and with the literature. By comparing the behavior of the hybrid membranes (Aq/HNT10, Aq/HNT-F10, Aq/HNT-S10 and Aq/HNT-SF10) it can be seen that fluorination (Aq/HNT-F10 and Aq/HNT-SF10) lead to lower storage modulus whatever the RH. Indeed, Aq/HNT-F10 and Aq/HNT-SF10 have a lower G' at 15 and 65%RH than Aq/HNT-S10 and Aq/HNT-10.

Finally, functionalization are interesting at low T (50°C) for HNT pretreated hybrid membranes, whereas sulfo-fluorinated functionalization is interesting for non-pretreated HNT hybrid membranes at high temperatures.

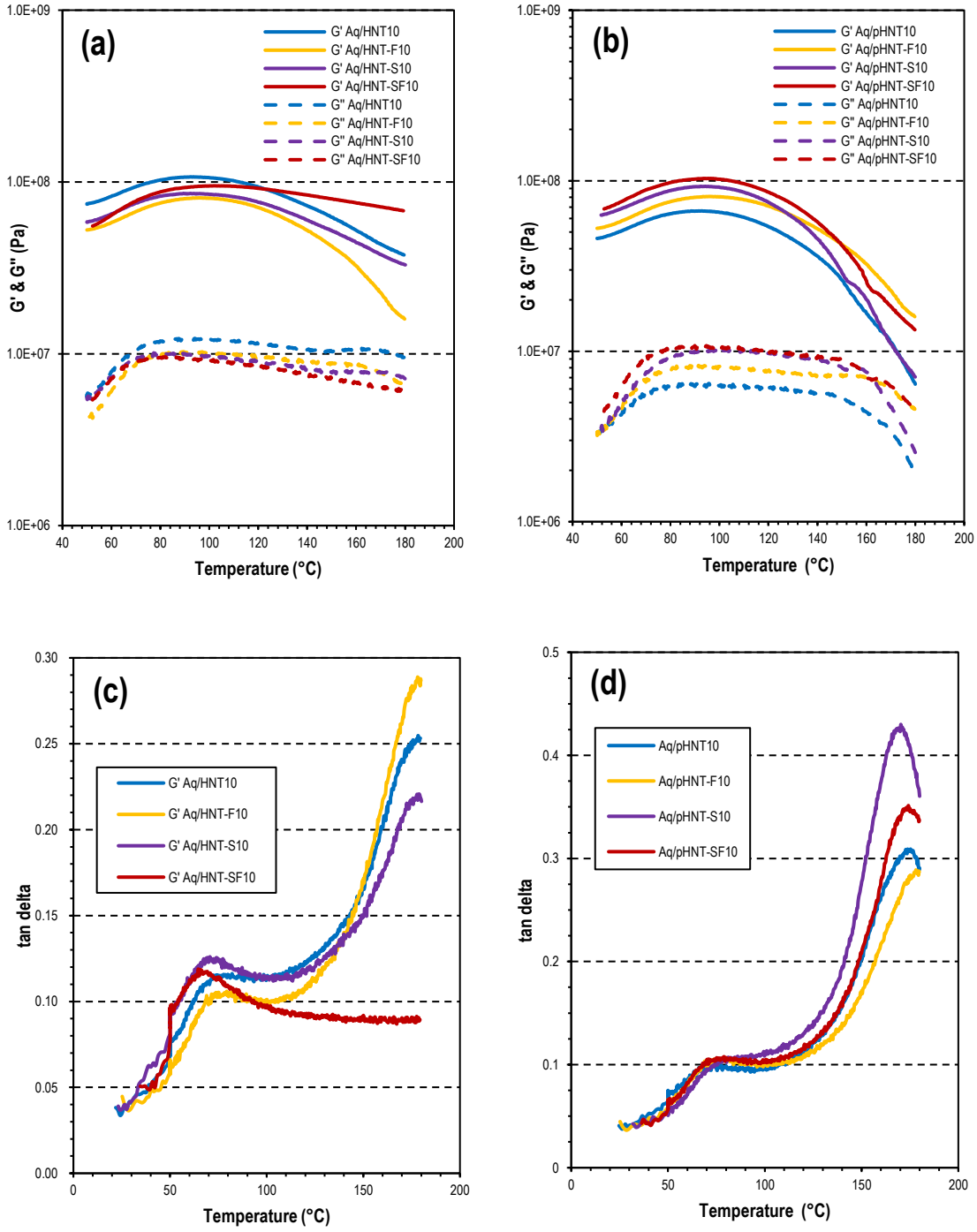

Fig. 4.10. DMA results on G' & G'' of composite membranes containing 10wt% of (a) non-pretreated and (b) pretreated HNTs. DMA data on tan delta of electrolyte membranes blended with 10wt% of (c) non-pretreated and (d) pretreated HNTs.

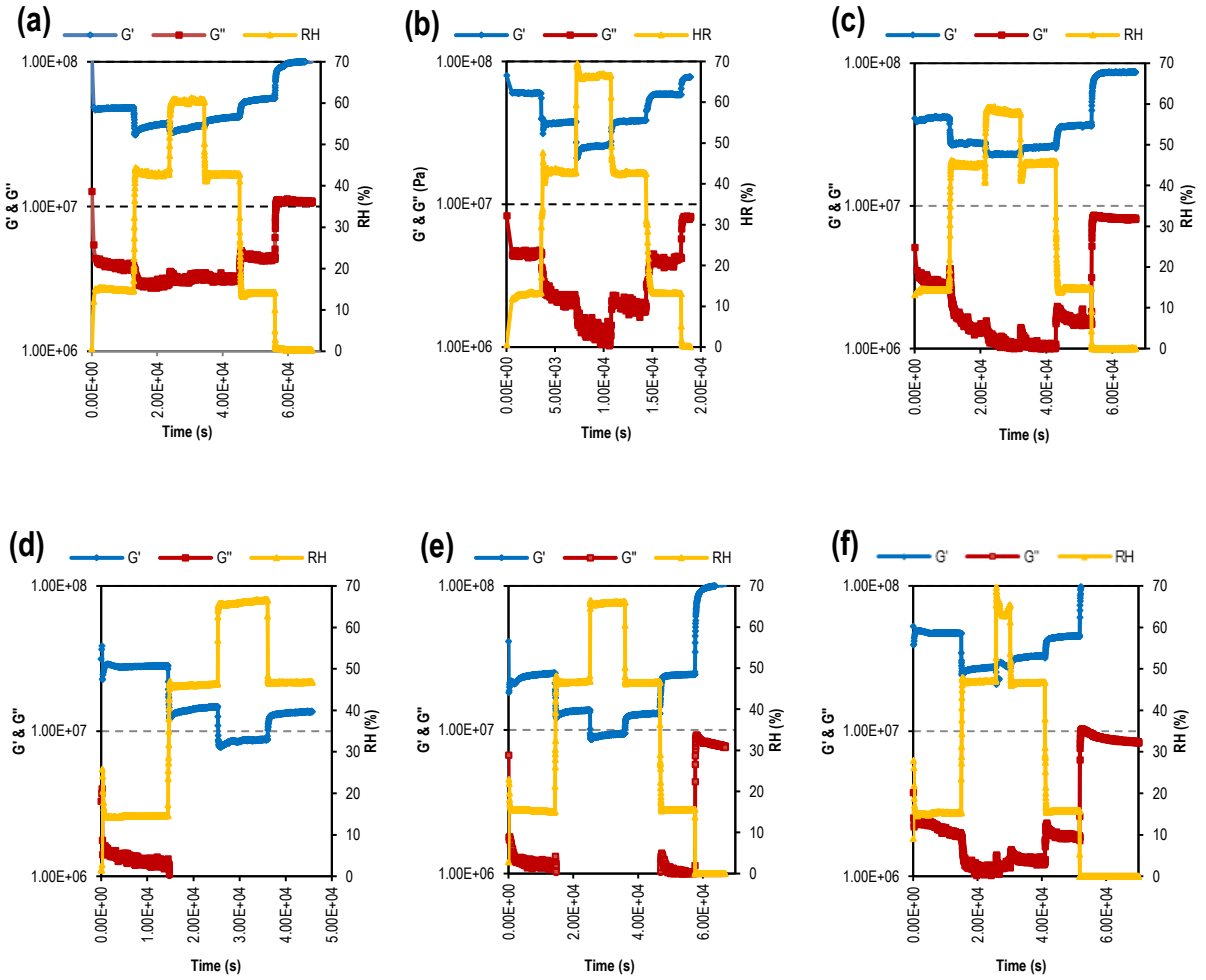

Fig. 4.11. DMA tests performed under different relative humidity (RH%) from 15 to 65% for (a) Nafion HP, (b) pristine Aquivion, (c) Aq/HNT10, (d) Aq/HNT-F10, (e) Aq/HNT-S10 and (f) Aq/HNT-SF10.

4.7. Chemical stability

PFSA membranes can be chemically degraded by free radicals such as HO· and HO_2· attacking the C-F bonds during operation of hydrogen fuel cells. This ultimately affects the permeability of the membrane, resulting in an increase in H_2 crossover. Numerous research engineers have reported that Fe_2O_3 is present in halloysites [185, 186]. Divalent iron ions can then react with H_2O_2 to form OH radicals and accordingly attack C-F bonds [13, 58, 60, 61]. To assess the chemical stability of our membranes and the possible role of such iron ions, they were immerged in H_2O_2/H_2SO_4 solution at 80°C for up to 96 h and the concentration of fluoride ions in the solution was measured.

It came out that, whatever the composites, the fluoride ion concentration raised with the immersion time (see Fig. 4.12), the evolution being very limited in the case of the Gore Select membrane.

The pristine Aquivion membrane exhibited less chemical stability than commercial membranes, Gore Select and Nafion® HP. That type of membrane most probably contains some antioxidant component which makes them more chemically stable.

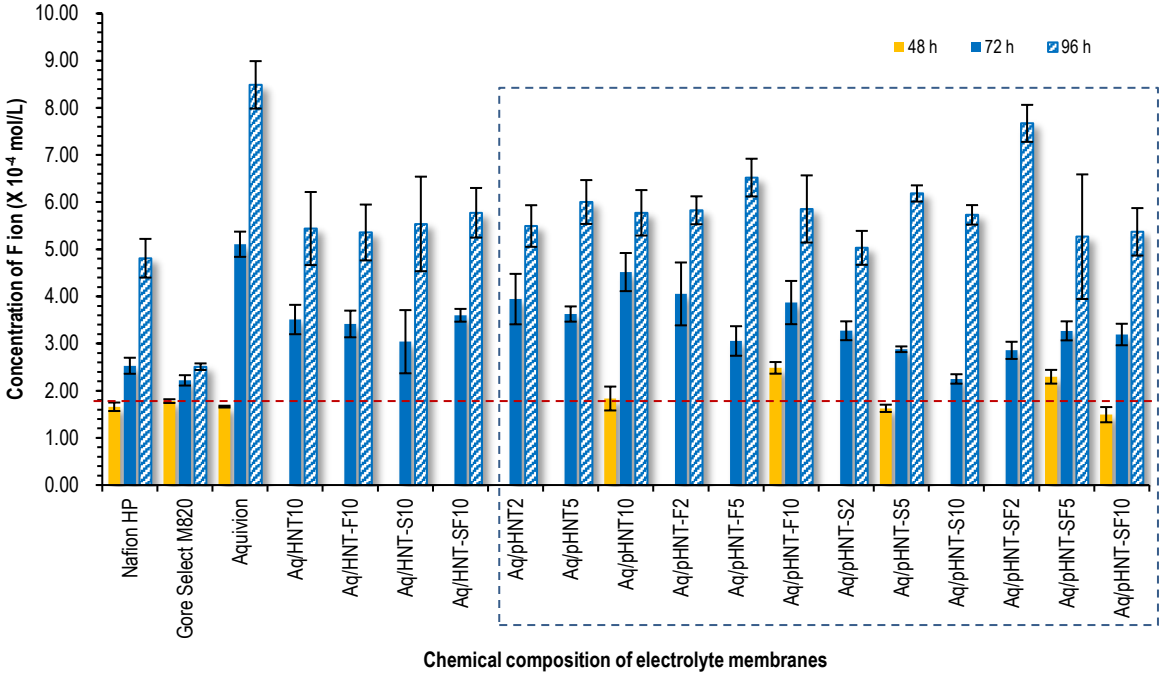

Fig. 4.12. Fluoride (F^-) concentration analyzed after immersion in H_2O_2/H_2SO_4 for Nafion HP, Gore Select M820, pristine Aquivion, Aq/HNT, Aq/HNT-F, Aq/HNT-S, Aq/HNT-SF, Aq/pHNT, Aq/pHNT-F, Aq/pHNT-S and Aq/pHNT-SF membranes. Red dotted line represents the fluorine concentration of 4.4 M H_2O_2/1.25 mM H_2SO_4 solution (blank test): $0.82\times10^{-4} \pm 0.08\times10^{-4}$ mol/L.

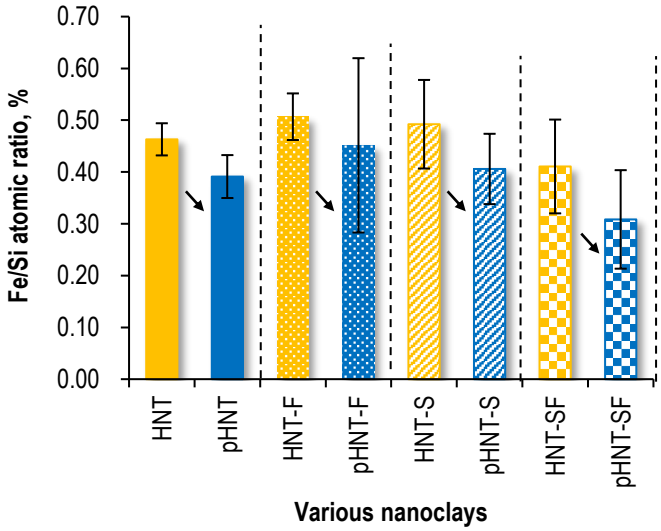

Fig. 4.13. Comparison of Fe/Si atomic ratio (%) regarding HNT, pHNT, HNT-F, pHNT-F, HNT-SF, pHNT-SF, HNT-S and pHNT-S clay nanotubes used for preparing composite membranes.Yellow and blue represent non-pretreated and pretreated nanoclays, respectively.

The presence of halloysites in Aquivion resulted in a lower production of fluoride ion showing an improved chemical stability of the composites compared to pristine Aquivion. True strictly speaking, if it is systematic, the difference is very limited and the amount of F very small because small membrane samples were used to analyze. On the other hand, if a full-size electrolyte membrane is used and considered in the fuel cell stack, the difference in fluorine concentration will be larger. For this reason, it is needed to real experiment with MEA tests or stacks, based on fluoride concentration and antioxidative activity, for further work.

Blending of functionalized halloysite also showed similar tendency to that of pristine halloysite. That is, when pristine halloysite or functionalized halloysite was mixed in Aquivion matrix, cracks or destruction didn't occur even when the composite membrane reacted with H_2O_2/H_2SO_4 solution. Such phenomenon is similar to when pristine sepiolite or fluorinated sepiolite is added. From these results, it can be concluded that the nanoclays reduce the concentration of fluoride ions by preventing the cracks or destruction behavior of composite membrane, compared with pristine Aquivion membrane.

The role of the pretreatment was to remove most of the iron from the halloysite. However, the composite membranes with pretreated halloysites showed similar fluoride concentrations to those without pretreatment. The reason can be explained by the amount of iron analyzed by EDS. As shown in Fig. 4.13, the iron (Fe^{2+}) removal by the pretreatment process is rather limited. For future experiment, a stronger and more effective pretreatment process may be required to remove divalent iron from halloysites.

Reducing the amount of halloysite did not impact the fluorine concentration. Either the concentration measured can be considered as negligeable or the amount of iron in the 2 wt% loaded composites is large enough to contribute to the degradation.

4.8. Proton conductivity (EIS)

High proton conductivity resulting from movement of the ion carriers is a prerequisite for fuel cell membranes. In the study, the through plane proton resistance of each membrane was measured in various temperatures (50℃, 70℃, and 90℃) and relative humidity (25%, 50%, 75%, and 90%) conditions.

Figs. 4.14 and 4.15 display the proton conductivity obtained by substituting the thickness of each membrane measured in the wet state into equation (5).

Pristine Aquivion with shorter side chains than Nafion led to higher proton conductivity. Large crystallinity and lower equivalent weight of Aquivion can also lead to higher proton conductivity [50, 51]. The commercial membrane, Gore Select, displayed a value close to approximately 260 mS/cm at 90℃ and 90% RH, which is higher than that of pristine Aquivion and Nafion HP. Cooper's group reported aound 80 - 120 mS/cm, which relatively lower proton conductivity of Gore Select (18 and 35 μm thickness) than data obtained in this study [187]. The reason is that multiple factors may work: 1) higher temperature operating condition, 2) low pH value of DI-water (destilled water) used for relative humidity controls and 3) reduced resistance of DI-water. More specifically, the reason for showing higher proton conductivity is that Gore Select measured in this study was sulfonated using sulfuric acid solution, thereby making the membranes better conductive. Other reason is because the proton conductivity improves as the temperature increases under similar relative humidity (i.e., approximately 10℃ gap of operating temperatures). That is, proton conductivity is proportional to the temperature. The proton

conductivity for temperature can be described by the following Arrhenius equation [188].

$$\sigma = \sigma_0 exp^{-E_a/RT} \qquad (6)$$

Where E_a, σ_0, R and T represent the activation energy for proton conductivity, pre-exponenital factor, universal gas constant and Kelvin temperature, respectively.

Third reason may be that the acidity (pH) of the distilled water used for relative humidity control is slightly lower. DI-water is 5.17 ± 0.08, which means helping to improve proton conductivity because the more acidic the water is, the higher the degree of dissociation of H^+, accordingly the resistance of water used as relative humidity controls may be relatively lower. The pH of DI-water used for relative humidity control in the reference was not measured but can be considered as a question. In addition, there may be another question or doubts as to whether trace amounts of sulfuric acid may be present in the treated Gore Select. However, the trace amount of sulfuric acid inside the membrane in the homemade cell with a drain can not remain at 90% RH operating conditions as sulfuric acid is diluted away by clean DI-water during being measured all days. Therefore, these hypotheses are not correct.

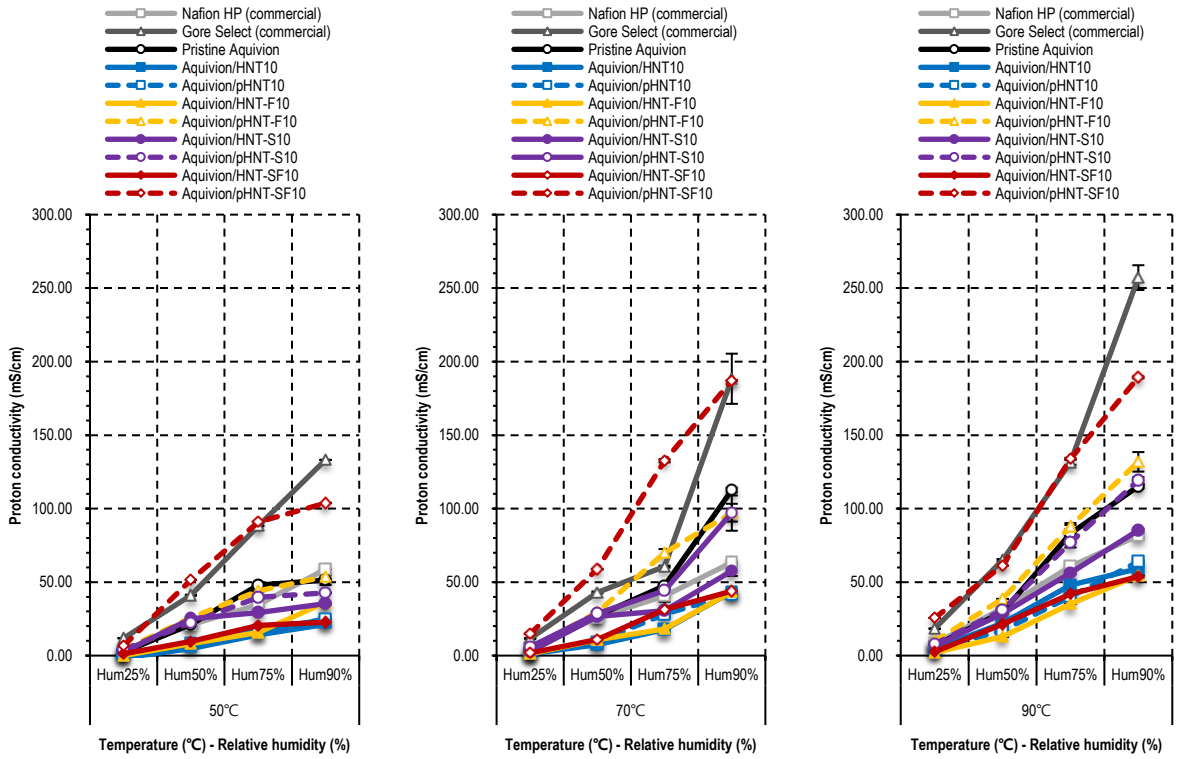

Fig. 4.14. Proton conductivity comparison of non-pretreated and functionalized vs. pretreated and functionalized nanoclays on composite membranes under various temperature and relative humidity: Nafion HP, Gore Select M820, pristine Aquivion, Aquivion/HNT, Aquivion/HNT-F, Aquivion/HNT-S, Aquivion/HNT-SF, Aquivion/pHNTs, Aquivion/pHNTs-F, Aquivion/pHNTs-S and Aquivion/pHNTs-SF composite membranes incorporated with 10wt% contents.

The proton conductivity of all composite membranes prepared with unpretreated halloysites (pristine HNT-10, fluorinated HNT-F10, sulfonated HNT-S10 and fluorosulfonated HNT-SF10) was relatively low compared with that of the pristine Aquivion membrane.

Composite membranes with pretreated nanoclays displayed improved proton conductivity, except in the case of pure halloysite due to improved nanoclay dispersion leading to homogeneous property. The pretreatment process had a positive influence, but the results varied depending on the functional group. In the case of fluorinated or sulfonated halloysite, the proton conductivity reached the level of pristine Aquivion.. Among the membranes tested, blending of pretreated and perfluoro-sulfonated halloysite exhibited the greatest improvement, reaching much higher a conductivity than that obtained with Aquivion, and even similar conductivity as the Gore select (190 and 280 mS/cm at 90℃ and 90% RH) for 10 wt% and 5 wt% added to Aquivion, respectively.

In terms of contents, composite membranes showed better proton conductivity when fluorinated or perfluoro-sulfonated halloysites was mixed with 5 wt% instead of 10 wt%. Then a maximum though-plane proton conductivity of 280 mS/cm was reached at 90°C and 90% RH. The proton conductivity is closely related to the IEC and water content in the membrane. The addition of 5 wt% pretreated and functionalized halloysites showed both higher IEC and water uptake values than 2 or 10 wt% (see Fig. 4.5 and 4.6). Accordingly, the membranes containing 5 wt% content showed the highest proton conductivity.

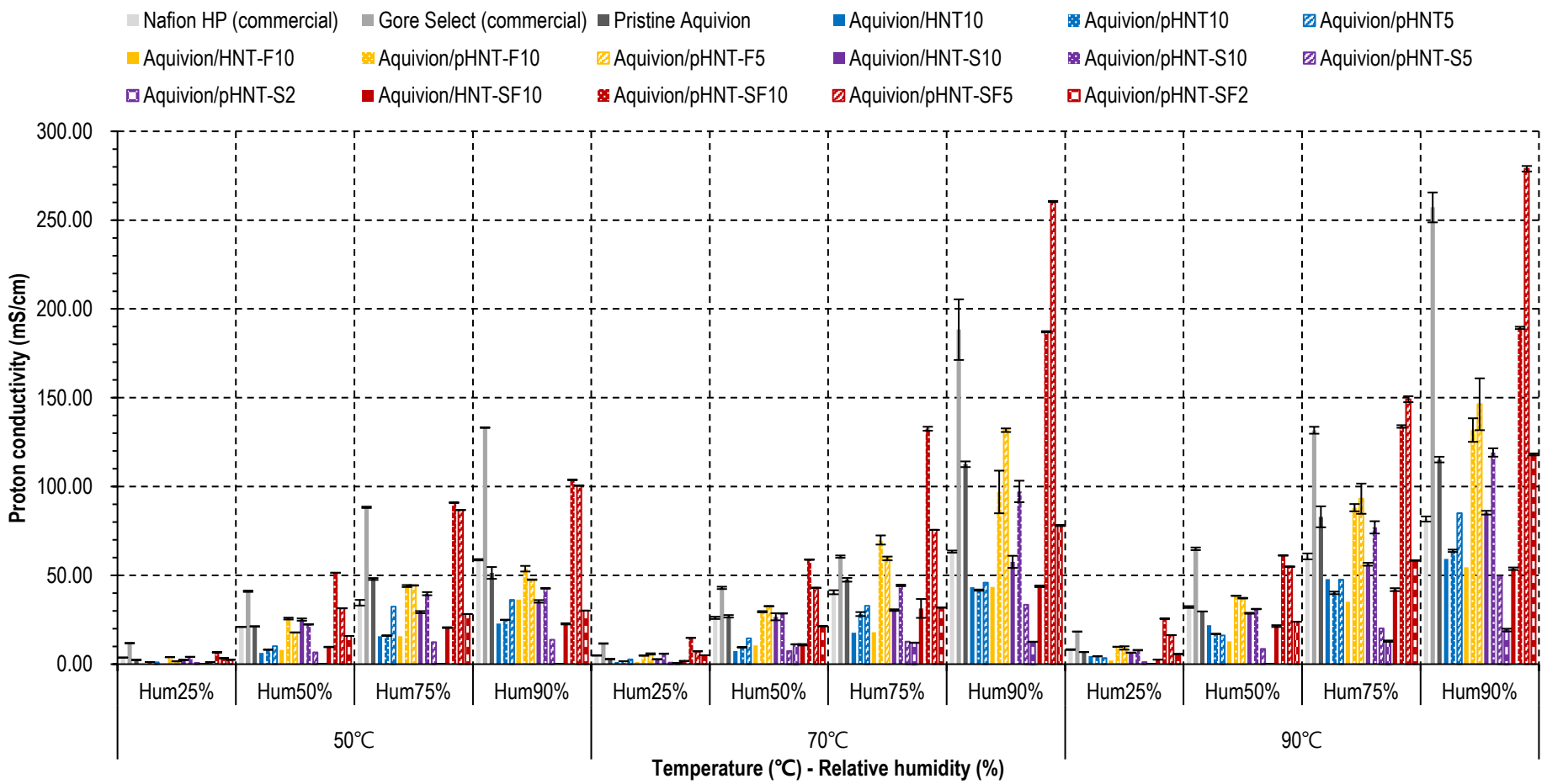

Fig. 4.15. Influence of temperature and relative humidity on proton conductivity (mS/cm) for various PEMs: Nafion HP, Gore Select, pristine Aquivion, Aquivion/HNT, Aquivion/HNT-F, Aquivion/HNT-S, Aquivion/HNT-SF, Aquivion/pHNTs, Aquivion/pHNTs-F, Aquivion/pHNTs-S and Aquivion/pHNTs-SF composite membranes incorporated with 10wt%, 5wt% and 2wt% contents.

Conclusions

Halloysite surface was successfully functionalized with fluorinated, sulfonated, or perfluorosulfonated group. Aquivion composite membranes were prepared by incorporating grafted halloysites. Their physicochemical properties were compared with Nafion HP and Gore Select M820. A number of conclusions related with properties of prepared membranes can be drawn:

- Blending pure halloysite into Aquivion phase resulted in improved water uptake, swelling ratio and mechanical properties. The composite membrane displayed similar IEC, but showed reduced proton conductivity compared to Nafion HP and Gore Select. In addition, they had heavy thickness compared with pristine Aquivion and commercially available membranes.
- Functionalized clay nanotubes resulted in stiffer (for Aq/HNT-SF10) and thinner composite membranes than pure halloysite. However, similar composite homogeneity, swelling, chemical stability, water uptake and IEC were obtained, regardless of functionalization types.
- The pretreatment associated to the functionalization of halloysites proved to benefit to composite homogeneity and proton conductivity. In particular, blending of pretreated and perfluoro-sulfonated halloysite into Aquivion matrix led to the highest proton conductivity among the membranes tested. Moreover, Aq/pHNT-SF10 was particularly interesting as it displayed improved mechanical property (better stiffness). However, according to the fluoride ion concentration, the pretreatment did not affect the chemical stability as expected.
- The amount of pretreated and functionalized clay nanotubes is impacting the IEC, the water uptake and the proton conductivity with a maximum reached for 5 wt% Besides, the smaller the content, the better the dispersion state of additives.

Based on characterization, it is suggested that improved physicochemical properties of Aquivion/pretreated and perfluoro-sulfonated halloysite electrolyte membrane have a potential in PEMFC operation, under wide ranged condition.

In terms of further study, it is needed to conduct MEA tests under various operating conditions. The thickness of composite membranes also needs to be optimized to reduce the resistance loss of the MEAs.

Chapter 5

Quercetin grafting effect of anti-oxidative activity on electrolyte membranes

Summary

Quercitine was grafted to halloysite to improve the chemical stability of composite membranes.

Halloysites were grafted with pure quercetin, amino group/quercetin or fluorine group/quercetin. Functionalized halloysites were pretreated using oxalic acid ($C_2H_2O_4$) and hydrogen chloride (HCl) to remove divalent iron. Pristine halloysite or modified halloysite was blended with Aquivion dispersion to improve membrane characteristics. Electrolyte membranes were cast and then evaporated prior to sulfuric acid (H_2SO_4) treatment.

Various functionalized halloysites were analyzed by ATR-FTIR (attenuated total reflection-Fourier-transform infrared spectroscopy), TGA (thermal gravimetric analysis), as well as Py-GC/MS (pyrolysis-gas chromatography mass spectrometry).

Regarding FTIR spectra, HNT-Q spectrum shows peaks at 1520, 1435, 1380, 1335 and 1285 cm^{-1} attributed to stretching vibrations of the quercetin part. N-H (bending) of the amide function and C-F bonds of the perfluorinated group (for HNT-FQ) appeared at 1535 and 1250 cm^{-1}, respectively. C-H (scissoring and wagging) of the propyl fragment of HNT-NQ was confirmed at 1505, 1362 and 1273 cm^{-1}.

With respect to TGA result, HNT-Q, HNT-FQ and HNT-NQ display weight losses of about 0.54, 1.39 and 1.00wt%, respectively. The second step of functionalization to obtain HNT-FQ and HNT-NQ from HNT-Q was verified for both samples with an augmentation of the weight loss of about 0.85 and 0.45wt% attributed to the fluorinated and amino grafting agents respectively. For Py-GC/MS, the results obtained for HNT-Q, HNT-FQ and HNT-NQ demonstrated the presence of an organic moiety after each HNT modification. No peak was observed for pristine halloysite, but chromatograms of functionalized halloysite nanotubes exhibit various peaks corresponding to molecules obtained by thermal decomposition of the grafted parts.

Mixing of Aquivion dispersion with halloysite grew water uptake and thickness compared to commercially available membranes used as reference. On the other hand, the electrolyte membrane showed similar oxidation resistance and IEC.

The addition of halloysite grafted with quercetin, fluorine group/quercetin or amino group/quercetin into Aquivion phase slightly increased the thickness with IEC. Moreover, these membranes had a reduced ratio of swelling compared with Nafion HP. Blending of halloysite grafted with fluorine group/quercetin could improve composite homogeneity. By incoporating fluorine group/quercetin- or amino group/quercetin-grafted HNT, water uptake values of composite membranes were raised. In addition, in 96 h, blending with quercetin grafted halloysites helped the composite membrane to show improved chemical stability over the Nafion HP. This displayed even higher antioxidant functions than pure Aquivion or pristine HNT-incorporated membranes.

By pretreating the functionalized halloysites, composite membranes were thicker than the commercial membranes. The water uptake of all the membranes except the membrane containing amino group/quercetin-grafted halloysite showed similar values. The overall IEC was similar. The swelling ratio was similar or slightly higher than Gore Select M820, but lower than Nafion HP. The proton conductivity of composite membranes was improved compared with Nafion HP when Aquivion dispersion was blended with pure quercetin-grafted halloysite.

Variety of additive content displayed different results of water uptake. For example, water uptake of 5 wt% additive-mixed membranes retained the highest values among the membranes tested. Concerning proton conductivity, the higher the contents, the higher the values. On the other hand, antioxidant function and thickness of electrolyte were not affected by the change of contents.

Résumé

Un groupe quercitine a été greffé sur l'halloysite pour améliorer la stabilité chimique des membranes composites.

Des halloysites ont été greffés avec de la quercétine pure, un groupe amino / quercétine ou un groupe fluor / quercétine. Les halloysites fonctionnalisés ont été prétraitées à l'aide d'acide oxalique ($C_2H_2O_4$) et de d'acide chlorhydrique (HCl) pour éliminer le fer divalent. Le différentes halloysites ont été mélangées à une dispersion d'Aquivion pour améliorer les caractéristiques des membranes composites. Les membranes ont été préparées par coulée/ évaporation avant de subir un traitement à l'acide sulfurique (H_2SO_4).

Les chargers argileuses ont été caractériées par ATR-FTIR (spectroscopie infrarouge à transformée de Fourier totale à réflexion totale atténuée), TGA (analyse gravimétrique thermique), ainsi que Py-GC / MS (spectrométrie de masse à pyrolyse-chromatographie en phase gazeuse).

En ce qui concerne les spectres FTIR, le spectre HNT-Q présente des pics à 1520, 1435, 1380, 1335 et 1285 cm^{-1} attribués auxvibrations de la quercétine. La liaison N-H (flexion) de la fonction amide et les liaisons C-F du groupe perfluoré (pour HNT-FQ) apparaissent à 1535 et 1250 cm^{-1}, respectivement. La liaison C-H du fragment propyle de HNT-NQ a été confirmée à 1505, 1362 et 1273 cm^{-1}.

En ce qui concerne le résultat d'ATG, HNT-Q, HNT-FQ et HNT-NQ affichent des pertes de masse d'environ 0,54, 1,39 et 1,00% respectivement.

Pour Py-GC / MS, les résultats obtenus pour HNT-Q, HNT-FQ et HNT-NQ ont démontré la présence d'une fraction organique après chaque modification HNT. Aucun pic n'a été observé pour l'halloysite brute, mais les chromatogrammes d'halloysites fonctionnalisés présentent divers pics correspondant à des molécules obtenues par décomposition thermique des parties greffées.

Le mélange de la dispersion Aquivion avec de l'halloysite a permis d'augmenter l'absorption d'eau et l'épaisseur de la membrane composite par rapport aux membranes disponibles dans le commerce utilisées comme référence. Par ailleurs, la membrane électrolytique présentait une résistance à l'oxydation et une capacité d'échangionique comparables à celles des membranes de référence.

L'addition d'halloysite greffée avec de la quercétine, un groupe fluor / quercétine ou un groupe amino / quercétine dans la phase Aquivion a légèrement augmenté l'épaisseur et la capacité d'échangionique. De plus, ces membranes avaient un taux de gonflement réduit par rapport au Nafion HP. Le mélange d'halloysite greffé avec un groupe fluor/quercétine pourrait améliorer l'homogénéité des composites. En incorporant un HNT greffé groupe fluor/quercétine ou amino/quercétine, l'absorption d'eau des membranes composites a été augmentée. De plus, en 96 h, un mélange avec des halloysites greffées avec de la quercétine a permis à la membrane composite de montrer une stabilité chimique améliorée leper rapport à la membrane Nafion HP. Elle présentait un comportement antioxydant encore plus élevé que les membranes Aquivion pure ou incorporant dans de l'halloysite non modifiée.

En prétraitant les halloysites fonctionnalisées, les membranes composites étaient plus épaisses que les membranes commerciales. L'absorption d'eau de toutes les membranes était similaire, à l'exception de la membrane contenant le groupe amino/halloysite greffé avec de la quercétine. La capacité d'échange ionique était similaire. Le taux de gonflement était similaire ou légèrement supérieur à celui de Gore Select M820, mais inférieur à celui de Nafion HP. La conductivité protonique des membranes composites a été améliorée par rapport au Nafion HP lorsque la dispersion d'Aquivion a été mélangée à de l'halloysite greffé à la quercétine pure.

La quantité d'eau absorbée dépend du taux d'argile dans la membrane composite. Par exemple, l'absorption d'eau

la plus élevée a été enregistrée pour une membrane chargée à 5% en masse. En ce qui concerne la conductivité des protons, plus le taux d'argile augmente, plus les valeurs sont élevées. Par contre, il n'a pas d'incidence sur le comportement antioxydant et l'épaisseur de la membrane.

1. Introduction

The divalent iron (Fe^{2+}) contained in HNT may be responsible of the formation of OH and OH_2 radicals which can then attack C-F bonds of the membrane during fuel cell operation [189] resulting in severe membrane degradation. The free radical formation pathway at the cathode can be described by the following equations [13, 58]:

1) $O_2 + 2H^+ + 2e^- \rightarrow H_2O_2$
2) $H_2O_2 + Fe^{2+} \rightarrow Fe^{3+} + HO\cdot + HO^-$
3) $HO\cdot + H_2O_2 \rightarrow H_2O + HO_2\cdot$

An attempt to avoid those composite membranes oxidation is necessary to improve PEMFC durability. The introduction of quercetin can lead to the anti-oxidative properties of the composite membrane. That is, PFSA-based electrolyte membranes can be chemically stabilized due to the effect of quercetin. The antioxidant activity of quercetin is related to its chemical structure, especially the presence and location of the hydroxyl (-OH) substitutions and the catechol-type ring B [190, 191]. The structural properties of a potent antioxidant capacity is due to the presence of (1) a catechol or ortho-dihydroxy group in the ring B, (2) a 2,3-double bond, and (3) hydroxyl substitution at positions 3 and 5 (see Fig. 5.1) [192]. Based on these structural properties, electron resonance between aromatic ring A and ring B plays an important role in antioxidative effect of quercetin [190, 191]. Moreover, introduction of the quercetin grafted with fluorine or amino groups has the potential to show improved dispersion state of additives inside PFSA phase.

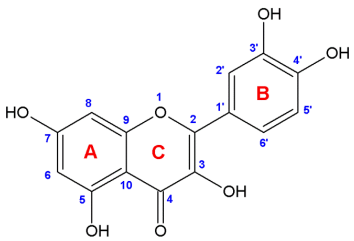

Fig. 5.1. Chemical structure of quercetin used for grafting.

So far, it has not been fully evidenced that quercetin-grafted halloysite-based Aquivion membranes show improved fuel cell performance. In addition, the influence of anti-oxidant properties on quercetin-grafted halloysites in Aquivion membranes has not been fully investigated for PEMFC application. If improved performance is achieved by blending with functionalized and pretreated halloysites, this approach will be a great advantage for operating a PEMFC.

The present study focuses on physicochemical properties and oxidation prevention of halloysite nanotube-based Aquivion membranes which can be operated at low relative humidity. It was demonstrated that the incorporation of modified halloysites into Aquivion improved the properties of composite membrane compared to those of pristine Aquivion membrane. In particular, composite membranes containing pure quercetin-, fluorinated group/quercetin- or aminized group/quercetin-grafted HNT showed increased chemical stability, represented by anti-oxidation. Moreover, mechanical strength and MEA of the prepared membranes were characterized.

2. Membrane preparation

All membrane samples with a size of 13 × 13 cm^2 were prepared via casting and evaporation. Aquivion and nanoclay were blended within casting dispersion in vials.

To begin with, 3.23 g of Aquivion dispersion (24 wt%, D83-24B), 0.078 g of nanoclay and 12.27 g of isopropanol were blended so as to obtain a 5 wt% Aquivion casting dispersion resulting in a 10 wt% clay loaded composite membrane.

Table 2.2. Information on nine different types of membranes prepared based on the available nanoclays (reproduced from chapter 2).

Membrane reference	PFSA ionomer	Nanoclay reference/content (wt%)	Type of nanoclay	Modification of nanoclay	Pretreatment of nanoclay
Aquivion		-	-	-	
Aq/HNT		HNT10		pristine	
Aq/HNT-Q		HNT-Q10		quercetine	
Aq/HNT-FQ		HNT-FQ10		Fluo + quercetin	
Aq/HNT-NQ		HNT-NQ10		Amino + quercetin	
Aq/pHNT	Aquivion	pHNT2/5/10	Halloysite	pristine	○
Aq/pHNT-Q		pHNT-Q2/5/10		quercetine	○
Aqn/pHNT-FQ		pHNT-FQ2/5/10		Fluo + quercetin	○
Aq/pHNT-NQ		pHNT-NQ2/5/10		Amino + quercetine	○

Different kinds of casting dispersions, obtained with different clays, were stirred for 15 mins at 80 rpm. Afterward, nanoclay dispersions in vials were dispersed using ultrasound (HD 2070, Bandelin, Germany) titanium alloyed microtip (MS73-529, Sonopuls, Bandelin) for 2 min at 60 W power and 20% pulsation level. The resultant dispersions were poured on a 13x13cm^2 mold at 15.578 g, after which it was heated at 80℃ for 18 h and then at 170℃ for 2 h. Prepared membranes were treated using 0.5M H_2SO_4 for 1 h and rinsed with DI-water for 1 h, at 100℃.

All the membranes were prepared using mold to have a dry thickness of around 20 μm, in order to follow commercial trends and reduce resistance.

Various membranes were prepared by addition of four available nanoclays: pristine halloysite (HNT), sulfonated halloysite (HNT-S), fluorinated halloysite (HNT-F) and sulfo-fluorinated halloysite (HNT-SF). The modification of halloysite is briefly presented in chapter 2. The obtained membanes were labeled as listed in table 2.2.

3. Nanoclay functionalization and characterization

3.1. Functionalization of halloysites

3.1.1. Grafting of halloysite with quercetin (HNT-Q)

Into a 250 ml flask fitted with a condenser were introduced 10 g of halloysite, 1 g of quercetin hydrate and 100 ml of ethanol (see scheme 5.1). The mixture was then stirred and heated at solvent reflux for 15 h. The mixture was next centrifuged (5000 rpm) to eliminate the liquid phase and washed twice with ethanol and acetone. Finally, the modified filler was dried under vacuum before characterization.

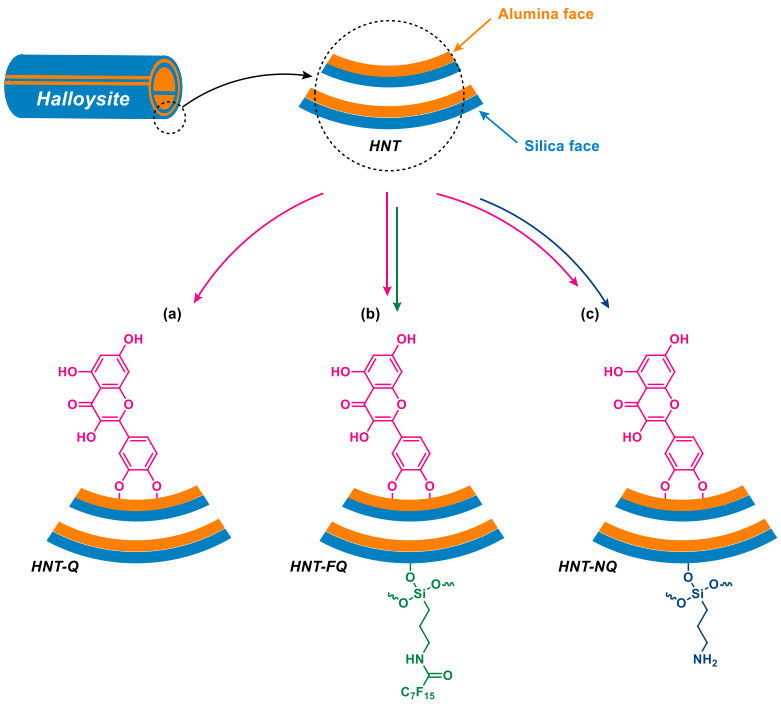

Scheme 5.1. Schematic representation of halloysite nanotubes grafted with (a) quercetin, (b) quercetin/fluorinated groups, and (c) quercetin/amino groups.

3.1.2. Grafting of halloysite with quercetin and fluorinated groups (HNT-FQ)

Into a 250 ml flask fitted with a condenser were introduced 10 g of halloysite previously modified with quercetin (HNT-Q), 1 g of N-(3-triethoxysilylpropyl)perfluorooctanoamide and 100 ml of an ethanol/water (90/10 wt%) solution. The mixture was then stirred and heated at solvent reflux for 15 h. The mixture was next centrifuged (5000 rpm) to eliminate the liquid phase and washed twice with acetone and THF. Finally, the modified filler was dried under vacuum before characterization.

3.1.3. Grafting of halloysite with quercetin and amino groups (HNT-NQ)

The same procedure than for HNT-FQ was used with only the replacement of N-(3-triethoxysilylpropyl)-perfluorooctanoamide with APTES.

3.2. Characterization of functionalized halloysites

ATR-FTIR, TGA, Py-GC/MS were performed at IMT MINES Alès.

FTIR was used to investigate the HNT, HNT-Q, HNT-FQ and HNT-NQ clay nanotubes. The different analyses show almost similar spectra generally observed for HNT (see Fig. 5.2) [109]. Two peaks are observed at 3693 and 3628 cm^{-1}, characteristic of O–H stretching vibrations of inner-surface Al–OH and inner Al–OH, respectively. The band at 1647 cm^{-1} is assigned to strongly bending vibrations of the adsorbed water. The band at 1124 cm^{-1} corresponds to the perpendicular Si–O stretching vibration, and the band at 1020 cm^{-1} can be assigned to in-plane Si–O stretching vibrations. The band observed at 908 cm^{-1} is assigned to the deformation of O–H of inner Al–OH. The bands at 530 and 465 cm^{-1} are characteristic of the deformations of Al-O-Si and Si-O-Si respectively.

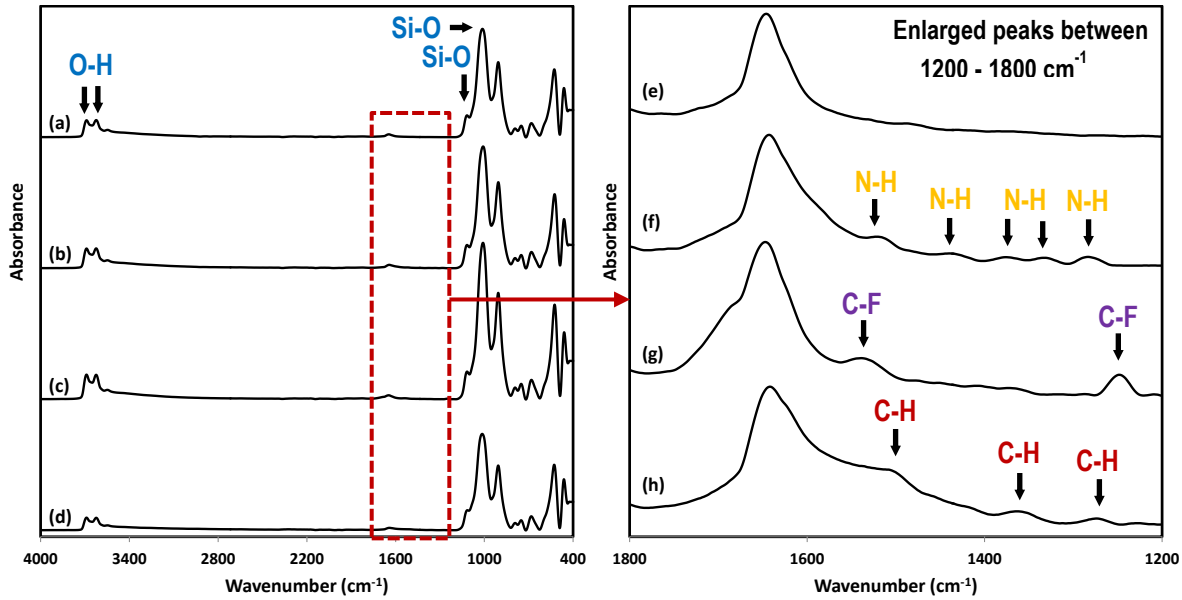

Fig. 5.2. ATR-FTIR spectra of (a) & (e) pristine halloysite, (b) & (f) HNT-Q, (c) & (g) HNT-FQ and (d) & (h) HNT-NQ.

Compared to the unmodified halloysite, the introduction of organic groups onto halloysite surface exhibits some new peaks between 1200 and 1800 cm^{-1}. Indeed HNT-Q spectrum shows peaks at 1520, 1435, 1380, 1335 and 1285 cm^{-1} attributed to stretching vibrations of the quercetin moiety [193]. HNT-FQ shows essentially peaks characteristic of the fluorinated grafting agent. Indeed as already observed in a previous chapter for HNT modified with N-(3-triethoxysilylpropyl)perfluorooctanoamide, two peaks appear at 1535 and 1250 cm^{-1} and were attributed respectively to the N-H (bending) of the amide function and C-F bonds of the perfluorinated group. We can also observe the enlargement at the highest wavenumbers of the peak centered at 1647 cm^{-1} which was attributed to the C=O stretching vibration of the amide function. HNT-NQ spectrum shows peaks at 1505, 1362 and 1273 cm^{-1} attributed to the deformation of C-H (scissoring and wagging) of the propyl fragment of the grafted APTES [109].

The different modified HNT samples were also characterized using thermogravimetric analyses (see Fig. 5.3). The grafted samples show an augmentation of the weight loss in comparison of pristine HNT. These weight losses were attributed to the decomposition of the grafted organic. As observed with FTIR analyses, TGA results prove

the efficiency of the functionalization procedures used. Indeed HNT-Q, HNT-FQ and HNT-NQ show weight losses of about 0.54, 1.39 and 1.00 wt% respectively. So the second step of functionalization to obtain HNT-FQ and HNT-NQ from HNT-Q was verified for both samples with an increase of the weight loss of about 0.85 and 0.45wt% attributed to the fluorinated and amino grafting agents respectively.

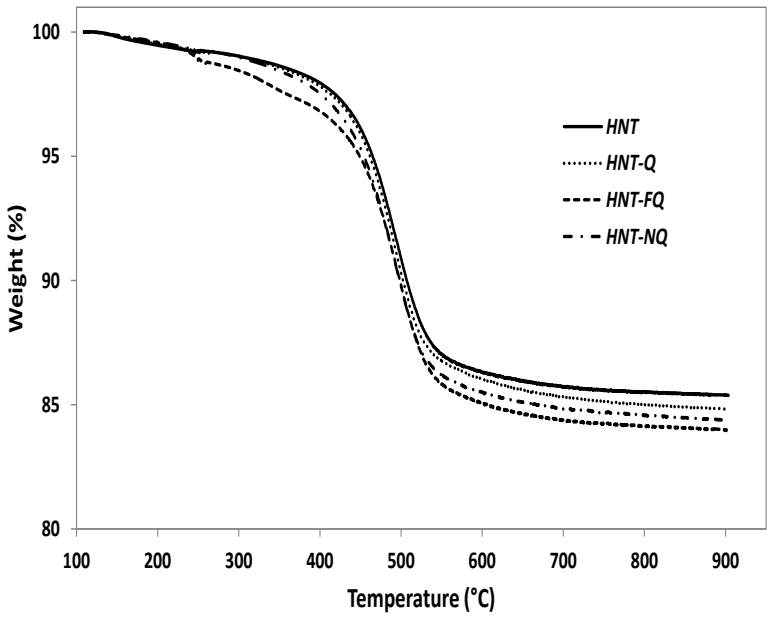

Fig. 5.3. TGA under nitrogen of HNT, HNT-Q, HNT-FQ and HNT-NQ samples from 110 °C to 900 °C after an isotherm at 110 °C for 10 min.

Lastly, Py–GC/MS was used to confirm the surface modifications of halloysite samples. The pyrolysis step was carried out at 900°C to decompose the organic part that may be present at the HNT surface after the different grafting procedures. The results obtained for HNT-Q, HNT-FQ and HNT-NQ (Figs. 5.4a-c) confirmed the presence of an organic part after each HNT modification. Whereas no peak was observed for pristine halloysite, chromatograms of functionalized clays show several peaks corresponding to molecules obtained by thermal degradation of the grafted parts. Formation of various aromatic molecules (e.g., benzene, toluene, styrene, phenol) is observed when HNT-Q is pyrolyzed (see Fig. 5.4a). Release of these molecules is due to the decomposition of quercetin molecules grafted at the inner surface of HNT. The peak of the fluorinated grafting agent of HNT-FQ is originated from perfluorooctanoic acid (PFOA) (see Fig. 5.4b). As for HNT-Q, peaks corresponding to aromatic molecules are also observed but with low intensities in comparison to the peak of PFOA. Pyrolysis of HNT-NQ release also essentially aromatic products but the spectrum shape change in comparison to HNT-Q with appearance of new molecules at early times and modification of peaks ratio for common products (see Fig. 5.4c).

As already demonstrated by FTIR and TG characterizations, Py-GC/MS analyses confirmed also the presence of the different grafting agents on the surface of modified HNTs after the grafting procedures.

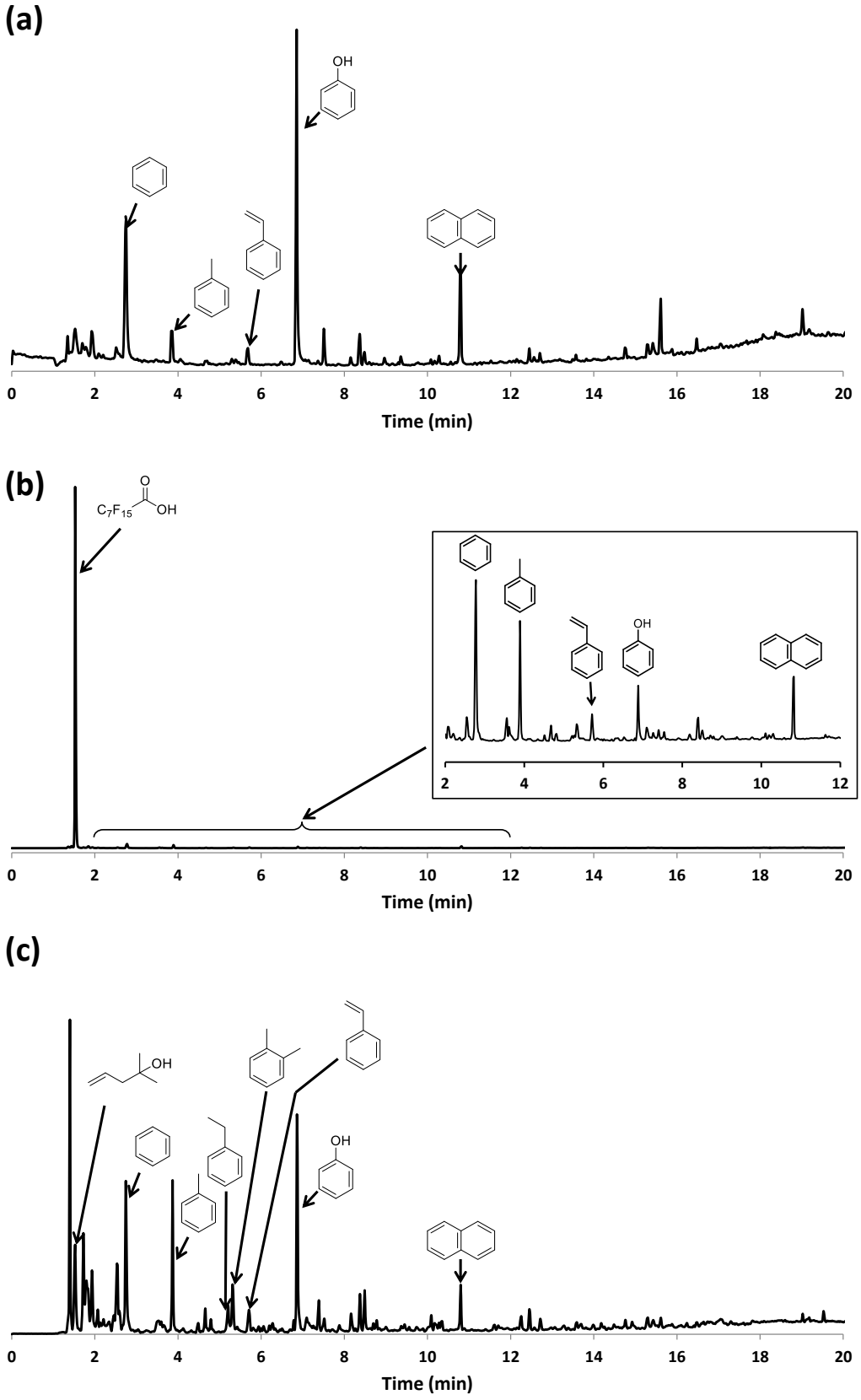

Fig. 5.4. Py–GC/MS chromatograms obtained for (a) HNT-Q, (b) HNT-FQ and (c) HNT-NQ samples pyrolyzed at 900°C.

4. Membrane characterization

4.1. Homogeneity of composite membranes (FE-SEM and EDS)

Cross section of various commercially available membranes and prepared membranes was investigated. using FE-SEM as shown in Fig. 5.5. Analytical method was followed as described in experimental section. Chemical composition at both edge and the center of membrane cross section were analyzed to get insights on the nanoclay repartition. Silicon and fluorine are respectively originated from halloysite and Aquivion, thus Si/F atomic ratio was obtained to verify composite homogeneity and aggregate loading inside Aquivion matrix.

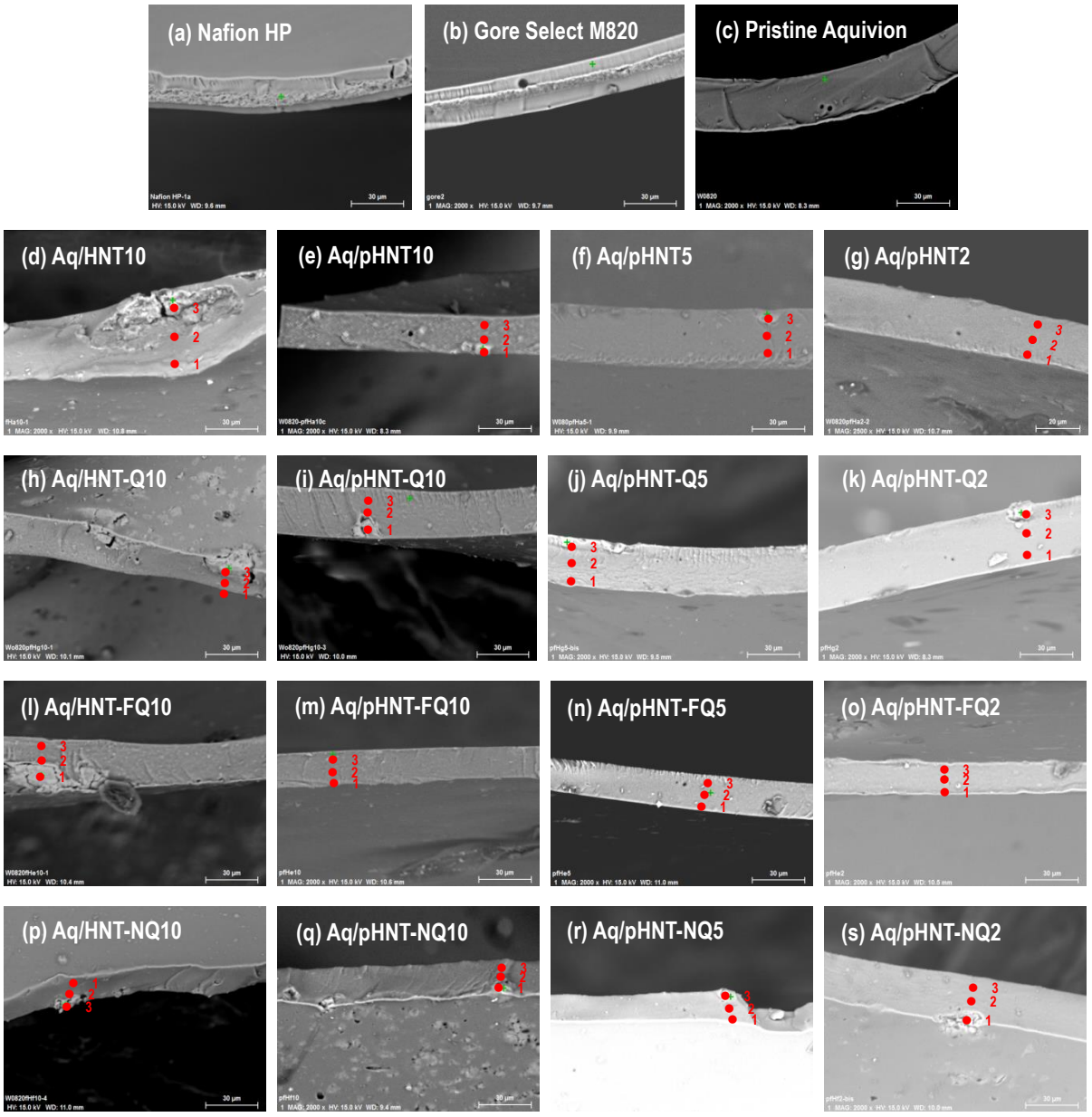

Fig. 5.5. FE-SEM images regarding (a) commercially available Nafion HP, (b) Gore Select M820 (Aquivion), (c) pristine Aquivion, and (d – s) composite membranes blended with HNT, HNT-Q, HNT-FQ and HNT-NQ.

Incorporating of pristine halloysite displays large aggregates at cross section, compared with that of functionalized halloysites as shown in Fig. 5.5d. The comparative analysis based on EDS results showed similar trends with other functionalization (see Fig. 5.6). It is difficult to say that each membrane have composite homogeneity according to lack of Si/F uniformity between points 1 and 3.

For impact of pretreated nanoclays on membrane cross section, the addition of pristine halloysites led to reduced scale of nanoclay aggregate within polymer phase as can be seen in Figs. 5.5d and 5.5e.

Reducing pristine halloysite and various halloysites with quercetin/fluorine group or quercetin/amino group contents did not display good uniformity of Si/F atomic ratio at cross section. In contrast, blending pHNT-FQ 2 wt% and 5 wt% with Aquivion displayed improvement of composite homogeneity among the membranes tested. According to EDS result, edges of pristine membrane cross section were similar Si/F atomic ratio to that of pHNT-Q and pHNT-NQ incorporated membranes, for 5, or 10 wt% contents. However, addition of pretreated and fluorinated quercetin-grafted halloysite shown an exceptionally reduced tendency at 2 wt%. In addition, blending pretreated and aminized quercetin-grafted halloysite with Aquivion doesn't show better composite homogeneity caused by compatibility reduction. Even if clay nanotube content was reduced from 10 to 2 wt%, uniformity of Si/F atomic ratio was difficult to find.

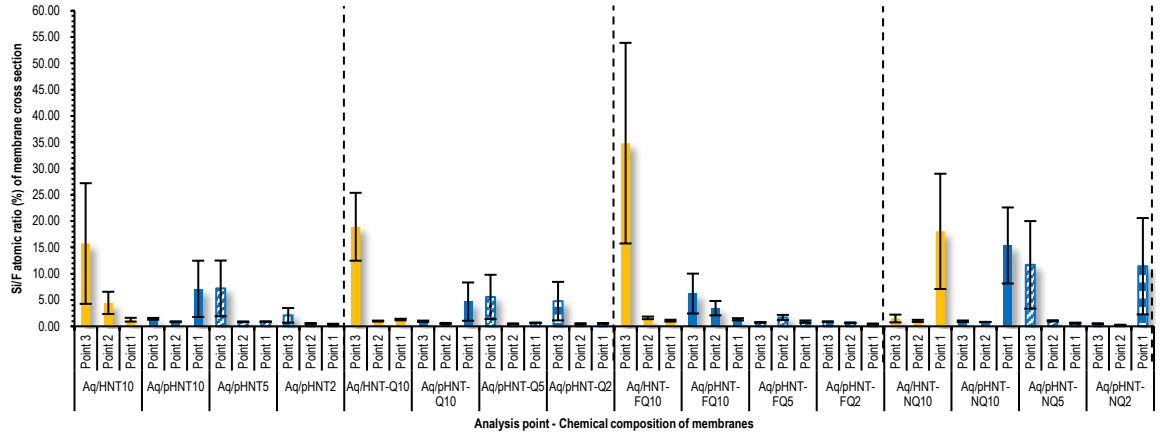

Fig. 5.6. Si/F atomic ratio verified using EDS regarding commercially available Nafion HP, Gore Select (Aquivion), pristine Aquivion, and Aquivion composite membranes incorporated with HNT, HNT-Q, HNT-FQ and HNT-NQ. Yellow and blue bars represent non-pretreated and pretreated nanoclays, respectively.

4.2. Thickness of hydrated membranes (micrometer)

Membrane thickness is considered as an important factor to decrease the resistance during operation under same conditions [182, 184], but reduce fuel cell operating efficiency caused by hydrogen crossover occurrence when the membrane thickness is reduced. To obtain the benefits, the membrane thickness was targeted to 20 μm measured at dry condition. As mentioned previously, Nafion HP and Gore Select M820 display about 23 – 27 μm similar to the thickness of pristine Aquivion at wet condition. All data are gathered in Fig. 5.7.

The composite membranes incorporated with 10 wt% of different kinds of halloysites into the polymer phase

are thicker than the pristine Aquivion membrane.

Blending of 10 wt% pure halloysite allowed membrane to be thicker compared with pristine Aquivion (Aq/HNT10 – 31.9 μm).

For quercetin introduction, blending of HNT-Q, HNT-FQ, or HNT-NQ with Aquivion ionomer kept a constant thickness in between that of pure Aquivion and Aq/HNT10. Such thickness can be due to density changes and affinity improvement, caused by functionalized halloysites incorporated inside other membranes.

In terms of pretreatment of various quercetin halloysites in oxalic acid and hydrogen chloride, similar thickness was achieved for the pretreated halloysites-based composite membranes, regardless of functionalization and nanoclay content (2 wt% and 5wt%) except for 10 wt% content for HNT and HNT-FQ. This implies that 10 wt% contents seem that different membrane thickness can be due to density change.

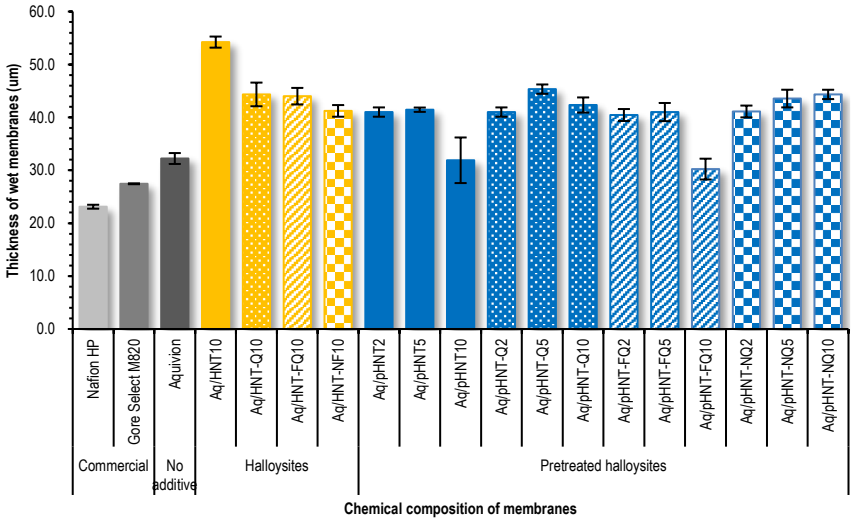

Fig. 5.7. Data on thickness: commercially available Nafion HP and Gore Select M820, and pristine Aquivion and Aquivion composite membranes containing quercetin-grafted halloysites. Yellow and blue bars represent non-pretreated and pretreated nanoclays, respectively.

4.3. IEC

IEC indicates the available number of sulfonic acid groups, and affects proton conductivity of electrolyte membranes in accordance with Grotthuss mechanism [183]. Similar IEC was obtained for commercially available, pristine and composite membranes. They exhibited values between 0.85 and 1.20 meq/g, as can be seen in Fig. 5.8. The reasons why Aq/pHNT2 membrane exhibits different IEC can be a combination of factors: (1) the measured temperature and (2) the limits of the calculation and weighing processes. More specifically, these are reasonable error values that can be taken into consideration by the temperature difference during the analysis. Other reasons for the deviations of the measured values can be due to the limitations of the calculation and weighing procedures to determine the amount of polymer added into the casting dispersion.

Grafting various quercetin on halloysite surface doesn't have a great influence on IEC, compared with non-grafting.

Concerning pretreatment, the values reduced depending on pHNTs amount. Quercetin-grafted pHNTs and pristine pHNTs showed a similar tendency approximately 1.10 meq/g as shown in Fig. 5.7. However, blending with pHNT2 with Aquivion was approximately 0.85 meq/g, which is slightly reduced value. The deviation can be due to the limitations of how to calculate or weigh the polymer content as described above.

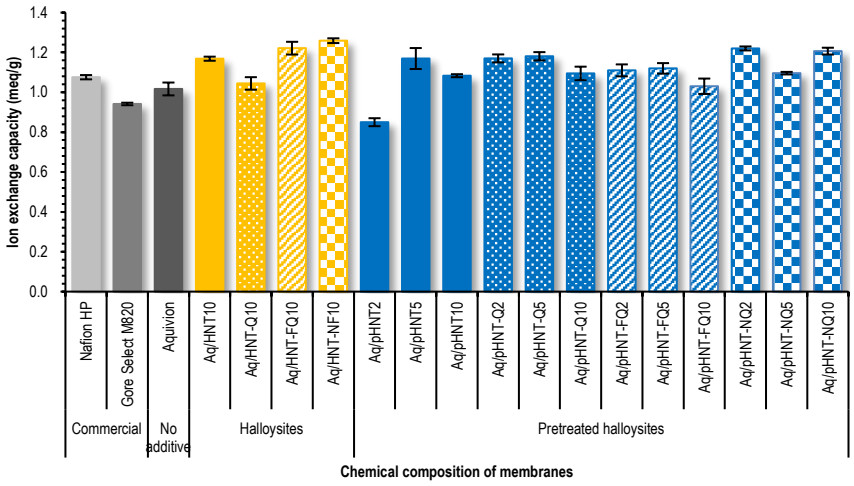

Fig. 5.8. Data on ion exchange capacity: commercially available Nafion HP and Gore Select M820, and pristine Aquivion and Aquivion composite membranes containing quercetin-grafted halloysites. Yellow and blue bars represent non-pretreated and pretreated nanoclays, respectively.

4.4. Water uptake

Water molecules affect proton conductivity inside polymer matrix according to Grotthuss and vehicle mechanisms [182, 184]. Water uptake (%) is an essential factor to measure the proton transfer for PEMFC application.

As shown in Fig. 5.9, water uptake of Gore Select was similar to that of pristine Aquivion as only 7% difference, while Nafion HP exhibited the lowest value among the membranes tested.

Addition of pristine HNT improved water uptake value by about 10%, compared with water uptake of Aquivion, and they displayed similar values to Gore Select M820.

Blending Aquivion with quercetin-grafted HNT showed very similar value than when mixing with pure HNT. On the other hand, quercetin grafted fluorinated or aminized HNTnot only displayed 24 - 34% higher water uptake than Aquivion, but 27 - 37% better than Gore Select M820. Water uptake of Nafion HP was up to 40% lower than that of Aq/HNT-FQ10.

Pretreatment process doesn't have great influence on the hygroscopicity of composite membranes at 10 wt% content. However, Aq/pHNT-NQ10 showed a somewhat higher water uptake than other membranes with functionalized and pretreated HNTs, or membrane with pretreated pure HNT.

Incorporating with 5 wt% pHNT or pHNT-Q led to improved water uptake of composite membrane. It is not the case with 5 wt% pHNT-FQ or pHNT-NQ. 5wt% quercetin-grafted halloysite blending showed grew in

hydrophilicity, whereas 2 and 10wt% contents were rather low. The reason for decreasing the water uptake at 10 wt% clay contents is that too much nanoclay inside Aquivion matrix blocks the sulfonic group, which has hydrophilicity. Blending with quercetin-grafted fluorinated or aminated halloysite showed higher water uptake of electrolyte membranes as the content was lower. This may be due to change in compatibility between Aquivion and modified halloysites.

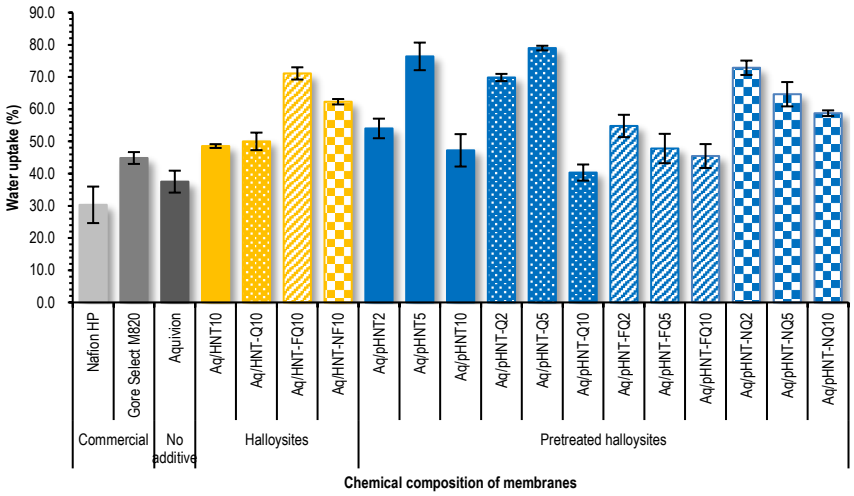

Fig. 5.9. Data on water uptake: commercially available Nafion HP and Gore Select M820, and pristine Aquivion and Aquivion composite membranes containing quercetin-grafted halloysites. Yellow and blue bars represent non-pretreated and pretreated nanoclays, respectively.

4.5. Swelling ratio

Swelling ratio affects fuel cell performance during operation. Fig. 5.10 exhibits swelling ratio of various electrolyte membranes.

Nafion HP and Gore Select M820 were selected as reference membranes to compare with swelling ratio of prepared membranes. The swelling of Nafion HP and Gore Select showed around 6 and 1%, respectively. That is, they showed smaller swelling ratio compared with pristine Aquivion. It should be noted that increase of mechanical strength is related with reduced swelling [38].

The incorporation of 10 wt% of halloysites has influence on swelling ratio, which decreases from 15% for pristine Aquivion membane to about 3% for composite membranes regardless of HNT functionalization, maybe due to reinforcement. HNT-based membranes reinforced by blending of cylinder type nanotubes were already discussed in former publications. That is, reduced swelling is probably due to stronger interfacial interaction between Aquivion and additives. In addition to this, swelling behavior is related with water uptake. Adding the HNTs inside polymer matrix is propitious to the membrane dimensional stability, and thereby repressing the membrane swelling. [30, 40, 42].

Pre-treatment of functionalized halloysites seems to have similar influence on thickness swelling. The swelling ratio of the membranes ranged between approximately 1 and 6%.

Increasing the amount of halloysites from 5 wt% to 10 wt% has impact, based on pretreated and functionalized groups. 10% of pretreated pristine halloysite blending led to reduced swelling compared with 5 wt% blending except for Aq/HNT. For example, through pretreatment of aminized group/quercetin-grafted HNT (resp. fluorinated group/quercetin-grafted HNT), the swelling ratio of membranes was reduced from 4% (resp. 6%), to 2% between 5 at 10 wt% content.

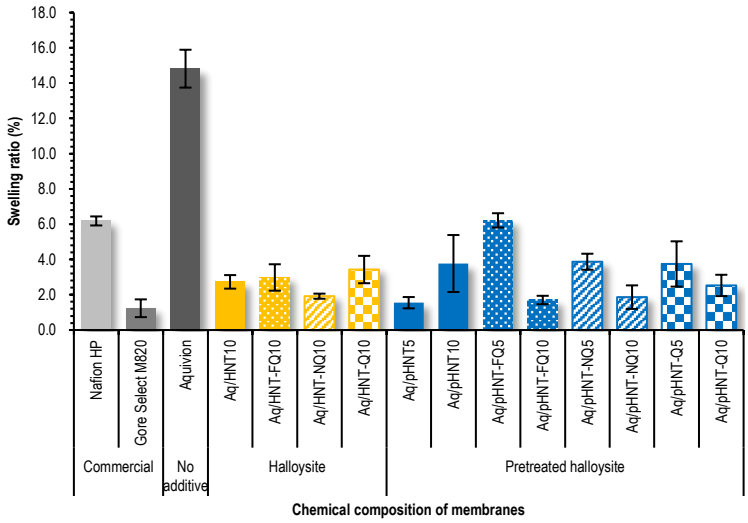

Fig. 5.10. Data on swelling ratio: commercially available Nafion HP and Gore Select M820, and pristine Aquivion and Aquivion composite membranes containing quercetin-grafted halloysites. Yellow and blue bars represent non-pretreated and pretreated nanoclays, respectively.

4.6. Chemical stability

Free radicals such as OH· and OH_2· attacks C-F bonds of the PFSA ionomers, and hence PFSA membranes suffer from chemical degradation during fuel cell operation. Accordingly, it affects the permeability of electrolyte membrane, resulting in an augmentation in hydrogen crossover. According to the protocol described in this study, various membranes were immersed in H_2O_2/H_2SO_4 solution for up to 96 h and reacted at 80℃.

Pristine Aquivion was chemically less stable compared with commercially available membranes. Gore Select M820 showed a decrease in fluoride ion concentration over Nafion HP after 96 h of reaction. This means that Gore Select is more stable than Nafion HP.

The addition of halloysites inside polymer phase caused improved chemical stability compared with pristine Aquivion, resulting in lower concentration of fluoride ion. During the experiment, pristine Aquivion easily damaged, while the composites did not change apparently during chemical reaction in the H_2O_2/H_2SO_4 solution. For more detailed surface analysis, observation using FE-SEM and EDS may be needed for further work. Numerous research groups have reported that Fe_2O_3 is present in halloysites [185, 186]. C-F bonds are usually attacked by divalent iron (Fe^{2+}). To be specific, the divalent iron ion reacts with H_2O_2 to form OH radicals and accordingly attack C-F bonds [13, 58, 60, 61].

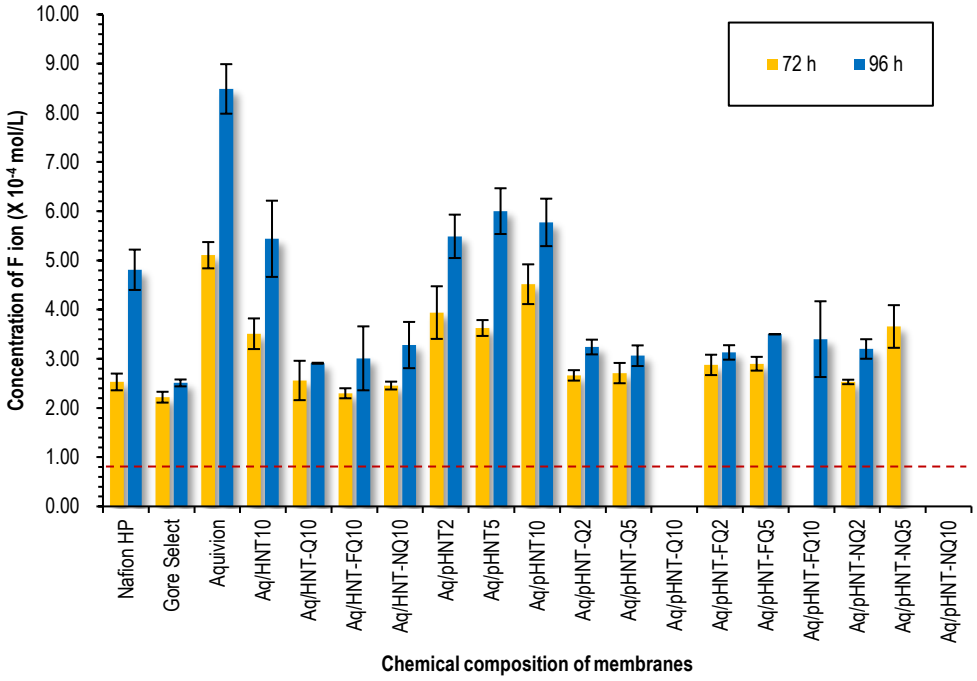

Fig. 5.11. Fluoride (F^-) concentration analyzed after immersion in H_2O_2/H_2SO_4 for Nafion HP, Gore Select M820 (Aquivion), pristine Aquivion, Aq/HNT, Aq/HNT-Q, Aq/HNT-FQ, Aq/HNT-NQ, Aq/pHNT, Aq/pHNT-Q, Aq/pHNT-FQ and Aq/pHNT-NQ membranes. Red dotted line represents the fluorine concentration of 4.4 M H_2O_2/1.25 mM H_2SO_4 solution (blank test): $0.82\times10^{-4} \pm 0.08\times10^{-4}$ mol/L.

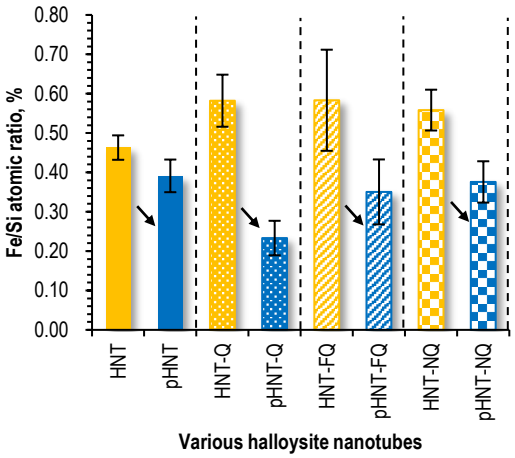

Fig. 5.12. Comparison of Fe/Si atomic ratio (%) regarding HNT, pHNT, HNT-Q, pHNT-Q, HNT-FQ, pHNT-FQ, HNT-NQ and pHNT-NQ nanoclays used for preparing composite membranes. Yellow and blue bars represent non-pretreated and pretreated nanoclays, respectively.

Blending of Aquivion with quercetin-grafted halloysite led to reduced fluoride concentration. Moreover, comparing the results of 72 h and 96 h, blending of pure HNT showed a higher fluoride concentration over time. On the other hand, when different kinds of quercetin-grafted HNTs were incoporated, 96 h reaction results displayed a comparatively small gap compared to 72 h reaction results. This is attributed to oxidation prevention caused by quercetin effect. Introduction of fluorinated group/quercetin, or aminized group/quercetin on halloysite surface seems to have similar results. The antioxidant activity of quercetin is related to chemical structure. In particular, hydroxyl (-OH) substitutions and the catechol-type ring B are important determinant factor for scavenging free radicals [190, 191]. The structural properties of a potent antioxidant capacity was mentioned in introduction section of this chapter (see Fig. 5.1) [192]. Free radical species scavenging occurs through donating electron from free hydroxyls of the flavonoid nucleus with the formation of less reactive flavonoid aroxyl radicals [190, 191].

The concentration of fluoride released from composite membranes containing pretreated halloysite (i.e., pHNT) did not show a significant decrease compared to those without pretreatment. The reason can be explained by the amount of iron. As shown in Fe/Si atomic ratio analyzed using EDS (see Fig. 5.12), the iron (Fe^{2+}) removal did not have a great effect by pretreatment process. In addition to this, the content of iron present in halloysites is very low, so the pretreatment process may have been meaningless for only chemical stability experiment (except for proton conductivity). It should be noted that Fe and Si are originated from iron (III) oxide and siloxane group of halloysites. However, various quercetin-grafted pHNTs exhibited a much lower amount of iron than pure pHNT. In addition to this, quercetin's structural properties above-mentioned also led to much improved anti-oxidation of each composite membrane containing various quercetin-grafted HNT series. According to analysis shown in Fig. 5.12, iron decrease eventually contributed to the antioxidant function of composite membrane. More specifically, blending with various quercetin-grafted HNTs exhibited lower fluoride values than the addition of pure pHNT, and the concentration differences became more pronounced over time. Nafion HP and Gore Select M820 released more fluoride ions over time, while the quercetin effect allowed the composite membrane to become chemically stable, maintaining fluoride concentrations similar to at 72 h reaction, even after 96 h reaction.

For further work, more effective strategy to pretreat halloysites may be needed to remove divalent iron.

4.7. Proton conductivity (EIS)

The movement of ion carriers is a prerequisite for high proton conductivity. As mentioned in section 4.4, movement phenomenon occurs according to Grotthouss and vehicular mechanisms. Proton conductivity experiments were performed at various temperatures (50℃, 70℃, and 90℃) and relative humidity (25%, 50%, 75%, and 90%). Afterwards, thickness of wet membranes was substituted into equation (5) to obtain the proton conductivity as shown in Fig. 5.13ab.

The pristine Aquivion membrane showed higher proton conductivity than Nafion HP because it has a shorter side-chain than the Nafion HP. Large crystallinity, and lower equivalent weight of Aquivion is also one of the factors to improve proton conductivity [50, 51]. The proton conductivities (115 mS/cm at 90°C and 90% RH) of pristine Aquivion membrane obtained in this study were very similar to that found in the literature in similar conditions as shown in Fig. 5.13c. Among the membranes tested, Gore Select M820 composed of Aquivion displayed the highest value, which is close to about 260 mS/cm at 90℃ and 90% RH [52, 194, 195].

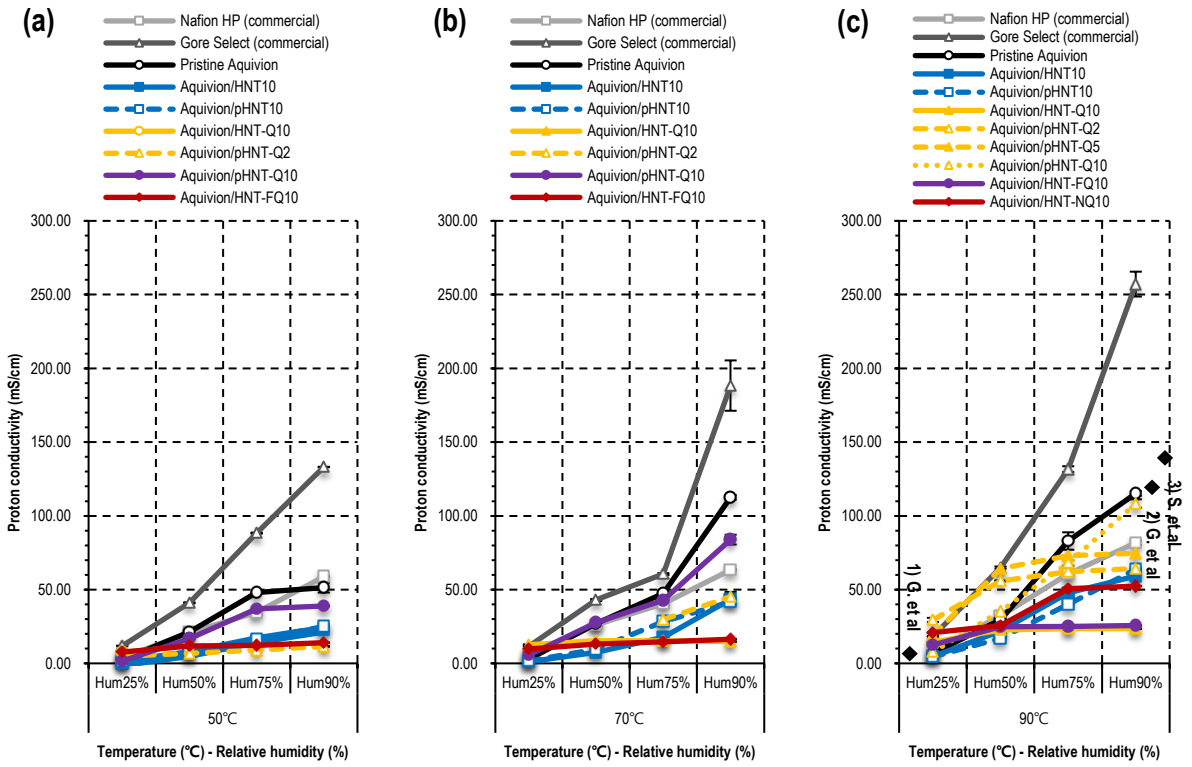

Fig. 5.13. Influence of temperature (a) 50℃, (b) 70℃ and (c) 90℃, and relative humidity on proton conductivity (mS/cm) for various PEMs: Nafion HP, Gore Select (Aquivion), pristine Aquivion, Aquivion/HNT, Aquivion/HNT-Q, Aquivion/HNT-FQ, Aquivion/HNT-NQ, Aquivion/pHNTs, Aquivion/pHNTs-Q, Aquivion/pHNTs-FQ and Aquivion/pHNTs-NQ composite membranes incorporated with 2, 5 and 10 wt% contents.

---

1) Gebert et al, 10 mS/cm at 95℃ , 25% (Aquivion E79-03S) [194].

2) Giancola et al, 118 mS/cm at 80℃, 95% RH (Aquivion EW 830 g/eq) [52]

3) Skulimowska et al, 138 mS/cm at 90℃, 95% (Aquivion E87-12S) [195]

Pure halloysite-incorporated membrane exhibited relatively lower value compared with pristine Aquivion. Pure quercetin-, or fluorinated group/quercetin-grafted halloysites introducing in the Aquivion phase led to similar values between 23 – 25 mS/cm, whereas blending of amino group/quercetin-grafted halloysite slightly raised to 53 mS/cm at 90℃ and 90 RH%.

Composite membranes with pretreated nanoclays displays increased proton conductivity, except for pure halloysite-blended membrane. The pretreatment process led to improved proton conductivity. That is, membranes containing pretreated quercetin-grafted halloysite allow to improve proton movement inside ion channers leading to showing higher values than the other membranes.

Concerning the additive content, quercetin-grafted halloysite membrane at 10wt% content displayed higher proton conductivity than 2 and 5 wt%. This means that the lower the content, the lower the conductivity value. Contrary to expectations, proton conductivity of composite membranes showed different tendency from the afore-mentioned IEC and water uptake data.

Conclusions

In conclusion, halloysites were grafted with pure quercetin (HNT-Q), fluorine group/quercetin (HNT-FQ) or amino group/quercetin (HNT-NQ). Pristine halloysite or modified halloysite was blended with Aquivion dispersion to improve membrane characteristics. Physicochemical properties of prepared membranes were compared with those of commercially available membranes (i.e., Nafion HP and Gore Select M820). The following conclusions can be drawn regarding membrane properties:

- Pristine Aquivion showed similar values to IEC compared to Nafion HP and Gore Select. Water uptake was lower than Gore Select, but higher than Nafion HP. Also, for proton conductivity, pristine Aquivion has benefit over Nafion HP.
- Blending of halloysite with Aquivion dispersion led to augmented thickness and water uptake of composite membrane compared to commercial membranes. Composite membrane showed similar IEC as well as chemical stability.
- The incorporation of halloysite grafted with quercetin, fluorine group/quercetin or amino group/quercetin into Aquivion matrix showed slightly increase in thickness and IEC. Moreover, they exhibited reduced swelling behavior compared to Nafion HP. Addition of fluorine group/quercetin-grafted halloysite led to improved dispersion state. The composite membranes containing fluorine group/quercetin- or amino group/quercetin-grafted HNT also displayed augmented water uptake. Moreover, improvement in chemical stability by quercetin grafting was verified compared to Nafion HP at 96 h, even and exhibited reduced values compared with pristine Aquivion or HNT-blended membrane (due to reduced iron amount as well as anti-oxidative activity).
- Through pretreatment process, composite membranes were thicker than commercially available membranes, except that of both Aq/pHNT10 and Aq/pHNT-FQ10 were 30 μm. Water uptake and IEC of composite membranes showed similar values, but the membrane with amino group/quercetin-grafted halloysite exceptionally displayed improved water uptake. Membrane swellings exhibited a similar or slightly raised value compared to that of Gore Select, but were lower than those of Nafion HP. Prepared membranes showed lower proton conductivity than Gore Select, but blending with pure quercetin-grafted halloysite showed higher values than Nafion HP.
- The results of the water uptake were different when varying the additive content. Blending of 5 wt% content showed increased water uptake value compared to that of 10 wt% or 2 wt% content. In terms of proton conductivity, the reduced content showed a reduced value. The anti-oxidative effect and thickness were not affected by the change of contents.

Based on characterization, it is suggested that anti-oxidant activity of composite membranes can be improved through iron amount reduction inside modified halloysites as well as quercetin effect, compared with Nafion HP, pristine Aquivion and halloysite-blended membranes. In addition, augmented water uptake and reduced swelling ratio by blending with modified halloysites also shows potential in PEMFC operation.

For further work, it is need to improve proton conductivity through increased additive contents and then obtain MEA results.

Chapter 6

Impact of fluorinated and pretreated sepiolite on electrolyte membrane

Summary

Several composite membranes were prepared with pristine or fluorinated sepiolite, pretreated or not. Sepiolite was successfully grafted with the fluorine group (-C_7F_{15}) and treated with oxalic acid and hydrogen chloride to remove possible traces of iron. Pristine sepiolite or modified sepiolite was added to the Aquivion matrix to improve electrolyte membrane properties and fuel cell performance. Composite membranes were prepared by casting - evaporation, and the physicochemical properties of prepared membranes were compared with pure Aquivion membrane and commercially available membranes Nafion HP and Gore Select M820 as reference.

The functionalized sepiolite was analyzed using ATR-FTIR, TGA and Py-GC/MS.

Concerning FTIR spectrum, the band at 1240 cm^{-1} indicated C-F bonds of the fluorinated fragment, meaning that sepiolite was successfully fluorinated.

According to TGA curve, grafted sepiolite showed increased weight loss caused by decomposition of the grafted organic part.

Py-GC/MS was also used to validate the procedure of functionalization of sepiolite nanofibers. Whereas no peak was observed for pristine sepiolite, chromatogram of functionalized nanoclay shows peaks corresponding to organic molecules generated by thermal degradation of the grafted part.

Adding pure sepiolite into Aquivion matrix improved water uptake and mechanical strength. Additionaly, this displayed reduced swelling ratio compared with Nafion HP and pristine Aquivion. The composite membrane also displayed similar IEC and chemical stability, but showed reduced proton conductivity, with higher thickness compared to Nafion HP as well as Gore Select M820.

The fluorination of sepiolite proved to be beneficial. It resulted in better dispersion state of the additive inside the polymer phase of the composite membrane. The mechanical strength as well as the proton conductivity were improved, without impacting the water uptake, the thickness, the IEC, and even the chemical stability.

Incorporating the sepiolite pretreated with acidic solutions showed similar water uptake, IEC and swelling ratio of composite membrane to that of non-pretreated sepiolite. Also, blending of pretreated sepiolite showed improvement in water uptake compared with Nafion HP and Gore Select M820.

In terms of pretreatment influence, composite membranes incorporated with fluorinated and pretreated sepiolite showed similar IEC and chemical stability compared to commercial membranes. Moreover, these membranes exhibited better proton conductivity regardless of additive contents among the membranes tested, but displayed decreased mechanical strength.

The behavior in single cell MEA test was also assessed. Pretreated and fluorinated sepiolite-blended membrane showed the greatest performance at intermediate current density and low relative humidity among the membranes tested,.

Based on characterization, it is indicated that improved physicochemical properties of Aquivion/fluorinated and pretreated sepiolite composite membrane lead to good result on MEAs test during PEMFC operation, under low relative humidity condition.

Résumé

Plusieurs membranes composites ont été préparées avec de la sépiolite pure ou fluorée, prétraitée ou non.

La sépiolite a été greffée avec succès avec le groupe fluor (-C_7F_{15}) et traitée avec de l'acide oxalique et de l'acide chlorhydrique pour éliminer toute trace de fer. De la sépiolite brute ou de la sépiolite modifiée a été ajoutée à la matrice Aquivion pour améliorer les propriétés de la membrane électrolytique et les performances de la pile à combustible. Les membranes composites ont été préparées par coulée - évaporation, et les propriétés physicochimiques des membranes préparées ont été comparées à la membrane Aquivion pur et aux membranes disponibles dans le commerce, Nafion HP et Gore Select M820, à titre de référence.

La sépiolite fonctionnalisée a été analysée par ATR-IRTF, ATG et Py-GC / MS.

En ce qui concerne le spectre FTIR, la bande à 1240 cm^{-1} montre les liaisons C-F du fragment fluoré, ce qui signifie que la sépiolite a été fluorée avec succès.

Selon la courbe ATG, la sépiolite greffée présentait une perte de masse accrue due à la décomposition de la partie organique greffée.

Py-GC / MS a également été utilisé pour valider la procédure de fonctionnalisation des nanofibres de sépiolite. Alors qu'aucun pic n'a été observé pour la sépiolite brute, le chromatogramme de la nanoargile fonctionnalisée montre des pics correspondant aux molécules organiques obtenues par dégradation thermique de la partie greffée.

L'ajout de sépiolite pure dans la matrice Aquivion améliorait l'absorption d'eau et la résistance mécanique. De plus, cela montrait un taux de gonflement et une conductivité protonique réduits par rapport au Nafion HP. La membrane composite présentait également une capacité d'échange ionique et une stabilité chimique similaires, mais une conductivité protonique réduite ainsi qu'une épaisseur plus importante par rapport au Nafion HP et au Gore Select M820.

La fluoration de la sépiolite s'est avérée bénéfique. Il en résultait un meilleur état de dispersion de l'additif dans la phase polymère de la membrane composite. La résistance mécanique ainsi que la conductivité protonique ont été améliorées, sans impact sur l'absorption d'eau, l'épaisseur, la capacité d'échange ionique et même la stabilité chimique.

L'incorporation de la sépiolite prétraitée avec des solutions acides a montré une absorption d'eau, une capacité d'échange ionique et un taux de gonflement de la membrane composite similaires à ceux de la sépiolite non prétraitée. En outre, le mélange de sépiolite prétraitée a montré une amélioration de l'absorption d'eau par rapport au Nafion HP et au Gore Select M820.

En ce qui concerne l'influence du prétraitement, les membranes composites incorporant de la sépiolite fluorée et prétraitée présentaient une stabilité chimique et une capacité d'échange ionique similaires aux membranes commerciales. De plus, la conductivité était supérieure à la conductivité protonique indépendamment des teneurs en additifs parmi les membranes testées, mais présentait une résistance mécanique réduite.

Le comportement dans des conditions de test des AMEs en monocellule a également été évalué. Les membranes obtenues avec la sépiolite fluorée et prétraitée ont montré les meilleures performances parmi les membranes testées, à une densité de courant intermédiaire et à une faible humidité relative.

Sur la base de la caractérisation, il est indiqué que les propriétés physicochimiques améliorées de la membrane composite Aquivion / sépiolite fluorée et prétraitée donnent de bons résultats au test en AME lors du fonctionnement de PEMFC, dans des conditions de faible humidité relative

1. Introduction

Sepiolite (SEP) is a natural nanoclay with a fibrous morphology (so called needle-like structure) which consists of parallel tunnels formed by blocks. Hence, it is able to improve the tensile strength of the membrane by effect of chain packing [38, 39, 42, 46, 47]. The authors already demonstrated in previous studies that the incorporation of sepiolite can lead to improved mechanical property of Nafion composite membranes [38, 39]. However, aggregated nanoclays inside polymer matrix can hinder the expected benefit. Hence, controlling the dispersion state of sepiolite has been considered as a crucial challenge in order to enhance the performance. To this end, surface modification of sepiolite has been achieved, namely sulfonation [32, 39, 49] or perfluorosulfonation [38].

To date, the influence of the incorporation of sepiolite in Aquivion membranes has not been fully investigated for PEMFC application even though Aquivion is a prominent candidate as one of PFSA ionomers. Moreover, the impact of sepiolite modification on Aquivion membrane features has not been fully demonstrated. If so, modified sepiolite-based Aquivion composite membranes can enhance fuel cell performance under the wide range of PEMFCs operating conditions.

The present study proposes a novel sepiolite-based Aquivion composite membrane which can be applied in low relative humidity and intermediate temperature. In the study, the authors evidenced that fluorinated sepiolite improved the properties of Aquivion composite membrane, compared with pristine sepiolite-based composite membranes. The membrane actually displayed superior water uptake and proton conductivity compared with commercially available membranes such as Nafion HP membranes, selected as reference, on top of increased mechanical property compared with pristine Aquivion membrane. Chemical stability against radical attack was, moreover, demonstrated. Lastly, the polarization curves and hydrogen crossover were investigated at various operating conditions (i.e., wet, dry, low pressure and HAST - highly accelerated stress tests).

2. Sepiolite functionalization

Into a 250 ml flask fitted with a condenser were introduced 10 g of sepiolite, 1 g (1.6×10^{-3} mol) of SPFOA and 100 ml of an ethanol/water (90/10 wt%) solution. The mixture was then stirred and heated at solvent reflux for 15 h. The mixture was next centrifuged (5000 rpm) to eliminate the liquid phase and washed twice with acetone and THF. Finally, the modified filler was dried under vacuum before characterization.

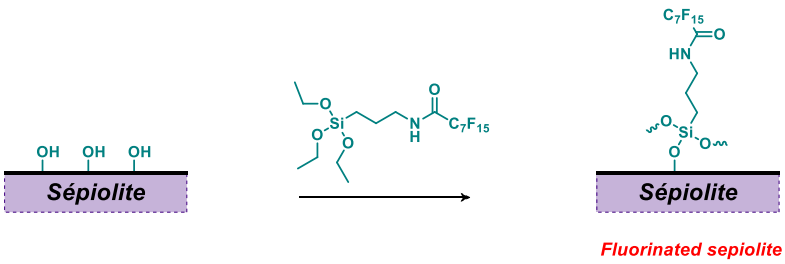

Scheme 6.1. Schematic representation of sepiolite nanofiber perfluorination grafted with N-(3-triethoxysilylpropyl)-perfluorooctanoamide (SPFOA).

All sepiolite materials (pristine or modified) were filtered using different membrane filters (45 µm and 25 µm pore sizes, Merck Millipore) and then dehydrated in oven at 80 °C for 16 h.

In terms of nomenclature, pristine sepiolite and fluorinated sepiolite are labeled as SEP and SEP-F, respectively.

3. Sepiolite characterization (ATR-FTIR, TGA, and Py-GC/MS)

All sepiolite characterizations were performed at IMT MINES Alès.

Fluorinated and pristine sepiolite have been analyzed by FTIR spectroscopy (see Fig. 6.1) and show similar spectra with few differences. As already described for sepiolite samples, both spectra show O-H stretching vibrations from Mg_3OH in the 3600 cm^{-1} region [39]. The bands which appear at 978, 1008 and 1214 cm^{-1} were attributed to Si–O bonds within silica tetrahedra. Moreover a band around 1670 cm^{-1} was attributed to water molecules hydrogen bonded to the surface. Finally the bands appearing at 788, 685 and 646 cm^{-1} were also attributed to O-H vibrations from Mg_3OH (deformation at 788 cm^{-1} and bending at 685 and 646 cm^{-1}).

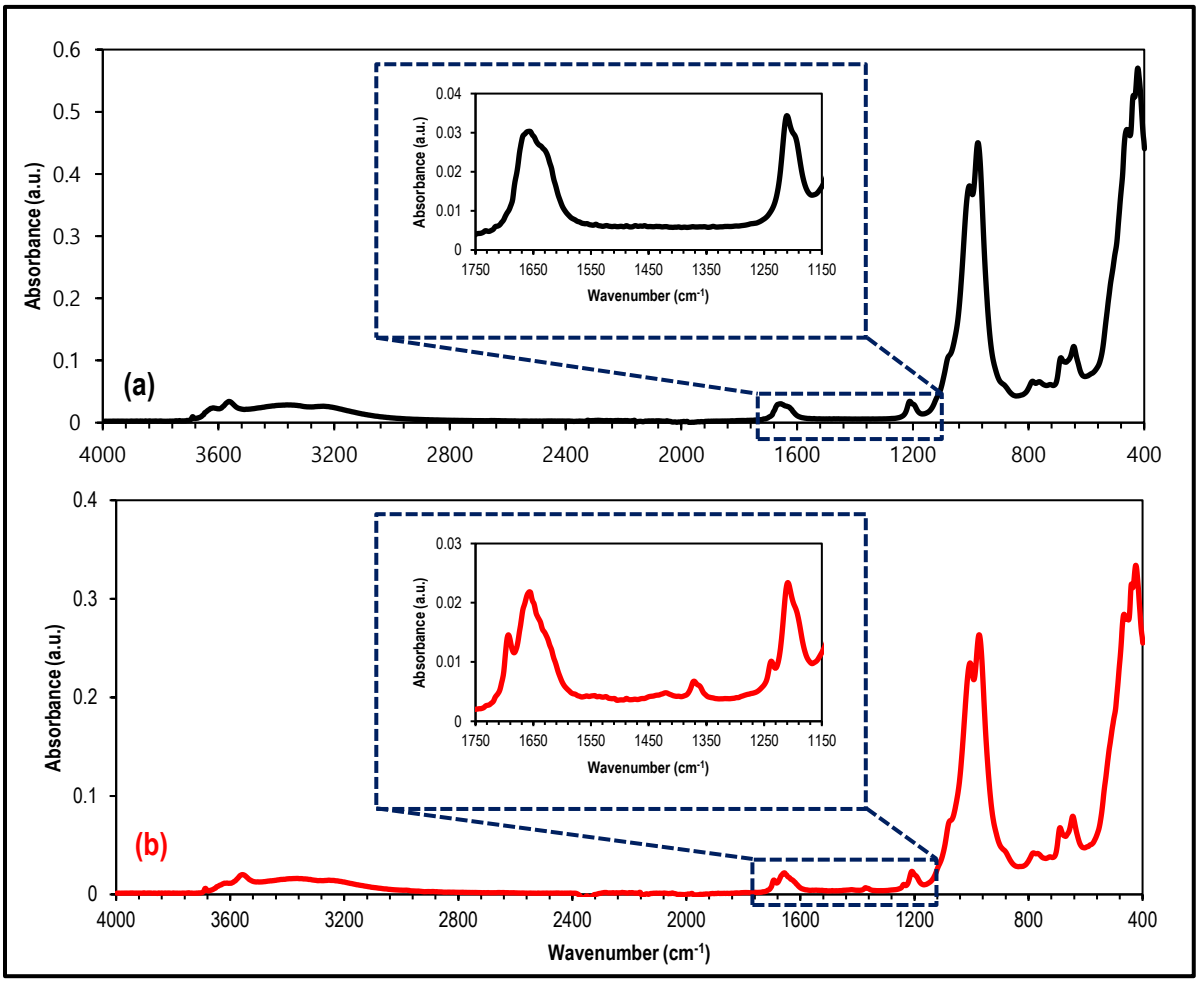

Fig. 6.1. ATR-FTIR spectra of (a) pristine sepiolite and (b) functionalized sepiolite.

For functionalized sepiolite, the FTIR spectrum shows some additional absorption peaks around 1240, 1370, 1420 and 1690 cm^{-1} attributed to the grafted organic part. Indeed, the band at 1240 cm^{-1} was attributed to the C-F bonds of the perfluorinated fragment. The bands at 1370 and 1420 cm^{-1} were attributed to C-H stretching vibrations of the alkyl part of the grafting agent. And finally the band at 1240 cm^{-1} was attributed to C=O stretching vibration of the amide function. The presence of these new bands proves the presence of the grafting agent for modified sepiolite after the functionalization procedure. Moreover, the shape of the band around 1670 cm^{-1} changes after the sepiolite treatment.

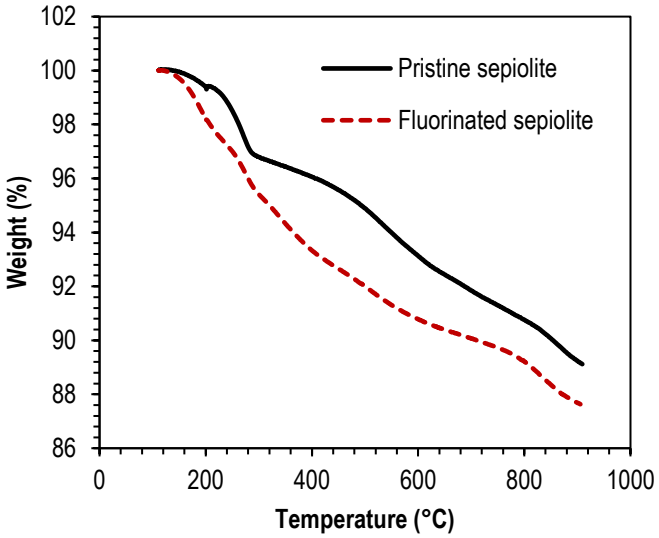

Fig. 6.2. TGA under nitrogen of pristine sepiolite and fluorine grafted sepiolite from 110 °C to 900 °C after an isotherm at 110 °C for 10 min.

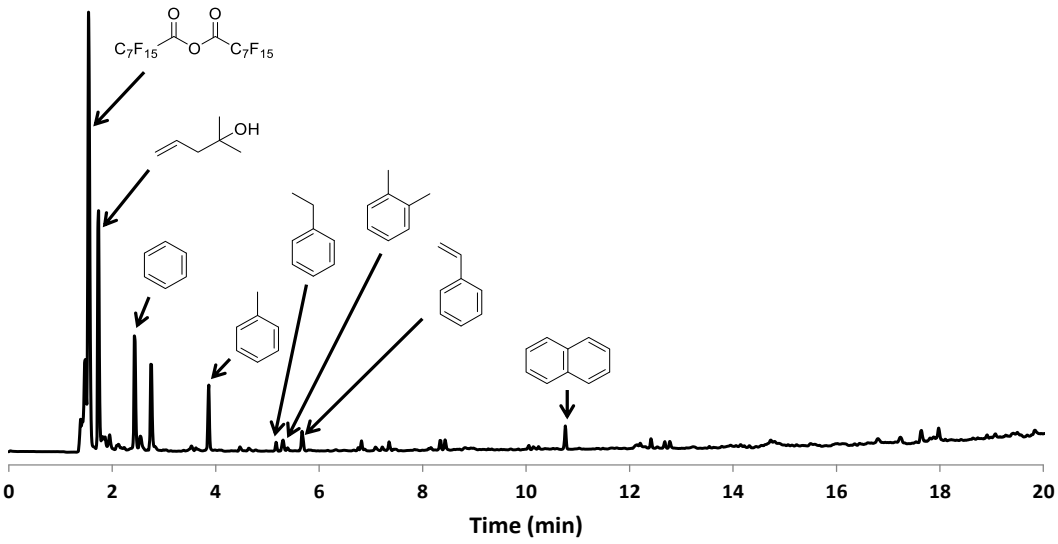

Fig. 6.3. Py–GC/MS chromatograms obtained for modified sepiolite sample pyrolyzed at 900°C.

Thermogravimetric analyses were used to characterize the functionalization of the sepiolite surface as shown in Fig. 6.2. Modified filler showed an augmented weight loss after grafting of about 1.4%. This weight loss was attributed to the decomposition of the grafted organic part which tends to prove, along with FTIR results, the efficiency of the functionalization procedure used.

Py–GC/MS was also used to validate the procedure of functionalization of sepiolite nanofibers. The analysis used a pyrolysis step at 900 °C to evaluate the presence and the nature of the organic molecules on the fillers surface. The results obtained for modified sepiolite sample (see Fig. 6.3) confirmed the TGA results. Whereas no peak was observed for pristine sepiolite, chromatogram of functionalized clay shows peaks corresponding to organic molecules obtained by thermal degradation of the grafted part. Presence of fluorinated molecules is observed due to the perfluorinated group of the grafting agent. Different molecules like aromatic molecules are also observed. Their structure, which is far from that of the grafting agent, is due to fracture/recombination processes occurring during the thermal decomposition. So Py-GC/MS analysis confirmed the presence of the fluorinated grafting agent on the modified sepiolite nanofibers.

4. Membrane preparation

All membrane samples with a size of 13 × 13 cm^2 were prepared via casting and evaporation. Aquivion and nanoclay were blended within casting dispersion in vials.

To begin with, 3.23 g of Aquivion dispersion (24 wt%, D83-24B), 0.078 g of nanoclay and 12.27 g of isopropanol were blended so as to obtain a 5 wt% Aquivion casting dispersion resulting in a 10 wt% clay loaded composite membrane.

Table 2.2. Information on nineteen different kinds of membranes prepared based on the available nanoclays (reproduced from chapter 2).

Membrane reference	PFSA ionomer	Nanoclay reference/content (wt%)	Type of nanoclay	Modification of nanoclay	Pretreatment of nanoclay
Aquivion		-	-	-	
Aq/SEP		SEP10		pristine	
Aq/SEP-F	Aquivion	SEP-F10	Sepiolite	fluorination	
Aq/pSEP		pSEP2/5/10		pristine	○
Aq/pSEP-F		pSEP-F2/5/10		fluorination	○

Different kinds of casting dispersions, obtained with different clays, were stirred for 15 mins by stirrer at 80 rpm. Afterward, nanoclay dispersions in vials were dispersed using ultrasound (HD 2070, Bandelin, Germany) and titanium alloyed microtip (MS73-529, Sonopuls, Bandelin) for 2 min at 60 W power and 20% pulsation level. The resultant dispersions were poured on a 13x13cm² mold at 15.578 g, after which it was heated at 80℃ for 18 h and then at 170℃ for 2 h. Prepared membranes were treated using 0.5M H_2SO_4 for 1 h and rinsed with DI-water for 1 h, at 100℃.

All the membranes were prepared using mold to have thickness of around 20 μm, in order to follow commercial trends and reduce resistance. Various membranes were prepared by addition of nine available nanoclays and they were labeled as listed in table 2.2.

5. Membrane characterization

5.1. Homogeneity of composite membranes (FE-SEM and EDS)

Fig. 6.4 displays FE-SEM cross-section images of the different studied membranes. EDS analysis was performed at both edge of membranes as well as in the center of the cross section in order to follow the chemical composition through the membranes to get insights on the nanoclay repartition. To this end, silicon, representative of sepiolite, and fluor, mainly representative of Aquivion, were specifically analyzed. Their ratio (Si/F) was then considered as an indicator for homogeneity. Constant value of Si/F and the nanoclay can be considered as homogeneously distributed though the membrane. Otherwise, nanoclay agglomeration can be suspected.

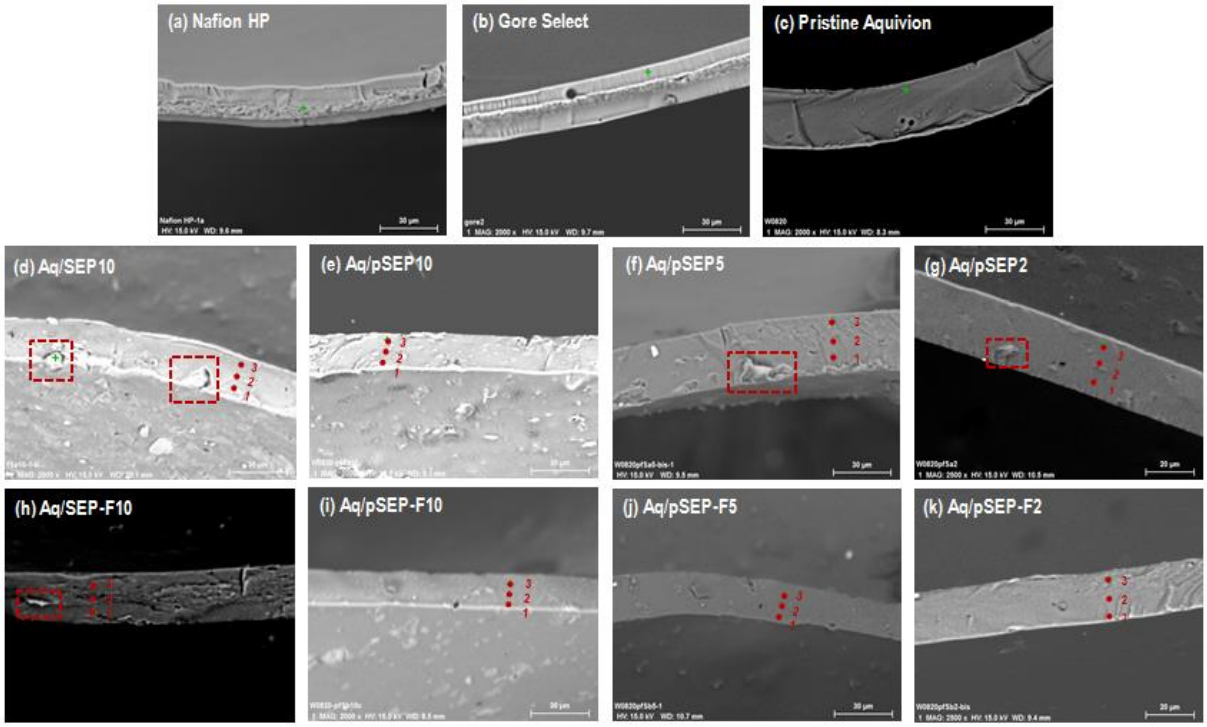

Fig. 6.4. FE-SEM images on (a) commercially available Nafion HP, (b) Gore Select (Aquivion), (c) pristine Aquivion, (d) Aq/SEP10, (e) Aq/pSEP10, (f) Aq/pSEP5, (g) Aq/SEP2, (h) Aq/SEP-F10, (ih) Aq/pSEP-F10, and (j) Aq/pSEP-F5 and (k) Aq/pSEP-F2 membranes.

The addition of pristine sepiolite resulted in rather inhomogeneous composite membrane (Aq/SEP10). The large difference in Si/F values analyzed through the membrane is consistent with the presence of large agglomerates observed on Fig. 6.4d.

The fluorination seems to improve the homogeneity of the composite membrane. Less agglomerates can be observed on the cross section of Aq/SEP-F10 (Fig. 4g). The difference in Si/F ratios is also smaller as can be seen in Fig. 6.5. Such a functionalization was expected to improve the compatibility between sepiolite and Aquivion. Perfluorinated groups (i.e., $-C_7F_{15}$) of N-(3-triethoxysilylpropyl)-perfluorooctanoamide grafting agent should indeed lead to good interaction with hydrophobic domains of Aquivion, resulting in improved compatibility and homogeneity [38]. Still the repartition of nanoclays can be improved further.

The pretreatment in oxalic acid and hydrogen chloride was meant to remove iron ions from sepiolite in order to multiply its chemical stability. It is noticeable that it seems to prevent the aggregation of sepiolite in the composite membranes [196-199], whatever the amount of sepiolite (2, 5 or 10 wt%), be it fluorinated or not. That is, very few agglomerates can be seen as shown in Figs. 6.4e-g. The best homogeneity was obtained for fluorinated and pretreated sepiolite among the membranes tested, since no visible agglomerates could be observed and quite constant Si/F values could be calculated across the membranes.

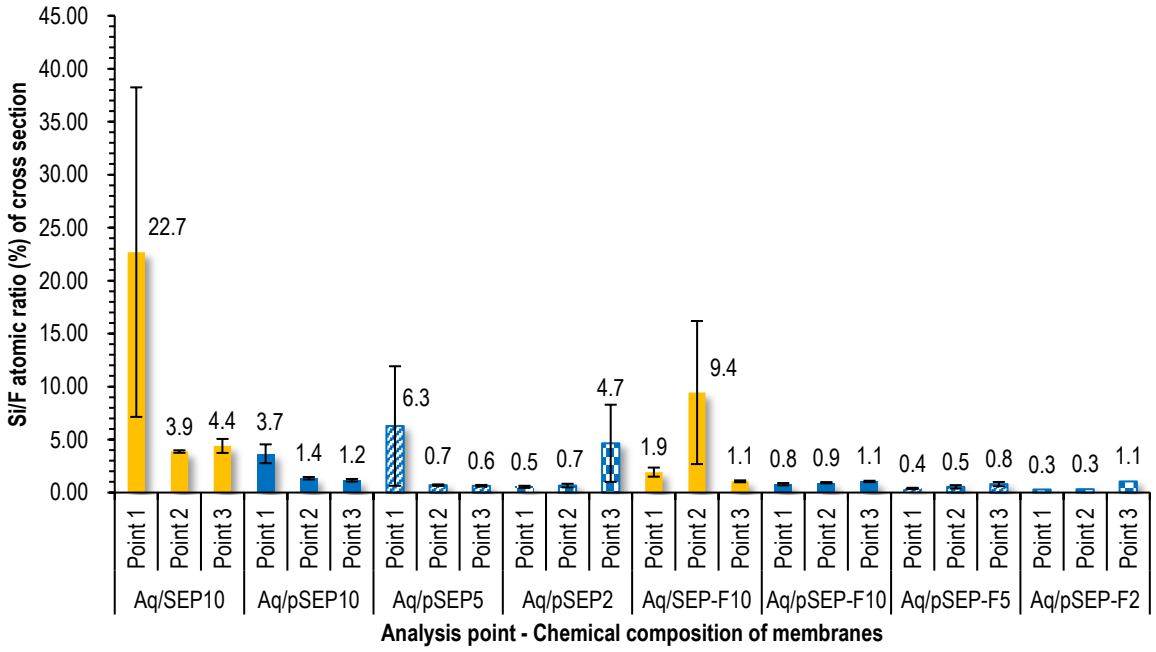

Fig. 6.5. Si/F atomic ratio (%) analyzed using EDS regarding sepiolite-based membranes: Aq/SEP10, Aq/pSEP5, Aq/pSEP2, Aq/pSEP10, Aq/SEP-F10, Aq/pSEP-F5, Aq/pSEP-F2 and Aq/pSEP-F10. Yellow and blue bars represent non-pretreated sepiolites and pretreated sepiolites, respectively. The different patterns represent different additive contents.

5.2. Thickness of hydrated membranes (micrometer)

The thickness of membranes is an important indication for PEMFC application as thin membrane can lead to reduced resistance under same condition [51], but often at the expense of a higher hydrogen crossover. Hence, the membranes were prepared targeting a thickness of approximately 20 µm under dry condition, similar to that of state-of-the-art membranes Nafion HP or Gore Select. Seven different kinds of our membranes were recovered by dipping, in DI-water, the glass plate they are prepared on. The thickness is thus measured in a wet state at room temperature and so is expected to be larger than in a dry state due to swelling. For comparison, the thickness of Nafion HP and Gore Select membranes was measured in the same conditions. All data are gathered in Fig. 6.6.

Pristine Aquivion membrane prepared in this study is slightly thicker than that of the references: 32 µm versus 23 µm and 27 µm for Nafion HP and Gore Select membranes, respectively.

In general, the incorporation of additives in Aquivion results in much thicker composite membranes, from 38 µm to 55 µm, depending on the additive amount and type and pre-treatment in oxalic acid and hydrogen chloride.

The thicker membrane was obtained with 10 wt% of pristine sepiolite (Aq/SEP10 - 55 µm).

Fluorination of sepiolite does not impact the thickness of the composite membrane (Aq/SEP-F10 - 54 µm).

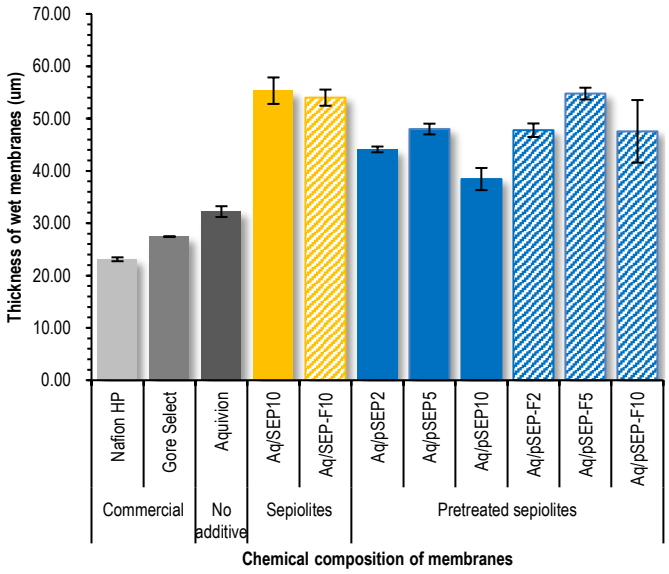

Fig. 6.6. Thickness, IEC, water uptake and swelling ratio of commercially available Nafion HP and Gore Select, and pristine Aquivion and Aquivion composite membranes containing various sepiolites. Gray bars represent referece membranes. Yellow and blue bars represent non-pretreated sepiolites and pretreated sepiolites, respectively. The diagonal line patterns represent fluorinated sepiolites.

The pretreatment of sepiolite in oxalic acid and hydrogen chloride seems to result in thinner composite membranes for 10 wt% of sepiolite at least for pristine sepiolite (Aq/pSEP10 - 38 µm vs Aq/SEP10 - 55 µm). The influence is less pronounced for 10 wt% of fluorinated sepiolite (Aq/pSEP-F10 - 47 µm vs Aq/SEP-F10 - 54 µm).

Surprisingly, it was not expected that decreasing amount of sepiolite to 5 wt% would result in slightly thicker composite membranes for both pSEP and pSEP-F sepiolites. On the contrary, composite membranes prepared with 2 wt% of pSEP or pSEP-F were thinner than those prepared with 5 wt%.

5.3. IEC

IEC is a representative indicator of the available number of ion exchange groups. It strongly influences the proton transfer through PEM, in particular Grotthuss-type transfer [183]. The IEC of composite membranes showed similar values compared with that of pristine Aquivion and reference membranes as shown in Fig. 6.7. Hence, the incorporation of sepiolite-type fillers, regardless of functionalization and pre-treatment process, does not impact the IEC. More specifically, the IEC of pristine Aquivion membrane displayed approximately 1.02 meq/g, whereas sepiolite-loaded composite membranes displayed values between 0.96 and 1.20 meq/g. Nafion HP membrane also exhibited similar IEC (1.08 meq/g) to pristine Aquivion membrane, whereas that of the Gore Select membrane is slightly lower. This result showed similar tendency to water uptake data except for 10 wt% sepiolite-blended membrane. This error value can be attributed to temperature difference while analyzing IEC or water uptake value.

For pretreated sepiolites, composite membrane with 5 wt% additive content exhibited the highest IEC among the membranes tested.

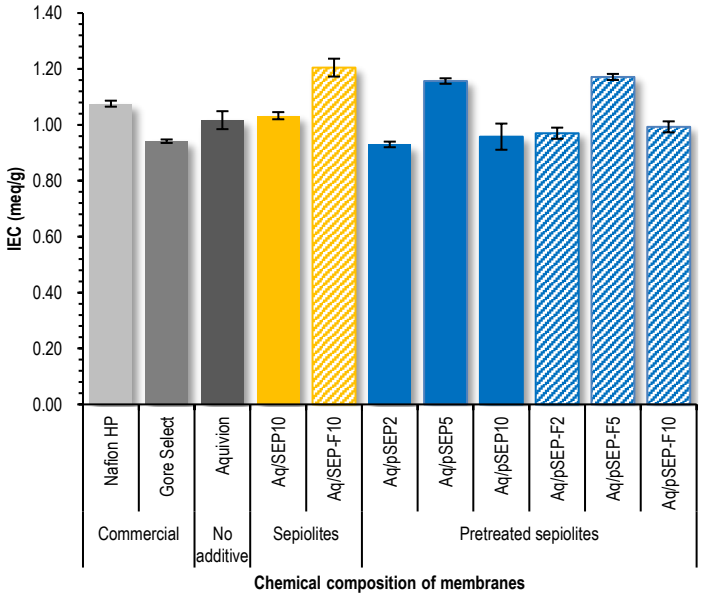

Fig. 6.7. IEC of commercially available Nafion HP and Gore Select, and pristine Aquivion and Aquivion composite membranes containing various sepiolites. Gray bars represent referece membranes. Yellow and blue bars represent non-pretreated sepiolites and pretreated sepiolites, respectively. The diagonal line patterns represent fluorinated sepiolites.

5.4. Water uptake

Water molecules are essential during proton transfer in ionomeric polymer matrix according to hopping, named Grotthuss mechanism, or vehicle mechanisms. The former means that protons randomly hop between neighbored protonic species with hydrolyzed ionic sites ($H_3O^+SO_3^-$) through hydrogen-network, whereas the latter

implies that protons are diffused together with water molecules by forming hydronium ions, e.g., H_3O^+, $H_5O_2^+$, and $H_9O_4^+$, caused by electrochemical difference [47, 182, 200]. Hence, the water uptake of membranes impacts the proton transfer during PEMFC operation.

As shown in Fig. 6.8, the introduction of sepiolite in Aquivion is beneficial to the water uptake. The obtained composite membranes displayed raised values compared to that of Nafion HP, Gore Select and pristine Aquivion membrane. Regardless of sepiolite fluorination and pretreatment process, 15 to 33% higher water uptake to that of pristine Aquivion membrane was achieved. The difference values between the two types of membranes were very tiny and negligible. This result can be attributed to the hydroscopic property of the numerous silanol groups (Si-OH) available in sepiolites.

Reducing the amount of sepiolite to 5 or 2 wt% does not significantly impact the results.

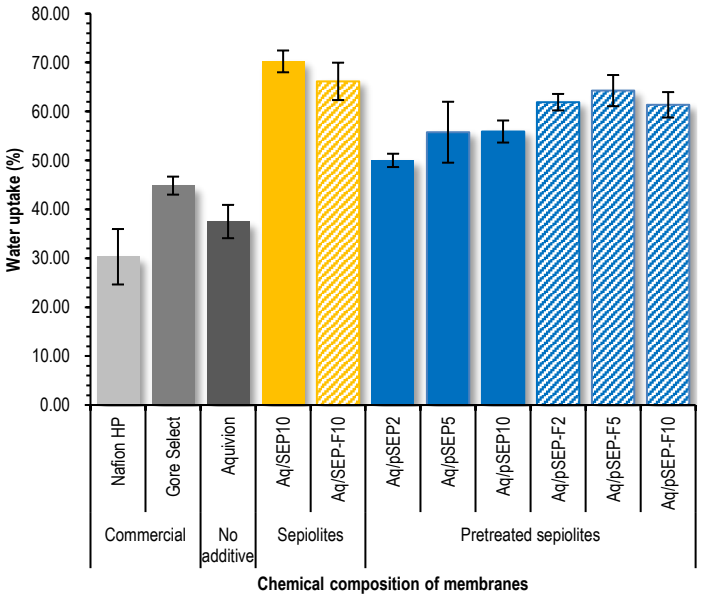

Fig. 6.8. Water uptake of commercially available Nafion HP and Gore Select, and pristine Aquivion and Aquivion composite membranes containing various sepiolites. Gray bars represent referece membranes. Yellow and blue bars represent non-pretreated sepiolites and pretreated sepiolites, respectively. The diagonal line patterns represent fluorinated sepiolites.

5.5. Swelling ratio

Swelling is another important feature since too high a value can impact fuel cell performance during operation.

As shown in Fig. 6.9, reference membranes Nafion HP and Gore Select, both reinforced membranes, showed rather low swelling, 6% and 1.2%, respectively. Our pristine Aquivion membrane, not reinforced, showed a much higher value of approximately 15%.

The insertion of sepiolite, regardless of the functionalization or pre-treatment, resulted in a very significant reduction of the thickness swelling for composite membranes. The addition of 10 wt% pristine sepiolite entailed

50% reduced swelling for the Aquivion membrane. This can be ascribed to the acicular nature of sepiolite. Such a nanofiber clay acts indeed as a reinforcement as already discussed in our former work on Nafion composite membranes [38, 39].

The fluorination of sepiolite has a positive impact on the swelling, making it decrease from 7% (Aq/SEP10) to 4.5% (Aq/SEP-F10). The presence of -C_7F_{15} groups in the modified sepiolite (SEP-F10) probably improves the nanophase distribution and the affinity between the filler and the hydrophobic domains of the Aquivion matrix, thereby inducing a better mechanical reinforcement of needle-like sepiolite [38, 47].

The pre-treatment in oxalic acid and hydrogen chloride seems to have a similar impact on the thickness swelling as the sepiolite fluorination (5% for Aq/pSEP10).

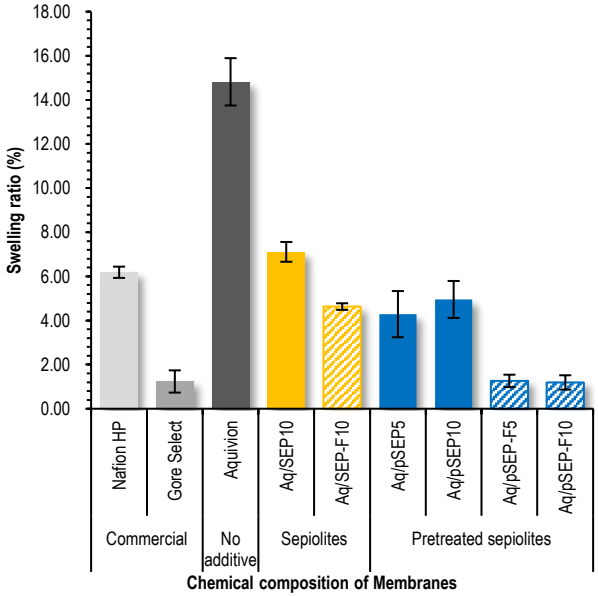

Fig. 6.9. Swelling ratio of commercially available Nafion HP and Gore Select, and pristine Aquivion and Aquivion composite membranes containing various sepiolites. Gray bars represent referece membranes. Yellow and blue bars represent non-pretreated sepiolites and pretreated sepiolites, respectively. The diagonal line patterns represent fluorinated sepiolites.

Mixing both, fluorination of sepiolite and pre-treatment in oxalic acid and hydrogen chloride, resulted in a very significant decrease of the thickness swelling which reached 1%, the same value than that obtained for the Gore-Select reinforced membrane. Such a synergic effect is consistent with the impact observed on the homogeneity of the composite membranes. The most homogenous membrane has actually been obtained with pre-treated and fluorinated sepiolite (pSEP-F10).

Note that reducing the amount of sepiolite (pSEP or pSEP-F) to 5 wt% has no impact on the beneficial effect observed.

5.6. *Dynamic mechanical analysis (DMA)*

The mechanical strength of membranes can be analyzed by DMA, comparing the different behaviors obtained in shear mode as described in the experimental section.

Regarding the pure membranes, it is clear from Fig. 6.10 that Aquivion is more mechanically stable at intermediate temperatures than Gore-Select and Nafion HP. The drop of G' arose indeed at much higher temperature for Aquivion, showing a higher stiffness. As a consequence, the Aquivion membrane exhibited a higher glass transition temperature (T_g) of about 140°C.

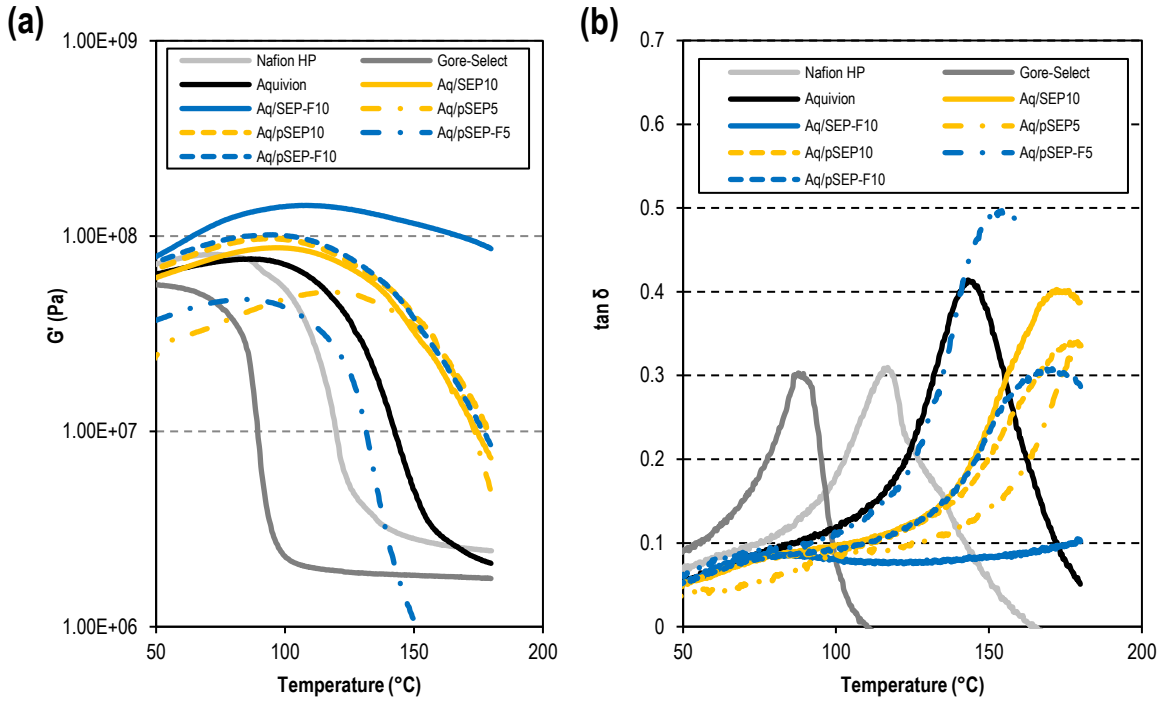

Fig. 6.10. Data on DMA - (a) G' and (b) tan delta - concerning Nafion HP, Gore-Select M820, pristine Aquivion, and Aquivion composite membranes blended with sepiolite and pretreated sepiolite.

Adding 10wt% of sepiolite in Aquivion (Aq/SEP-10) resulted in improved performance. The composite membrane is stiffer than the pure Aquivion membrane, with a T_g shifted to 170°C. The fluorination of sepiolite does not seem to result in a higher stiffness. However the T_g of the prepared composite membrane (Aq/SEP-F10) seems to be higher than 170°C.

Composite membranes with pretreated sepolite do not have impact on mechanical strength. Composite membranes exhibited similar or rather lower glass transition temperatures compared to non-pretreated sepiolite-based membranes regardless of functionalization.

The mechanical strength of composite membrane increased as the addition amount augmented. Blending of 10 wt% nanoclays displayed higher G' as well as T_g, compared to that of 5 wt% nanoclays. Incorporating fluorinated sepiolite 10 wt% led to the highest stiffness among the membranes tested. This also showed remarkable T_g value compared with the membranes tested.

5.7. Chemical stability

PFSA membranes are chemically degraded by free radical species which can be formed during fuel cell operation, i.e., HO· and HO_2· with strong oxidative property. Such free radical chemically attacks C-F bonds thus impacting the permeability of the membrane resulting in an increase of H_2 crossover [57]. The formation of H_2O_2 can be generated at the cathode side in MEA following a two-electron reduction reaction of oxygen. H_2O_2 can then react with divalent iron (Fe^{2+}) to form free radical species such as HO· and HO_2· [13, 58, 60, 61]. The free radicals are generated from H_2O_2 and Fe^{2+} as afore-mentioned in chapter 5 [13, 58].

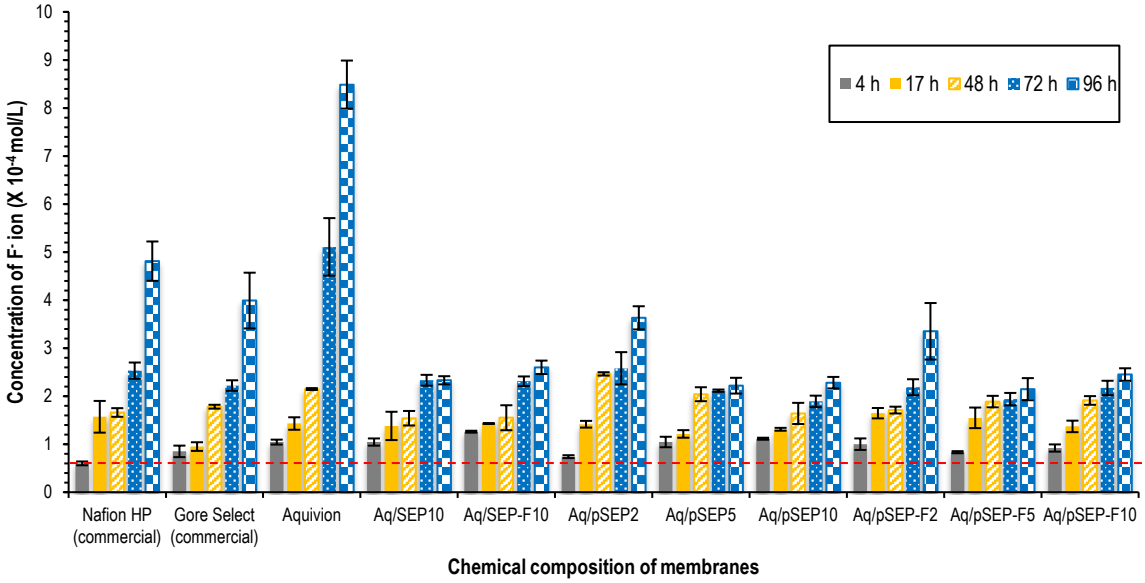

Fig. 6.11. Fluoride (F^-) concentration analyzed after immersion in H_2O_2/H_2SO_4 for Nafion HP, Gore Select (Aquivion), pristine Aquivion, Aq/SEP, Aq/SEP-F, Aq/pSEP and Aq/pSEP-F membranes. Red dotted line represents the fluorine concentration of 4.4 M H_2O_2/1.25 mM H_2SO_4 solution (blank test): $0.82\times10^{-4} \pm 0.08\times10^{-4}$ mol/L.

Sepiolite may contain some iron ions which could participate to the membrane degradation in the presence of hydrogen peroxide. For this reason, it was verified whether composite membranes containing sepiolite are chemically stable or not in the conditions of a modified Fenton test, according to the analytical method explained in chapter 2. Basically, the membrane sample is immersed in a mixture of H_2O_2 and H_2SO_4, the hypothesized source of Fe^{2+} being the sepiolite. The concentration of fluorine ions originated from the degradation is followed with a specific electrode. The influence of the fluorination and that of the pre-treatment in oxalic acid were studied.

Results for all the membranes tested at different reaction time from 4 to 96 h are shown in Fig. 6.11.

The evolution of the fluoride (F^-) concentration with time is similar for all the membranes tested: the longer the treatment the higher the F^- concentration. That one is slightly higher for the reference membranes, approximately twice more for our pristine Aquivion membrane. However the F^- concentration is rather limited even after 96 h of treatment since it is always quite close to that measured for the blank solution.

It is noticeable that the presence of sepiolite does not amplify the membrane degradation. The fluoride concentration measured for composite membranes is even smaller compared to that measured for the reference

membranes. No significant difference could be observed among the various composite membranes. The fluorination and the pre-treatment of sepiolite have no impact on the degradation of the composite membranes. It can be concluded that the fluorination is not detrimental while the pre-treatment is not beneficial to the membrane chemical stability.

Rio's group reported that sepiolite does not contain any Fe^{2+} ions, based on the analysis of twenty kinds of different sepiolites from various provenances such as Madrid, Toledo, Zaragoza, California and so on [201]. This is consistent with our observation. Sepiolite (Tolsa company) used for the membrane preparation in this study is mined at Madrid, Spain. The fact that no degradation could be evidenced showed that Fe^{3+} ions from sepiolite are not reduced to Fe^{2+}. It should be noted that the iron ion can circulate between Fe^{2+} and Fe^{3+} when free radicals are present [202, 203].

Blending of 2 or 5wt% sepiolite with Aquivion led to similar chemical stability to that of 10 wt% sepiolites regardless of fluorination and pre-treatment process.

5.8. Proton conductivity (EIS)

A fuel cell membrane requires high proton conductivity originating from the mobility of ion carriers. The proton transfer phenomena in ionomeric polymer matrices are classified into Grotthuss and vehicular mechanisms, which were already described in section 5.4. In the study, the resistance of prepared membranes was measured using AC impedance spectroscopy under conditions of different temperature (50℃, 70℃, and 90℃) and relative humidity (25%, 50%, 75%, and 90%). The proton conductivity is then calculated from the measured resistance taking the membrane thickness into account. It was not possible to measure the thickness during the resistance measurement. Since the membrane was hydrated in the measurement cell we chose to consider the thickness measured in wet conditions to calculate the proton conductivities. The real conductivities may vary from the calculated ones. Nevertheless, it is noteworthy that the conductivities calculated for Aquivion at 90°C and 25 %RH or 90 %RH are close to values reported in literature (cf. Fig. 5.13 and 6.13).

As a general rule, Fig. 6.12 shows that, for each membrane, the higher the temperature and/or relative humidity, the higher the proton conductivity (i.e., the lower the resistance). As expected, the impact of the relative humidity is much more pronounced than that of the temperature.

Based on Fig. 6.13, all membranes can be classified as follows: Aq/pSEP-F5 > Gore Select (Aquivion) > Aq/pSEP-F10 > Aq/SEP-F10 > pristine Aquivion $\geq$ Aq/pSEP5 $\cong$ Nafion HP $\geq$ Aq/pSEP10 > Aq/SEP10.

Pristine Aquivion membrane generally showed a better conductivity than Nafion HP. It is well known that Aquivion has improved properties compared to Nafion series due to shorter side-chains, larger crystallinity and higher glass transition temperature [50, 51]. Among selected reference membranes, Gore Select showed the best proton conductivity, two to three times that of Nafion HP, reaching almost 260 mS/cm at 90°C and 90% RH. The proton conductivity of pristine Aquivion membrane obtained in this study were very similar to that found in the literature in similar conditions [194, 195]. It reached approximately 115 mS/cm at 90°C and 90% RH. It should be noted that Aquivion E79-03S, Aquivion EW830 and Aquivion E87-12S respectively showed 10 mS/cm (95℃, 25%), 118 mS/cm (80℃, 95%), and 138 mS/cm (90℃, 95%) according to the literature [52, 194, 195] (see Fig. 6.13).

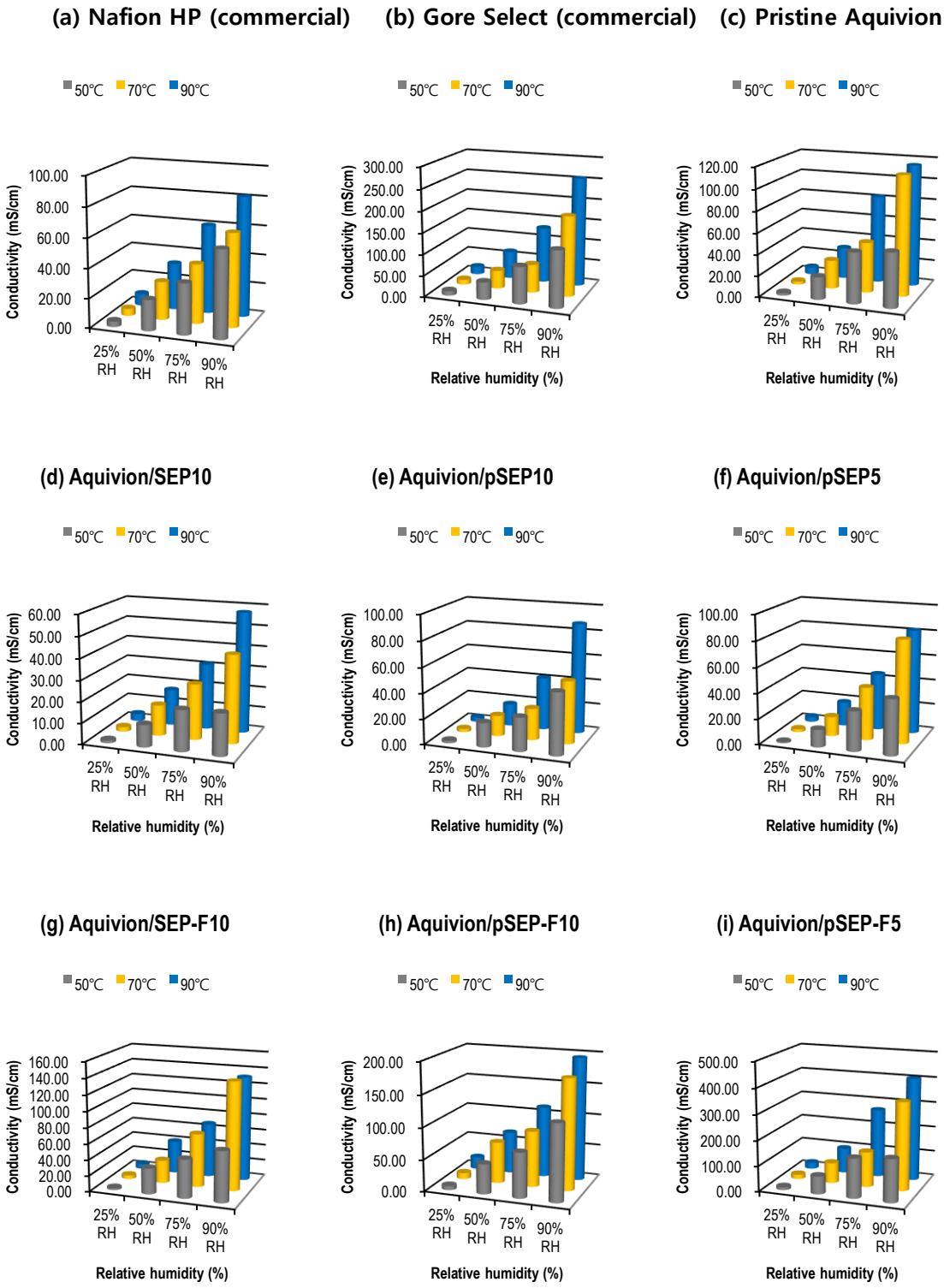

Fig. 6.12. 3D cylinder graphs depending on temperature (50°C, 70°C, and 90°C) regarding proton conductivity of various PEMs: (a) Nafion HP, (b) Gore Select (Aquivion), (c) pristine Aquivion, (d) Aquivion/SEP10, (e) Aquivion/pSEP10, (f) Aquivion/pSEP5, (g) Aquivion/SEP-F10, (h) Aquivion/pSEP-F10, and (i) Aquivion/pSEP-F5 membranes.

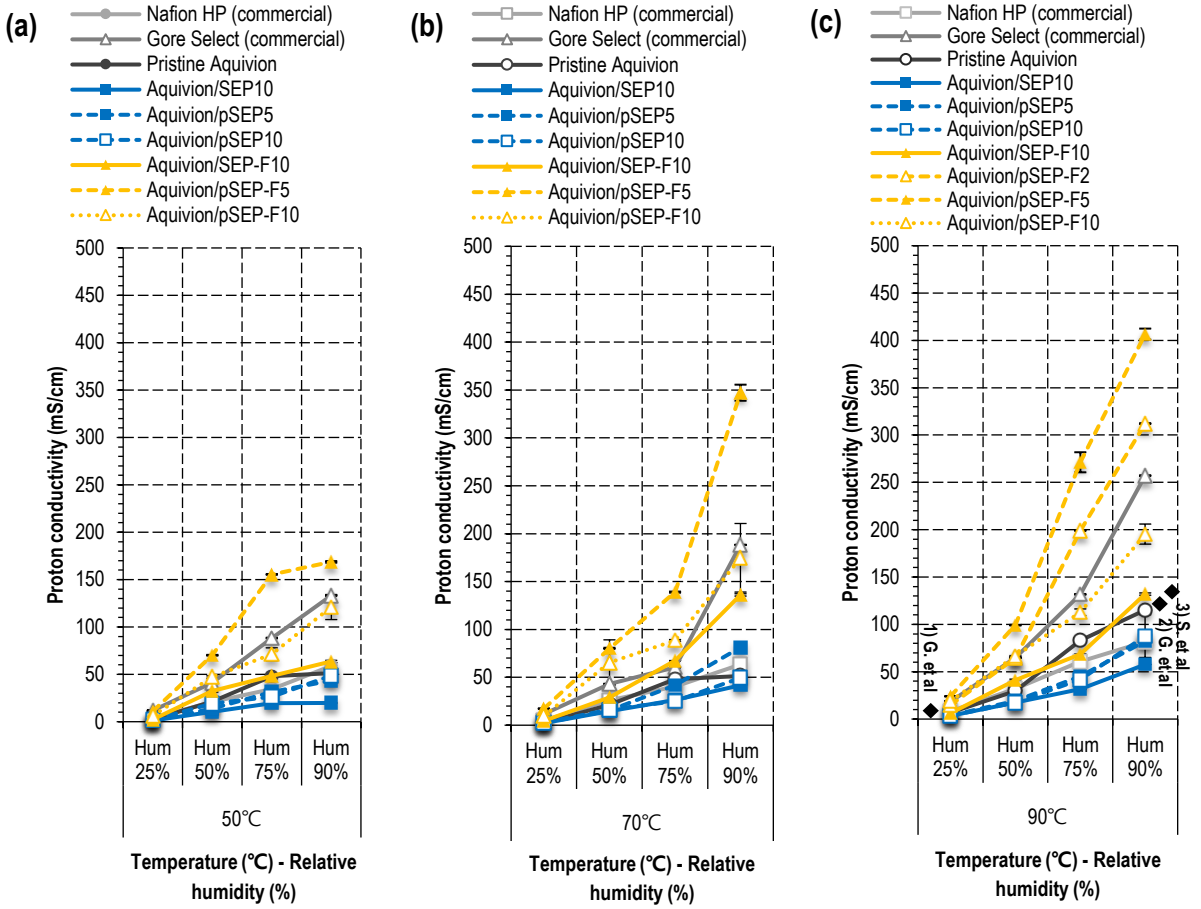

Fig. 6.13. Influence of temperature (a) 50℃, (b) 70℃, (c) 90℃ and relative humidity on proton conductivity for various PEMs: Nafion HP, Gore Select (Aquivion), pristine Aquivion, Aquivion/SEP10, Aquivion/pSEP5, Aquivion/pSEP10, Aquivion/SEP-F10, Aquivion/pSEP-F2, Aquivion/pSEP-F5, and Aquivion/pSEP-F10 membranes.

1) Gebert et al, 10 mS/cm at 95℃, 25% (Aquivion E79-03S) [194].
2) Giancola et al, 118 mS/cm at 80℃, 95% RH (Aquivion EW 830 g/eq) [52]
3) Skulimowska et al, 138 mS/cm at 90℃, 95% (Aquivion E87-12S) [195]

Blending pristine sepiolite (SEP10) with Aquivion resulted in a decrease of the proton conductivity compared with pristine Aquivion membrane and Nafion HP. This may be related to the observed agglomeration of sepiolite and possible blocking of the ionic path thus hindering smooth movement of protons within the composite membranes.

The fluorination of sepiolite (SEP-F10) allowed enhancing the conductivity of the composite membrane to a level close to that of pristine Aquivion or even slightly higher, depending on the conditions. This may be due to the improved affinity of the functionalized nanoclay with the ionomer, as already described in section 5, or to a better ionomer chain organization during membrane formation resulted from better interaction between the fluorinated backbone (C-F) and the fluorinated sepiolite.

The pretreatment of sepiolite led to similar or slightly higher proton conductivity compared with that of the composite membrane blended with pristine sepiolites. Still the proton conductivity stays below that of pristine Aquivion membrane. Exploiting both modifications, fluorination and pre-treatment of sepiolite (pSEP-F), was

very beneficial to the proton conductivity. As previously mentioned, there might be a synergetic effect between fluorination and pre-treatment. The membrane prepared with 10 wt% of pretreated and fluorinated sepiolite showed a proton conductivity larger than that of the membrane blended with fluorinated only or pretreated only sepiolite. The proton conductivity is even significantly larger than that obtained with the pristine Aquivion membrane, 195 vs 115 mS/cm at 90°C and 90 %RH.

The amount of sepiolite impacts the proton conductivity of composite membranes. If for pretreated sepiolite, reducing the amount to 5 wt% has quite no influence, for both pretreated and fluorinated sepiolite the proton conductivity is almost doubled and for the first time above that of the Gore select membrane, under any conditions of temperature and relative humidity (407 vs. 260 mS/cm at 90 °C and 90% RH). Mixing the nanofiber with 5wt% content had much improved impact on proton conductivity of composite membrane than 2wt% content.

The proton conductivity is related to the concentration of acid sites, related to the IEC, to the amount of water in the membrane (RH and water uptake) and to the mobility of protons. The IEC and the water uptake calculated for membranes containing 5 wt% of sepiolite (pretreated, or fluorinated and pretreated) are similar or slightly larger than for 10 wt%. Since the proton conductivity is improved only with fluorinated and pretreated sepiolite, the main effect should be here the homogeneity of the dispersion that influences the mobility of protons as previously mentioned.

5.9. Impact of the acidic treatment on nanoclays

It was shown that pretreated and fluorinated sepiolite allowed to significantly improve the properties of the composite membrane prepared with Aquivion. The impact of fluorination can be ascribed to a better affinity of the filler with the polymer matrix both possessing fluorine available for interactions. Additional structural analysis was performed to try to understand the role of the pre-treatment.

The structure of pristine or fluorinated sepiolite turned to become mainly amorphous after pre-treatment as shown in Fig. 6.14. Followed by EDS, the relative concentration of cations such as Mg^{2+}, Al^{3+} and Fe^{3+}, all present inside sepiolite, significantly decreased after pre-treatment in oxalic acid and hydrochloric acid, all the more so that sepiolite was fluorinated and mainly for Mg^{2+} and Fe^{3+} (see Fig. 6.15). As for palygorskite [204], such a cation leaching may result in the structure modification observed by XRD. This leads to a fraction of octahedral vacancies at the edges of channels, which form silanol groups (Si-OH) and as a consequence to a modification of the surface area [196, 205, 206]. The leaching resulted only in a partial modification of the structure, allowing maintaining the overall morphology. We assume that the defects created during the acid treatment allowed improving the interface with the polymer matrix and the repartition of fillers, thereby being beneficial to the proton conductivity of the composite membranes.

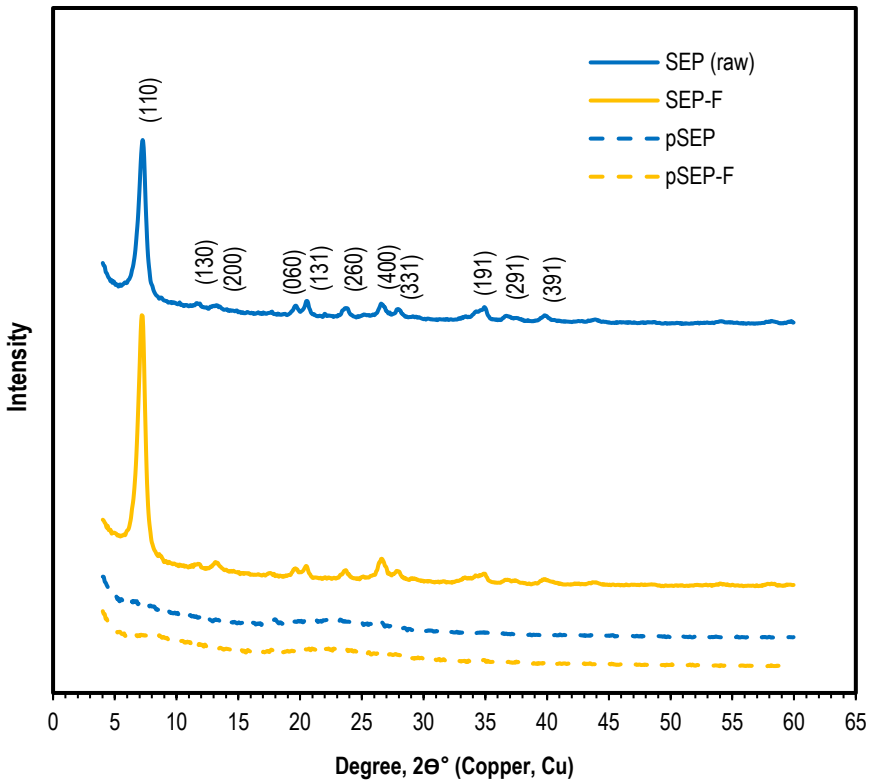

Fig. 6.14. XRD pattern of pretreated sepiolites: SEP (blue), SEP-F (yellow), pSEP (blue, dashed line) and pSEP-F (yellow dashed line) nanoclays used for preparing composite membranes.

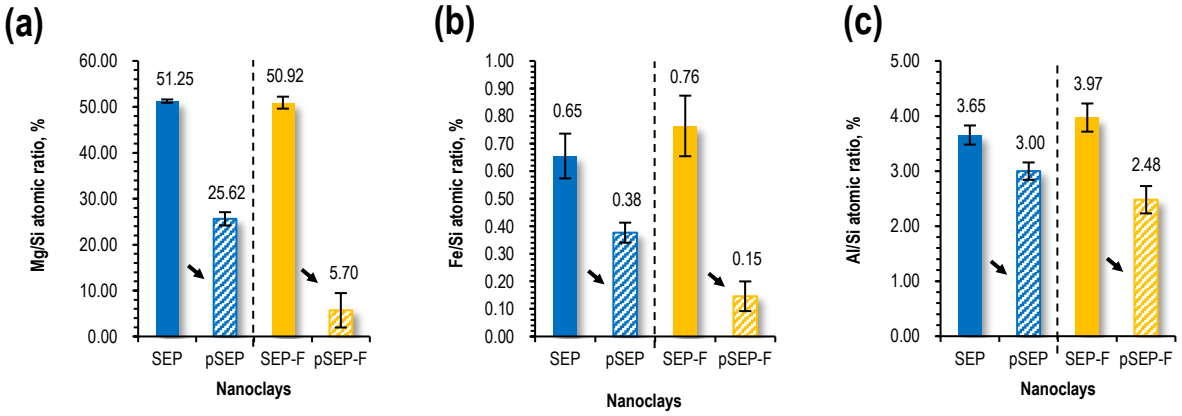

Fig. 6.15. Comparison of (a) Mg/Si, (b) Fe/Si and (c) Al/Si atomic ratio (%) regarding SEP, pSEP, SEP-F, and pSEP-F nanoclays used for preparing composite membranes.

In addition to this, the amorphous structure of sepiolite, which was formed through pretreatment, may offer advantages in improving the proton conductivity of composite membranes. The phenomena can be explained

through diffusion coefficient [207]:

$$D = D_0 e^{-E_a/kT} \quad \rightarrow \quad D \propto \frac{1}{E_a} \qquad (7)$$

Where D_0, E_a, k and T represent pre-exponential factor, activation energy, gas constant and temperature, respectively.

Pretreatment promotes water diffusivity by reducing the activation energy by forming an amorphous structure of sepiolite. More specifically, the lack of crystalline properties (i.e., amorphous structure), caused by removal of Al_2O_3, Fe_2O_3 and MgO, makes it difficult to bind to crystalline solids. Hence, as the water swells the amorphous sepiolite (compared to crystalline sepiolite), diffusion and penetration of water molecules in the amorphous structure becomes faster under same relative humidity conditions by reduced activation energies, and accordingly this makes ion mobility much easier (see Fig. 6.16). It should be noted that the higher the ion diffusivity, the higher the ionic conductivity based on Nernst-Einstein equation [208].

Also, it is notable that the reason why the water absorption of the composite membranes containing pretreated sepiolite is similar to the absorption of the composite membranes containing sepiolite is related to the diffusion rate (i.e., diffusion coefficient), but is not related to the number of water molecules moving through the swelled parts.

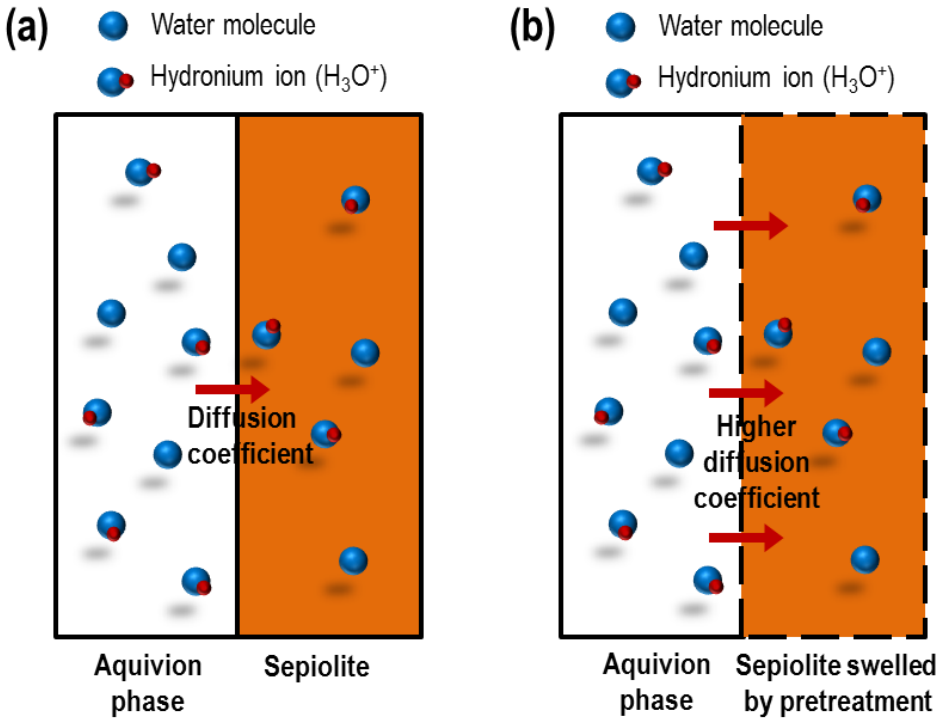

Fig. 6.16. Diffusion coefficient of water molecules and protons to (a) sepiolite and (b) pretreated sepiolite. The water molecules diffuse relatively easily to swelled sepiolite, which makes the ionic mobility easier.

5.10. Fuel cell performances

Pristine Aquivion membrane, two different kinds of composite membranes (Aq/SEP10, Aq/SEP-F10) and Nafion HP were selected to conduct MEA test.

In wet conditions the initial polarization curves are rather similar (see Fig. 6.17a). The mass transport limitation occurs at lower cell voltages for the Aquivion and composite membranes. This may be due to the presence of sepiolite for the latter.

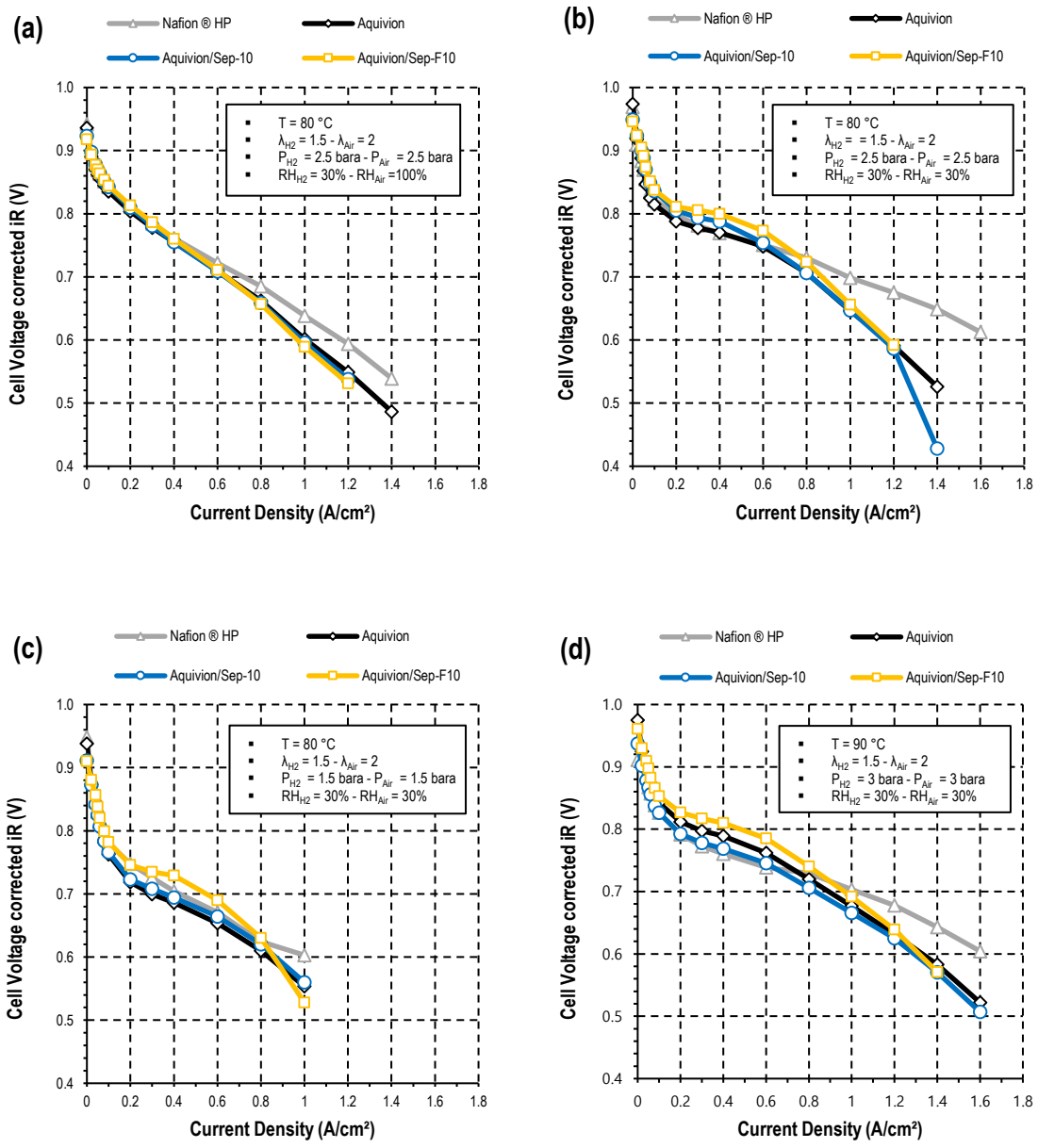

Fig. 6.17. Polarization curves of membrane electrode assemblies (MEAs) based on Nafion HP and different Aquivion membranes: (a) wet, (b) dry, (c) low pressure and (d) HAST initial conditions.

In all other dryer conditions (dry, low pressure and HAST conditions) the performances of the composite membranes are slightly better before 0.8 A/cm² compared with pristine Aquivion and Nafion HP, especially when the sepiolite is fluorinated (see Figs. 6.17b - d). The presence of sepiolite in the composite membranes is thus beneficial in dry conditions. In so-called "dry conditions" (see Fig. 6.17b) the mass transport limitations looks however much more pronounced than in wet conditions (see Fig. 6.17a).

The HAST cycles proved very severe on all MEAs, all tests were interrupted after less than 15 hours. The tests all finished in the same way, with a drastic augmentation in crossover currents, short resistances lower than 1 ohm.cm² and a significant decrease in OCV and fuel cell performances.

.

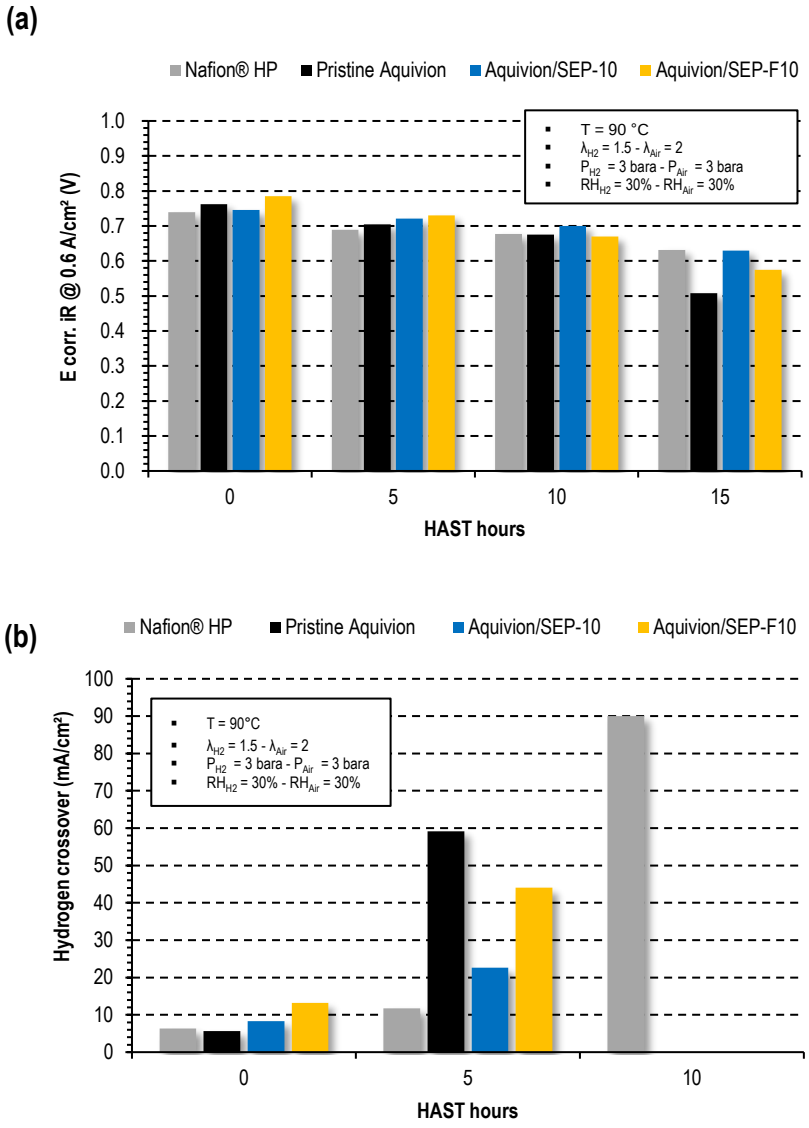

Fig. 6.18. Evolution of (a) the voltage at 0.6 A/cm² and (b) the hydrogen crossover for the different MEAs during the HAST.

At 0.6 A/cm², the cell voltage of the MEA incorporating Aquivion based membranes, pristine or composite, is, until 10 h of cycling, systematically higher than that of the Nafion® HP based MEA (see Fig. 18a). The decrease in performance with time after HAST cycles is comparable for all the tested membranes except pristine Aquivion. After 10 h of cycling, the performance of the pristine Aquivion based MEA dropped significantly. It is noteworthy that the incorporation of sepiolite in Aquivion resulted in a limited decrease of performance. The presence of sepiolite does not however significantly impact the durability of the MEA in the tested conditions

The initial hydrogen crossover of the composite membranes is slightly higher than that of the pristine Aquivion membrane or Nafion® HP (see Fig. 6.18b). This impacted the open circuit voltage (OCV) which was slightly lower for composites membranes compared to that of pristine Aquivion based MEAs (see Fig. 6.18d). Surprisingly, if the fluorination of sepiolite did impact the initial hydrogen crossover, the effect on the OCV is rather limited. The hydrogen crossover increased with time during HAST tests for all membranes tested and only that of Nafion® HP could be measured after 10 h of cycling. From the results obtained after 5 hours of cycling it looks clear that the hydrogen cross over is much more limited for sepiolite based composite membranes compared to the pristine Aquivion membrane. So even if the level of hydrogen crossover was still higher than that obtained with Nafion® HP, it came out that the presence of sepiolite, modified or not, may thus be beneficial. However the fluorination of sepiolite did not reduce the hydrogen crossover even if improved compatibility with Aquivion was expected. Further minimizing the hydrogen crossover is a promising route for improvement that should result in much better performances.

Finally, considering that our composite membranes are much thicker than the Aquivion or the Nafion HP ones (55 µm vs 32 µm or 23 µm respectively), it is reasonable to expect much better performance for similar thickness. The preparation process will be adapted to prepare thinner composite membranes which will be tested in a further study.

Conclusions

Sepiolite was successfully grafted with fluorinated group and pretreated using acidic solutions. Aquivion composite membranes were prepared by blending with sepiolite (i.e., SEP or pSEP) or fluorine grafted sepiolite (i.e., SEP-F or pSEP-F), and they were compared with commercially available Nafion HP and Gore Select M820. A number of conclusions related to physicochemical properties of composite membranes can be drawn:

- The incorporation of sepiolite into Aquivion matrix led to improved water uptake, swelling ratio and mechanical properties. The composite membrane displayed similar IEC and chemical stability, but showed reduced dispersion of fillers and proton conductivity, with heavy thickness compared to Aquivion and Nafion HP.
- The fluorination of sepiolite proved to be beneficial. It resulted in better dispersion of the additive inside the polymer phase of the composite membrane. The mechanical strength as well as the proton conductivity were improved, without impacting the water uptake, the thickness, the IEC, and even the chemical stability.
- Concerning pretreatment influence, composite membranes blended with fluorinated and pretreated sepiolite showed similar IEC and chemical stability compared to commercially available membranes. In

addition, the composite membranes were superior to proton conductivity regardless of filler contents among the membranes tested, but displayed reduced swelling and mechanical stability.

- Electrolyte membranes were incorporated in MEAs to be tested in single cell fuel cells. Slightly better performances were achieved with composites membranes compared to Nafion HP or pristine Aquivion, especially at intermediate current density and low relative humidity. The best performance was obtained with the fluorinated sepiolite based composite membrane.
- Based on characterization, it can be suggested that improved physicochemical properties of Aquivion/fluorinated sepiolite electrolyte membrane lead to good result on MEAs test during PEMFC operation, under low relative humidity condition.

Further study is needed to optimize the amount of nanofiber additives inside Aquivion phase, in order to optimize the membrane characteristics and especially reduce the hydrogen crossover. The composite membrane thickness also has to be reduced in order to limit the resistance loss of the MEAs.

Conclusions and perspectives

1. Summary

PEMFCs have been used for automobile applications due to their advantages. Among PFSA (perfluorosulfonic acid) materials used for PEM, Aquivion has been selected because of good properties. However, PFSA is not suitable for use at high operating temperatures (i.e., 120 - 150℃) and low relative humidity. Hence, inorganic oxide, zeolite or nanoclay can be blended with polymer phase of composite membranes.

Incorporation of nanoclays into a polymer matrix can overcome limitations regarding thermo-mechanically resistance and relative humidity. Addition of nanoclay particularly prevents dehydration due to hydroscopicity. Halloysite or sepiolite can be incorporated inside polymeric phase in order to improve characteristics of proton exchange membranes. Nevertheless, this method still has limitations regarding the restricted temperature and sensitive relative humidity resulting in reduced proton conductivity during operation. This result is due to aggregated nanoclay inside polymer matrix, and hence dispersion of nanoclay is an important aspect for formation of homogeneous membranes. Controlling the dispersion state of nanoclay within polymeric phase has been a key issue for numerous researchers, but the achievement is difficult as relationship between polymer and inorganic filler shows bad compatibility caused by poor affinity. However, if fibrous and layered nanoclays can be functionalized, the modified nanoclays ultimately can help composite membranes to have improved homogenous characteristic.

So far, the influence of the incorporation of sepiolite or halloysite in Aquivion membranes has not been fully determined for PEMFC application even though Aquivion is a prominent candidate as one of the PFSA ionomers. Moreover, the impact of halloysite and sepiolite modification on Aquivion membrane features has not been fully demonstrated. In addition, although iron in nanoclays may cause oxidation, no studies have been conducted to verify it using anti-oxidant material such as quercetin. If so, modified fibrous nanoclay-based Aquivion composite membranes may enhance fuel cell performance under the wide range of PEMFCs operating conditions.

This Ph.D. thesis proposed a novel nanoclay-based PFSA composite membrane which could be applied at low relative humidity and intermediate temperature. In the study, it was discovered that the shorter the blenidng time the better the composite homogeneity. Moreover, it was confirmed that the addition of modified nanoclay improved the dispersion state of composite membrane, compared with blending of natural nanoclay with Aquivion dispersion. On top of the functionalization, a specific pre-treatment allows to enhance the fuel cell performance. Aquivion/nanoclay composite membrane shows improved water uptake, swelling behavior, mechanical and chemical stability as well as proton conductivity compared with pristine Aquivion and commercially available membranes based on Nafion HP or Gore Select. They are thus expected to be very interesting alternatives for low relative humidity and intermediate temperature operation of PEMFCs (proton exchange membrane fuel cells).

Sepiolite was fluorinated, and halloysite was fluorinated, sulfonated or perfluorosulfonated, and also functionalized with amino group/quercetin or fluorine group/quercetin. Afterward, to remove most of iron contained in nanoclays, they were pretreated using oxalid acid and hydrogen chloride solutions. Membranes were prepared via casting and evaporation. In addition, Nafion/halloysite or Nafion/sepiolite composite membranes were prepared with varying blending times to improve homogeneity.

In terms of characterization, nanoclay modification was analyzed using ATR-FTIR, Py-GC/MS, TGA, XRD and EDS. Physicochemical properties of commercially available, pristine and composite membranes were verified by water uptake, swelling ratio, ion exchange capacity, SEM, EDS, chemical stability, mechanical strength, proton conductivity and MEA test.

2. Achievements

At the beginning of this Ph.D. thesis, the purpose of this study was described through general introduction. Briefly, three scientific objectives can be presented as follows:

- Influence of blending time of halloysite or sepiolite inside Nafion membranes;
- Effect of halloysite or sepiolite filler incorporating into Aquivion composite membranes;
- Influence of functionalized halloysite or sepiolite additive on Aquivion electrolyte membranes;
- Impact of quercetin grafting on Aquivion composite membranes; and
- Effect of pretreated nanoclays and their various contents on Aquivion composite membranes

2.1. Influence of blending time of halloysite or sepiolite inside Nafion membranes

In general, the addition of halloysite or sepiolite filler led to improved membrane properties: larger water uptake and reduced swelling compared with pristine Nafion membranes, without any impact on the IEC. It is noteworthy that the introduction of sepiolite and halloysite resulted in similar improved performance: 60% water uptake and 2 - 3% swelling ratio for 1 h blending, versus 40% and 14% respectively for the Nafion membrane prepared in the same conditions.

Moreover, it is clear from our results that the shorter the blending the better the homogeneity and as a consequence the performance, especially the water uptake. The impact seems to be more pronounced for halloysite than for sepiolite. In the first case macroscopic inhomogeneity appeared from 5 h blending, 24 h in the second case.

Additionally, it can be concluded that sepiolite is much easier to disperse than halloysite inside Nafion matrix.

2.2. Effect of halloysite or sepiolite filler incorporating into Aquivion composite membranes

Blending of halloysite with Aquivion dispersion led to raised water uptake, swelling ratio as well as mechanical strength. Compared with Nafion HP and Gore Select M820, composite membranes exhibited similar IEC, but reduced proton conductivities. In addition, they showed a thicker thickness compared to pristine Aquivion and commercially available membranes.

Adding pure sepiolite into Aquivion matrix improved water uptake and mechanical strength. Additionaly, this displayed reduced swelling ratio and proton conductivity compared with Nafion HP. The composite membrane also displayed similar IEC and chemical stability, but showed reduced proton conductivity, with heavy thickness compared to Nafion HP as well as Gore Select M820.

2.3. Influence of functionalized halloysite or sepiolite additive on Aquivion electrolyte membranes

With respect to functionalization with fluorination, sulfonation or perfluorosulfonation group, functionalized halloysite-incoporated membranes showed reduced thickness and improved mechanical strength compared to

pristine halloysite-blended membrane. On the other hand, similar composite homogeneity, swelling, antioxidant activity, hydrophilicity, and IEC values were verified, regardless of functionalization type.

The fluorination of sepiolite proved to be beneficial. It resulted in better dispersion state of the additive inside the polymer phase of the composite membrane. The mechanical strength as well as the proton conductivity were improved, without impacting the water uptake, the thickness, the IEC, and even the chemical stability.

2.4. Impact of quercetin grafting on Aquivion composite membranes

Pristine Aquivion showed increased water uptake and proton conductivity compared with Nafion HP. However, water uptake and thickness of pristine Aquivion was reduced than those of composite membranes containing quercetin grafted HNTs. The incorporation of halloysite grafted with quercetin, fluorine group/quercetin or amino group/quercetin into Aquivion matrix showed slightly augmentation in thickness and IEC. Moreover, they can decrease the swelling compared to Nafion HP. Addition of fluorine group/quercetin-grafted halloysite led to improved dispersion state at cross section. The composite membranes containing fluorine group/quercetin- or amino group/quercetin-grafted HNT also displayed raised water uptake. Moreover, improvement in chemical stability by quercetin grafting was verified compared to Nafion HP at 96 h, even and exhibited reduced values compared with pristine Aquivion or HNT-blended membrane (due to reduced iron amount as well as anti-oxidative activity).

2.5. Effect of pretreated nanoclays and their various contents on Aquivion composite membranes

The pretreatment associated to the functionalization (-F, -S, or -SF) of halloysites proved to benefit to composite homogeneity and proton conductivity. In particular, blending of pretreated and perfluoro-sulfonated halloysite into Aquivion matrix led to the highest proton conductivity among the membranes tested. Moreover, Aq/pHNT-SF10 was particularly interesting as it displayed improved mechanical property caused by better stiffness. However, according to the fluoride ion concentration, the pretreatment did not affect the chemical stability as expected.

The amount of pretreated and functionalized clay nanotubes (-F, -S, or –SF) is impacting the IEC, the water uptake and the proton conductivity with a maximum reached for 5 wt% Besides, the smaller the content, the better the dispersion state of additives.

Through pretreatment process, quercetin grafted halloysite-based composite membranes were thicker than commercially available membranes, except that both Aq/pHNT10 and Aq/pHNT-FQ10 were 30 μm. Water uptake and IEC of composite membranes showed similar values, but the membrane with amino group/quercetin-grafted halloysite exceptionally displayed improved water uptake. Membrane swellings exhibited a similar or slightly raised value to that of Gore Select, but were lower than those of Nafion HP. Prepared membranes showed lower proton conductivity than Gore Select, but blending with pure quercetin-grafted halloysite showed higher values than Nafion HP.

The results of the water uptake were different when varying quercetin grafted-halloysite content. Blending of 5 wt% content showed increased water uptake value compared to that of 10 wt% or 2 wt% content. In terms of proton conductivity, 5 wt% loaded membrane showed better value than 10 wt% or 2 wt% loaded membranes. The anti-oxidative effect and thickness were not affected by the change of contents.

Composite membranes blended with fluorinated and pretreated sepiolite showed similar IEC and chemical stability compared to commercially available membranes. In addition, the composite membranes were superior to proton conductivity regardless of filler contents among the membranes tested, but displayed reduced swelling and mechanical stability.

For electrolyte membranes incorporated in MEAs to be tested in single cell fuel cells, slightly better performances were achieved with composites membranes compared to Nafion HP or pristine Aquivion, especially at intermediate current density and low relative humidity.

3. Perspectives

Regarding further work, it is needed to find novel strategies to more effectively pretreat sepiolites and halloysites using a variety of chemical solutions or processes.

Moreover, other chemical modification methods that can further grow the grafting ratio of sepiolite and halloysite to further improve the physicochemical properties of the membrane are needed to be considered. Afterward, such modified additives inside polymer matrix are needed to be optimized with varying contents.

A variety of PFSA ionomers and hydrocarbon polymers, which have not been reported so far, can be also used to study composite membranes.

In addition to the blending time, functionalization and pretreatment effect, other methods can be sought so that the dispersion state of sepiolites or halloysites within PFSA polymers is homogeneous, thereby having improved physicochemical properties.

Finally, it would be good to get a variety of results through MEA testing with various electrolyte membranes.

Annex

Table A1. Summary data on membrane casting dispersions composed of montmorillonite and ionomer, and proton conductivity of prepared membranes.

Filler type	Additives	Polymer powder/ polymer dispersion	Solvent/ non-solvent	Preparation method of composite membrane	Additive content over the casting dispersion (wt%)	Operating temp. (℃)	RH (%)	Proton conductivity of modified membrane (S cm^{-1})	Year of publication	Ref.
MMT	Cloisite® Na/[BVBI][Cl]	Styrene	DMF	Casting-evaporation process	3.5 g	-	-	0.0779	2016	[84]
MMT	Cloisite® Na/[BVBI][Cl]	HEMA	DMF	Casting-evaporation process	3.5 g	-	-	0.0425	2016	[84]
MMT	Cloisite® Na/[BVBI][Cl]	Acrylic acid	DMF	Casting-evaporation process	3.5 g	-	-	0.0524	2016	[84]
MMT	H^+ MMT	Nafion	-	Casting-evaporation process	6	25	50	0.0376	2016	[129]
MMT	Na^+ MMT	Nafion	-	Casting-evaporation process	6	25	50	0.0385	2016	[129]
MMT	Ca^{2+} MMT	Nafion	-	Casting-evaporation process	6	25	50	0.036	2016	[129]
MMT	Mg^{2+}MMT	Nafion	-	Casting-evaporation process	6	25	50	0.0365	2016	[129]
MMT	K^+ MMT	Nafion	-	Casting-evaporation process	6	25	50	0.037	2016	[129]
MMT	GPTMS-modified MMT	CS	Acetic acid	Casting-evaporation process	5	-	-	0.00466	2016	[85]
MMT	10% Sulfonated H^+ MMT	PVA	Water	Casting-evaporation process	20	Room	100	0.0060	2015	[137]
MMT	Cloisite® Na/[HMIM]Cl	ABPBI	Methanesulfonic acid (MSA)	Casting-evaporation process	10	220	-	< 0.02237	2015	[139]
MMT	Cloisite® Na/[TMG][BF_4]	ABPBI	Methanesulfonic acid (MSA)	Casting-evaporation process	10	220	-	< 0.01005	2015	[139]
MMT	3-MPTMS-modified MMT	Nafion	-	Casting-evaporation process	8	25	-	0.084	2015	[143]
MMT	CTAB-modified MMT	SPPESK	NMP	Casting-evaporation process	4	80	-	0.143	2014	[169]

Filler type	Additives	Polymer powder/ polymer dispersion	Solvent/ non-solvent	Preparation method of composite membrane	Additive content over the casting dispersion (wt%)	Operating temp. (℃)	RH (%)	Proton conductivity of modified membrane (S cm^{-1})	Year of publication	Ref.
MMT	MMT H+	PBI/PPA	-	Casting-evaporation process	50	160	20	0.436	2014	[80]
MMT	HDTMA-modified MMT	ABPBI	DMAc	Casting-evaporation process	-	-	-	-	2014	[88]
MMT	Cloisite® Na+	Poly(St-co-NaSS)	DMF	Casting-evaporation process	3.5 g	25	-	0.0779	2014	[142]
MMT	Cloisite® Na+	Poly(HEMA-co-NaSS)	DMF	Casting-evaporation process	3.5 g	25	-	0.0425	2014	[142]
MMT	Cloisite® Na+	Poly(AAc-co-NaSS)	DMF	Casting-evaporation process	3.5 g	25	-	0.0524	2014	[142]
MMT	Cloisite® Na+/PAA	PEO	-	Electrospinning	-	-	-	-	2014	[89]
MMT	Cloisite® 30B	SPSU	NMP	Casting-evaporation process	5	25	-	0.000511	2014	[166]
MMT	Cloisite® Na+	CS/PWA	-	Casting-evaporation process	2	25	-	0.0132	2013	[168]
MMT	Cloisite® 15A	CS/PWA	-	Casting-evaporation process	2	25	-	0.0108	2013	[168]
MMT	Cloisite® 30B	CS/PWA	-	Casting-evaporation process	2	25	-	0.0146	2013	[168]
MMT	AMPS-modified MMT	SPEEK	DMAc	Casting-evaporation process	10	-	-	0.006	2013	[154]
MMT	pristine MMT	Nafion	DMF/IPA	Casting-evaporation process	-	-	-	-	2012	[35]
MMT	Cloisite® 30B	SPSU (modified with chlorosulfonic acid)	DMF	Casting-evaporation process	1	Room	-	0.0005581	2012	[165]
MMT	Cloisite® 30B	SPSU (modified with trimethyl silyl chlorosulfonate)	DMF	Casting-evaporation process	1	Room	-	0.002126	2012	[165]

Filler type	Additives	Polymer powder/ polymer dispersion	Solvent/ non-solvent	Preparation method of composite membrane	Additive content over the casting dispersion (wt%)	Operating temp. (℃)	RH (%)	Proton conductivity of modified membrane (S cm^{-1})	Year of publication	Ref.
MMT	Closite Na	PSU	DMF	Casting-evaporation process	1	60	100	0.000000333	2012	[82]
MMT	Cloisite® 93A	PSU	DMF	Casting-evaporation process	1	60	100	0.000000341	2012	[82]
MMT	Cloisite® 30B	PSU	DMF	Casting-evaporation process	1	60	100	0.000000331	2012	[82]
MMT	3-MPTMS-modified MMT	SPAES	-	IR ramp	2	80	100	1.05	2012	[91]
MMT	Cloisite® 15A/TAP	SPEEK	DMSO	Doctor blande method	0.25 g/0.5g	-	-	0.0175	2017	[121]
MMT	Cloisite® 15A/TAP	SPEEK	DMSO	Casting-evaporation process	7.5/10 (corresponding to amount of SPEEK)	Room	100	0.00595	2012	[68]
MMT	DMDO-modified MMT	SPEEK	DMAc	Casting-evaporation process	15	80	100	0.151	2011	[153]
MMT	SA-modified MMT	SPEEK	DMAc	Casting-evaporation process	15	80	100	0.06	2011	[153]
MMT	AMPS-modified MMT	SPEEK	DMAc	Casting-evaporation process	15	80	100	0.065	2011	[153]
MMT	SO_3H-functionalized MMT	cross-linked PVA/PSSA	-	Casting-evaporation process	20	70	-	0.012	2011	[71]
MMT	1,3-propane sulfone-modified MMT/SPSU-BP	PTFE	NMP	Casting-evaporation process	3/97 (unkown for PTFE amount)	25	100	0.028 (through-plane)/0.073 (in-plane)	2011	[156]
MMT	MMT/STA	SPEEK	DMAc	Casting-evaporation process	1/0.5	Room	100	0.00608	2011	[152]
MMT	Cloisite® 30B	Cross-linked SPEEK	DMAc	Casting-evaporation process	5	80	-	0.0197	2011	[164]
MMT	SO_3H-functionalized MMT	PVA/PSSA	-	Casting-evaporation process	20/10	70	-	0.012	2011	[155]

Filler type	Additives	Polymer powder/ polymer dispersion	Solvent/ non-solvent	Preparation method of composite membrane	Additive content over the casting dispersion (wt%)	Operating temp. (℃)	RH (%)	Proton conductivity of modified membrane (S cm^{-1})	Year of publication	Ref.
MMT	Cloistie® 15A/TAP	SPEEK	DMSO	Casting-evaporation process	1/1(corresponding to amount of SPEEK)	Room	-	0.00387	2009	[162]
MMT	Cloisite® 15A/TAP	SPEEK	DMSO	Casting-evaporation process	2.5/7.5 (corresponding to amount of SPEEK)	Room	100	0.000704	2011	[209]
MMT	Cloisite® Na+	SSEBS	THF	Casting-evaporation process	10	Room	-	0.142	2011	[118]
MMT	Cloisite® 15A	SSEBS	THF	Casting-evaporation process	10	Room	-	0.03	2011	[118]
MMT	Cloisite® 20A	SSEBS	THF	Casting-evaporation process	10	Room	-	0.038	2011	[118]
MMT	Cloisite® 30B	SSEBS	THF	Casting-evaporation process	10	Room	-	0.027	2011	[118]
MMT	AMPS-modified MMT	Nafion	-	Casting-evaporation process	10	90	95	0.13	2011	[150]
MMT	CS-modified MMT	Nafion	-	Casting-evaporation process	10	25	-	0.045	2010	[170]
MMT	HSO_3-R-modified MMT	Nafion	-	Casting-evaporation process	5	100	98	0.1	2010	[145]
MMT	HSO_3-RSR-modified MMT	Nafion	-	Casting-evaporation process	5	100	98	0.16	2010	[145]
MMT	Cloisite® 15A	SPES	DMAc	Casting-evaporation process	10	Room	-	0.002	2010	[167]
MMT	Cloisite® 15A	H_3PO_4-doped PBI	DMAc	Casting-evaporation process	10	70	-	0.01	2010	[78]
MMT	CS-modified MMT	Nafion	-	Casting-evaporation process	10	25	95	0.025	2009	[171]
MMT	H+ MMT (Aldrich)	PVA	water	Casting-evaporation process	20	70	0	0.0278	2009	[73, 138]

Filler type	Additives	Polymer powder/ polymer dispersion	Solvent/ non-solvent	Preparation method of composite membrane	Additive content over the casting dispersion (wt%)	Operating temp. (℃)	RH (%)	Proton conductivity of modified membrane (S cm^{-1})	Year of publication	Ref.
MMT	Cloistie® 15A	SPPO	DMAc	Casting-evaporation process	3	Room	-	0.008	2009	[163]
MMT	H+ MMT	Nafion	Aliphatic alcohols	Casting-evaporation process	10	-	100	0.072	2009	[210]
MMT	Cloistie® 15A	SPEEK	DMAc	Casting-evaporation process	10	Room	-	0.0009	2010, 2008	[70, 161]
MMT	4-sulfophthalic acid-modified MMT	SPEEK	DMF	Casting-evaporation process	5	100	100	0.03	2008	[151]
MMT	Cloisite® 15A	SPPO	DMAc	Casting-evaporation process	2	Room	-	0.0108	2008	[81]
MMT	Dodecylamine-exchanged MMT	Nafion	-	Casting-evaporation process	5	80	0	0.7	2008	[149]
MMT	Cloisite® 30B	GPTMS/EHTES	H_3PO_4	Sol-gel procedure	10	140	30	0.026	2008	[132]
MMT	Cloisite® Na+	SPVA	-	Casting-evaporation process	5	-	-	0.016	2008	[75]
MMT	MMT synthesized with Krytox®	Nafion	-	Casting-evaporation process	3? 5?	100	100	0.032	2007	[130]
MMT	DOA-modified MMT	PBI	DMAc	Casting-evaporation process	-	-	-	-	2007	[76]
MMT	POPD230-modified MMT	Nafion	-	Casting-evaporation process	5	Room	-	0.07	2007	[211]
MMT	POPD400-modified MMT	Nafion	-	Casting-evaporation process	5	Room	-	0.092	2007	[211]
MMT	POPD2000-modified MMT	Nafion	-	Casting-evaporation process	5	Room	-	0.06	2007	[211]
MMT	POPD400-modified MMT	Nafion	-	Casting-evaporation process	-	Room	-	-	2007	[148]

Filler type	Additives	Polymer powder/ polymer dispersion	Solvent/ non-solvent	Preparation method of composite membrane	Additive content over the casting dispersion (wt%)	Operating temp. (℃)	RH (%)	Proton conductivity of modified membrane (S cm^{-1})	Year of publication	Ref.
MMT	POPD400-PS-modified MMT	Nafion	-	Casting-evaporation process	6	Room	-	0.115	2007	[148]
MMT	1,3-PS-modified MMT	Nafion	NMP/DMAc	Casting-evaporation process	10	Room	-	0.076	2007	[157]
MMT	1,4-BS-modified MMT	Nafion	NMP/DMAc	Casting-evaporation process	5	Room	-	-	2007	[157]
MMT	FMES-modified MMT	Nafion	NMP/DMAc	Casting-evaporation process	5	Room	-	-	2007	[157]
MMT	pristine MMT	Nafion	DMF	Casting-evaporation process	1	25	100	0.075	2007	[36]
MMT	No additive (see ratio of solvents)	Nafion	NMP/DMAc (100/0)	Inokin 2 roll reverse die coater	-	Room	-	0.096	2007	[147]
MMT	No additive (see ratio of solvents)	Nafion	NMP/DMAc (50/50)	Inokin 2 roll reverse die coater	-	Room	-	< 0.098	2007	[147]
MMT	No additive (see ratio of solvents)	Nafion	NMP/DMAc (10/90)	Inokin 2 roll reverse die coater	-	Room	-	< 0.105	2007	[147]
MMT	1,3-PS-modified MMT	Nafion	NMP/DMAc (10/90)	Inokin 2 roll reverse die coater	10	Room	-	0.077	2007	[147]
MMT	Cloisite® Na+; Cloisite® 20A	SSEBS	THF/methanol	Casting-evaporation process	-	-	-	-	2007	[93]
MMT	Dodecylamine-modified MMT	Nafion	-	Sol-gel procedure	-	-	-	-	2007	[144]
MMT	Cloisite® Na^+	PVA (40 wt%)	-	Casting-evaporation process	15	Room	100	0.0027	2006	[44]
MMT	1,4-BS-modified MMT	Nafion	-	Casting-evaporation process	5	50	98	0.11	2006	[146]

Filler type	Additives	Polymer powder/ polymer dispersion	Solvent/ non-solvent	Preparation method of composite membrane	Additive content over the casting dispersion (wt%)	Operating temp. (℃)	RH (%)	Proton conductivity of modified membrane (S cm^{-1})	Year of publication	Ref.
MMT	1,3-PS-modified MMT	Nafion	-	Casting-evaporation process	5	50	98	0.115	2006	[146]
MMT	FMES-modified MMT	Nafion	-	Casting-evaporation process	5	50	98	0.13	2006	[146]
MMT	o-BNPOB-modified MMT	6F-PEAA (Fluoro-poly(ether amic acid))	NMP	Casting-evaporation process	-	-	-	-	2006	[212]
MMT	Zonyl-modified MMT	Nafion	-	laboratory two-roll mill	4	Room	100	0.095	2006	[8]
MMT	PFPE-NR3-modified MMT	Nafion	-	laboratory two-roll mill	4	Room	100	0.081	2006	[8]
MMT	POP230-modified MMT	Vinyl ester	-	Bulk molding compound (BMC) process	4	-	-	-	2006	[94]
MMT	POP400-modified MMT	Vinyl ester	-	Bulk molding compound (BMC) process	4	-	-	-	2006	[94]
MMT	POP2000-modified MMT	Vinyl ester	-	Bulk molding compound (BMC) process	4	-	-	-	2006	[94]
MMT	Dodecylamine-modified MMT	Nafion	DMF	Casting-evaporation process	5	25		0.071	2005	[159]
MMT	CTAC-modified MMT	SPEEK	DMAc	Casting-evaporation process	10	90	100	0.0088	2005	[160]
MMT	DMOSPA-modified MMT	Nafion	water/aliphatic alcohol/ethylene glycol	Casting-evaporation process	-	-	-	-	2005	[102]
MMT	ACA-modified MMT	Nafion	water/aliphatic alcohol/ethylene glycol	Casting-evaporation process	4	Room	100	0.091	2005	[102]
MMT	BHB-modified MMT	Nafion	water/aliphatic alcohol/ethylene glycol	Casting-evaporation process	4	Room	100	0.088	2005	[102]

Filler type	Additives	Polymer powder/ polymer dispersion	Solvent/ non-solvent	Preparation method of composite membrane	Additive content over the casting dispersion (wt%)	Operating temp. (℃)	RH (%)	Proton conductivity of modified membrane (S cm^{-1})	Year of publication	Ref.
MMT	Cloisite® 10A	Nafion	DMAc	Casting-evaporation process	10	50-70	-	0.02	2004	[43]
MMT	Dodecylamine-modified MMT	Nafion	-	Hot pressing (at 200 - 230°C and 6000 psi)	3	110	100	0.0772	2003	[123]
MMT	Pristine MMT	SPEK	DMF/ NMP	Casting-evaporation process	20	-	-	0.046	2005	[141]
MMT	Cloisite® treated with 1 M H_2SO_4	SPEEK	DMAc	Casting-evaporation process	10	60	-	0.0027	2003	[34]
MMT	Pristine MMT	Nafion	DMF	Experimental set-up under electric field	-	-	-	-	2003	[100]

Bibliography

[1] G. A. Florides and P. Christodoulides, "Global warming and carbon dioxide through sciences," *Environment international,* vol. 35, no. 2, pp. 390-401, 2009.

[2] C. Change, "Global Warming," *TAPPI JOURNAL,* 1998.

[3] M. Winter and R. J. Brodd, "What are batteries, fuel cells, and supercapacitors?," ed: ACS Publications, 2004.

[4] B. C. Steele and A. Heinzel, "Materials for fuel-cell technologies," in *Materials For Sustainable Energy: A Collection of Peer-Reviewed Research and Review Articles from Nature Publishing Group*: World Scientific, 2011, pp. 224-231.

[5] P. Costamagna and S. Srinivasan, "Quantum jumps in the PEMFC science and technology from the 1960s to the year 2000: Part II. Engineering, technology development and application aspects," *Journal of power sources,* vol. 102, no. 1-2, pp. 253-269, 2001.

[6] J. M. Moore, J. B. Lakeman, and G. O. Mepsted, "Development of a PEM fuel cell powered portable field generator for the dismounted soldier," *Journal of Power Sources,* vol. 106, no. 1-2, pp. 16-20, 2002.

[7] L. Schlapbach, "Technology: Hydrogen-fuelled vehicles," *Nature,* vol. 460, no. 7257, p. 809, 2009.

[8] J.-M. Thomassin, C. Pagnoulle, D. Bizzari, G. Caldarella, A. Germain, and R. Jérôme, "Improvement of the barrier properties of Nafion® by fluoro-modified montmorillonite," *Solid State Ionics,* vol. 177, no. 13-14, pp. 1137-1144, 2006.

[9] K. Kreuer, "On the development of proton conducting polymer membranes for hydrogen and methanol fuel cells," *Journal of membrane science,* vol. 185, no. 1, pp. 29-39, 2001.

[10] M. Ciureanu, "Effects of Nafion® dehydration in PEM fuel cells," *Journal of Applied Electrochemistry,* vol. 34, no. 7, pp. 705-714, 2004.

[11] H. Lee *et al.*, "Pinhole formation in PEMFC membrane after electrochemical degradation and wet/dry cycling test," *Korean Journal of Chemical Engineering,* vol. 28, no. 2, pp. 487-491, 2011.

[12] G. Lin and T. Van Nguyen, "Effect of thickness and hydrophobic polymer content of the gas diffusion layer on electrode flooding level in a PEMFC," *Journal of The Electrochemical Society,* vol. 152, no. 10, pp. A1942-A1948, 2005.

[13] S. Peighambardoust, S. Rowshanzamir, and M. Amjadi, "Review of the proton exchange membranes for fuel cell applications," *International journal of hydrogen energy,* vol. 35, no. 17, pp. 9349-9384, 2010.

[14] R. Nagarale, W. Shin, and P. K. Singh, "Progress in ionic organic-inorganic composite membranes for fuel cell applications," *Polymer Chemistry,* vol. 1, no. 4, pp. 388-408, 2010.

[15] A. K. Mishra, S. Bose, T. Kuila, N. H. Kim, and J. H. Lee, "Silicate-based polymer-nanocomposite membranes for polymer electrolyte membrane fuel cells," *Progress in polymer Science,* vol. 37, no. 6, pp. 842-869, 2012.

[16] W. Zhengbang, H. Tang, and P. Mu, "Self-assembly of durable Nafion/TiO2 nanowire electrolyte membranes for elevated-temperature PEM fuel cells," *Journal of membrane science,* vol. 369, no. 1-2, pp. 250-257, 2011.

[17] B. Matos, E. Aricó, M. Linardi, A. Ferlauto, E. Santiago, and F. Fonseca, "Thermal properties of Nafion–TiO2 composite electrolytes for PEM fuel cell," *Journal of thermal analysis and calorimetry,* vol. 97, no. 2, p. 591, 2009.

[18] V. Di Noto, R. Gliubizzi, E. Negro, and G. Pace, "Effect of SiO2 on relaxation phenomena and mechanism of ion conductivity of [Nafion/(SiO2) x] composite membranes," *The Journal of Physical Chemistry B,* vol. 110, no. 49, pp. 24972-24986, 2006.

[19] F. Pereira, K. Vallé, P. Belleville, A. Morin, S. Lambert, and C. Sanchez, "Advanced mesostructured hybrid silica− nafion membranes for high-performance PEM fuel cell," *Chemistry of Materials,* vol. 20, no. 5, pp. 1710-1718, 2008.

[20] N. H. Jalani, K. Dunn, and R. Datta, "Synthesis and characterization of Nafion®-MO2 (M= Zr, Si, Ti) nanocomposite membranes for higher temperature PEM fuel cells," *Electrochimica Acta,* vol. 51, no. 3, pp. 553-560, 2005.

[21] A. Saccà *et al.*, "Phosphotungstic Acid Supported on a Nanopowdered ZrO2 as a Filler in Nafion-Based Membranes for Polymer Electrolyte Fuel Cells," *Fuel Cells,* vol. 8, no. 3-4, pp. 225-235, 2008.

[22] A. D'Epifanio *et al.*, "Composite nafion/sulfated zirconia membranes: effect of the filler surface properties on proton transport characteristics," *Chemistry of Materials,* vol. 22, no. 3, pp. 813-821, 2009.

[23] Y. Zhai, H. Zhang, J. Hu, and B. Yi, "Preparation and characterization of sulfated zirconia (SO42−/ZrO2)/Nafion composite membranes for PEMFC operation at high temperature/low humidity," *Journal of membrane science,* vol. 280, no. 1-2, pp. 148-155, 2006.

[24] D. J. Kim, M. J. Jo, and S. Y. Nam, "A review of polymer–nanocomposite electrolyte membranes for fuel cell application," *Journal of Industrial and Engineering Chemistry,* vol. 21, pp. 36-52, 2015.

[25] P. Kongkachuichay and S. Pimprom, "Nafion/Analcime and Nafion/Faujasite composite membranes for polymer electrolyte membrane fuel cells," *Chemical Engineering Research and Design,* vol. 88, no. 4, pp. 496-500, 2010.

[26] E. Şengül, H. Erdener, R. G. Akay, H. Yücel, N. Bac, and İ. Eroğlu, "Effects of sulfonated polyether-etherketone (SPEEK) and composite membranes on the proton exchange membrane fuel cell (PEMFC) performance," *international journal of hydrogen energy,* vol. 34, no. 10, pp. 4645-4652, 2009.

[27] B. P. Tripathi, M. Kumar, and V. K. Shahi, "Highly stable proton conducting nanocomposite polymer electrolyte membrane (PEM) prepared by pore modifications: an extremely low methanol permeable PEM," *Journal of Membrane Science,* vol. 327, no. 1-2, pp. 145-154, 2009.

[28] A. Carbone, A. Saccà, I. Gatto, R. Pedicini, and E. Passalacqua, "Investigation on composite S-PEEK/H-BETA MEAs for medium temperature PEFC," *International Journal of Hydrogen Energy,* vol. 33, no. 12, pp. 3153-3158, 2008.

[29] A. Filippov *et al.*, "Transport properties of novel hybrid cation-exchange membranes on the base of MF-4SC and halloysite nanotubes," *Journal of Materials Science and Chemical Engineering,* vol. 3, no. 01, p. 58, 2015.

[30] G. Cavallaro, R. De Lisi, G. Lazzara, and S. Milioto, "Polyethylene glycol/clay nanotubes composites," *Journal of thermal analysis and calorimetry,* vol. 112, no. 1, pp. 383-389, 2013.

[31] M. Oroujzadeh, S. Mehdipour-Ataei, and M. Esfandeh, "Microphase separated sepiolite-based nanocomposite blends of fully sulfonated poly (ether ketone)/non-sulfonated poly (ether sulfone) as proton exchange membranes from dual electrospun mats," *RSC Advances,* vol. 5, no. 88, pp. 72075-72083, 2015.

[32] F. J. Fernandez-Carretero, K. Suarez, O. Solorza, E. Riande, and V. Compan, "PEMFC performance of MEAs based on Nafion® and sPSEBS hybrid membranes," *Journal of New Materials for Electrochemical Systems,* vol. 13, no. 3, pp. 191-199, 2010.

[33] P. Bébin, M. Caravanier, and H. Galiano, "Nafion®/clay-SO3H membrane for proton exchange membrane fuel cell application," *Journal of Membrane Science,* vol. 278, no. 1-2, pp. 35-42, 2006.

[34] J.-H. Chang, J. H. Park, G.-G. Park, C.-S. Kim, and O. O. Park, "Proton-conducting composite membranes derived from sulfonated hydrocarbon and inorganic materials," *Journal of Power Sources,* vol. 124, no. 1, pp. 18-25, 2003.

[35] I. Nicotera, A. Enotiadis, K. Angjeli, L. Coppola, and D. Gournis, "Evaluation of smectite clays as nanofillers for the synthesis of nanocomposite polymer electrolytes for fuel cell applications," *international journal of hydrogen energy,* vol. 37, no. 7, pp. 6236-6245, 2012.

[36] F. Mura, R. Silva, and A. Pozio, "Study on the conductivity of recast Nafion®/montmorillonite and Nafion®/TiO2 composite membranes," *Electrochimica acta,* vol. 52, no. 19, pp. 5824-5828, 2007.

[37] K. Fatyeyeva *et al.*, "Grafting of p-styrene sulfonate and 1, 3-propane sultone onto Laponite for proton exchange membrane fuel cell application," *Journal of membrane science,* vol. 366, no. 1-2, pp. 33-42, 2011.

[38] C. Beauger, G. Lainé, A. Burr, A. Taguet, and B. Otazaghine, "Improvement of Nafion®-sepiolite composite membranes for PEMFC with sulfo-fluorinated sepiolite," *Journal of Membrane Science,* vol. 495, pp. 392-403, 2015.

[39] C. Beauger, G. Lainé, A. Burr, A. Taguet, B. Otazaghine, and A. Rigacci, "Nafion®–sepiolite composite membranes for improved proton exchange membrane fuel cell performance," *Journal of membrane science,* vol. 430, pp. 167-179, 2013.

[40] H. Zhang, T. Zhang, J. Wang, F. Pei, Y. He, and J. Liu, "Enhanced proton conductivity of sulfonated poly (ether ether ketone) membrane embedded by dopamine-modified nanotubes for proton exchange membrane fuel cell," *Fuel Cells,* vol. 13, no. 6, pp. 1155-1165, 2013.

[41] A. K. Mishra, T. Kuila, N. H. Kim, and J. H. Lee, "Effect of peptizer on the properties of Nafion–Laponite clay nanocomposite membranes for polymer electrolyte membrane fuel cells," *Journal of membrane science,* vol. 389, pp. 316-323, 2012.

[42] X. Liu *et al.*, "Proton conductivity improvement of sulfonated poly (ether ether ketone) nanocomposite membranes with sulfonated halloysite nanotubes prepared via dopamine-initiated atom transfer radical polymerization," *Journal of Membrane Science,* vol. 504, pp. 206-219, 2016.

[43] M.-K. Song, S.-B. Park, Y.-T. Kim, K.-H. Kim, S.-K. Min, and H.-W. Rhee, "Characterization of polymer-layered silicate nanocomposite membranes for direct methanol fuel cells," *Electrochimica Acta,* vol. 50, no. 2-3, pp. 639-643, 2004.

[44] J.-M. Thomassin, C. Pagnoulle, G. Caldarella, A. Germain, and R. Jérôme, "Contribution of nanoclays to the barrier properties of a model proton exchange membrane for fuel cell application," *Journal of membrane science,* vol. 270, no. 1-2, pp. 50-56, 2006.

[45] R. Kamble, M. Ghag, S. Gaikawad, and B. K. Panda, "Halloysite Nanotubes and Applications: A Review," *Journal of Advanced Scientific Research,* vol. 3, no. 2, 2012.

[46] H. Zhang, Y. He, J. Zhang, L. Ma, Y. Li, and J. Wang, "Constructing dual-interfacial proton-conducting pathways in nanofibrous composite membrane for efficient proton transfer," *Journal of Membrane Science,* vol. 505, pp. 108-118, 2016.

[47] H. Zhang, C. Ma, J. Wang, X. Wang, H. Bai, and J. Liu, "Enhancement of proton conductivity of polymer electrolyte membrane enabled by sulfonated nanotubes," *International journal of hydrogen energy,* vol. 39, no. 2, pp. 974-986, 2014.

[48] D. Bielska, A. Karewicz, T. Lachowicz, K. Berent, K. Szczubiałka, and M. Nowakowska, "Hybrid photosensitizer based on halloysite nanotubes for phenol-based pesticide photodegradation," *Chemical Engineering Journal,* vol. 262, pp. 125-132, 2015.

[49] F. Fernandez-Carretero, V. Compan, and E. Riande, "Hybrid ion-exchange membranes for fuel cells and separation processes," *Journal of power sources,* vol. 173, no. 1, pp. 68-76, 2007.

[50] J. Li, M. Pan, and H. Tang, "Understanding short-side-chain perfluorinated sulfonic acid and its application for high temperature polymer electrolyte membrane fuel cells," *RSC Advances,* vol. 4, no. 8, pp. 3944-3965, 2014.

[51] A. Stassi *et al.*, "Performance comparison of long and short-side chain perfluorosulfonic membranes for high temperature polymer electrolyte membrane fuel cell operation," *Journal of Power Sources,* vol. 196, no. 21, pp. 8925-8930, 2011.

[52] S. Giancola *et al.*, "Composite short side chain PFSA membranes for PEM water electrolysis," *Journal of membrane science,* vol. 570, pp. 69-76, 2019.

[53] D. Jones, *https://www.sigmaaldrich.com/technical-documents/articles/materials-science/perfluorosulfonic-acid-membranes.html*.

[54] A. Aricò *et al.*, "High temperature operation of a solid polymer electrolyte fuel cell stack based on a new ionomer membrane," *Fuel Cells,* vol. 10, no. 6, pp. 1013-1023, 2010.

[55] A.-C. Dupuis, "Proton exchange membranes for fuel cells operated at medium temperatures: Materials and experimental techniques," *Progress in Materials Science,* vol. 56, no. 3, pp. 289-327, 2011.

[56] A. Chandan *et al.*, "High temperature (HT) polymer electrolyte membrane fuel cells (PEMFC)–A review," *Journal of Power Sources,* vol. 231, pp. 264-278, 2013.

[57] J. Qiao, M. Saito, K. Hayamizu, and T. Okada, "Degradation of perfluorinated ionomer membranes for PEM fuel cells during processing with H2O2," *Journal of The Electrochemical Society,* vol. 153, no. 6, pp. A967-A974, 2006.

[58] Q. Guo, P. N. Pintauro, H. Tang, and S. O'Connor, "Sulfonated and crosslinked polyphosphazene-based proton-exchange membranes," *Journal of Membrane Science,* vol. 154, no. 2, pp. 175-181, 1999.

[59] S. J. Peighambardoust, S. Rowshanzamir, and M. Amjadi, "Review of the proton exchange membranes for fuel cell applications," *International journal of hydrogen energy,* vol. 35, no. 17, pp. 9349-9384, 2010.

[60] F. N. Büchi, B. Gupta, O. Haas, and G. G. Scherer, "Study of radiation-grafted FEP-G-polystyrene membranes as polymer electrolytes in fuel cells," *Electrochimica Acta,* vol. 40, no. 3, pp. 345-353, 1995.

[61] J. Xie, D. L. Wood, D. M. Wayne, T. A. Zawodzinski, P. Atanassov, and R. L. Borup, "Durability of PEFCs at high humidity conditions," *Journal of the Electrochemical Society,* vol. 152, no. 1, pp. A104-A113, 2005.

[62] C. A. Daniels, *Polymers: structure and properties*. CRC Press, 1989.

[63] Y. Tang, A. M. Karlsson, M. H. Santare, M. Gilbert, S. Cleghorn, and W. B. Johnson, "An experimental investigation of humidity and temperature effects on the mechanical properties of perfluorosulfonic acid membrane," *Materials Science and Engineering: A,* vol. 425, no. 1-2, pp. 297-304, 2006.

[64] N. Uematsu, N. Hoshi, T. Koga, and M. Ikeda, "Synthesis of novel perfluorosulfonamide monomers and their application," *Journal of fluorine chemistry,* vol. 127, no. 8, pp. 1087-1095, 2006.

[65] S. Subianto *et al.*, "Physical and chemical modification routes leading to improved mechanical properties of perfluorosulfonic acid membranes for PEM fuel cells," *Journal of Power Sources,* vol. 233, pp. 216-230, 2013.

[66] V. Arcella and A. Ghielmi, "Solvay Solexis EP1238999 B1," 2006.

[67] J. A. Kolde, B. Bahar, M. S. Wilson, T. A. Zawodzinski, and S. Gottesfeld, "Advanced composite polymer electrolyte fuel cell membranes," *ECS Proceedings Volumes,* vol. 1995, pp. 193-201, 1995.

[68] J. Jaafar, A. Ismail, and T. Matsuura, "Effect of dispersion state of Cloisite15A® on the performance of SPEEK/Cloisite15A nanocomposite membrane for DMFC application," *Journal of Applied Polymer Science,* vol. 124, no. 2, pp. 969-977, 2012.

[69] M. Othman, A. Ismail, and A. Mustafa, "Proton conducting composite membrane from sulfonated poly (ether ether ketone) and boron orthophosphate for direct methanol fuel cell application," *Journal of membrane science,* vol. 299, no. 1-2, pp. 156-165, 2007.

[70] M. M. Hasani-Sadrabadi, S. H. Emami, R. Ghaffarian, and H. Moaddel, "Nanocomposite membranes made from sulfonated poly (ether ether ketone) and montmorillonite clay for fuel cell applications," *Energy & Fuels,* vol. 22, no. 4, pp. 2539-2542, 2008.

[71] C.-C. Yang, "Fabrication and characterization of poly (vinyl alcohol)/montmorillonite/poly (styrene sulfonic acid) proton-conducting composite membranes for direct methanol fuel cells," *International Journal of Hydrogen Energy,* vol. 36, no. 7, pp. 4419-4431, 2011.

[72] C.-C. Yang, S.-J. Chiu, and S.-C. Kuo, "Preparation of poly(vinyl alcohol)/montmorillonite/poly(styrene sulfonic acid) composite membranes for hydrogen–oxygen polymer electrolyte fuel cells," *Current Applied Physics,* vol. 11, no. 1, Supplement, pp. S229-S237, 2011/01/01/ 2011, doi: https://doi.org/10.1016/j.cap.2010.11.043.

[73] C.-C. Yang, Y.-J. Lee, and J. M. Yang, "Direct methanol fuel cell (DMFC) based on PVA/MMT composite polymer membranes," *Journal of Power Sources,* vol. 188, no. 1, pp. 30-37, 2009.

[74] B. S. Pivovar, Y. Wang, and E. Cussler, "Pervaporation membranes in direct methanol fuel cells," *Journal of Membrane Science,* vol. 154, no. 2, pp. 155-162, 1999.

[75] P. Duangkaew and J. Wootthikanokkhan, "Methanol permeability and proton conductivity of direct methanol fuel cell membranes based on sulfonated poly (vinyl alcohol)–layered silicate nanocomposites," *Journal of applied polymer science,* vol. 109, no. 1, pp. 452-458, 2008.

[76] S.-W. Chuang, S. L.-C. Hsu, and C.-L. Hsu, "Synthesis and properties of fluorine-containing polybenzimidazole/montmorillonite nanocomposite membranes for direct methanol fuel cell applications," *Journal of Power Sources,* vol. 168, no. 1, pp. 172-177, 2007.

[77] J.-M. Bae, I. Honma, M. Murata, T. Yamamoto, M. Rikukawa, and N. Ogata, "Properties of selected sulfonated polymers as proton-conducting electrolytes for polymer electrolyte fuel cells," *Solid State Ionics,* vol. 147, no. 1-2, pp. 189-194, 2002.

[78] M. M. Hasani-Sadrabadi, N. M. Dorri, S. R. Ghaffarian, E. Dashtimoghadam, K. Sarikhani, and F. S. Majedi, "Effects of organically modified nanoclay on the transport properties and electrochemical performance of acid-doped polybenzimidazole membranes," *Journal of Applied Polymer Science,* vol. 117, no. 2, pp. 1227-1233, 2010.

[79] J. Peron, E. Ruiz, D. J. Jones, and J. Rozière, "Solution sulfonation of a novel polybenzimidazole: a proton electrolyte for fuel cell application," *Journal of Membrane Science,* vol. 314, no. 1-2, pp. 247-256, 2008.

[80] F. Ublekov, H. Penchev, V. Georgiev, I. Radev, and V. Sinigersky, "Protonated montmorillonite as a highly effective proton-conductivity enhancer in p-PBI membranes for PEM fuel cells," *Materials Letters,* vol. 135, pp. 5-7, 2014/11/15/ 2014, doi: https://doi.org/10.1016/j.matlet.2014.07.128.

[81] M. M. Hasani-Sadrabadi, S. H. Emami, and H. Moaddel, "Preparation and characterization of nanocomposite membranes made of poly (2, 6-dimethyl-1, 4-phenylene oxide) and montmorillonite for direct methanol fuel cells," *Journal of Power Sources,* vol. 183, no. 2, pp. 551-556, 2008.

[82] L. Unnikrishnan, S. Mohanty, S. K. Nayak, and N. Singh, "Synthesis and characterization of polysulfone/clay nanocomposite membranes for fuel cell application," *Journal of Applied Polymer Science,* vol. 124, no. S1, pp. E309-E318, 2012.

[83] F. Wang, M. Hickner, Y. S. Kim, T. A. Zawodzinski, and J. E. McGrath, "Direct polymerization of sulfonated poly (arylene ether sulfone) random (statistical) copolymers: candidates for new proton exchange membranes," *Journal of Membrane Science,* vol. 197, no. 1-2, pp. 231-242, 2002.

[84] Y.-S. Kim, K.-S. Seo, and S.-H. Choi, "Polymeric nanocomposite proton exchange membranes prepared by radiation-induced polymerization for direct methanol fuel cell," *Radiation Physics and Chemistry,* vol. 118, pp. 35-41, 2016.

[85] M. Purwanto *et al.*, "Biopolymer-based electrolyte membranes from chitosan incorporated with montmorillonite-crosslinked GPTMS for direct methanol fuel cells," *RSC Advances,* vol. 6, no. 3, pp. 2314-2322, 2016.

[86] X. Bao, F. Zhang, and Q. Liu, "Sulfonated poly (2, 5-benzimidazole)(ABPBI)/MMT/ionic liquids composite membranes for high temperature PEM applications," *international journal of hydrogen energy,* vol. 40, no. 46, pp. 16767-16774, 2015.

[87] Z. Hu, G. He, S. Gu, Y. Liu, and X. Wu, "Montmorillonite-reinforced sulfonated poly (phthalazinone ether sulfone ketone) nanocomposite proton exchange membranes for direct methanol fuel cells," *Journal of Applied Polymer Science,* vol. 131, no. 3, 2014.

[88] B. Eren, R. Aydin, and E. Eren, "Morphology and thermal characterization of montmorillonite/polybenzimidazole nanocomposite," *Journal of Thermal Analysis and Calorimetry,* vol. 115, no. 2, pp. 1525-1531, 2014.

[89] M. Prasad, S. Mohanty, and S. K. Nayak, "Study of polymeric nanocomposite membrane made from sulfonated polysulfone and nanoclay for fuel cell applications," *High Performance Polymers,* vol. 26, no. 5, pp. 578-586, 2014.

[90] D.-J. Kim, H.-Y. Hwang, S.-b. Jung, and S.-Y. Nam, "Sulfonated poly (arylene ether sulfone)/Laponite-SO3H composite membrane for direct methanol fuel cell," *Journal of Industrial and Engineering Chemistry,* vol. 18, no. 1, pp. 556-562, 2012.

[91] D. J. Kim, H. Y. Hwang, S. Y. Nam, and Y. T. Hong, "Characterization of a composite membrane based on SPAES/sulfonated montmorillonite for DMFC application," *Macromolecular research,* vol. 20, no. 1, pp. 21-29, 2012.

[92] L. C. Battirola, L. H. Gasparotto, U. P. Rodrigues-Filho, and G. Tremiliosi-Filho, "Poly (imide)/organically-modified montmorillonite nanocomposite as a potential membrane for alkaline fuel cells," *Membranes,* vol. 2, no. 3, pp. 430-439, 2012.

[93] A. Ganguly and A. K. Bhowmick, "Sulfonated styrene-(ethylene-co-butylene)-styrene/montmorillonite clay nanocomposites: synthesis, morphology, and properties," *Nanoscale research letters,* vol. 3, no. 1, p. 36, 2008.

[94] C.-Y. Yen, S.-H. Liao, Y.-F. Lin, C.-H. Hung, Y.-Y. Lin, and C.-C. M. Ma, "Preparation and properties of high performance nanocomposite bipolar plate for fuel cell," *Journal of Power Sources,* vol. 162, no. 1, pp. 309-315, 2006.

[95] S. Xie, S. Zhang, F. Wang, M. Yang, R. Séguéla, and J.-M. Lefebvre, "Preparation, structure and thermomechanical properties of nylon-6 nanocomposites with lamella-type and fiber-type sepiolite," *Composites science and technology,* vol. 67, no. 11-12, pp. 2334-2341, 2007.

[96] S. Trabia, K. Choi, Z. Olsen, T. Hwang, J.-D. Nam, and K. Kim, "Understanding the Thermal Properties of Precursor-Ionomers to Optimize Fabrication Processes for Ionic Polymer-Metal Composites (IPMCs)," *Materials,* vol. 11, no. 5, p. 665, 2018.

[97] S. Siracusano, V. Baglio, A. Stassi, L. Merlo, E. Moukheiber, and A. Aricò, "Performance analysis of short-side-chain Aquivion® perfluorosulfonic acid polymer for proton exchange membrane water electrolysis," *Journal of membrane science,* vol. 466, pp. 1-7, 2014.

[98] B. Matos, E. Aricó, M. Linardi, A. Ferlauto, E. Santiago, and F. Fonseca, "Thermal properties of Nafion–TiO2 composite electrolytes for PEM fuel cell," *Journal of thermal analysis and calorimetry,* vol. 97, no. 2, pp. 591-594, 2009.

[99] C. Felice, S. Ye, and D. Qu, "Nafion− montmorillonite nanocomposite membrane for the effective reduction of fuel crossover," *Industrial & Engineering Chemistry Research,* vol. 49, no. 4, pp. 1514-1519, 2010.

[100] C. Karthikeyan *et al.*, "Aligned Nafion® nanocomposites: Preparation and morphological characterization," *Macromolecular Materials and Engineering,* vol. 288, no. 2, pp. 175-180, 2003.

[101] L. d. A. Prado, C. Karthikeyan, K. Schulte, S. Nunes, and I. L. de Torriani, "Organic modification of layered silicates: structural and thermal characterizations," *Journal of Non-Crystalline Solids,* vol. 351, no. 12-13, pp. 970-975, 2005.

[102] J.-M. Thomassin, C. Pagnoulle, G. Caldarella, A. Germain, and R. Jérôme, "Impact of acid containing montmorillonite on the properties of Nafion® membranes," *Polymer,* vol. 46, no. 25, pp. 11389-11395, 2005.

[103] I. Nicotera, V. Kosma, C. Simari, C. D'Urso, A. Aricò, and V. Baglio, "Methanol and proton transport in layered double hydroxide and smectite clay-based composites: influence on the electrochemical behavior of direct methanol fuel cells at intermediate temperatures," *Journal of Solid State Electrochemistry,* vol. 19, no. 7, pp. 2053-2061, 2015.

[104] B. Ruzicka and E. Zaccarelli, "A fresh look at the Laponite phase diagram," *Soft Matter,* vol. 7, no. 4, pp. 1268-1286, 2011.

[105] G. Tartaglione, D. Tabuani, and G. Camino, "Thermal and morphological characterisation of organically modified sepiolite," *Microporous and Mesoporous Materials,* vol. 107, no. 1-2, pp. 161-168, 2008.

[106] Z. Tabatabaei-Yazdi and S. Mehdipour-Ataei, "Poly (ether-imide) and related sepiolite nanocomposites: investigation of physical, thermal, and mechanical properties," *Polymers for Advanced Technologies,* vol. 26, no. 4, pp. 308-314, 2015.

[107] E. Bilotti, H. Fischer, and T. Peijs, "Polymer nanocomposites based on needle-like sepiolite clays: Effect of functionalized polymers on the dispersion of nanofiller, crystallinity, and mechanical properties," *Journal of applied polymer science,* vol. 107, no. 2, pp. 1116-1123, 2008.

[108] F. Fernandez-Carretero, E. Riande, C. Del Rio, F. Sánchez, J. Acosta, and V. Compañ, "Preparation and characterization of hybrid membranes based on Nafion® using partially sulfonated inorganic fillers," *Journal of New Materials for Electrochemical Systems,* vol. 13, no. 2, pp. 83-93, 2010.

[109] P. Yuan *et al.*, "Functionalization of halloysite clay nanotubes by grafting with γ-aminopropyltriethoxysilane," *The Journal of Physical Chemistry C,* vol. 112, no. 40, pp. 15742-15751, 2008.

[110] Y. Xie, D. Qian, D. Wu, and X. Ma, "Magnetic halloysite nanotubes/iron oxide composites for the adsorption of dyes," *Chemical Engineering Journal,* vol. 168, no. 2, pp. 959-963, 2011.

[111] M. E. Mackay *et al.*, "General strategies for nanoparticle dispersion," *Science,* vol. 311, no. 5768, pp. 1740-1743, 2006.

[112] R. Krishnamoorti, "Strategies for dispersing nanoparticles in polymers," *MRS bulletin,* vol. 32, no. 4, pp. 341-347, 2007.

[113] G. J. Fleer, "Polymers at interfaces and in colloidal dispersions," *Advances in colloid and interface science,* vol. 159, no. 2, pp. 99-116, 2010.

[114] Y. S. Lipatov, "Polymer blends and interpenetrating polymer networks at the interface with solids," *Progress in Polymer Science,* vol. 27, no. 9, pp. 1721-1801, 2002.

[115] C. R. Vestal and Z. J. Zhang, "Atom transfer radical polymerization synthesis and magnetic characterization of MnFe2O4/polystyrene core/shell nanoparticles," *Journal of the American Chemical Society,* vol. 124, no. 48, pp. 14312-14313, 2002.

[116] T. L. Wang, C. C. Ou, and C. H. Yang, "Synthesis and properties of organic/inorganic hybrid nanoparticles prepared using atom transfer radical polymerization," *Journal of applied polymer science,* vol. 109, no. 5, pp. 3421-3430, 2008.

[117] H. Hosseini, S. Shojaee-Aliabadi, S. Hosseini, and L. Mirmoghtadaie, "Nanoantimicrobials in Food Industry," in *Nanotechnology Applications in Food*: Elsevier, 2017, pp. 223-243.

[118] H. Y. Hwang, S. J. Kim, D. Y. Oh, Y. T. Hong, and S. Y. Nam, "Proton Conduction and Methanol Transport through Sulfonated Poly (styrene-b-ethylene/butylene-b-styrene)/Clay Nanocomposite," *Macromolecular Research,* vol. 19, no. 1, pp. 84-89, 2011.

[119] P. Bordes, E. Pollet, and L. Avérous, "Nano-biocomposites: biodegradable polyester/nanoclay systems," *Progress in Polymer Science,* vol. 34, no. 2, pp. 125-155, 2009.

[120] A. Rico-Zavala *et al.*, "Synthesis and characterization of composite membranes modified with Halloysite nanotubes and phosphotungstic acid for electrochemical hydrogen pumps," *Renewable Energy,* vol. 122, pp. 163-172, 2018.

[121] M. T. Salleh *et al.*, "Stability of SPEEK/Cloisite®/TAP nanocomposite membrane under Fenton reagent condition for direct methanol fuel cell application," *Polymer Degradation and Stability,* vol. 137, pp. 83-99, 2017.

[122] S. H. Lee, W. J. Lee, T. K. Kim, M. K. Bayazit, S. O. Kim, and Y. S. Choi, "UV-crosslinked poly (arylene ether sulfone)–LAPONITE® nanocomposites for proton exchange membranes," *RSC Advances,* vol. 7, no. 45, pp. 28358-28365, 2017.

[123] D. Jung, S. Cho, D. Peck, D. Shin, and J. Kim, "Preparation and performance of a Nafion®/montmorillonite nanocomposite membrane for direct methanol fuel cell," *Journal of Power Sources,* vol. 118, no. 1-2, pp. 205-211, 2003.

[124] J. Zhang, G.-P. Yin, Z.-B. Wang, Q.-Z. Lai, and K.-D. Cai, "Effects of hot pressing conditions on the performances of MEAs for direct methanol fuel cells," *Journal of power sources,* vol. 165, no. 1, pp. 73-81, 2007.

[125] T. Frey and M. Linardi, "Effects of membrane electrode assembly preparation on the polymer electrolyte membrane fuel cell performance," *Electrochimica Acta,* vol. 50, no. 1, pp. 99-105, 2004.

[126] V. Mehta and J. S. Cooper, "Review and analysis of PEM fuel cell design and manufacturing," *Journal of power sources,* vol. 114, no. 1, pp. 32-53, 2003.

[127] P. Liu, "Polymer modified clay minerals: A review," *Applied Clay Science,* vol. 38, no. 1-2, pp. 64-76, 2007.

[128] K. Adachi and Y. Tsukahara, "Macroinitiator and Macromonomer: Preparation and Application," in *Encyclopedia of Polymeric Nanomaterials*: Springer, 2015, pp. 1167-1175.

[129] X.-W. Wu, N. Wu, C.-Q. Shi, Z.-Y. Zheng, H.-B. Qi, and Y.-F. Wang, "Proton conductive montmorillonite-Nafion composite membranes for direct ethanol fuel cells," *Applied Surface Science,* vol. 388, pp. 239-244, 2016.

[130] R. Gosalawit, S. Chirachanchai, S. Shishatskiy, and S. P. Nunes, "Krytox–Montmorillonite–Nafion® nanocomposite membrane for effective methanol crossover reduction in DMFCs," *Solid State Ionics,* vol. 178, no. 29-30, pp. 1627-1635, 2007.

[131] M. K. Song, S. B. Park, Y. T. Kim, K. H. Kim, S. K. Min, and H. W. Rhee, "Characterization of polymer-layered silicate nanocomposite membranes for direct methanol fuel cells," *Electrochimica Acta,* vol. 50, no. 2-3, pp. 639-643, Nov 2004, doi: 10.1016/j.electacta.2003.12.078.

[132] R. Jana and H. Bhunia, "Thermal stability and proton conductivity of silane based nanostructured composite membranes," *Solid State Ionics,* vol. 178, no. 37-38, pp. 1872-1878, 2008.

[133] S. Moulik, B. A. Vaishnavi, H. Nagar, and S. Sridhar, "Water Competitive Diffusion," in *Encyclopedia of Membranes*, E. Drioli and L. Giorno Eds. Berlin, Heidelberg: Springer Berlin Heidelberg, 2016, pp. 1973-1983.

[134] Z. Wojnarowska and M. Paluch, "Recent progress on dielectric properties of protic ionic liquids," *Journal of Physics-Condensed Matter,* vol. 27, no. 7, Feb 2015, Art no. 073202, doi: 10.1088/0953-8984/27/7/073202.

[135] W. H. J. Hogarth, J. C. D. da Costa, and G. Q. Lu, "Solid acid membranes for high temperature (> 140 degrees C) proton exchange membrane fuel cells," *Journal of Power Sources,* vol. 142, no. 1-2, pp. 223-237, Mar 2005, doi: 10.1016/j.jpowsour.2004.11.020.

[136] S. Bureekaew *et al.*, "One-dimensional imidazole aggregate in aluminium porous coordination polymers with high proton conductivity," *Nature Materials,* vol. 8, no. 10, pp. 831-836, Oct 2009, doi: 10.1038/nmat2526.

[137] P. Bahavan Palani, R. Kannan, S. Rajashabala, S. Rajendran, and G. Velraj, "Effect of nano-composite on polyvinyl alcohol-based proton conducting membrane for direct methanol fuel cell applications," *Ionics,* journal article vol. 21, no. 2, pp. 507-513, February 01 2015, doi: 10.1007/s11581-014-1193-1.

[138] C.-C. Yang and Y.-J. Lee, "Preparation of the acidic PVA/MMT nanocomposite polymer membrane for the direct methanol fuel cell (DMFC)," *Thin Solid Films,* vol. 517, no. 17, pp. 4735-4740, 2009.

[139] X. Bao, F. Zhang, and Q. Liu, "Sulfonated poly(2,5-benzimidazole) (ABPBI)/ MMT/ ionic liquids composite membranes for high temperature PEM applications," *International Journal of Hydrogen Energy,* vol. 40, no. 46, pp. 16767-16774, 2015/12/14/ 2015, doi: https://doi.org/10.1016/j.ijhydene.2015.07.127.

[140] H. J. Kim *et al.*, "Synthesis of poly(2,5-benzimidazole) for use as a fuel-cell membrane," *Macromolecular Rapid Communications,* vol. 25, no. 8, pp. 894-897, Apr 2004, doi: 10.1002/marc.200300288.

[141] C. Karthikeyan, S. Nunes, and K. Schulte, "Ionomer-silicates composite membranes: Permeability and conductivity studies," *European polymer journal,* vol. 41, no. 6, pp. 1350-1356, 2005.

[142] Y.-S. Kim, Y. O. Kang, and S.-H. Choi, "Radiolytic synthesis of vinyl Polymer-Clay nanocomposite membranes for direct methanol fuel cell," *Journal of Nanomaterials,* vol. 2014, 2014.

[143] J.-W. Lee, Y.-T. Yoo, and J. Y. Lee, "Characterization of Nafion nanocomposites with spheric silica, layered silicate, and amphiphilic organic molecule and their actuator application," *Macromolecular Research,* journal article vol. 23, no. 2, pp. 167-176, February 01 2015, doi: 10.1007/s13233-015-3029-x.

[144] L. Zhang, J. Xu, G. Hou, H. Tang, and F. Deng, "Interactions between Nafion resin and protonated dodecylamine modified montmorillonite: A solid state NMR study," *Journal of colloid and interface science,* vol. 311, no. 1, pp. 38-44, 2007.

[145] Y. Kim, Y. Choi, H. K. Kim, and J. S. Lee, "New sulfonic acid moiety grafted on montmorillonite as filler of organic–inorganic composite membrane for non-humidified proton-exchange membrane fuel cells," *Journal of Power Sources,* vol. 195, no. 15, pp. 4653-4659, 2010.

[146] Y. Kim, J. S. Lee, C. H. Rhee, H. K. Kim, and H. Chang, "Montmorillonite functionalized with perfluorinated sulfonic acid for proton-conducting organic–inorganic composite membranes," *Journal of power sources,* vol. 162, no. 1, pp. 180-185, 2006.

[147] T. K. Kim *et al.*, "Preparation of Nafion-sulfonated clay nanocomposite membrane for direct menthol fuel cells via a film coating process," *Journal of Power Sources,* vol. 165, no. 1, pp. 1-8, 2007.

[148] Y.-F. Lin, C.-Y. Yen, C.-H. Hung, Y.-H. Hsiao, and C.-C. M. Ma, "A novel composite membranes based on sulfonated montmorillonite modified Nafion® for DMFCs," *Journal of Power Sources,* vol. 168, no. 1, pp. 162-166, 2007.

[149] H. Xiuchong, T. Haolin, and P. Mu, "Synthesis and performance of water-retention PEMs with nafion-intercalating-montmorillonite hybrid," *Journal of applied polymer science,* vol. 108, no. 1, pp. 529-534, 2008.

[150] M. M. Hasani-Sadrabadi, E. Dashtimoghadam, F. S. Majedi, K. Kabiri, M. Solati-Hashjin, and H. Moaddel, "Novel nanocomposite proton exchange membranes based on Nafion® and AMPS-modified montmorillonite for fuel cell applications," *Journal of Membrane Science,* vol. 365, no. 1-2, pp. 286-293, 2010.

[151] R. Gosalawit, S. Chirachanchai, S. Shishatskiy, and S. P. Nunes, "Sulfonated montmorillonite/sulfonated poly (ether ether ketone)(SMMT/SPEEK) nanocomposite membrane for direct methanol fuel cells (DMFCs)," *Journal of Membrane Science,* vol. 323, no. 2, pp. 337-346, 2008.

[152] S. Mohtar, A. Ismail, and T. Matsuura, "Preparation and characterization of SPEEK/MMT-STA composite membrane for DMFC application," *Journal of membrane science,* vol. 371, no. 1-2, pp. 10-19, 2011.

[153] H. Doğan, T. Y. Inan, M. Koral, and M. Kaya, "Organo-montmorillonites and sulfonated PEEK nanocomposite membranes for fuel cell applications," *Applied Clay Science,* vol. 52, no. 3, pp. 285-294, 2011.

[154] M. F. Samberan, M. M. Hasani-Sadrabadi, S. R. Ghaffarian, and A. Alimadadi, "Investigation of the effects of AMPS-modified nanoclay on fuel cell performance of sulfonated aromatic proton exchange membranes," *International Journal of Hydrogen Energy,* vol. 38, no. 32, pp. 14076-14084, 2013.

[155] C.-C. Yang, S.-J. Chiu, and S.-C. Kuo, "Preparation of poly (vinyl alcohol)/montmorillonite/poly (styrene sulfonic acid) composite membranes for hydrogen–oxygen polymer electrolyte fuel cells," *Current Applied Physics,* vol. 11, no. 1, pp. S229-S237, 2011.

[156] D. Xing, G. He, Z. Hou, P. Ming, and S. Song, "Preparation and characterization of a modified montmorillonite/sulfonated polyphenylether sulfone/PTFE composite membrane," *International journal of hydrogen energy,* vol. 36, no. 3, pp. 2177-2183, 2011.

[157] W. Lee, H. Kim, T. K. Kim, and H. Chang, "Nafion based organic/inorganic composite membrane for air-breathing direct methanol fuel cells," *Journal of membrane science,* vol. 292, no. 1-2, pp. 29-34, 2007.

[158] Y. Kim, J. S. Lee, C. H. Rhee, H. K. Kim, and H. Chang, "Montmorillonite functionalized with perfluorinated sulfonic acid for proton-conducting organic-inorganic composite membranes," *Journal of Power Sources,* vol. 162, no. 1, pp. 180-185, Nov 2006, doi: 10.1016/j.jpowsour.2006.07.041.

[159] R. Silva, S. Passerini, and A. Pozio, "Solution-cast Nafion®/montmorillonite composite membrane with low methanol permeability," *Electrochimica Acta,* vol. 50, no. 13, pp. 2639-2645, 2005.

[160] Z. Gaowen and Z. Zhentao, "Organic/inorganic composite membranes for application in DMFC," *Journal of Membrane Science,* vol. 261, no. 1-2, pp. 107-113, 2005.

[161] M. M. Hasani-Sadrabadi, E. Dashtimoghadam, K. Sarikhani, F. S. Majedi, and G. Khanbabaei, "Electrochemical investigation of sulfonated poly (ether ether ketone)/clay nanocomposite membranes for moderate temperature fuel cell applications," *Journal of Power Sources,* vol. 195, no. 9, pp. 2450-2456, 2010.

[162] J. Jaafar, A. F. Ismail, and T. Matsuura, "Preparation and barrier properties of SPEEK/Cloisite 15A®/TAP nanocomposite membrane for DMFC application," *Journal of Membrane Science,* vol. 345, no. 1-2, pp. 119-127, 2009.

[163] M. M. Hasani-Sadrabadi, S. R. Ghaffarian, N. Mokarram-Dorri, E. Dashtimoghadam, and F. S. Majedi, "Characterization of nanohybrid membranes for direct methanol fuel cell applications," *Solid State Ionics,* vol. 180, no. 32-35, pp. 1497-1504, 2009.

[164] V. R. Hande, S. K. Rath, S. Rao, and M. Patri, "Cross-linked sulfonated poly (ether ether ketone)(SPEEK)/reactive organoclay nanocomposite proton exchange membranes (PEM)," *Journal of membrane science,* vol. 372, no. 1-2, pp. 40-48, 2011.

[165] L. Unnikrishnan, P. Madamana, S. Mohanty, and S. K. Nayak, "Polysulfone/C30B nanocomposite membranes for fuel cell applications: effect of various sulfonating agents," *Polymer-Plastics Technology and Engineering,* vol. 51, no. 6, pp. 568-577, 2012.

[166] Z. Shami, N. Sharifi-Sanjani, B. Khanyghma, S. Farjpour, and A. Fotouhi, "Ordered exfoliated silicate platelets architecture: hydrogen bonded poly (acrylic acid)–poly (ethylene oxide)/Na–montmorillonite complex nanofibrous membranes prepared by electrospinning technique," *RSC Advances,* vol. 4, no. 77, pp. 40892-40897, 2014.

[167] M. M. Hasani-Sadrabadi, E. Dashtimoghadam, S. R. Ghaffarian, M. H. H. Sadrabadi, M. Heidari, and H. Moaddel, "Novel high-performance nanocomposite proton exchange membranes based on poly (ether sulfone)," *Renewable Energy,* vol. 35, no. 1, pp. 226-231, 2010.

[168] M. Tohidian, S. R. Ghaffarian, S. E. Shakeri, E. Dashtimoghadam, and M. M. Hasani-Sadrabadi, "Organically modified montmorillonite and chitosan–phosphotungstic acid complex nanocomposites as high performance membranes for fuel cell applications," *Journal of Solid State Electrochemistry,* vol. 17, no. 8, pp. 2123-2137, 2013.

[169] Z. Hu, G. He, S. Gu, Y. Liu, and X. Wu, "Montmorillonite-reinforced sulfonated poly(phthalazinone ether sulfone ketone) nanocomposite proton exchange membranes for direct methanol fuel cells," *Journal of Applied Polymer Science,* vol. 131, no. 3, 2014, doi: doi:10.1002/app.39852.

[170] M. M. Hasani-Sadrabadi *et al.*, "Novel high-performance nanohybrid polyelectrolyte membranes based on bio-functionalized montmorillonite for fuel cell applications," *Chemical Communications,* vol. 46, no. 35, pp. 6500-6502, 2010.

[171] M. M. Hasani-Sadrabadi, E. Dashtimoghadam, F. S. Majedi, and K. Kabiri, "Nafion®/bio-functionalized montmorillonite nanohybrids as novel polyelectrolyte membranes for direct methanol fuel cells," *Journal of Power Sources,* vol. 190, no. 2, pp. 318-321, 2009.

[172] D. Plackett *et al.*, "High-temperature proton exchange membranes based on polybenzimidazole and clay composites for fuel cells," *Journal of membrane science,* vol. 383, no. 1-2, pp. 78-87, 2011.

[173] K. Fatyeyeva, C. Chappey, F. Poncin-Epaillard, D. Langevin, J.-M. Valleton, and S. Marais, "Composite membranes based on Nafion® and plasma treated clay charges: elaboration and water sorption investigations," *Journal of membrane science,* vol. 369, no. 1-2, pp. 155-166, 2011.

[174] A. Filippov, D. Afonin, N. Kononenko, Y. Lvov, and V. Vinokurov, "New approach to characterization of hybrid nanocomposites," *Colloids and Surfaces A: Physicochemical and Engineering Aspects,* vol. 521, pp. 251-259, 2017.

[175] F. J. Fernandez-Carretero, E. Riande, C. del Rio, F. Sanchez, J. L. Acosta, and V. Compan, "Preparation and Characterization of Hybrid Membranes based on Nafion (R) using Partially Sulfonated Inorganic Fillers," *Journal of New Materials for Electrochemical Systems,* vol. 13, no. 2, pp. 83-93, Apr 2010. [Online]. Available: <Go to ISI>://WOS:000282032200001.

[176] M. Oroujzadeh, S. Mehdipour-Ataei, and M. Esfandeh, "Preparation and properties of novel sulfonated poly(arylene ether ketone) random copolymers for polymer electrolyte membrane fuel cells," *European Polymer Journal,* vol. 49, no. 6, pp. 1673-1681, Jun 2013, doi: 10.1016/j.eurpolymj.2013.03.008.

[177] H. Yang, W. Lee, B. Choi, and W. Kim, "Preparation of Nafion/Pt-containing TiO2/graphene oxide composite membranes for self-humidifying proton exchange membrane fuel cell," *Journal of Membrane Science,* vol. 504, pp. 20-28, 2016.

[178] R. Sothornvit, J.-W. Rhim, and S.-I. Hong, "Effect of nano-clay type on the physical and antimicrobial properties of whey protein isolate/clay composite films," *Journal of Food Engineering,* vol. 91, no. 3, pp. 468-473, 2009.

[179] S. H. Woo, A. Rigacci, and C. Beauger, "Influence of sepiolite and halloysite nanoclay additives on the water uptake and swelling of Nafion based composite membranes for PEMFC: impact of the blending time on composite homogeneity," *Chemistry Letters,* vol. 48, 2019.

[180] Y. S. Kim and B. Pivovar, "Comparing proton conductivity of polymer electrolytes by percent conducting volume," *ECS Transactions,* vol. 25, no. 1, pp. 1425-1431, 2009.

[181] A. Mokrini, A. Siu, L. Robitaille, L. Gonzalez, and F. Sanchez, "Investigation of advanced hybrid PEM based on sulfonyl fluoride PFSA and grafted inorganic nanoparticles," *ECS Transactions,* vol. 33, no. 1, pp. 823-838, 2010.

[182] N. Agmon, "The grotthuss mechanism," *Chemical Physics Letters,* vol. 244, no. 5-6, pp. 456-462, 1995.

[183] C. Zhao *et al.*, "Block sulfonated poly (ether ether ketone) s (SPEEK) ionomers with high ion-exchange capacities for proton exchange membranes," *Journal of power sources,* vol. 162, no. 2, pp. 1003-1009, 2006.

[184] T. Grancha *et al.*, "Insights into the Dynamics of Grotthuss Mechanism in a Proton-Conducting Chiral bio MOF," *Chemistry of Materials,* vol. 28, no. 13, pp. 4608-4615, 2016.

[185] E. Joussein, S. Petit, J. Churchman, B. Theng, D. Righi, and B. Delvaux, "Halloysite clay minerals–a review," ed: De Gruyter, 2005.

[186] B. Szczepanik, P. Rogala, P. M. Słomkiewicz, D. Banaś, A. Kubala-Kukuś, and I. Stabrawa, "Synthesis, characterization and photocatalytic activity of TiO2-halloysite and Fe2O3-halloysite nanocomposites for photodegradation of chloroanilines in water," *Applied Clay Science,* vol. 149, pp. 118-126, 2017.

[187] K. Cooper, "Characterizing through-plane and in-plane ionic conductivity of polymer electrolyte membranes," *ECS Transactions,* vol. 41, no. 1, pp. 1371-1380, 2011.

[188] J.-H. Fang, "Polyimide Proton Exchange Membranes," in *Advanced Polyimide Materials*: Elsevier, 2018, pp. 323-383.

[189] S. M. Andersen, C. F. Nørgaard, M. J. Larsen, and E. Skou, "Tin dioxide as an effective antioxidant for proton exchange membrane fuel cells," *Journal of Power Sources,* vol. 273, pp. 158-161, 2015.

[190] C. A. Rice-Evans, N. J. Miller, and G. Paganga, "Structure-antioxidant activity relationships of flavonoids and phenolic acids," *Free radical biology and medicine,* vol. 20, no. 7, pp. 933-956, 1996.

[191] L. Wang, Y.-C. Tu, T.-W. Lian, J.-T. Hung, J.-H. Yen, and M.-J. Wu, "Distinctive antioxidant and antiinflammatory effects of flavonols," *Journal of Agricultural and Food Chemistry,* vol. 54, no. 26, pp. 9798-9804, 2006.

[192] W. Bors, W. Heller, C. Michel, and M. Saran, "Radical chemistry of flavonoid antioxidants," in *Antioxidants in therapy and preventive medicine*: Springer, 1990, pp. 165-170.

[193] J. Hanuza *et al.*, "Molecular structure and vibrational spectra of quercetin and quercetin-5'-sulfonic acid," *Vibrational Spectroscopy,* vol. 88, pp. 94-105, 2017.

[194] M. Gebert, A. Ghielmi, L. Merlo, M. Corasaniti, and V. Arcella, "AQUIVION {trade mark, serif}--The Short-Side-Chain and Low-EW PFSA for Next-Generation PEFCs Expands Production and Utilization," *ECS Transactions,* vol. 26, no. 1, pp. 279-283, 2010.

[195] A. Skulimowska *et al.*, "Proton exchange membrane water electrolysis with short-side-chain Aquivion® membrane and IrO2 anode catalyst," *International Journal of Hydrogen Energy,* vol. 39, no. 12, pp. 6307-6316, 2014.

[196] A. Esteban-Cubillo, R. Pina-Zapardiel, J. Moya, M. Barba, and C. Pecharromán, "The role of magnesium on the stability of crystalline sepiolite structure," *Journal of the European Ceramic Society,* vol. 28, no. 9, pp. 1763-1768, 2008.

[197] A. Yebra-Rodriguez, J. Martin-Ramos, F. Del Rey, C. Viseras, and A. Lopez-Galindo, "Effect of acid treatment on the structure of sepiolite," *Clay Minerals,* vol. 38, no. 3, pp. 353-360, 2003.

[198] A. S. Aricò, V. Baglio, and V. Antonucci, "Composite membranes for high temperature direct methanol fuel cells," *Membranes for Energy Conversion,* vol. 2, pp. 123-167, 2007.

[199] L. Liang, "Effects of surface chemistry on kinetics of coagulation of submicron iron oxide particles ([alpha]-Fe2O3) in water," California Institute of Technology, 1988.

[200] K. D. Kreuer, A. Rabenau, and W. Weppner, "Vehicle mechanism, a new model for the interpretation of the conductivity of fast proton conductors," *Angewandte Chemie International Edition,* vol. 21, no. 3, pp. 208-209, 1982.

[201] M. S. del Río, E. García-Romero, M. Suárez, I. da Silva, L. Fuentes-Montero, and G. Martínez-Criado, "Variability in sepiolite: Diffraction studies," *American Mineralogist,* vol. 96, no. 10, pp. 1443-1454, 2011.

[202] K. Chemizmu and R. Fentona, "Fenton reaction-controversy concerning the chemistry," *Ecological chemistry and engineering,* vol. 16, pp. 347-358, 2009.

[203] W. Barb, J. Baxendale, P. George, and K. Hargrave, "Reactions of ferrous and ferric ions with hydrogen peroxide. Part I.—The ferrous ion reaction," *Transactions of the Faraday Society,* vol. 47, pp. 462-500, 1951.

[204] M. S. Barrios, L. F. González, M. V. Rodríguez, and J. M. Pozas, "Acid activation of a palygorskite with HCl: Development of physico-chemical, textural and surface properties," *Applied Clay Science,* vol. 10, no. 3, pp. 247-258, 1995.

[205] L. Gozalez, L. Ibarra, A. Rodriguez, J. Moya, and F. Valle, "Fibrous silica gel obtained from sepiolite by HCl attack," *Clay Minerals,* vol. 19, no. 1, pp. 93-98, 1984.

[206] A. Jiménez-López, J. d. D. López-González, A. Ramīrez-Sāenz, F. Rodrīguez-Reinoso, C. Valenzuela-Calahorro, and L. Zurita-Herrera, "Evolution of surface area in a sepiolite as a function of acid and heat treatments," *Clay Minerals,* vol. 13, no. 4, pp. 375-385, 1978.

[207] S. Kostinski, R. Pandey, S. Gowtham, U. Pernisz, and A. Kostinski, "Diffusion of water molecules in amorphous silica," *IEEE Electron Device Letters,* vol. 33, no. 6, pp. 863-865, 2012.

[208] O. Sel, L. To Thi Kim, C. Debiemme-Chouvy, C. Gabrielli, C. Laberty-Robert, and H. Perrot, "Determination of the diffusion coefficient of protons in Nafion thin films by ac-electrogravimetry," *Langmuir,* vol. 29, no. 45, pp. 13655-13660, 2013.

[209] J. Jaafar, A. Ismail, T. Matsuura, and K. Nagai, "Performance of SPEEK based polymer–nanoclay inorganic membrane for DMFC," *Journal of membrane science,* vol. 382, no. 1-2, pp. 202-211, 2011.

[210] R. H. Alonso, L. Estevez, H. Lian, A. Kelarakis, and E. P. Giannelis, "Nafion–clay nanocomposite membranes: morphology and properties," *Polymer,* vol. 50, no. 11, pp. 2402-2410, 2009.

[211] Y.-F. Lin, C.-Y. Yen, C.-C. M. Ma, S.-H. Liao, C.-H. Hung, and Y.-H. Hsiao, "Preparation and properties of high performance nanocomposite proton exchange membrane for fuel cell," *Journal of power sources,* vol. 165, no. 2, pp. 692-700, 2007.

[212] R. H. Vora and M. Vora, "1, 2′-Bis (4-aminophenoxy) benzene based designed fluoro-poly (ether-imide)/MMT clay nanocomposites: synthesis and properties for high performance applications," *Materials Science and Engineering: B,* vol. 132, no. 1-2, pp. 90-102, 2006.

ABSTRACT

This Ph.D. thesis introduces novel electrolyte membranes which can be operated at low relative humidity (below 50%) and intermediate temperature, i.e., 90℃. More specifically, the thesis takes benefit from hygroscopicity of microfibrous SEP (sepiolite) and tubular HNT (halloysite). Changes in Nafion membrane properties with blending time are studied. Moreover, these nanoclays are functionalized and pretreated to make them proton conductive and to improve their compatibility with short-side-chain PFSA (perfluorosulfonic acid) composite membranes based on Aquivion. To begin with, functionalized and pretreated clay nanoparticles are characterized prior to incorporation in polymer matrix: ATR-FTIR (attenuated total reflection-fourier transform infrared spectroscopy), Py-GC/MS (pyrolysis gas chromatography mass spectrometry), and TGA (thermogravimetric analysis). Composites membranes have them been prepared and characterized for proton conductivity, water uptake, swelling, thermo-mechanical strength and chemical stability. The dispersion state of SEP and HNT inside polymer phase was observed using SEM/EDS (field emission scanning electron microscopy/Energy dispersive X-ray spectroscopy). The properties of pretreated nanoclays are characterized using XRD (X-ray diffraction) and EDS. Chemical stability regarding radical attack against composite membranes is clarified using Ion meter through fluoride ion (F^-) analysis. Proton conductivity of composite membranes is also measured under condition of different relative humidity and temperature. Following this, it is demonstrated by DMA (dynamic mechanical analysis) results that the particular elongated morphology of SEPs and HNTs participates to improving mechanical property of the composite membranes with decreased swelling ratio. MEAs (membrane electrode assembly) performance are evaluated to understand the advantage of the presence of nanoclays in the composite membranes regarding the relative humidity of the feeding gas, the operating temperature of single cells, and the hydrogen crossover. Detailed abstracts including main results were provided at the beginning of each chapter.

KEYWORDS

Hydrogen fuel cell; Proton exchange membrane fuel cell (PEMFC) ; Electrolyte membrane; Composite membrane; Membrane electrode assembly (MEA); Ionomer; PFSA (perfluorosulfonic acid); Aquivion; Nafion; Nanoclay; Sepiolite; Halloysite; Low relative humidity; Intermediate temperature; Functionalization; Acidic pretreatment; Composite homogeneity; Water uptake; Chemical stability; Dynamic mechanical analysis (DMA); Electrochemical impedance spectroscopy (EIS); Proton conductivity; Hydrogen crossover; Swelling; Single cell

RÉSUMÉ

Cette thèse introduit de nouvelles membranes électrolytiques pouvant fonctionner à faible humidité relative (inférieure à 50%) et à une température intermédiaire, c'est-à-dire 90°C voire au-delà. Plus spécifiquement, la thèse tire profit de l'hygroscopicité de la morphologie d'argiles naturelles, lasépiolite microfibreuse et l'halloysite tubulaire . Ces nanoargiles ont été intégrées à des suspensions de Nafion® ou Aquivion pour préparer des membranes composites. Elles ont été fonctionnalisées et prétraitées pour les rendre conductrices protoniques et améliorer leur compatibilité avec les matrices perfluorosulfoniques utilisés. Ces argiles ont d'abord été caractérisées avant leur incorporation dans la matrice polymère : ATR-FTIR (spectroscopie infrarouge à transformée de Fourier totale atténuée), Py-GC/MS (spectrométrie de masse par chromatographie en phase gazeuse à pyrolyse) et ATG (analyse thermogravimétrique). Les propriétés des nanoargiles prétraitées ont enfin été caractérisées par XRD (diffraction des rayons X) et EDS. Les membranes composites préparées ont ensuite été caractérisées pour la conductivité protonique, l'absorption d'eau, le gonflement, la résistance thermomécanique et la stabilité chimique. L'état de dispersion des argiles à l'intérieur de la phase de polymère a été observé par SEM/EDS (microscopie électronique à balayage à émission de champ / spectroscopie à rayons X à dispersion d'énergie). La stabilité chimique vis-à-vis de l'attaque radicale contre les membranes composites a été étudiée par mesure de la formation d'ions fluorure (F^-). La conductivité protonique des membranes composites a également été calculée à partir des résistances mesurées dans dans une large gamme d'humidités relatives et de températures. Des mesures thermomécaniques par analyse mécanique dynamique ont montré que la morphologie allongée particulière des argiles choisies participe à l'amélioration des propriétés mécaniques des membranes composites tout en réduisant le taux de gonflement. Les performances en assemblage membrane électrodes ont été évaluées pour mettre en évidence l'avantage de la présence de ces nanoargiles dans les membranes composites en ce qui concerne l'humidité relative du gaz d'alimentation, la température de fonctionnement de la cellule et la perméation à l'hydrogène. Des résumés détaillés comprenant les principaux résultats ont été fournis au début de chaque chapitre.

MOTS CLÉS

Pile à combustible à membrane d'échange de protons (PEMFC); Membrane électrolytique; Membrane composite; Aquivion; Nafion; Nanoclay; Sepiolite; Halloysite; Faible humidité relative; Température intermédiaire; Fonctionnalisation; Prétraitement acide; Homogénéité; Absorption d'eau; Stabilité chimique; Analyse mécanique dynamique (AMD); Spectroscopie d'impédance électrochimique (EIS); Conductivité protonique; Perméation à l'hydrogène; Gonflement. ; assemblage membrane électrode (AME); Courbes de polarisation.